NASA CR-111772

# DEMONSTRATION OF A STERILIZABLE SOLID PROPELLANT ROCKET MOTOR

By L. Weinberg



Prepared under Contract No. NAS1-8937 by
United Technology Center
Division of United Aircraft Corporation
Sunnyvale, California

for

NATIONAL AERONAUTICS AND SPACE ADMINISTRATION

CONTENTS


| Section | | Page |
|---|---|---|
| 1.0 | INTRODUCTION | 1-1 |
| 2.0 | SUMMARY OF RESULTS | 2-1 |
| 3.0 | PROPELLANT CHARACTERIZATION | 3-1 |
| | 3.1 Propellant Development Background | 3-1 |
| | 3.2 Propellant Constituents | 3-8 |
| | 3.3 Propellant Physical and Ballistic Properties | 3-11 |
| | 3.3.1 Strand Burning Rates | 3-11 |
| | 3.3.2 Stress-Strain Characteristics of Propellants for Demonstration Motors | 3-14 |
| | 3.3.3 Propellant Density | 3-15 |
| | 3.3.4 Propellant Volatile Stability and Dimensional Stabilities | 3-16 |
| 4.0 | LINER/INSULATION EVALUATION | 4-1 |
| | 4.1 Liner and Insulation Development Background | 4-1 |
| | 4.2 Liner and Insulation Constituents | 4-2 |
| | 4.3 Program Evaluation Tests for Liner and Insulation | 4-4 |
| | 4.3.1 Liner and Insulation Tensile Properties | 4-4 |
| | 4.3.2 Volatile Stability of Liner and Insulation | 4-5 |
| | 4.3.3 Insulation-to-Titanium Peel Tests | 4-8 |
| | 4.4 Supplemental Development Activities on Liner and Insulation | 4-12 |
| 5.0 | STERILIZATION CYCLE DETERMINATION | 5-1 |
| | 5.1 Aging Degradation Analysis | 5-6 |
| | 5.2 Oven Tests Using An Empty Motor Case | 5-17 |
| | 5.3 Oven Tests Using An Inert Propellant Motor | 5-44 |
| | 5.4 Sterilization Heating Cycle Using Live Propellant | 5-55 |
| | 5.5 Conclusions and Recommendations | 5-63 |
| 6.0 | MOTOR DESIGN, DESCRIPTION, AND PERFORMANCE SUMMARY | 6-1 |
| | 6.1 Grain Design and Performance Summary | 6-2 |
| | 6.2 Motor Case Design | 6-7 |
| | 6.3 Nozzle/Aft Closure Assembly Design | 6-11 |
| | 6.4 Case Insulation Design | 6-26 |
| | 6.5 Igniter Design and Sizing | 6-30 |
| | 6.5.1 Design | 6-30 |
| | 6.5.2 Sizing | 6-32 |
| | 6.5.3 Igniter Thermal Analysis | 6-33 |

CONTENTS (Continued)


| Section | | | Page |
|---|---|---|---|
| | 6.6 | Motor Loading and Curing | 6-36 |
| | | 6.6.1 Processing Procedures | 6-36 |
| | | 6.6.2 Processing Propellant for Evaluation | 6-41 |
| | | 6.6.3 Processing Propellant for Demonstration Motors | 6-44 |
| | 6.7 | Inspection and Quality Control | 6-45 |
| | | 6.7.1 Propellant Inspections | 6-47 |
| | | 6.7.2 Motor Case and Loaded Motor Inspections | 6-49 |
| | 6.8 | Motor Environmental Tests | 6-53 |
| 7.0 | SUPPLEMENTAL TESTS | | 7-1 |
| 8.0 | CONCLUSIONS AND RECOMMENDATIONS | | 8-1 |

ILLUSTRATIONS


| Figure | | Page |
|---|---|---|
| 3-1 | Strand Burning Rate vs Pressure - UTP-11439-5/1 | 3-12 |
| 3-2 | Strand Burning Rate vs Pressure - UTP-11439-5/2 | 3-13 |
| 4-1 | Volatile Stability Test Specimen | 4-6 |
| 4-2 | Measurement of Distance Between Scribe Lines on Volatile Stability Test Specimens | 4-7 |
| 4-3 | Weight Loss vs Sterilization Cycles | 4-11 |
| 5-1 | Arrhenius Plot Showing the Effect of Temperature on the Usable Storage Life of Propellant | 5-3 |
| 5-2 | Predicted Propellant Degradation Factor for Temperature Change | 5-4 |
| 5-3 | Location and Model for Thermal Analysis of Sterilization Cycle Optimization | 5-9 |
| 5-4 | Internal and Interface Temperatures at Constant Oven Air Temperature = 300°F | 5-10 |
| 5-5 | Internal and Interface Temperatures at Variable Oven Air Cycle 1 | 5-11 |
| 5-6 | Internal, Interface, and External Temperatures at Case Temperature Cycle 2 | 5-14 |
| 5-7 | Internal, Interface, and External Temperatures at Case Temperature Cycle 4, Modified | 5-15 |
| 5-8 | Internal, Interface, and External Temperatures (Cooling to 60°F) | 5-16 |
| 5-9 | Thermocouple Locations on Motor Case and Propellant | 5-18 |
| 5-10 | Motor Positions in Oven | 5-19 |
| 5-11 | Typical Recording of Thermocouple Responses on Empty Motor Case Tests | 5-20 |
| 5-12 | Empty Case Position Number 1, Test 1 Low Value Case Temperatures | 5-22 |

ILLUSTRATIONS (Continued)


| Figure | | Page |
|---|---|---|
| 5-13 | Empty Case Position Number 1, Test 1 High Value Case Temperatures | 5-23 |
| 5-14 | Empty Case Position Number 1, Test 1 Low Value Case Temperatures, HTC Results | 5-24 |
| 5-15 | Empty Case Position Number 1, Test 1 High Value Case Temperatures, HTC Results | 5-25 |
| 5-16 | Empty Case Position Number 4, Test 2 Low Value Case Temperatures | 5-26 |
| 5-17 | Empty Case Position Number 4, Test 2 High Case Temperature Values | 5-27 |
| 5-18 | Empty Case Position Number 4, Test 2 Low Value Case Temperatures, HTC Results | 5-28 |
| 5-19 | Empty Case Position Number 4, Test 2 High Case Temperature Values, HTC Results | 5-29 |
| 5-20 | Empty Case Position Number 2, Test 3 Low Case Temperature Values, Pre-Heat Oven | 5-30 |
| 5-21 | Empty Case Position Number 2, Test 3 High Case Temperature Values, Pre-Heat Oven | 5-31 |
| 5-22 | Empty Case Position Number 2, Test 3 Low Case Temperature Values, Pre-Heat Oven, HTC Results | 5-32 |
| 5-23 | Empty Case Position Number 2, Test 3 High Case Temperature Values, Pre-Heat Oven, HTC Results | 5-33 |
| 5-24 | Empty Case Position Number 3, Test 4 Low Case Temperature Values | 5-34 |
| 5-25 | Empty Case Position Number 3, Test 4 High Case Temperature Values | 5-35 |
| 5-26 | Empty Case Position Number 3, Test 4 Low Case Temperature Values, HTC Results | 5-36 |
| 5-27 | Empty Case Position Number 3, Test 4 High Case Temperature Values, HTC Results | 5-37 |

ILLUSTRATIONS (Continued)


| Figure | | Page |
|---|---|---|
| 5-28 | Empty Case Position Number 4, Test 5 Low Case Temperature Values | 5-38 |
| 5-29 | Empty Case Position Number 4, Test 5 High Case Temperature Values | 5-39 |
| 5-30 | Empty Case Position Number 4, Test 5 Low Case Temperature Values, HTC Results | 5-40 |
| 5-31 | Empty Case Position Number 4, Test 5 High Case Temperature Values, HTC Results | 5-41 |
| 5-32 | Empty Case Position Number 4, Test 5 Cool Down Test | 5-42 |
| 5-33 | Empty Case Position Number 4, Test 5 Cool Down Test, HTC Results | 5-43 |
| 5-34 | Test 1, Position 1, High Case | 5-45 |
| 5-35 | Test 1, Position 1, High Case | 5-46 |
| 5-36 | Test 1, Position 1, High Case | 5-48 |
| 5-37 | Test 1, Position 1, Low Case | 5-49 |
| 5-38 | Test 1, Position 1, Low Case | 5-50 |
| 5-39 | Test 2, Position 2, Low Case | 5-51 |
| 5-40 | Test 2, Position 2, Low Case | 5-52 |
| 5-41 | Test 2, Position 2, High Case | 5-53 |
| 5-42 | Test 2, Position 2, High Case | 5-54 |
| 5-43 | First Cycle, Position 1, Impressed Heat Conduction Run Using First Live Motor Data | 5-56 |
| 5-44 | First Cycle, Position 1, Impressed Profiles From Heat Conduction Run Using First Live Motor Data | 5-57 |
| 5-45 | Prediction From Inert Motor Data for Low Value HTC | 5-58 |
| 5-46 | Prediction From Inert Motor Data for High Value HTC | 5-59 |

ILLUSTRATIONS (Continued)


| Figure | | Page |
|---|---|---|
| 5-47 | Final Cycle Prediction for Live Motor Based Upon First Live Motor Data | 5-61 |
| 5-48 | Profiles for Final Live Motor Cycle Prediction | 5-62 |
| 6-1 | Grain Design | 6-5 |
| 6-2 | Burning Surface Area vs Web Burnback | 6-6 |
| 6-3 | Sea Level Thrust vs Time (Nominal ~ 70°F) | 6-8 |
| 6-4 | Motor Pressure vs Time (Nominal ~ 70°F) | 6-9 |
| 6-5 | Thermal Analysis Stations for Nozzle | 6-14 |
| 6-6 | Ablation Rate vs Heat Flux for Silica and Asbestos Rubber Insulation | 6-16 |
| 6-7 | Ablation Rate vs Heat Flux for Silica Cloth Phenolic Insulation | 6-17 |
| 6-8 | Thermal Properties of G-90 Graphite | 6-18 |
| 6-9 | Thermal Properties of Silica Phenolic | 6-19 |
| 6-10 | Sterilizable Motor Nozzle, Station 10-30 | 6-20 |
| 6-11 | Station 40, Throat, G-90 Graphite | 6-21 |
| 6-12 | Station 50, Aft End of Throat Insert at O-Ring | 6-22 |
| 6-13 | Sterilizable Motor Nozzle, Station 70 | 6-23 |
| 6-14 | Insulated Motor Case | 6-27 |
| 6-15 | Sterilizable Motor Case Insulation | 6-29 |
| 6-16 | Igniter Schematic Showing Location of Thermal Analysis | 6-35 |
| 6-17 | Motor Processing Chart | 6-38 |
| 6-18 | Hydrotest Assembly | 6-39 |
| 6-19 | Remote Casting Installation | 6-42 |

ILLUSTRATIONS (Continued)


| Figure | | Page |
|---|---|---|
| 6-20 | Master Inspection Plan | 6-48 |
| 6-21 | Radiographic Inspection Technique | 6-52 |
| 6-22 | X-Ray Report Graph, Part No. CO5856, S/N 0176 | 6-56 |
| 6-23 | X-Ray Report Graph, Part No. CO5856, S/N 0177 | 6-57 |

TABLES


| Table | | Page |
|---|---|---|
| 3-I | Results of Initial Screening of Polymer Lots | 3-2 |
| 3-II | Effect of Curative Ratio on Physical Properties | 3-5 |
| 3-III | Summary of Sterilizable Propellant Properties vs Batch Size | 3-7 |
| 3-IV | Propellant Constituents | 3-8 |
| 3-V | Analysis of Ammonium Perchlorate | 3-10 |
| 3-VI | Differential Scanning Calorimeter Analysis of Ammonium Perchlorate | 3-11 |
| 3-VII | Stress-Strain Characteristics of Sterilized Propellant | 3-14 |
| 3-VIII | Stress-Strain Characteristics of UTP-11439 at Elevated Temperatures | 3-15 |
| 3-IX | Propellant Density Measurements | 3-16 |
| 3-X | Evaluation of Volatile Stability for Propellant UTP-11439 | 3-16 |
| 3-XI | Evaluation of Dimensional Change for Propellant UTP-11439 | 3-17 |
| 4-I | Composition and Properties of UTL-0026 Liner | 4-3 |
| 4-II | Hitco-2820 Compound Ingredients | 4-3 |
| 4-III | Tensile Properties vs Sterilization Cycles, UTL-0026 Liner and Hitco-2820 Insulation | 4-5 |
| 4-IV | Volatile Stability — UTL-0026 Liner | 4-9 |
| 4-V | Volatile Stability — Hitco-2820 | 4-10 |
| 4-VI | Insulation-to-Titanium Peel Tests | 4-13 |
| 5-I | Results of Transient Heating and Cooling Analyses on the Propellant/Case Interface for Several Transient Variations | 5-13 |
| 6-I | Design Summary | 6-3 |
| 6-II | Drawing List | 6-4 |

TABLES (Continued)


| Table | | Page |
|---|---|---|
| 6-III | Ballistics Summary (Predicted) Nominal - Sea Level - 70°F | 6-7 |
| 6-IV | Five-Gallon Characterization Batches (UTP-11439) | 6-43 |
| 6-V | UTX-12335 Stress-Strain Properties | 6-44 |
| 6-VI | Propellant Physical Properties | 6-46 |
| 6-VII | Propellant Data - Motors No. 1 and 2 | 6-50 |
| 6-VIII | Loaded Case, Sterilizable Motor (Project 2348) P/N C05856-01-01, S/N 0176 - Motor No. 1 | 6-54 |
| 6-IX | Loaded Case, Sterilizable Motor (Project 2348) P/N C05856-01-01, S/N 0177 - Motor No. 2 | 6-55 |
| 6-X | Discrepancy Summary | 6-58 |
| 7-I | Measured Strain in Analog Motors | 7-2 |

## ABBREVIATIONS

| | |
|---|---|
| AP | ammonium perchlorate |
| BDMA | N,N-dimethylbenzyl amine |
| CTPB | carboxy-terminated polybutadiene |
| CTPIB | carboxy-terminated polyisobutylene |
| EED | electroexplosive device |
| GFE | Government-furnished equipment |
| HTC | heat transfer coefficient |
| ICC | Interstate Commerce Commission |
| ICRPG | Interagency Chemical Rocket Propulsion Group |
| ID | inside diameter |
| IDR | inspection discrepancy report |
| JANNAF | Joint Army-Navy-NASA-Air Force |
| LRC | Langley Research Center |
| LSBR | liquid strand burning rate |
| MAPO | tris [1-(2-methyl) aziridinyl] phosphine oxide |
| MEOP | maximum expected operating pressure |
| MS | military standard |
| NASA | National Aeronautics and Space Administration |
| NDT | nondestructive testing |
| OD | outside diameter |
| PBAN | polybutadiene-acrylonitrile |
| P/N | part number |
| S/N | serial number |
| UTC | United Technology Center |
| $\Delta T$ | differential temperature |
| $\epsilon_m$ | stress at maximum load |
| $S_m$ | measured strain |

# 1.0 INTRODUCTION

This is the final report documenting and summarizing the results of laboratory, subscale, and full-scale tests demonstrating the ability of a flightweight solid propellant rocket motor (exclusive of igniter and nozzle) to withstand sterilization requirements for unmanned planetary landers. The work was sponsored by the Langley Research Center, National Aeronautics and Space Administration and was performed during the period February 1969 through July 1970. Mr. M. Lucy was the NASA project engineer.

The program covered five main tasks:

A. The laboratory evaluation of a propellant, liner, and insulation before and after exposure to repeated sterilization cycling and at mission temperature extremes,

B. The design of a flightweight motor meeting specific performance requisites and capable of withstanding NASA's sterilization requirements,

C. The measurement of temperature gradients in an inert "thermal control motor" and the optimization of sterilization heatup and cooldown periods for minimum propellant thermal degradation,

D. The evaluation of inspection procedures and techniques for identifying discrepancies due to sterilization effects,

E. The thermal cycling of flightweight motors processed in a practical manner and utilizing NASA-supplied motor cases and aft closures to provide a significant demonstration of the ability of a solid propellant rocket motor to withstand sterilization requirements for interplanetary missions.

The NASA sterilization policy requires that all spacecraft for planetary landings be thermally sterilized so that the probability of contaminating a planet with viable earth organisms is very small. For this program LRC specified that each full-scale motor successfully survive six dry-heat sterilization cycles which maintain the most thermally remote point in the motor at a temperature of 275°F for 53 hr.

The most significant effects of sterilization are:

A. The degradation of propellant physical properties as the result of extended exposure to high temperature,

B. The effect of temperature on the structural integrity of bonds due to the weakening of adhesive forces and/or the migration of ingredients from contiguous surfaces.

As would be expected, these phenomena absorbed the major effort during the program.

Particular attention was given the transition from laboratory tests to prototype tests. Although emphasis was placed upon duplicating motor conditions in the laboratory, problems arose and failures occurred in full-scale tests which were neither predicted by analysis nor indicated by laboratory work.

The result was that although the CTPIB-based propellant had remarkable thermal stability and physical properties during and after sterilization cycling and although the liner and insulation displayed more than adequate physical

properties as individual components, the flightweight motors (and subsequently subscale analog motors) suffered propellant separation at or adjacent to the propellant/liner interface. When this first happened, the fault was attributed to migration of plasticizer from the insulation even though most of the plasticizer was removed prior to casting propellant. However, when the same thing occurred in analog motors with no insulation, it became apparent that the tensile and/or shear stress imposed on the system during heatup exceeded the allowable strength. This phenomena was not evident during laboratory tests and consequently was not discovered until the first full-scale motor was sterilized.

Thus the results of this study show that the ability of a solid propellant rocket motor (loaded with propellant UTP-11439) to successfully survive dry heat sterilization depends upon the high temperature strength of the bond between propellant and liner as well as the structural adequacy of the propellant. The determination of the mechanics of failure could not be made within the limitations of the contract; however, it is obvious that additional work with the propellant system is required.

The data and results are presented in accordance with the tasks previously described. Section 7.0, Supplemental Tests, describes the analog test motor work performed subsequent to propellant separation in the full-scale motor. This section contains the hypothesis for motor failure.

## 2.0 SUMMARY OF RESULTS

The propellant characterization tests conducted on this program have confirmed the results of previous work on the development of a sterilizable solid propellant motor. Propellant physical and mechanical properties are essentially not affected by dry-heat sterilization, as indicated by the results of testing after subjecting the propellant to six cycles of 53 hr per cycle at 275°F. In addition, both liner and insulation systems survived the necessary sterilization with no substantial deterioration of properties. During the first sterilization cycle the insulation sustained weight losses higher than those of the propellant or liner. However, these results had been obtained previously. As a matter of fact, the high volatility of the insulation during the first cycle was accounted for in the processing procedure by the introduction of a presterilization cycle which was designed to eliminate most of the volatiles before loading the demonstration motors.

Hazard testing, both at UTC and by the ICC, indicated a class II propellant. Autoignition time at 300°F, which is of the order of 100 hr for typical AP propellants, is at least an order of magnitude higher with sterilizable propellant.

Systems tests involving the insulation/liner/propellant system in the bond-in-tension configuration indicated acceptable properties for the system for six sterilization cycles. However, complete motor castings in 13-in. spherical demonstration motors yielded substantial debonding between liner and propellant after sterilization.

Initial efforts to eliminate this problem were based on the belief that techniques devised to eliminate volatiles and antitack agents from the Hitco-2820

insulation were not being effectively applied. However, in analog motor tests involving only propellant and UTL-0026 (a CTPB liner-insulation formulation), debonding was also experienced during sterilization. The conclusion reached from these observations is that the system failures are caused by a low high-temperature bond strength between propellant and liner. This causes the bond to fail when transient conditions impose an unfavorable combination of high-temperature tensile and/or shear stresses, upon the propellant/liner bond stress.

# 3.0 PROPELLANT CHARACTERIZATION

## 3.1 PROPELLANT DEVELOPMENT BACKGROUND

Inasmuch as the CTPIB used on this program had not had an extensive history in propellants, it was necessary to conduct a brief screening program on the available lots of polymers to select those lots which should be used for this program. In general, all of the available polymer lots had equivalent weight values in the range of 888 to 1,010 g. The polymer can be treated in a number of ways to remove low molecular weight fractions and thereby increase the equivalent weight of the polymer up to 50%. The most obvious benefit obtained by removing low molecular weight fractions is to minimize the existence of fractions tending to be volatile or migratory in the propellant at sterilization temperatures. As might be expected, the effect of polymer equivalent weight on propellant physical properties is generally to effect modest reductions in stress capability and modest increases in strain capability with increases in equivalent weight.

Table 3-I represents the results of initial screening of polymer lots in preparation for this program. The polymer samples were processed in the standard UTP-11439 composition which was developed for sterilizable applications. A curative-to-carboxyl ratio of 1.2:1 was generally used in the experimental mixes. As a part of the polymer screening process an evaluation of promising techniques for upgrading the "as-received" CTPIB polymer was conducted. This work is also included in the table 3-I.

Lot No. 50276A (equivalent weight 949 g) yielded unacceptable specimens when used with no pretreatment. Blended with lot No. DL-448 as a 1:1 or a 3:1

# TABLE 3-I

## RESULTS OF INITIAL SCREENING OF POLYMER LOTS

| Batch No. | 11,486 | 11,487 | 11,488 | 11,489 | 11,490 | 11,486A | 11,491 | 11,492 | 11,493 | 11,494 | 11,495 | 11,496 | 11,497 | 11,498 | 12,401 | 12,403 |
|---|---|---|---|---|---|---|---|---|---|---|---|---|---|---|---|---|
| Polymer Lot No. | DL-448 | 50276A | 0.5 448<br>0.5 50276A | 0.25 448<br>0.75 50276A | 50276A | DL-448 | 0-1(66) | 0-2(66) | 0-4(66) | 4-8(69) | 50276A | 50276A | 50276A | 50276A | 5 | 8 |
| Polymer Equivalent Weight, g | 983 | 949 | -- | -- | 1,595 | 983 | 980 | 1,031 | 1,000 | 1,020 | 1,027 | 1,069 | 1,020 | 1,122 | 1,001 | 888 |
| Polymer Treatment | -- | -- | -- | -- | Acetone | -- | -- | -- | -- | -- | HCl | Silica gel | Celite Filtration | HCl Silica gel | -- | -- |
| Mechanical Properties | | | | | | | | | | | | | | | | |
| Test Temperature, 76°F | | | | | | | | | | | | | | | | |
| After cure | | Cracked | | | | | | | | | | | | | | |
| Stress, psi | 123 | Cracked | 78 | 97 | 92 | 110 | 106 | 81 | 108 | 55 | 138 | 156 | 80 | 99 | 226 | 145 |
| Strain, % | 17 | Cracked | 26 | 14 | 21 | 18 | 14 | 18 | 13 | 8 | 16 | 14 | 23 | 19 | 11 | 12 |
| After six cycles at 275°F | | | | | | | | | | | | | | | | |
| Stress, psi | 206 | Cracked | 97 | 184 | 115 | 173 | 157 | 115 | 182 | 88 | 188 | 200 | 150 | 158 | 271 | 211 |
| Strain, % | 16 | Cracked | 16 | 8 | 20 | 15 | 7 | 10 | 11 | 3 | 14 | 12 | 15 | 16 | 11 | 11 |
| Test Temperature, 275°F | | | | | | | | | | | | | | | | |
| After cure | | | | | | | | | | | | | | | | |
| Stress, psi | 40 | Cracked | 32 | 28 | 22 | 53 | 28 | 15 | 47 | 19 | -- | -- | -- | -- | 63 | 44 |
| Strain, % | 14 | Cracked | 18 | 20 | 34 | 15 | 15 | 15 | 8 | 8 | -- | -- | -- | -- | 4 | 8 |

| Batch No. | 12,405 | 12,406 | 12,407 | 12,408 | 12,409 | 12,410 | 12,411 | 12,412 | 12,413 | 12,414 | 12,415 | 12,401-2 | 12,417 | 12,418 | 12,419 |
|---|---|---|---|---|---|---|---|---|---|---|---|---|---|---|---|
| Polymer Lot No. | 5 | 8 | 5 | 8 | 5 | 8 | 69-1-1 | DL-476 | 0.5 474<br>0.5 8 | 0.255 474<br>0.319 8<br>0.426 5 | 0.200 474<br>0.137 8<br>0.667 69-1-1 | 5 | Blend 2 | DL-476 | 69-1-1 |
| Polymer Equivalent Weight, g | 1,420 | 1,426 | 1,048 | 947 | 1,445 | 1,436 | 1,241 | 1,017 | -- | -- | -- | 1,001 | 1,419 | 1,529 | 1,722 |
| Polymer Treatment | Acetone | Acetone | Acid | Acid | Acetone and acid | Acetone and acid | -- | -- | -- | -- | -- | -- | Acetone | Acetone | Acetone |
| Mechanical Properties | | | | | | | | | | | | | | | |
| Test Temperature, 76°F | | | | | | | | | | | | | | | |
| After cure | | | | | | | | | | | | | | | |
| Stress, psi | 163 | 144 | 196 | 196 | 200 | 148 | No | 150 | 119 | 168 | Crumbly | 253 | 188 | 153 | Poor cure |
| Strain, % | 14 | 17 | 13 | 13 | 10 | 16 | Cure | 11 | 8 | 12 | Cure | 10 | 15 | 19 | Hard and flaky |
| After six cycles at 275°F | | | | | | | | | | | | | | | |
| Stress, psi | 273 | 251 | 306 | 320 | 236 | 286 | -- | 223 | 254 | 226 | -- | 304 | 248 | 241 | -- |
| Strain, % | 13 | 17 | 13 | 10 | 10 | 16 | -- | 11 | 13 | 9 | -- | 11 | 13 | 16 | -- |
| Test Temperature, 275°F | | | | | | | | | | | | | | | |
| After cure | | | | | | | | | | | | | | | |
| Stress, psi | 66 | 60 | 73 | 67 | 108 | 67 | -- | 50 | 52 | 63 | -- | 82 | 88 | 58 | -- |
| Strain, % | 7 | 9 | 7 | 7 | 7 | 9 | -- | 12 | 8 | 8 | -- | 5 | 8 | 13 | -- |

blend, good properties were obtained. In terms of the net change in strain capability after six sterilization cycles, lot No. DL-448 (equivalent weight 983 g) and lot No. 50276A after acetone treatment (equivalent weight 1,595 g) yielded the most acceptable properties. Other types of treatment evaluated with lot No. 50276A include (1) washing with HCl, (2) drying with silica gel, (3) filtration through celite, and (4) a combination of acid wash and drying with silica gel. Any one of these treatments resulted in an improved combination of propellant physical properties compared to specimens prepared with untreated polymer from lot No. 50276A. An increase in the polymer equivalent weight of 10% to 15% was obtained by each of these treatments. However, the acetone fractionation resulted in an equivalent weight change from 949 to 1,595 g and also resulted in the highest strain capability (20% before and after six sterilization cycles).

Two lots of polymer (lots No. 5 and 8) were formed by combining a number of smaller lots. These polymer lots were evaluated in propellant mixes, and various polymer treatments were compared. For these two polymer lots, propellant mechanical properties are relatively insensitive to the changes in equivalent weights resulting from the various polymer treatments. As an extreme example, lot No. 8 polymer with an equivalent weight of 888 g yielded the following propellant mechanical properties: $S_m$ = 145 psi after cure and 211 psi after six sterilization cycles, $\epsilon_m$ = 12% after cure and 11% after six cycles. The same polymer after acetone fractionation, which increased its equivalent weight to 1,426 g, yielded propellant with similar properties, i.e., $S_m$ = 144 psi after cure and 251 psi after sterilization and $\epsilon_m$ = 17%, both after cure and after sterilization cycling.

Table 3-I also presents data concerning the evaluation of a pilot production polymer lot, lot No. 69-1-1, and the results of attempting to upgrade lots No. 5 and 8 through blending or acetone fractionation. Polymer lot No. 69-1-1 failed to cure in propellant even when blended with other polymer lots (see batch No. 12,411) and therefore was not used further on this program. This lot may have had subnormal functionality since its equivalent weight was 1,241 g, which increased to 1,722 g after acetone fractionation. These figures indicate a probable reduction in functionality of 15% to 20% compared to other polymer lots.

After the preliminary screening of available polymer lots and a comparison of techniques for upgrading the polymer, lots No. DL-474A and DL-476 were selected for primary use on this program. Lot No. DL-474A is a blend of lots No. DL-474, 8, and 5, and was acetone fractionated subsequent to blending. The equivalent weight of lot No. DL-474A after fractionating was 1,405 g. Lot No. DL-476 was manufactured in 1969 and was subjected to acetone fractionation prior to use in characterization batches.

Essentially all of the polymer evaluation work conducted just prior to this contract was accomplished in propellant batches formulated at a curative/carboxyl equivalence ratio of 1.2. At the same time that the initial prepolymer quality screening was being done, a range of curative levels was explored. Early work with low solids loadings was generally conducted at a curative/carboxyl ratio of 1.3. After a plasticized, aluminized formulation was developed at a solids loading of 84%, the curative level was again evaluated. A series of propellants having curative/carboxyl ratios of 1.0 to 1.3 were tested. These results are presented in table 3-II. The equivalent weight of the polymer used in this series of mixes was 916 g. On the basis of the

mechanical properties obtained from these mixes, it was concluded that a curative/carboxyl ratio of 1.1 yielded the best combination of properties (UTX-10,730).

TABLE 3-II

EFFECT OF CURATIVE RATIO ON PHYSICAL PROPERTIES

| | Formulation | | | |
|---|---|---|---|---|
| | UTX-10,720 | UTX-10,726 | UTX-10,728 | UTX-10,730 |
| Total cure equivalent ratio | 1.30 | 1.20 | 1.00 | 1.10 |
| Stress, psi | | | | |
| End of cure | 189 | 190 | 69 | 121 |
| Cycle 1 | 328 | 330 | 179 | 191 |
| Strain, % | | | | |
| End of cure | 11.5 | 12.9 | 24.0 | 18.1 |
| Cycle 1 | 10.2 | 6.4 | 12.7 | 15.7 |

As can be noted from the data presented in these tables, although the general trend is to lower stress values and higher strain values as the curative level is reduced, or as the polymer equivalent weight is increased, it is nevertheless quite difficult to tailor the propellant strain capability by making adjustments in the curative level or the polymer equivalent weight. The propellant stress capability is somewhat more sensitive to these parameters so that lowering the curative level, for example, generally results in a significant reduction in stress capability and generally a very minor increase in strain capacity.

Prior to processing 5-gal. characterization batches, subscale propellant batches were processed for the purpose of anticipating the propellant characteristics resulting from the use of each polymer lot or sublot. For example, separate portions of polymer lot No. DL-476 were subjected to an acetone fractionation step at separate times resulting in sublots No. 476A and 476A-2.

The pint scale batches indicated that the untreated lot No. DL-476 (equivalent weight 1,010 g) yielded unacceptably low strain values of 11%, whereas a pint scale batch using lot No. DL-476A (equivalent weight 1,318 g) yielded strain values of 19% after cure and 16.5% after six sterilization cycles.

However, the strain capability increases as the propellant mixing scale is increased. For example (see table 3-III) in propellant batches containing polymer lot No. DL-476A, a pint propellant mix yielded strain values of 15% after cure and 13% after six sterilization cycles, a 1-gal. mix yielded strain values of 15% after cure and 11% after four sterilization cycles, and a 5-gal. mix (76 lb) yielded strain values of 22.5% after cure and 17.5% after six cycles. A similar trend is apparent in a series with a batch using polymer lot No. DL-476. Pint batches yielded strain values of 11% before and after six sterilization cycles. Comparable values for a 1-gal. mix were 13% and 13.8%, and for a 5-gal. mix the values were 21.9% and 18.2%.

A possible explanation for the effect of scaleup on strain properties is based on the fact that MAPO is an excellent wetting agent for the oxidizer and has a tendency to polymerize on the oxidizer surface. This reaction is in competition with the aziridine-carboxyl cure reaction. The cure reaction is favored at the higher cure temperatures. However, in the larger batch sizes, the propellant has a chance to cool somewhat between the time the mixing is completed and the time the propellant is cast and the specimens are moved to the cure oven. This time is minimal and the motor and casting tooling are preheated, therefore some cooldown is inevitable. Although the brief cooldown encountered due to the casting time required is not necessarily deleterious to the propellant, it complicates the problem of using mechanical property tests from small-scale mixes to predict the properties of large propellant batches.

TABLE 3-III

SUMMARY OF STERILIZABLE PROPELLANT PROPERTIES VERSUS BATCH SIZE

| Polymer Lot No. | DL-474A | DL-476 | DL-476A | DL-476A2 | DL-476A2 |
|---|---|---|---|---|---|
| Polymer Equivalent Weight, g | 1,405 | 1,010 | 1,318 | 1,566 | 1,566 |
| Curative Ratio | 1.2 | 1.2 | 1.2 | 1.2 | 1.1 |
| Pint Scale (1 lb) | | | | | |
| After cure, $S_m - \epsilon_m$ | 188-15 | 150-11 | 153-19 | -- | -- |
| After six cycles,* $S_m - \epsilon_m$ | 248-13 | 223-11 | 240-16 | -- | -- |
| One-Gallon Scale (10 lb) | | | | | |
| After cure, $S_m - \epsilon_m$ | 220-15 | 163-13 | -- | 116-16 | 81-21 |
| After one cycle, $S_m - \epsilon_m$ | 281-11 | 210-13 | -- | 142-17 | 109-18 |
| After four cycles, $S_m - \epsilon_m$ | 307-11 | 228-14 | -- | 163-17 | 112-21 |
| After six cycles, $S_m - \epsilon_m$ | -- | -- | -- | 157-15 | 123-18 |
| Five-Gallon Scale (65 lb) | | | | (10-day cure) | |
| After cure, $S_m - \epsilon_m$ | 111-22 | 114-22 | 95-22 | 115-17 | 57-22 |
| After one cycle, $S_m - \epsilon_m$ | 213-16 | 207-13 | 172-14 | -- | 53-37 |
| After two cycles, $S_m - \epsilon_m$ | -- | -- | -- | 166-14 | 28-33 |
| After five cycles, $S_m - \epsilon_m$ | -- | -- | -- | -- | 31-32 |
| After six cycles, $S_m - \epsilon_m$ | 167-17 | 202-18 | 162-20 | -- | -- |

* Each cycle represents at least 53 hr at 275°F

## 3.2 PROPELLANT CONSTITUENTS

The propellant constituents are obtained in accordance with the appropriate UTC material specifications. The following table outlines the propellant ingredients, the UTC specification number, and the function of each item.

TABLE 3-IV

PROPELLANT CONSTITUENTS

| Ingredient | Specification | Function |
|---|---|---|
| CTPIB polymer | UTC-MS-53 | Binder |
| MAPO | UTC-MS-44 | Curative |
| EPON X-801 | UTC-MS-54 | Curative |
| Plasticizer | UTC-MS-55 | Plasticizer |
| Uteflo A-2 | UTC-MS-50 | Surfactant and stabilizer |
| Antioxidant | UTC-MS-56 | Antioxidant |
| Aluminum Powder | UTC-MS-8 | Fuel |
| AP | UTC-MS-57 (Pureox grade) | Oxidizer |

The ingredients used during this program were either from the same lot used during preprogram development or were procured to the same material specification and functionally qualified in a number of laboratory and pilot-scale propellant batches. The polymer which was one of the most critical items used was sampled extensively. The equivalent weight of each lot, each sample, and in fact each container of polymer was obtained prior to and subsequent to any treatment of the polymer. In addition, 1-lb propellant mixes were made

from all polymer lots. These batches were subjected to uniaxial constant strain rate tensile tests after cure and after exposure to six sterilization cycles (53 hr at 275°F). Those polymer lots selected for use on this program were also evaluated in 10-lb (1-gal.) propellant batches.

The aziridine curative, MAPO, is a standard ingredient issued from UTC stores following acceptance testing detailed in specification UTC-MS-44. This lot has also been used in essentially all of the small-scale propellant batches. The epoxy curative, EPON X-801, was manufactured by Shell Chemical Co. for UTC, and all work done at UTC with EPON X-801 was from the same lot. The plasticizer and the surfactant, Uteflo A-2, used on this program were also from single lots and had been functionally confirmed prior to this contract. The lot of aluminum powder used is from a production lot which had received the full range of acceptance testing.

The AP was purchased specifically for this program per specification UTC-MS-57. The certificate of analysis indicates that this lot (No. 69014 HP) generally exceeds all of the requirements except that the pH of the aqueous solution (4.9) is slightly below the desired minimum of 5.5. However, all of the data obtained on this lot indicate that it should be a very thermally stable material. The chemical analysis and the particle size aralysis are presented in table 3-V.

A differential scanning calorimeter analysis was conducted at UTC on this lot. This test indicated a thermally stable material. The results of the analysis are presented in table 3-VI.

TABLE 3-V

ANALYSIS OF AMMONIUM PERCHLORATE

(Lot UTC-69014 HP)

| | Analysis* | Specification UTC-MS-57 Minimum | Maximum |
|---|---|---|---|
| Perchlorate as $NH_4ClO_4$, % | 99.7 | 98.7 | -- |
| Total moisture, % | 0.040 | -- | 0.06 |
| pH of aqueous solution | 4.9 | 5.5 | 6.5 |
| Water insolubles, % | 0.01 | -- | 0.15 |
| Sulfated ash, % | 0.01 | -- | 0.45 |
| Bromates as $NaBrO_3$, % | 0.001 | -- | 0.004 |
| Chlorate as $NaClO_3$, % | 0.01 | -- | 0.0035 |
| Chlorides as $NH_4Cl$, % | 0.01 | -- | 0.15 |
| Sodium, ppm | 8 | -- | -- |
| Potassium, ppm | 8 | -- | 50.0 |

Sieve Analysis

| Tyler Sieve No. | Opening, | Pacific Engineering Data, % | UTC Data % |
|---|---|---|---|
| 16 | 991 | 0 | -- |
| 48 | 295 | 8 | 3.2 |
| 65 | 208 | 34 | -- |
| 80 | 175 | -- | 47.8 |
| 100 | 147 | 74 | 63.8 |
| 150 | 104 | -- | 87.8 |
| 200 | 74 | 98 | 96.3 |
| 270 | 53 | -- | 98.6 |
| 325 | 43 | 100 | 99.2 |

* Certificate of analysis from Pacific Engineering

TABLE 3-VI

DIFFERENTIAL SCANNING CALORIMETER ANALYSIS* OF AMMONIUM PERCHLORATE

(Lot No. UTC 69014 HP)

| Run No. | Sample Weight, mg | Endotherm | Exotherm Onset, °C | Gas Evolution Onset, °C | Percent Weight Loss to 316°C |
|---|---|---|---|---|---|
| 1 | 22.0 | Normal | 293 | 301 | 3.18 |
| 2 | 18.8 | Normal | 295 | 303 | 3.54 |

* Analysis by UTC at 10°C/min heating rate

## 3.3 PROPELLANT PHYSICAL AND BALLISTIC PROPERTIES

### 3.3.1 Strand Burning Rates

Propellant linear burning rates versus pressure were measured in a strand bomb. Specimens from two separate 5-gal. propellant mixes were tested. Specimens subjected to the sterilization process were cycled as block propellant and then cut to individual strands at the conclusion of sterilization. Three strands were tested at each condition. The data are presented in figures 3-1 and 3-2. Good reproducibility between sterilized and unsterilized specimens was obtained. In each batch the sterilized specimens had very slightly reduced burning rates compared to nonsterilized propellant, although the reduction in burning rate was somewhat less than 3% in each case. Batch No. 1 yielded a burning rate of 0.21 in./sec at 1,000 psia compared to 0.19 in./sec for batch No. 2. A pressure exponent of approximately 0.25 was obtained for both mixes above 75 psia, increasing to about 0.7 below 75 psia.

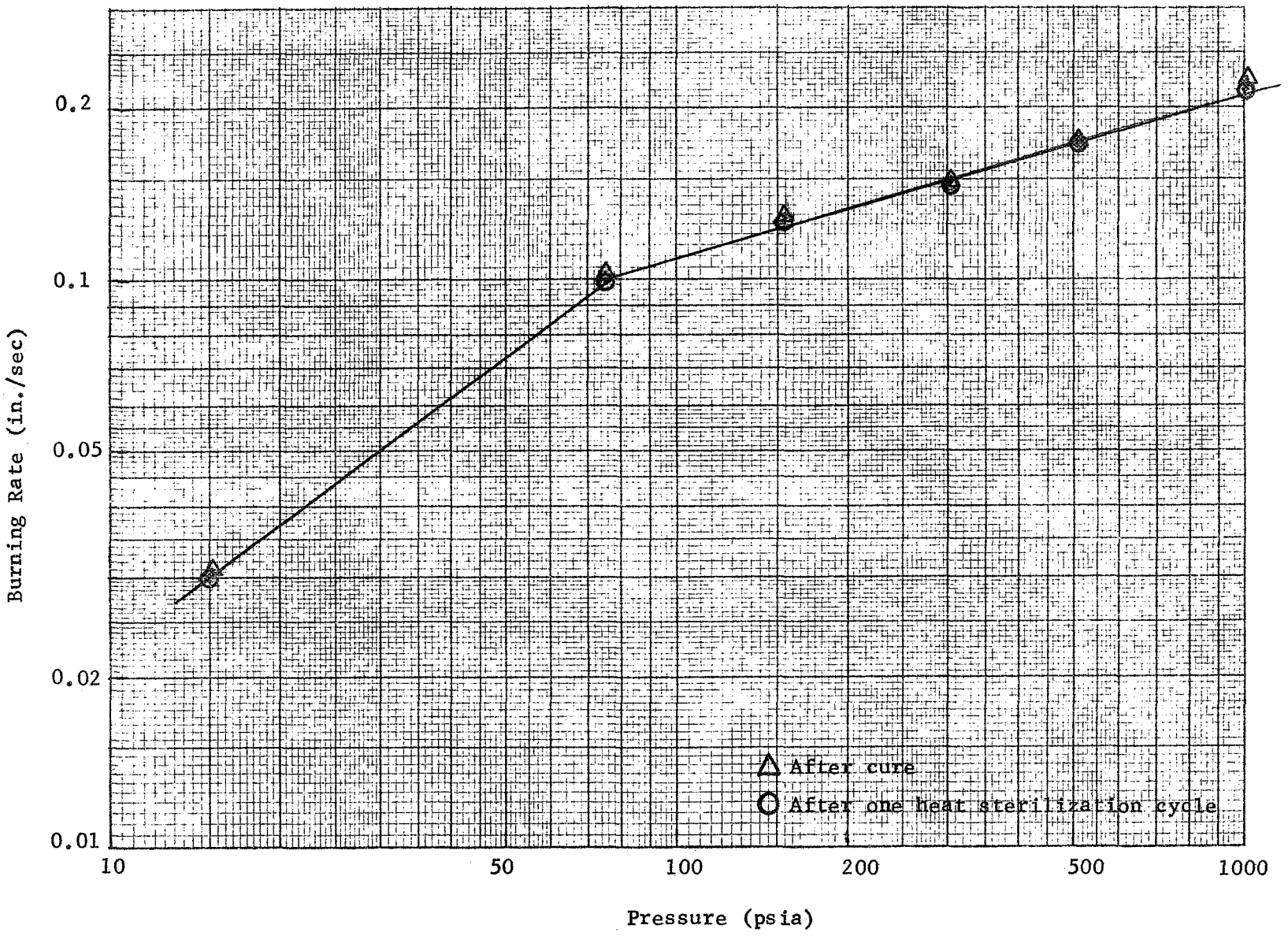


Figure 3-1. Strand Burning Rate vs Pressure - UTP-11439-5/1

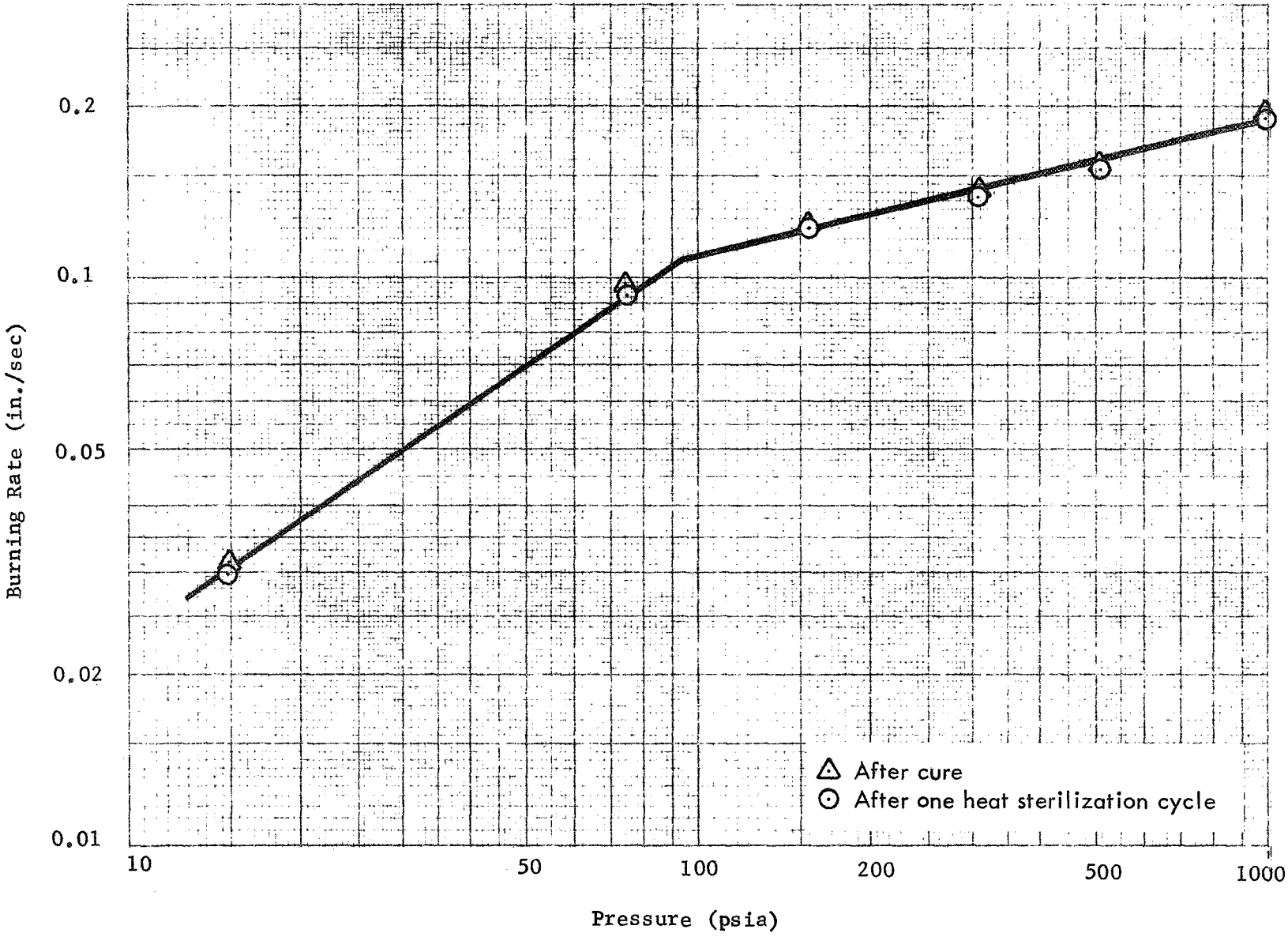


Figure 3-2. Strand Burning Rate vs Pressure - UTP-11439-5/2

3.3.2 Stress-Strain Characteristics of Propellants for Demonstration Motors

To demonstrate stress-strain characteristics for propellant batches planned for processing and loading into spherical demonstration motors under specification NAS 1-8937, a series of mixes was processed and tested using current lots of ingredients.

Stress-strain data were obtained for the candidate propellant at a crosshead speed of 2 in./min at 70° to 80°F and at 250°F after exposure to one and six sterilization cycles of 53 hr at 275°F. To avoid skin effects, the propellant was subjected to the sterilization environment in the form of 1 in. by 3 in. by 5 in. slabs and then machined to the appropriate configuration for testing.

The initial characterization was conducted on two 5-gal. propellant batches. A third characterization batch included stress-strain data after nine sterilization cycles, and in addition was used for obtaining stress-strain data at additional temperature points. The data for these propellant batches are included in tables 3-VII and 3-VIII.

TABLE 3-VII

STRESS-STRAIN CHARACTERISTICS OF STERILIZED PROPELLANT

| Number of Cycles | Temperature (°F) | UTP-11439-5/1 Stress (psi) | UTP-11439-5/1 Strain (%) | UTP-11439-5/2 Stress (psi) | UTP-11439-5/2 Strain (%) | UTP-11439-5/3 Stress (psi) | UTP-11439-5/3 Strain (%) |
|---|---|---|---|---|---|---|---|
| 0 | 75 | 111 | 22.5 | 114 | 21.9 | 94 | 22.4 |
| | 250 | 69.7 | 13.2 | 52.8 | 16.4 | 49.7 | 18.1 |
| 1 | 75 | 213 | 16.5 | 207 | 12.5 | 172.7 | 14.5 |
| | 250 | 85.4 | 13.9 | 92.2 | 15.0 | -- | -- |
| 3 | 75 | 179 | 15.3 | -- | -- | -- | -- |
| 6 | 75 | 167 | 19.3 | 202 | 18.2 | 162 | 19.6 |
| | 250 | -- | -- | 50.4 | 15.7 | 50.9 | 17.7 |
| 9 | 75 | -- | -- | -- | -- | 91.5 | 20.3 |
| | 250 | -- | -- | -- | -- | 28.5 | 20.9 |

TABLE 3-VIII

STRESS-STRAIN CHARACTERISTICS OF UTP-11439
AT ELEVATED TEMPERATURES
(UTP-11439-5/3)

| Test Temperature (°F) | Stress (psi) | Strain (%) |
|---|---|---|
| 75 | 95 | 22.4 |
| 225 | 72 | 11.0 |
| 250 | 50 | 18.1 |
| 275 | 57 | 15.1 |
| 300 | 51 | 14.1 |

Inasmuch as the spherical demonstration motors are exposed to 300°F during the programmed heatup portion of the sterilization cycle, the outer periphery of the propellant grain is exposed to temperatures in excess of 250°F. The data in table 3-IX indicate that no substantial degradation of propellant mechanical properties is experienced during the heatup step.

### 3.3.3 Propellant Density

Density measurements were made on the same two propellant batches characterized for strand burning rates and stress-strain properties. Measurements taken after cure and after the propellant was subjected to six sterilization cycles indicated a density increase of 0.3% to 0.5% as a result of the sterilization. The data are presented in table 3-IX.

TABLE 3-IX

PROPELLANT DENSITY MEASUREMENTS

| | UTP-11439-5/1 | UTP 11439-5/2 |
|---|---|---|
| Initial | 1.717 g/cc | 1.723 g/cc |
| Six cycles | 1.722 g/cc | 1.732 g/cc |
| Density change | +0.3% | +0.5% |

3.3.4 Propellant Volatile Stability and Dimensional Stabilities

Four 1-in. propellant cubes from each of three 5-gal. batches were subjected to six sterilization cycles and evaluated for weight loss as a result of propellant volatility. The samples were sealed in nitrogen during sterilization to minimize the possibility of degradation by atmospheric moisture or oxygen. A total of 12 cubes had an average weight loss of less than 0.06% after one sterilization cycle and a loss of approximately 0.22% after six cycles at 275°F. The data are presented in table 3-X.

TABLE 3-X

EVALUATION OF VOLATILE STABILITY
FOR PROPELLANT UTP-11439

(1-In. Propellant Cubes, 275°F for 53 Hr)

| Number of Cycles | Weight Loss, % | | | | | | | | | | | |
|---|---|---|---|---|---|---|---|---|---|---|---|---|
| | Batch 5/1 | | | | Batch 5/2 | | | | Batch 5/3 | | | |
| 1 | 0.4 | 0.4 | 0.4 | 0.4 | 0.11 | 0.06 | 0.06 | 0.08 | 0.05 | 0.04 | 0.06 | 0.05 |
| 6 | 0.21 | 0.20 | 0.18 | 0.22 | 0.30 | 0.23 | 0.24 | 0.27 | 0.21 | 0.20 | 0.20 | 0.24 |

In addition to the volatile stability tests, the cubes were measured dimensionally with a micrometer in all three axes to determine the dimensional stability of the propellant after one and six sterilization cycles. The changes in dimensions for all 12 cubes after one sterilization cycle ranged from 0.1% to 0.8% with an average change of 0.28%. Little additional change occurred after five more sterilization cycles, and the final average increase in dimensions after six cycles was 0.22%. The individual results are presented in table 3-XI.

TABLE 3-XI

EVALUATION OF DIMENSIONAL CHANGE
FOR PROPELLANT UTP-11439

(1-In. Propellant Cubes, 275°F for 53 Hr)

| Number of Cycles | Dimensional Grain (Loss), % | | | | | | | | | | | |
|---|---|---|---|---|---|---|---|---|---|---|---|---|
| | Batch 5/1 | | | | Batch 5/2 | | | | Batch 5/3 | | | |
| 1 | (0.3) | 0.4 | 0.3 | 0.2 | 0.3 | 0.1 | 0.1 | 0.8 | (1.1) | 0.3 | 0.1 | 0.6 |
| 6 | 0.2 | 0.3 | 0.2 | 0.3 | 0.1 | (0.1) | 0.1 | 0.5 | 0.1 | 0.2 | 0.2 | 0.3 |

# 4.0 LINER/INSULATION EVALUATION

## 4.1 LINER AND INSULATION DEVELOPMENT BACKGROUND

The development of the liner for this program was based on its compatibility with the CTPIB propellant system and its ability to bond to that propellant system and to the insulation after extended high temperature exposure. An additional important consideration is the absence of volatile materials which might be exuded from the liners during the six heat sterilization cycles.

The UTL-0026 liner formulation is based on a CTPB prepolymer cured with a mixed aziridine/epoxy curative similar to that of the propellant. It contains carbon black and resin-grade asbestos as reinforcing and insulating fillers. Extensive in-house development and evaluation studies with a wide variety of candidate liner prepolymers, demonstrated that the bonding characteristics of the CTPB liner are superior to those of CTPIB liners.

Adhesion of the liner to insulation and propellant was measured in bond-in-tension tests. Samples of steel, insulation, liner, and propellant were sandwiched between steel plates, repeat sterilization cycled, and then pulled to simulate motor conditions. Data from one test series through nine heat sterilization cycles was obtained.

In addition, shear tests were used to supplement the quantitative results from the bond-in-tension measurements. The liner-to-propellant shear was determined with a sandwich apparatus composed of steel, liner, propellant, liner, and steel. Shear tests using liner UTL-0026 and propellant UTP-11439 have been conducted at -65°, +75°, and +160°F. The mode of the failure was consistently in the propellant.

Failure in both the shear and bond-in-tension tests was consistently in the propellant, demonstrating that the liner/propellant bond is stronger than the propellant. Since the allowable strength of the propellant is the design criteria, this type of failure indicates system acceptability.

The liner was also evaluated for 470 hr at a temperature of 275°F and short-term tested at temperatures up to 500°F. In both cases strength at temperature was well above design allowables.

Liner UTL-0026 was subjected to nine 53-hr cycles at 275°F in the form of ICRPG tensile specimens. The stress values exceeded those of propellant UTP-11439 throughout the temperature range of 75° to 300°F by a factor of three. The strain values through six sterilization cycles are similar to those of UTP-11439 propellant. These results were all presented and discussed in UTC technical proposal 68-95 dated 23 December 1968.

A butyl rubber containing 45% silica-asbestos (Hitco-2820) had been selected for this program because of low weight loss (i.e., low weight-percent plasticizer) and overall superiority in erosion resistance and physical properties after being thermally cycled. During this program two important observations were made of factors which could have had serious reliability effects: (1) the type of tackifier and the manner in which it was applied could result in debonding during sterilization and (2) the manner in which the volatiles were driven off during the insulation pretreatment. These factors led to selection of a compatible tackifier and a manufacturing procedure which assured removal of the tackifier and liberated plasticizer during the pretreatment process.

## 4.2 LINER AND INSULATION CONSTITUENTS

The liner constituents are obtained in accordance with the appropriate UTC material specification. Table 4-I outlines the liner ingredients, the UTC specification number, the function of each item, and the liner processing properties.

TABLE 4-I

COMPOSITION AND PROPERTIES OF UTL-0026 LINER

| | Specification | Function |
|---|---|---|
| CTPB polymer | UTC MS-48 | Binder |
| MAPO | UTC MS-44 | Curative |
| ERL-0510 | UTC MS-3? | Curative |
| Glycerol | UTC MS-59 | Modifier |
| BDMA | UTC MS-16 | Catalyst |
| Elftex-5, carbon | UTC MS-10 | Reinforcement |
| Asbestos, resin, grade 144 (Union Carbide) | UTC MS-58 | Insulator |

Processing and Physical Properties

| | |
|---|---|
| Gel time at 160°F | 4 hr |
| Cure time at 160°F | 20 hr |
| Active life at 160°F | 2 days |
| Active life at 75°F after 4 hr precure at 160°F | 3 weeks |
| Active life at 75°F (no precure) | 3 weeks |

The percent by weight of the insulation constituents as certified by the insulation supplier are given in table 4-II.

TABLE 4-II

HITCO-2820 COMPOUND INGREDIENTS

| Ingredients | Percent by Weight |
|---|---|
| Isobutylene-isoprene rubber | 45 |
| Hydrated silica | 20 |
| Asbestos fibers | 25 |
| Curing agents and processing aids | 10 |

## 4.3 PROGRAM EVALUATION TESTS FOR LINER AND INSULATION

### 4.3.1 Liner and Insulation Tensile Properties

A test program was conducted to evaluate the effect of heat sterilization cycling upon the physical and mechanical properties of the liner and insulation materials to be used in the sterilizable solid rocket motor. In addition, the compatibility of the propellant/liner/insulation combination was evaluated. Three liner samples 1/2-in. thick and 6 in. wide by 12 in. long (of sufficient size to obtain 10 ICRPG, class C tensile test specimens) were prepared. One sample was cut into 10 ICRPG class C tensile test specimens. Five specimens were tested for tensile strength and elongation at 70° to 80°F and five were tested at 250°F.

The two remaining samples were placed in an oven and subjected to heat sterilization cycling. One sample was removed after one cycle (53 hr at 275°F) and the other after six cycles. Ten specimens were prepared from each sample and subjected to stress-strain testing at 70° to 80°F and at 250°F. The liner tests confirmed previous in-house tests which indicated that the liner physical properties were more than adequate.

Three insulation samples 1/2-in. thick and 6 in. wide by 12 in. long were prepared from stock obtained from the motor insulation supplier using the same process as that used in fabricating insulation for the motor cases. These samples were subjected to the same schedule of sterilization and testing as the liner samples except that the insulation was subjected to one additional cycle corresponding to the step required for motor processing to eliminate the major source of volatiles prior to casting propellant. The test results for both the liner and insulation are presented in table 4-III.

TABLE 4-III

TENSILE PROPERTIES VERSUS STERILIZATION CYCLES
UTL-0026 LINER AND HITCO-2820 INSULATION

| | Cycles at 275°F | Stress, psi | | Strain, % | |
|---|---|---|---|---|---|
| | | 70° to 80°F | 250° to 10°F | 70° to 80°F | 250° to 10°F |
| UTL-0026 liner | 0 | 867 | 443 | 70.6 | 38.6 |
| | 1 | 1,177 | 756 | 27.9 | 15.1 |
| | 6 | 882 | 430 | 47.7 | 22.4 |
| Hitco-2820 insulation | 0 | 1,216 | 500 | 30.1 | 36.7 |
| | 1 | 1,805 | 885 | 23.1 | 20.0 |
| | 7 | 1,761 | 1,012 | 11.9 | 11.0 |

4.3.2 Volatile Stability of Liner and Insulation

Three liner specimens and three insulation specimens approximately 1/2-in. thick and 4 in. in length and width were prepared. On each specimen a 3.5-in. square was scribed as shown in figure 4-1. The scribe lines were such that the distance between the lines could be accurately measured (within ± 0.010 in.) before and after heat sterilization cycling.

Each of the specimens were weighed to the nearest 0.01 g and three Shore A hardness readings were taken on the smoothest side of each specimen. The distance between the scribe lines on each specimen was measured to the nearest 0.01 in. at three places approximately equally spaced as shown in figure 4-2. On the insulation specimens, the scribe line measurements were taken with the grain and across the grain. Measurements were taken before the specimens were exposed to sterilization cycling and after they had been exposed to one, two, four, and six sterilization cycles. The specimens were allowed to cool to room temperature (70° to 80°F) after cycling prior to taking the

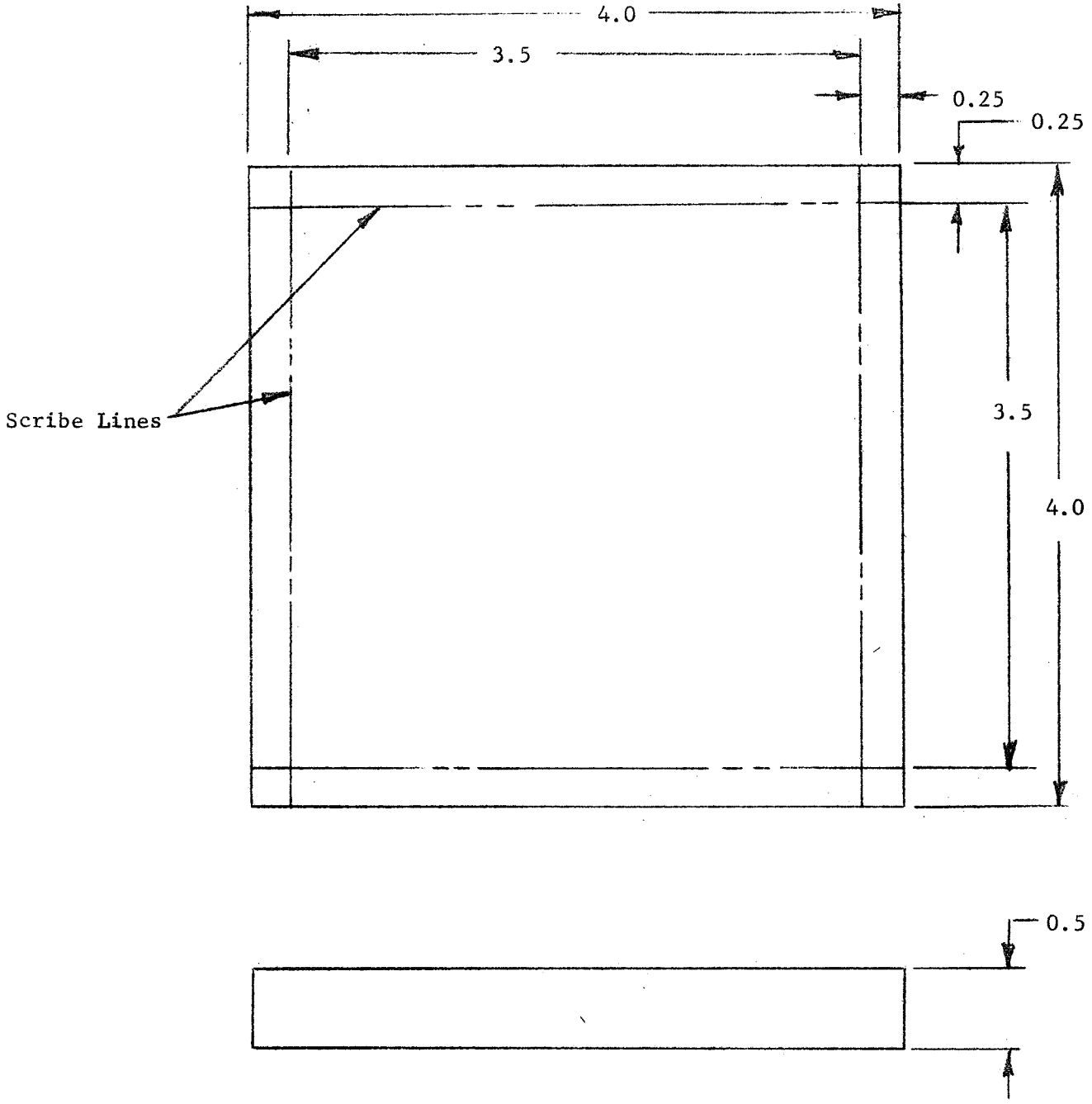


NOTE: All dimensions are in inches.

Figure 4-1. Volatile Stability Test Specimen

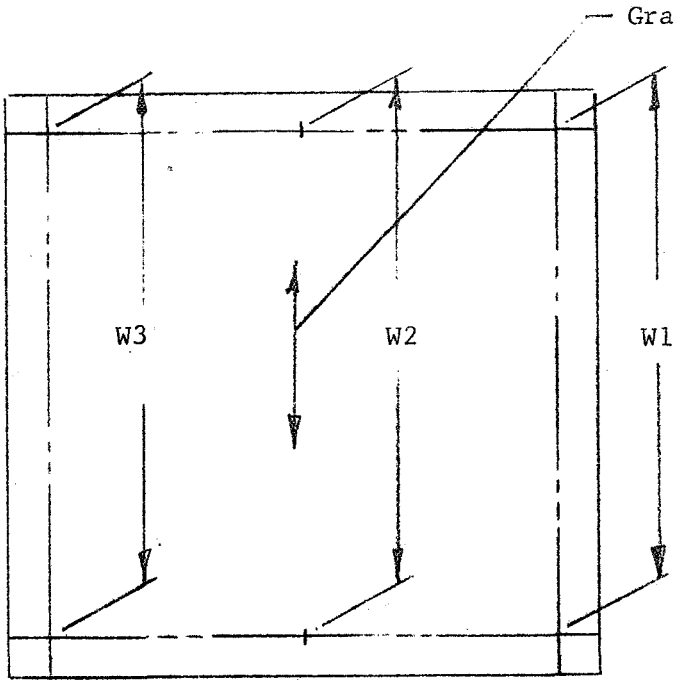


With Grain Measurements

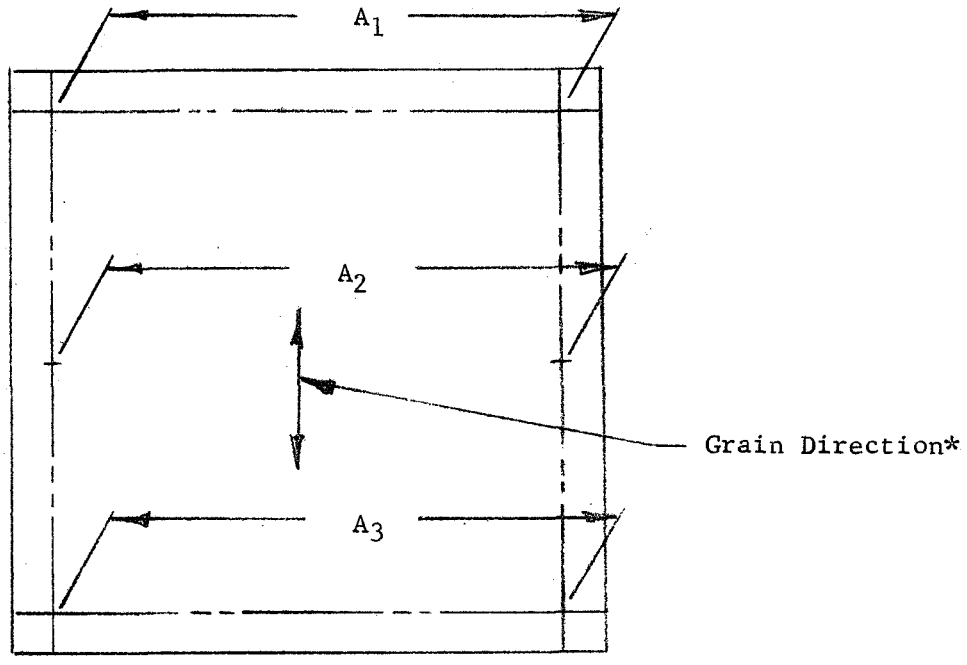


Across Grain Measurements

* Grain direction applies only to the insulation specimens

Figure 4-2. Measurement of Distance Between Scribe Lines On Volatile Stability Test Specimens

measurements. The volatile stability measurements of the liner and the insulation, as determined by dimensional change, weight loss, and change in hardness are presented in tables 4-IV and 4-V. It is apparent from these results that the insulation experiences its greatest weight loss during the first sterilization cycle and that the total weight loss for the insulation is considerably greater than that for either the liner or the propellant.

Figure 4-3 compares the weight loss as a function of the number of heat sterilization cycles for the propellant, liner, and insulation. It is apparent that the rate of weight loss for the insulation is twice as great as for the propellant, even after the first sterilization cycle has been completed.

### 4.3.3 Insulation-to-Titanium Peel Tests

Insulation-to-titanium peel tests were conducted on samples furnished by the motor insulation supplier to evaluate the adequacy of the bond at the case/insulation interface. The samples were prepared to the same specifications as those used to insulate the spherical motor cases except that the titanium sheet was not grit blasted. The titanium was cleaned with toluene, followed by a caustic-free detergent wash and distilled water rinse. The Hitco-2820 was bonded to the titanium, using Chemlok 205 primer and Chemlok 234 adhesive.

The samples were fabricated in 6-in. by 12-in. sections by the supplier. At UTC the samples were cut into 1-in.-wide strips for sterilization and testing. One set of nine specimens was tested prior to sterilization as a control. One set was tested after one sterilization cycle and another set after seven sterilization cycles at 275°F. Within each set three specimens were tested at each of three temperatures, 0°, 76°, and 254°F. All specimens were tested at a pull rate of 5 in. per minute. It is apparent that the sterilization environment does effect the case/insulation interface although

TABLE 4-IV

VOLATILE STABILITY - UTL-0026 LINER

| Specimen | Distance Between Lines | | Initial Value | Number of Cycles | | | |
|---|---|---|---|---|---|---|---|
| | | | | One | Two | Four | Six |
| A | E-W | 1 | 3.51 | 3.51 | 3.51 | 3.50 | 3.51 |
| | | 2 | 3.50 | 3.50 | 3.49 | 3.49 | 3.50 |
| | | 3 | 3.49 | 3.50 | 3.49 | 3.49 | 3.50 |
| | N-S | 1 | 3.46 | 3.48 | 3.46 | 3.45 | 3.46 |
| | | 2 | 3.49 | 3.48 | 3.48 | 3.47 | 3.48 |
| | | 3 | 3.49 | 3.50 | 3.50 | 3.49 | 3.49 |
| B | E-W | 1 | 3.51 | 3.52 | 3.51 | 3.51 | 3.51 |
| | | 2 | 3.51 | 3.52 | 3.51 | 3.51 | 3.51 |
| | | 3 | 3.51 | 3.52 | 3.51 | 3.51 | 3.51 |
| | N-S | 1 | 3.51 | 3.50 | 3.50 | 3.50 | 3.50 |
| | | 2 | 3.52 | 3.51 | 3.51 | 3.50 | 3.50 |
| | | 3 | 3.50 | 3.51 | 3.50 | 3.51 | 3.51 |
| C | E-W | 1 | 3.52 | 3.51 | 3.50 | 3.51 | 3.51 |
| | | 2 | 3.52 | 3.51 | 3.50 | 3.51 | 3.51 |
| | | 3 | 3.51 | 3.52 | 3.51 | 3.51 | 3.51 |
| | N-S | 1 | 3.51 | 3.51 | 3.50 | 3.50 | 3.50 |
| | | 2 | 3.52 | 3.51 | 3.52 | 3.51 | 3.51 |
| | | 3 | 3.54 | 3.54 | 3.53 | 3.53 | 3.53 |
| | | | | Specimen Weight, g | | | |
| A | | | 139.81 | 139.81 | 139.76 | 139.72 | 139.64 |
| B | | | 150.42 | 150.48 | 150.46 | 150.42 | 150.33 |
| C | | | 144.43 | 144.44 | 144.44 | 144.38 | 144.26 |
| | | | | Shore A-2 Hardness | | | |
| A | | | 86 | 87 | 87 | 87 | 88 |
| B | | | 88 | 89 | 89 | 89 | 88 |
| C | | | 89 | 89 | 88 | 88 | 88 |

TABLE 4-V

VOLATILE STABILITY - HITCO-2820

| Specimen | Distance Between Lines | | Initial Value | Number of Cycles | | | |
|---|---|---|---|---|---|---|---|
| | | | | One | Two | Four | Seven |
| A | Across grain | 1 | 3.51 | 3.48 | 3.47 | 3.47 | 3.48 |
| | | 2 | 3.51 | 3.48 | 3.47 | 3.47 | 3.47 |
| | | 3 | 3.50 | 3.47 | 3.47 | 3.47 | 3.47 |
| | With grain | 1 | 3.52 | 3.51 | 3.51 | 3.49 | 3.50 |
| | | 2 | 3.51 | 3.51 | 3.50 | 3.49 | 3.50 |
| | | 3 | 3.50 | 3.50 | 3.50 | 3.49 | 3.49 |
| B | Across grain | 1 | 3.49 | 3.47 | 3.46 | 3.46 | 3.46 |
| | | 2 | 3.50 | 3.47 | 3.47 | 3.46 | 3.46 |
| | | 3 | 3.49 | 3.47 | 3.46 | 3.46 | 3.46 |
| | With grain | 1 | 3.50 | 3.49 | 3.49 | 3.48 | 3.47 |
| | | 2 | 3.50 | 3.49 | 3.48 | 3.48 | 3.47 |
| | | 3 | 3.50 | 3.49 | 3.48 | 3.48 | 3.47 |
| C | Across grain | 1 | 3.48 | 3.46 | 3.46 | 3.46 | 3.45 |
| | | 2 | 3.49 | 3.47 | 3.46 | 3.45 | 3.45 |
| | | 3 | 3.50 | 3.47 | 3.47 | 3.46 | 3.45 |
| | With grain | 1 | 3.48 | 3.47 | 3.45 | 3.46 | 3.46 |
| | | 2 | 3.48 | 3.47 | 3.47 | 3.48 | 3.48 |
| | | 3 | 3.50 | 3.51 | 3.50 | 3.49 | 3.49 |
| | | | | Specimen Weight, g | | | |
| A | | | 158.22 | 156.10 | 155.96 | 155.61 | 155.29 |
| B | | | 155.35 | 153.21 | 153.06 | 152.71 | 152.36 |
| C | | | 150.78 | 148.61 | 148.49 | 148.16 | 147.81 |
| | | | | Shore A-2 Hardness | | | |
| A | | | 73 | 82 | 84 | 85 | 86 |
| B | | | 76 | 85 | 85 | 86 | 88 |
| C | | | 76 | 83 | 86 | 87 | 87 |

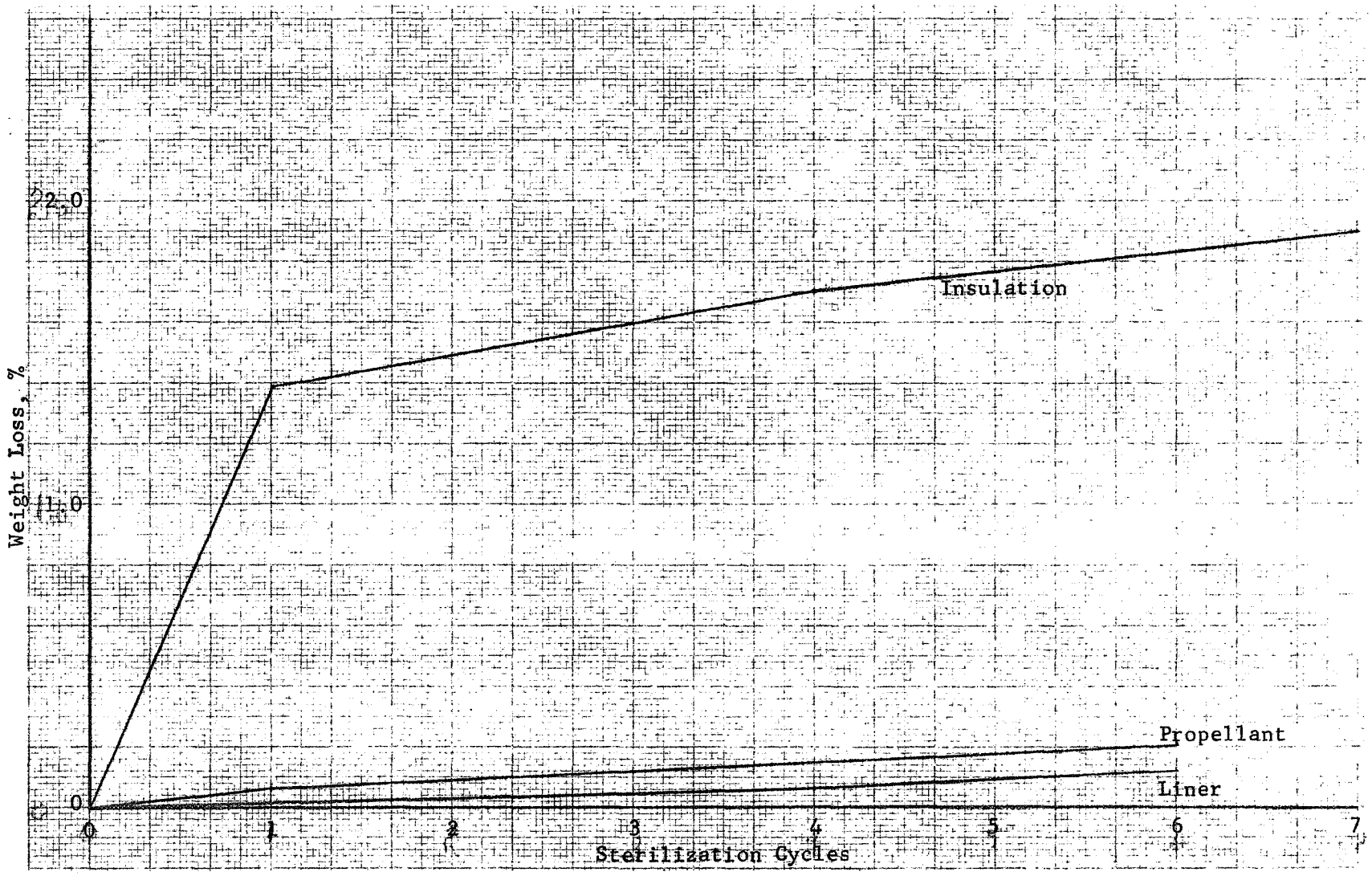


Figure 4-3. Weight Loss vs Sterilization Cycles

the relatively low numbers obtained at the elevated temperature are primarily the result of flexing the insulation material through a rather small radius to achieve the 180° required by the test. The test results were considered satisfactory and are presented in table 4-VI.

## 4.4 SUPPLEMENTAL DEVELOPMENT ACTIVITIES ON LINER AND INSULATION

The specific liner and insulation evaluation tests required for this program were successfully conducted. The results are presented in section 4.3. The tests described include tensile testing, volatile stability, and peel tests. In spite of the extensive background of laboratory scale testing of insulation, liner, and propellant (individually and in combination with one another), substantial debonding between insulation and propellant was observed in both small-scale and demonstration motors.

Several factors are involved, the two of greatest concern being (1) migration of materials from the insulation through the liner and into the propellant causing loss of bond strength near the propellant/liner interface and (2) the bond strength of propellant to liner during sterilization. Another factor may be the loss of propellant strength at sterilization temperatures when propellant is loaded at very low strain rates.

Prior experience with this type of insulation system indicated the possibility that the type of tackifiers typically used in these systems were potentially harmful to propellant/liner bond strength if such materials were able to migrate to the bond area.

Chemical characterization was conducted from vacuum oven condensate and volatile materials recovered from diced, vulcanized Hitco-2820 insulation by heating at 275°F for 48 hr at a pressure of 1 torr. Infrared spectroscopy and thin-layer chromatography of the materials revealed the presence of methyl

TABLE 4-VI

INSULATION-TO-TITANIUM PEEL TESTS

Results in Pounds/Inch Width
(Pull Rate 5 in./min)

| Test Temperature (°F) | 0 Cycle | | | 1 Cycle | | | 7 Cycles | | |
|---|---|---|---|---|---|---|---|---|---|
| | Average | Maximum | Minimum | Average | Maximum | Minimum | Average | Maximum | Minimum |
| 76 | 38.6 | 47.7 | 29.3 | 30.9 | 35.0 | 23.2 | 30.6 | 33.5 | 24.0 |
| | 26.4 | 43.5 | 17.6 | 37.4 | 43.6 | 31.1 | 14.4 | 16.7 | 12.4 |
| | 40.1 | 49.3 | 31.8 | 33.5 | 39.2 | 30.1 | 27.7 | 32.0 | 20.0 |
| | 35.0 | | | 33.9 | | | 24.2 | | |
| 0 | 63.2 | 71.8 | 54.7 | 59.5 | 71.0 | 45.3 | 14.6 | 33.7 | 10.3 |
| | 60.4 | 68.8 | 47.6 | 65.7 | 75.7 | 57.0 | 26.4 | 38.2 | 19.2 |
| | 73.8 | 81.5 | 69.8 | 57.4 | 70.5 | 37.7 | 64.3 | 67.0 | 63.4 |
| | 65.8 | | | 60.9 | | | 35.1 | | |
| 254 | 13.5 | 16.3 | 8.4 | 14.0 | 16.2 | 8.5 | 5.1 | 6.3 | 4.8* |
| | 11.7 | 13.3 | 7.9 | 12.2 | 14.6 | 9.9 | 9.5 | 10.2 | 9.1* |
| | 10.9 | 12.8 | 6.9 | 12.0 | 14.4 | 7.9 | 6.4 | 7.5 | 4.2* |
| | 12.0 | | | 12.7 | | | 7.0 | | |

*Mode of failure was tearing of insulation, not bond peel

hydroxystearate (Paracin 1), a hydrocarbon extender oil (plasticizer) and, possibly, an antioxidant. The presence of methyl hydroxystearate, a common antitack or mold release agent for butyl rubbers, was confirmed during discussions with Hitco.

Paracin 1 is commonly used as an antitack or mold release agent for butyl rubber compositions. Its effectiveness probably stems from its insolubility in the saturated polymer. Thus, methyl hydroxystearate tends to bleed to the surface of the composition and exert an effect greatly in excess of that expected on the basis of concentration in the formulation. Since the polymer backbones of butyl rubber and Utrez (CTPIB) binder are essentially identical, methyl hydroxystearate can be expected to impair bonding of Utrez propellant to any substrate. Qualitative laboratory tests have shown that application of the vacuum oven condensate to UTL-0026 liner inhibits bonding to UTP-11439 propellant.

Although their presence in the insulator has not been established, two other materials commonly used in butyl rubber processing are known to impair the tensile properties of Utrez propellant. These are stearic acid and zinc stearate. Stearic acid competes with the prepolymer in reaction with the crosslinking agents. Being monofunctional, stearic acid degrades the resulting crosslinked polymer network by production of sterile branches. Zinc stearate interferes with the cure reactions by a process which is not yet understood.

A modified Hitco-2820 insulation was prepared in which these potentially noxious ingredients were omitted. This insulation was bonded into analog motor cases and then lined with UTL-0030 (contains 10% asbestos). UTP-11439 propellant was cast and cured in these motors. After cure and one sterilization cycle, debonding at the propellant/liner interface was evident by X-ray analysis. This

insulation did not receive a heat sterilization cycle prior to propellant addition because the harmful ingredients had been eliminated.

Additional analog motors were insulated with modified Hitco-2820 and put into the heat sterilization cycle prior to lining and propellant casting. Debonding between the case and the insulation occurred. Formation of large blisters in the insulation indicated that the insulation supplier had not properly installed the insulation. Sufficient time was not available to have additional motors insulated and tested.

Concurrent with testing of the modified Hitco-2820 insulation system, a series of processing parameters were investigated by bond-in-tension tests. The test series included variations in insulation pretreatment, solvent used for wiping insulation, drying time, and liner thickness. All of the test results were similar so that no significant differences were observed in bond strength resulting from variations in processing.

Consideration was then given to using the liner material (UTL-0026) as the insulation. The thermal conductivity of 1.14 Btu/hr-ft$^2$-°F/in. and 9.8 mils/sec erosion rate at 625 psig for UTL-0026 is equal to Hitco-2820. There are no volatile materials in the UTL-0026 to migrate into the propellant as in Hitco-2820. Laboratory scale tests were then conducted to check the feasibility of using UTL-0026 as an insulation.

Since UTL-0026 has a low-temperature cure system (160°F) and can be cast in place, a sample was prepared of the material by laying up 1/10-in.-thick layers of UTL-0026 (up to four layers). Each layer was cured 2 to 3 hr at 200°F after application. After the final 200°F cure, the sample received an additional 24-hr cure at 160°F and all sections had an excellent chemical bond to each other. A boot was also prepared in this experiment and a satisfactory

bond line was demonstrated. From this experiment, it was concluded that UTL-0026 could be fabricated as an insulating material for use in this program.

Analog motors containing UTL-0026 as the insulating material were prepared by using an 0.187-in.-thick sheet of UTL-0026 and curing the sheet at 160°F. The sheet of UTL-0026 was bonded to the case wall and then lined. UTP-11439 propellant was cast into the cases and received the normal cure. X-ray analysis showed that this approach also caused debonding during cycling at 275°F at the propellant/liner interface. The insulation section did not debond from the case during the test.

All available evidence indicated that UTL-0026 should function satisfactorily as a motor insulation material since it was essentially free of volatiles and migrating ingredients and bonded readily to the case wall. Since the one obvious problem area remaining involved the debonding of the propellant during sterilization, a series of experiments was initiated to develop a liner that would exhibit the necessary stress-strain properties during sterilization. Liners were prepared and cast into molds and cured at 160°F. These samples were checked for stress-strain properties after cure, and after one 53-hr sterilization cycle. CTPB and CTPIB prepolymers were evaluated in combination with the following curatives: HX-868, MAPO, ERL-0510, EPON-X801, EPON-812, EPON-828, and STF-6.

Using 1-in.-wide by 2-in.-long strips of UTL-0026 insulation as the base, test liners were applied to the insulation and given the proper precure prior to propellant application. UTP-11439 was cast onto the liner and cured. These samples were evaluated through four sterilization cycles.

Formulations containing one equivalent of prepolymer and more than one equivalent of epoxy with one equivalent of MAPO or HX-868 produced liners

with high stress values (ranging from 200 psi or greater than 500 psi) after one sterilization cycle. The strain values were near 50%. Using 1 to 3 equivalents of HX-868 with the prepolymer and 0 to 1 equivalent of epoxy produced very high stress liners and again low elongation after one sterilization cycle. The liners with the highest elongation after sterilization were those containing 2 to 3 equivalents MAPO and 0.3 equivalent epoxy.

To evaluate systems of high elongation, liners were prepared using 2 and 3 equivalents of MAPO and 0.3 equivalent of EPON-X801 with a CTPB prepolymer and lined on UTL-0026 insulation in analog motors. These liners, when checked in the laboratory, had high elongation before and after sterilization. The liner did not have the high stress of UTL-0026 in samples of propellant, liner, and insulation tests but adhesion to the propellant and insulation after cycling at 275$^{o}$F was excellent.

These liners adhered well to the propellant and insulation during sterilization in the analog motors, but propellant debonding occurred as a result of propellant shrinkage. Since the liner was so elastic, the propellant was free to move, and shrinkage was observed on the ends of the grain and between the propellant and insulation. The liner adhered to the propellant and insulation after sterilization, but as a result of its low modulus it was not able to hold the propellant in place.

When tested with UTP-11439 and UTL-0026 insulation, many of the liners had a good physical bond at the end of cure. However, the bond was lost during sterilization cycling. The experimental liners exhibited good properties when tested alone. There is apparently a reaction at the propellant and liner interface resulting in a hardening of the surface and loss of bond strength.

# 5.0 STERILIZATION CYCLE DETERMINATION

Under the contract each motor assembly was to be sterilized by means of a series of six heating cycles, each of which would maintain the most remote point of the grain at a temperature of 275°F for a minimum of 53 hr. Since it is a well-established fact that degradation in polymeric systems increases with temperature and time, it is desirable to limit the time that the system is exposed to elevated temperatures. This section describes the analytical and experimental work which was conducted to determine an optimum heating cycle which would (1) minimize the degradation of the propellant caused by the elevated temperatures required for sterilization, (2) be compatible with the thermal stress constraints of the propellant and the propellant-to-liner bonds, and (3) be compatible with the practical and physical limitations of the oven hardware used for the sterilization cycles. It is important to note that the optimized cycle determined for the contraints listed above is only applicable for the specific motor geometry of this contract, the UTP 11439 propellant, and the particular ovens used for sterilization. However, the work recorded here should provide a basis for constructing an optimized sterilization cycle for any combination of motor, propellant, and oven hardware. Recommendations regarding suggested procedures for further applications are stated in section 5.5.

The first constraint in the determination of an optimum heating cycle is the need to minimize the aging degradation of the propellant. To develop an understanding of the accelerated degradation of propellant at elevated

temperatures, numerous storage studies and investigations of propellants under elevated temperature environments have been conducted by UTC and other investigators. As a result of these tests, it has been found that the degradation of most composite solid propellants containing AP and hydrocarbon binder occurs in a predictable pattern. The Arrhenius plot shown in figure 5-1 has been used successfully to estimate degradation and to correlate accelerated aging data at various temperatures. Using these data, it is possible to compute a multiplication factor which can be used to calculate the degradation at elevated temperatures in terms of the degradation which takes place at a selected standard temperature. Such a plot is shown in figure 5-2 and is based on a standard temperature of 275°F. Adding to the difficulty of minimizing degradation is the variation in heating rates in different portions of the grain. These variations arise from two causes: (1) the variation in heat transfer coefficient at the external motor case wall as a function of the location of the case in the oven and (2) the slower thermal response of the portions of the grain at a distance from the heated surface. Because of these variations, a heating cycle must be developed which assures that the slowest responding point in the grain is maintained at 275°F for 53 hr per cycle. The amount of degradation, on the other hand, must be calculated for the fastest responding point in the grain.

The second constraint in developing an optimum sterilization cycle is the necessity to minimize the thermal stress in the propellant and in the bond between liner and propellant. Since the difference between mean bulk temperatures of the motor case and propellant is an indication of the thermal stress, calculations were made to minimize this difference in

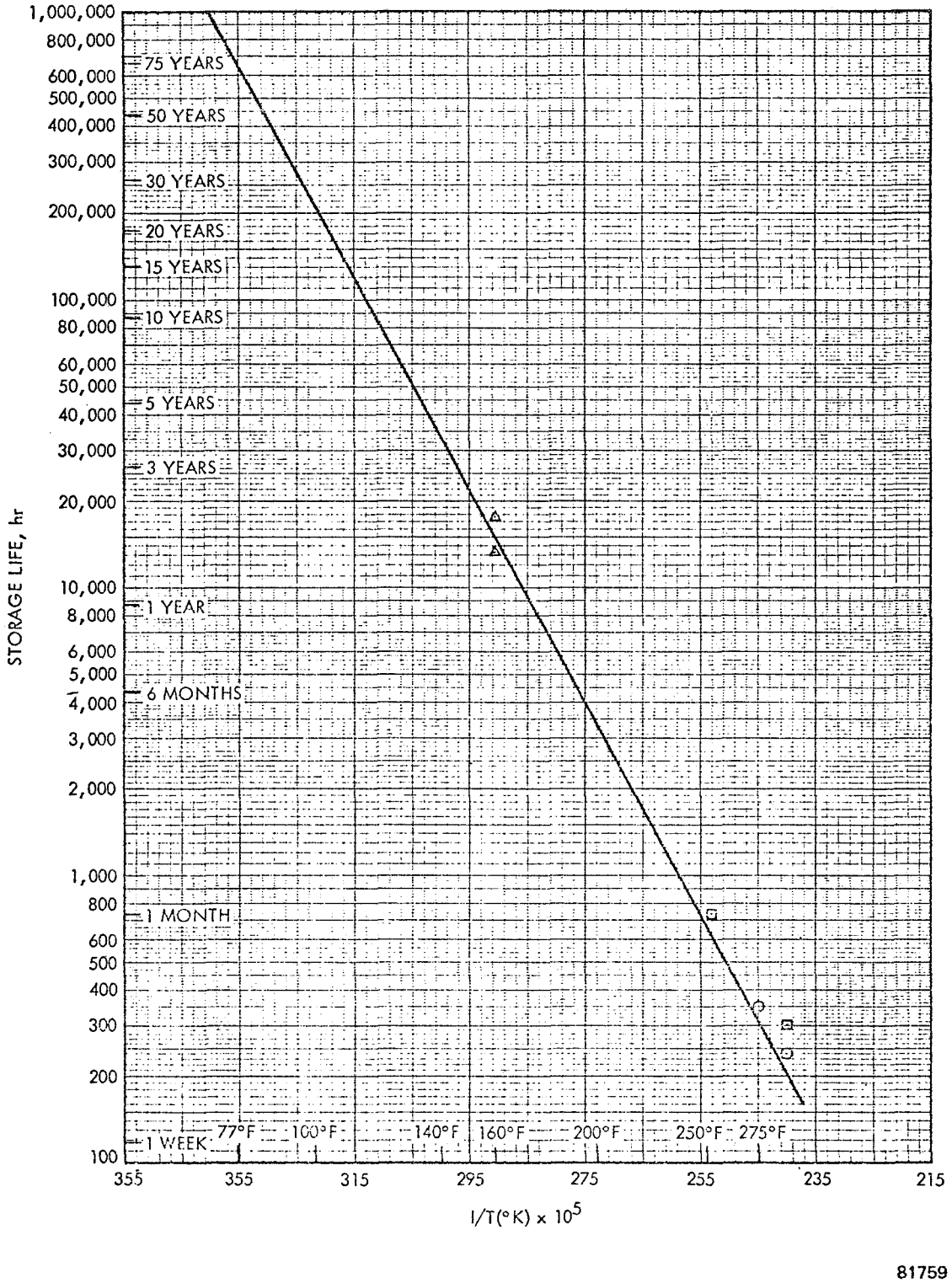


Figure 5-1. Arrhenius Plot Showing the Effect of Temperature on the Usable Storage Life of Propellant

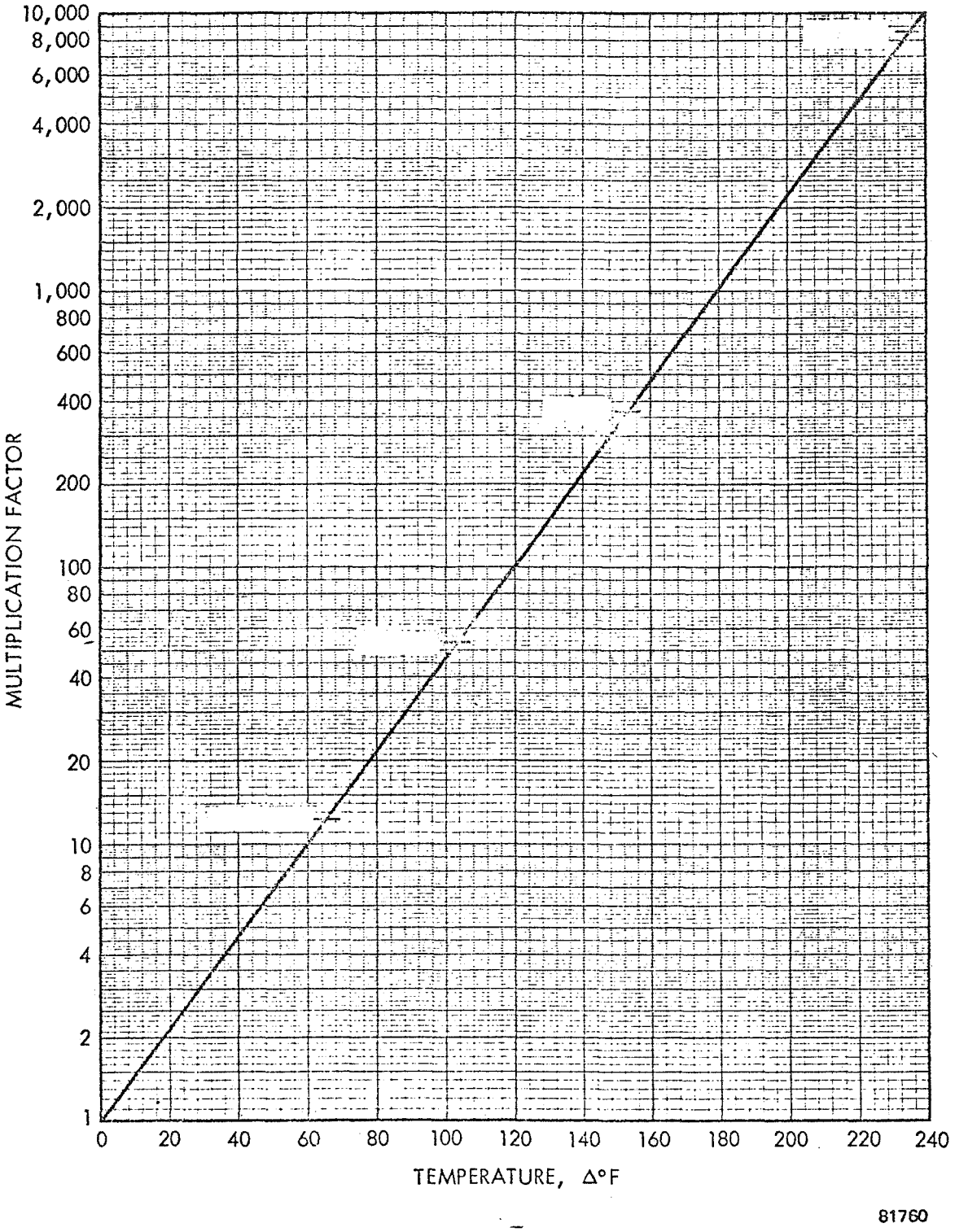


Figure 5-2. Predicted Propellant Degradation Factor for Temperature Change

developing an optimum cycle. The means for decreasing the mean bulk temperature difference is to heat the motor slowly. This tends to increase propellant degradation. Thus a compromise must be obtained between these factors.

The third constraint in developing a heating cycle involves the physical limitations of the hardware to be used for the temperature cycling. The oven used has a fixed geometry, air flow rate, and temperature limitation as described in section 6.4. Thermal cycles which minimize degradation and thermal stresses would require an automatic preprogrammed continuous temperature controller for the oven. Under this demonstration contract such a programmed controller was impractical and a stepwise manually controlled oven cycle was used.

With these three basic criteria in mind, the procedure followed to arrive at the optimum sterilization cycle for a live propellant was as follows:

A. Determine the approximate heating rate on the motor case for all locations within the oven for the air flow rates and temperatures to be used. This was accomplished using a thermocouple instrumented empty motor case which facilitated rapid tests since the rate of thermal response of the thin shell was high.

B. Using this range of heat transfer rates, make estimates of the response times of an inert propellant and motor case and determine a nearly optimum cycle in terms of aging degradation and thermal stress.

C. Using an inert loaded motor and the heating cycle calculated in paragraph B, measure external and internal surface temperature responses. Use this measured data to refine the heating rates measured

in paragraph A and to verify a heat conduction model for prediction of in-depth thermal response.

D. Finalize the optimum sterilization cycle using the latest heating rates and properties for the live propellant. This optimum cycle will be a compromise between cycles which minimize aging degradation and cycles which minimize thermal stress. The cycle must also meet the contraints of the oven hardware.

The following discussion will describe in greater detail the steps listed previously and will present the results for each of the major milestones. It should be noted that a significant amount of thermocouple data were taken and a large number of heat transfer computer runs were made during the course of this work. In this report, the thermocouple data are summarized by plotting the maximum, minimum, and any critical points. The great volume of data for the several thermocouples per test are not presented here; however, a sample from the strip charts used in the test is presented, and the data are on file at UTC for review. Only the final results of the heat conduction computer runs are presented, as no purpose would be served to present all of the runs made. However, a summary of the maximum degradation is presented for several of the cycles tried which led to the final cycle.

## 5.1 AGING DEGRADATION ANALYSIS

As mentioned previously, the propellant degradation or aging multiplication factor may be computed from the known thermal response of any point in a propellant and the plot shown in figure 5.2. For example, if it is known that a propellant has been at 295°F for 3 hr, the aging relative to 275°F would be computed in the following manner:

A. The $\Delta$ T is 295° to 275°F = 20°F.

B. Using figure 5-2, a $\Delta$T of 20°F gives a multiplying factor of 2.15.

C. Therefore, relative to 275°F the propellant has aged 2.15 times 3 hr, or 6.45 hr, in a actual time of 3 hr due to the elevated temperature.

For convenience of the analysis, a degradation factor has been defined as

$$DF = \frac{D_t}{D_s}$$

where

DF = The degradation factor

$D_t$ = The total degradation estimated by using the curve in figure 5-2 to calculate the equivalent degradation time at some base temperature (usually 275°F)

$D_s$ = The total degradation calculated using the data in figure 5-2 to determine the degradation value at the same base temperature as $D_t$ for the actual 53 hr at 275°F.

This factor actually represents the number of 53-hr 275°F periods that the propellant is aged or degraded when taken through each cycle of the sterilizing process. Obviously some points of the propellant must see the high temperatures for longer than 53 hr for the thermally remote regions to reach 275°F. This factor indicates the actual number of degraded hours realtive to the ideal cycle.

The computation of this factor has been computerized and may be calculated for any propellant response generated by the heat conduction computer program or oven cycle for a given temperature setting. The program,

designated AGING/CODE, uses the equation of the semi-log curve which describes the temperature degradation phenomenon (figure 5-2), and the time-temperature results from computations or measurements to compute the degradation time at any presecribed based temperature. The base temperature of 275°F was used for this study.

Figure 5-3 shows a schematic of the sterilizable motor and a thermal model used for the one-dimensional heat conduction computer program, LA15ZAZ, which is used to compute the temperatures within the propellant during a sterilization cycle. When a motor is heated from the external surface only, the point marked A will heat significantly faster than the thermally remote point B. The degradation computed for these two points generally will yield the maximum and minimum thermal degradation times.

To determine the effect of various cycles, several oven heatup transients were imposed on a preliminary propellant model. For each of the cycles the relative startup transient aging time was determined for the external point of the propellant, point A, and compared to the actual time required for the remote point B to reach 275°F. Figures 5-4 and 5-5 show the results for two oven air cycles, one for a constant 300°F and another in which the oven air is increased to 400°F for 2 hr and then reduced to 300°F. These runs were used to determine when the remote point B would reach 275°F. At that time the oven would normally be reduced to the 275°F value for the remainder of the 53 hr. Table 5-I lists the actual time and the relative aging time that resulted from the cycles. Note that although the cycle of figure 5-5 is shorter the aging time is longer, since the external temperature of figure 5-5 was higher than that for figure 5-4 for a longer time period. For these two oven cycles, the heat transfer coefficient was assumed to be

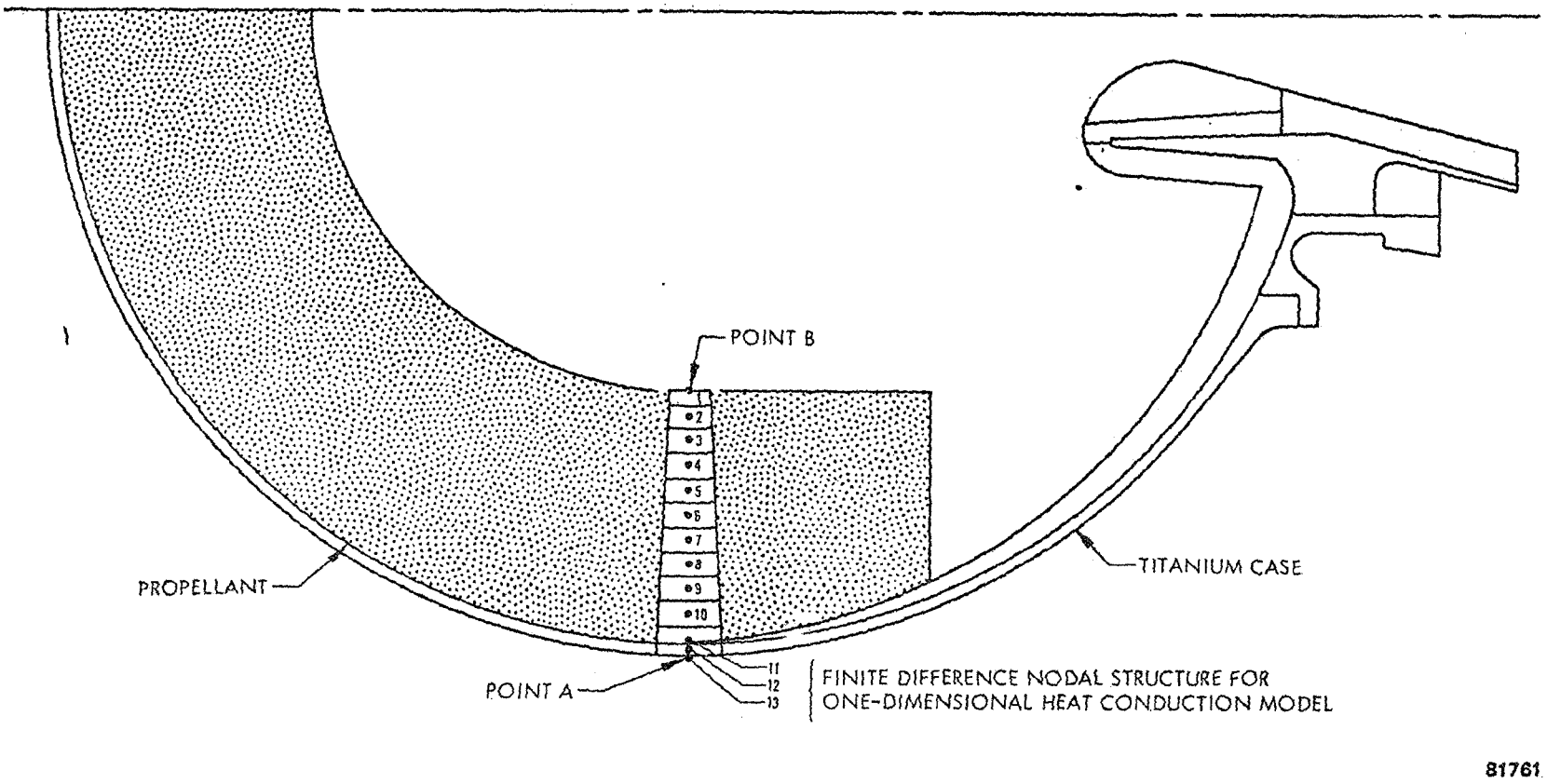


Figure 5-3. Location and Model for Thermal Analysis of Sterilization Cycle Optimization

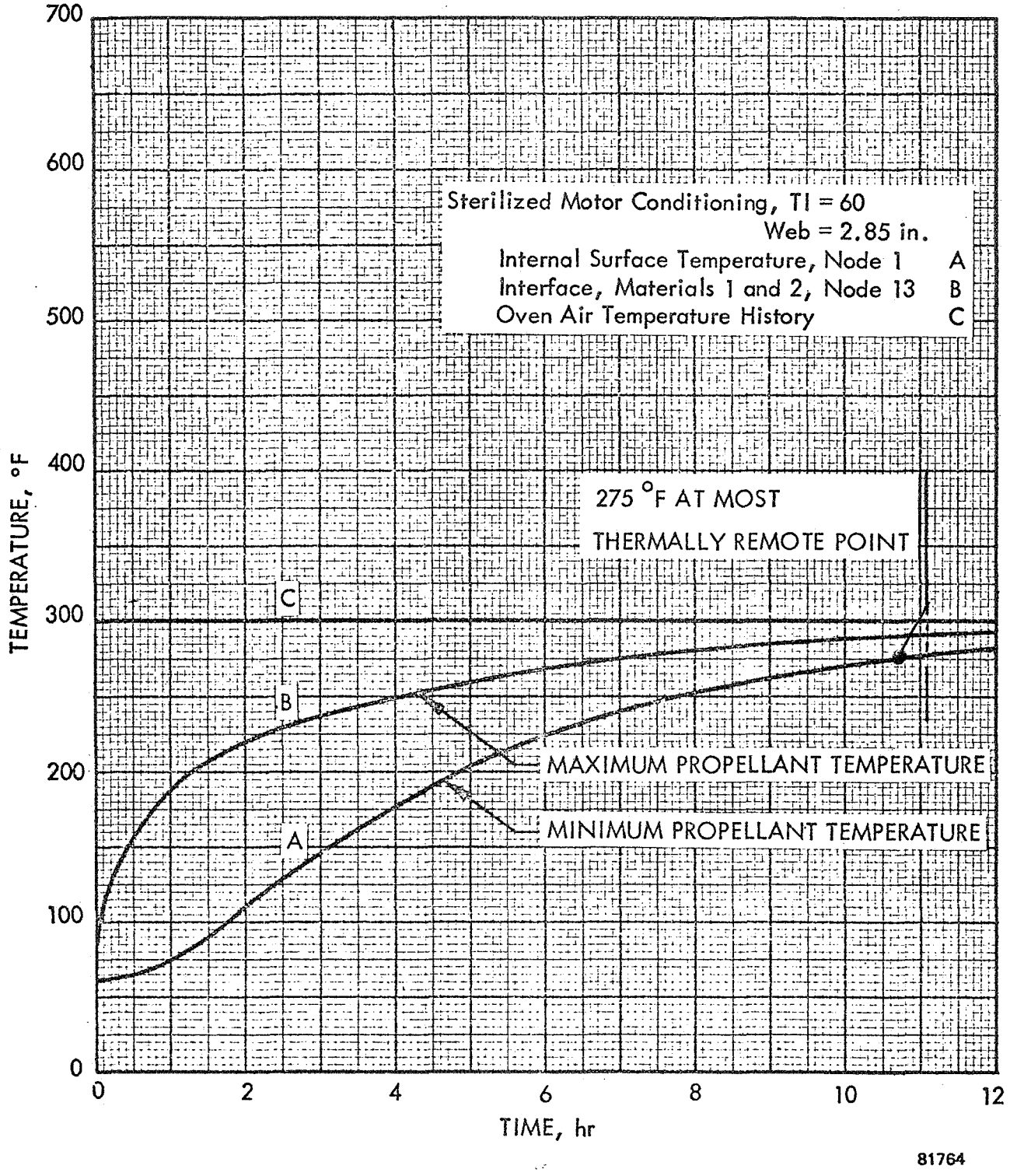


Figure 5-4. Internal and Interface Temperatures at Constant Oven Air Temperature = 300°F

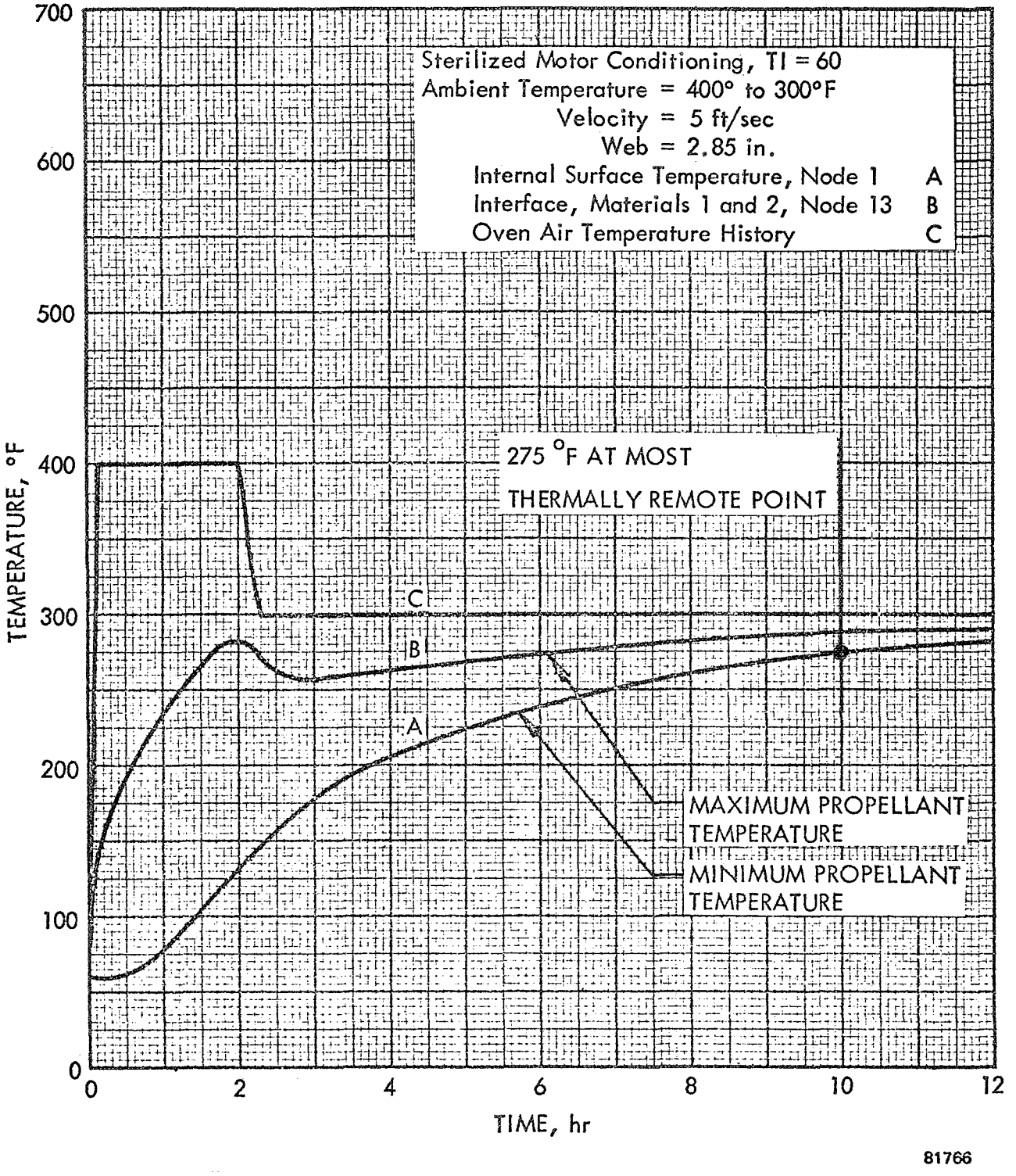


Figure 5-5. Internal and Interface Temperatures at Variable Oven Air Cycle 1

constant for the prescribed oven temperature, thus defining the external wall temperature. To attempt further optimization, a second approach was taken. Since it is the external surface temperature that defines the degradation, it was decided to prescribe the external surface temperature and then "back out" the oven temperature required to create that surface temperature response when the lowest surface temperature producing the lowest aging was found. Figures 5-6 and 5-7 show two typical external surface temperature runs, and table 5-I shows the relative aging times. Note that the cycle with the longer duration (figure 5-7) had the shortest relative aging time. Figure 5-7 also shows the "backed out" oven temperature which would be required to produce the external surface response.

The cooling transient was less critical since the temperatures are always less than the 275°F sterilization temperature. The major controlling factor for the cooling phase would be the compatibility with any structural requirements regarding the maximum cooling rate acceptable. A typical response is shown in figure 5-8 where the cooling air is maintained at a constant 60°F and the oven blowers are still on.

Table 5-I indicates the relative aging times for both the internal and external surfaces. The internal surface has the larger relative aging time because it lags during cooldown.

It should be noted that these examples assumed a specific oven air flow which causes a particular convective heating rate on the motor case. The runs were typical, although not final due to the fact that the specific oven response had not yet been determined. However, it was concluded from these and other runs that the surface temperatures must be kept as close to the sterilization temperature as possible to keep the degradation to a minimum.

TABLE 5-I

RESULTS OF TRANSIENT HEATING AND COOLING ANALYSES
ON THE PROPELLANT/CASE INTERFACE FOR SEVERAL TRANSIENT VARIATIONS

| Cycle | Reference Figure Number | Time for Point B to Reach 275°F | Relative Aging Time Hr | Transient Degradation Factor† |
|---|---|---|---|---|
| Constant oven air 300°F | 5-4 | 11.0 | 7.84 | 0.71 |
| Air cycle 1 | 5-5 | 10.0 | 9.35 | 0.94 |
| Case temperature cycle 2 | 5-6 | 6.55 | 12.05 | 1.8 |
| Case temperature cycle 4, modified | 5-7 | 7.5 | 7.4 | 0.99 |
| Cooling to 60°F | | | | |
| Outside | 5-8 | 12.0* | 0.11 | 0.01 |
| Inside | 5-8 | 12.0* | 1.19 | 0.1 |

*Time to reach 70°F on inside.

†Minimum degradation for the heating transient is desired. The degradation factor for these transients are only for reference because the total cycle of heating, holding, and cooling must be considered.

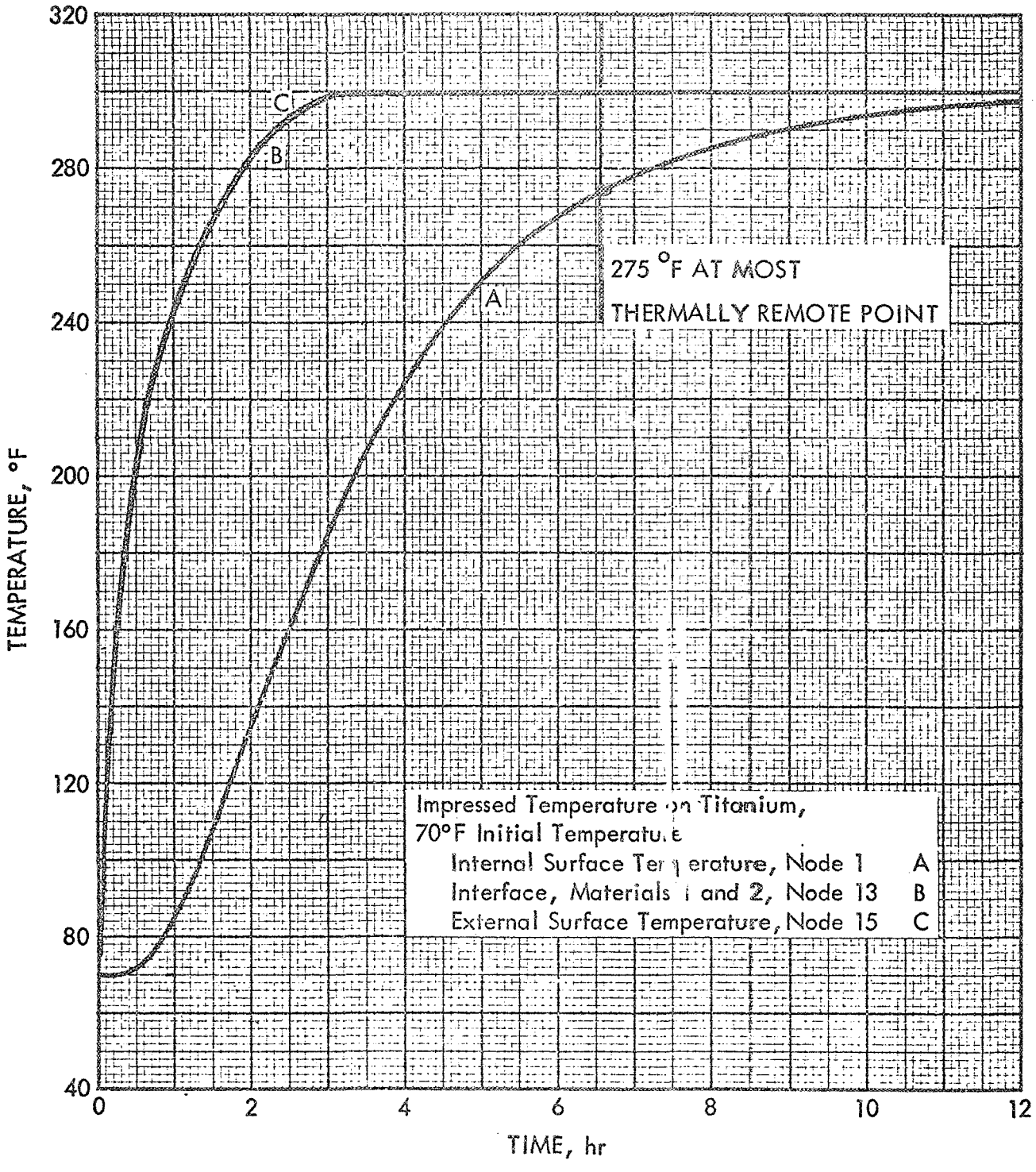


Figure 5-6. Internal, Interface, and External Temperatures at Case Temperature Cycle 2

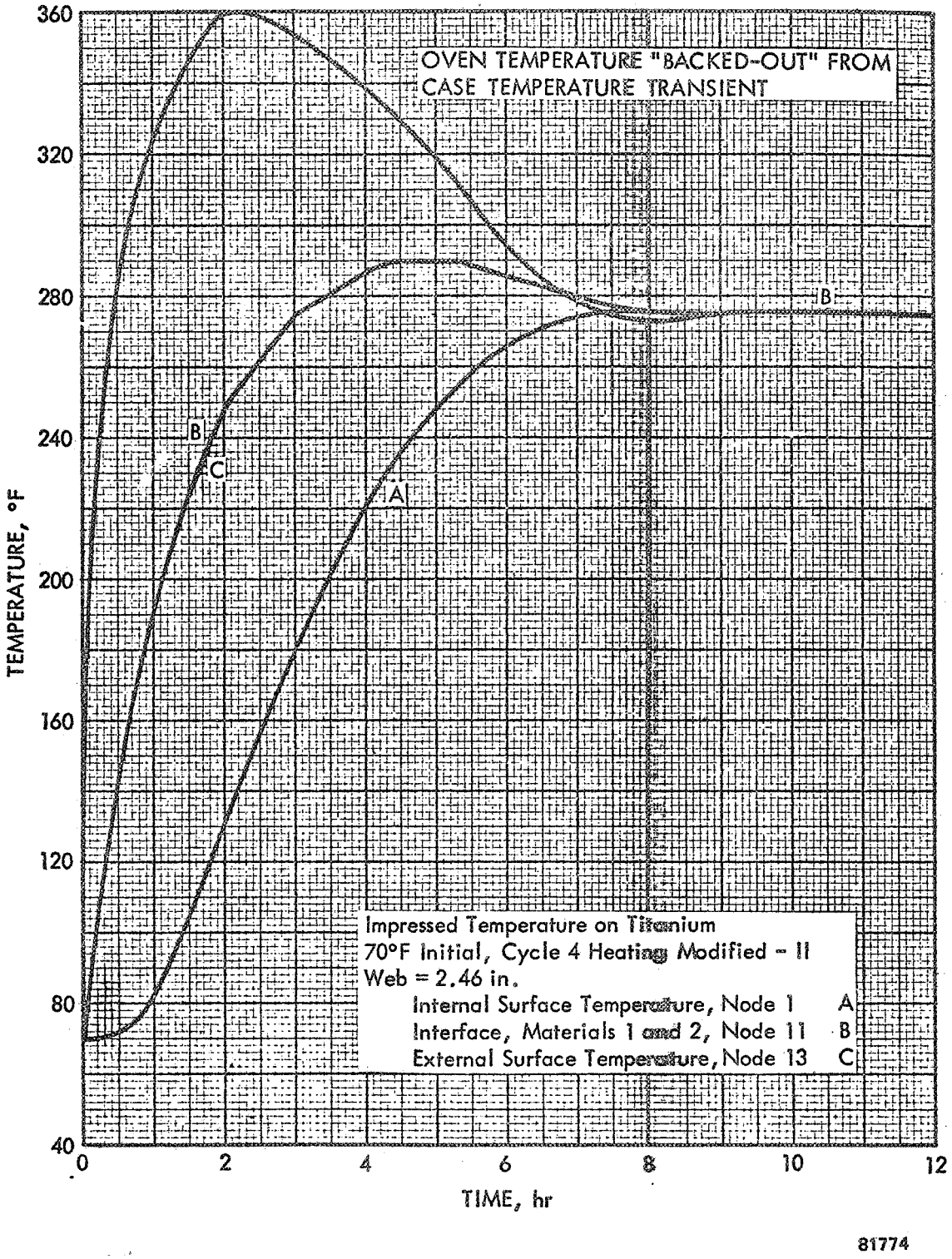


Figure 5-7. Internal, Interface, and External Temperatures at Case Temperature Cycle 4, Modified

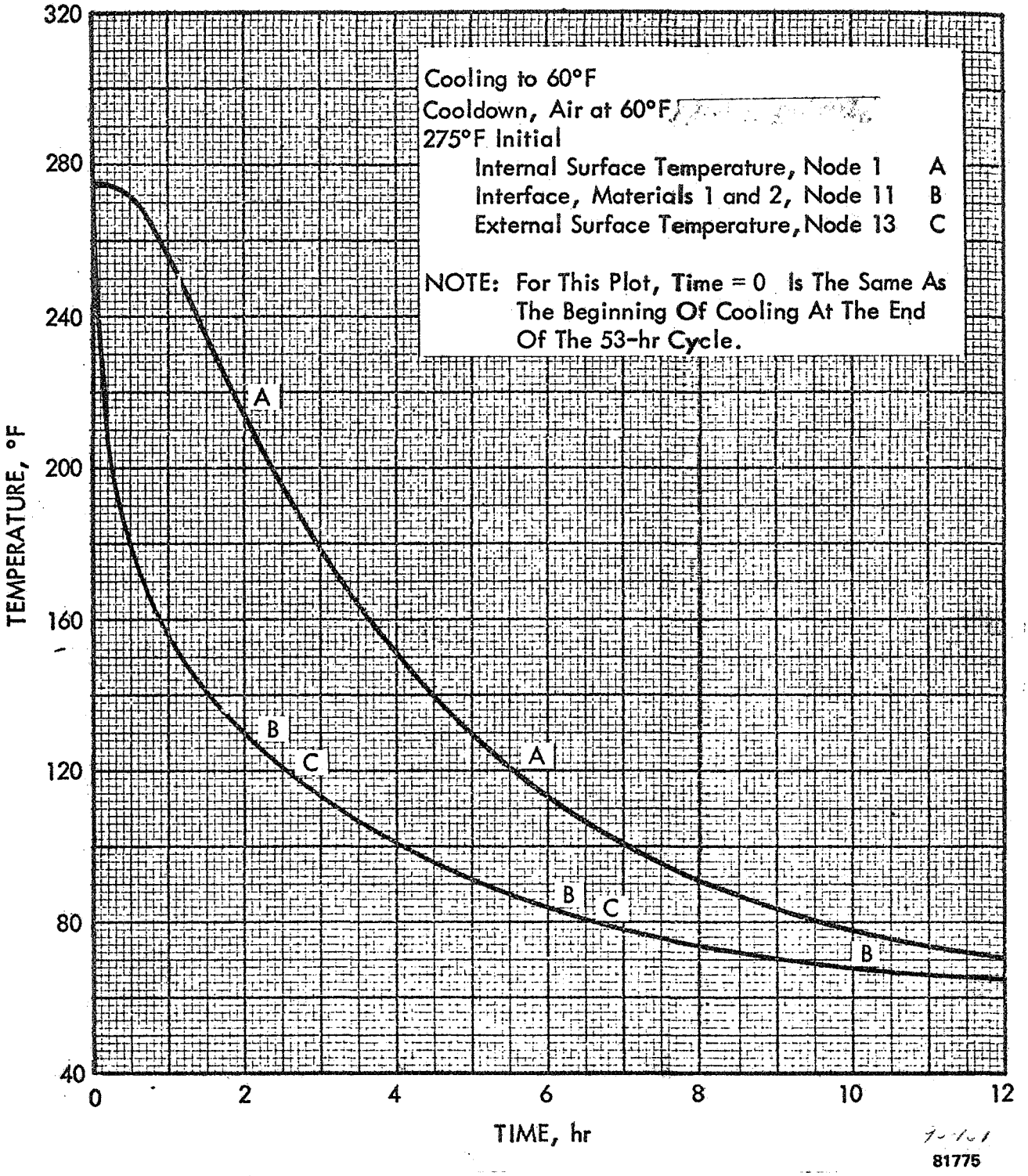


Figure 5-8. Internal, Interface, and External Temperatures (Cooling to 60°F)

## 5.2 OVEN TESTS USING AN EMPTY MOTOR CASE

To accurately develop oven cycles which will minimize the degradation of the propellant during sterilization, a thermal model must be developed which represents the heating process in the oven. This requires a knowledge of the convective heat transfer coefficient on the external surface of the motor case. A preliminary determination of the heat transfer coefficients was made using an empty motor case instrumented with thermocouples and placed in the oven. Thirteen thermocouples were located on the case, as shown in figure 5-9. These were formed using 28-gauge copper and constantan wire twisted together and spot welded to the case. A thermocouple was also placed inside the case to measure the inside air temperature. Two thermocouples were used to measure oven air temperature, one directly in front of the case (in terms of direction of air flow) and one behind the case. All thermocouples were checked for continuity and were connected to a recorder.

The instrumented empty case was then placed in oven position 1 as shown in figure 5-10. When all thermocouple readings were stabilized, the oven heat was turned on. The oven air temperature was allowed to rise naturally to 300°F and was subsequently held thermostatically at 300°F. This procedure was then repeated for oven positions 4, 2, and 3 and again for position 4. In the last test, the cooldown was also recorded and the data were reduced.

A typical recorded response of the thermocouples is shown in figure 5-11. Data representing the oven air temperature, the air temperature inside the motor case, and the maximum and minimum case temperatures were taken from these recorder strips. These data were used as input to the program CASE/TEMP which calculated the heat transfer coefficients based on a

FIGURE 5-9

THERMOCOUPLE LOCATIONS ON MOTOR CASE AND PROPELLANT

▲ CASE THERMOCOUPLES

● LIVE OR INERT PROPELLANT THERMOCOUPLES

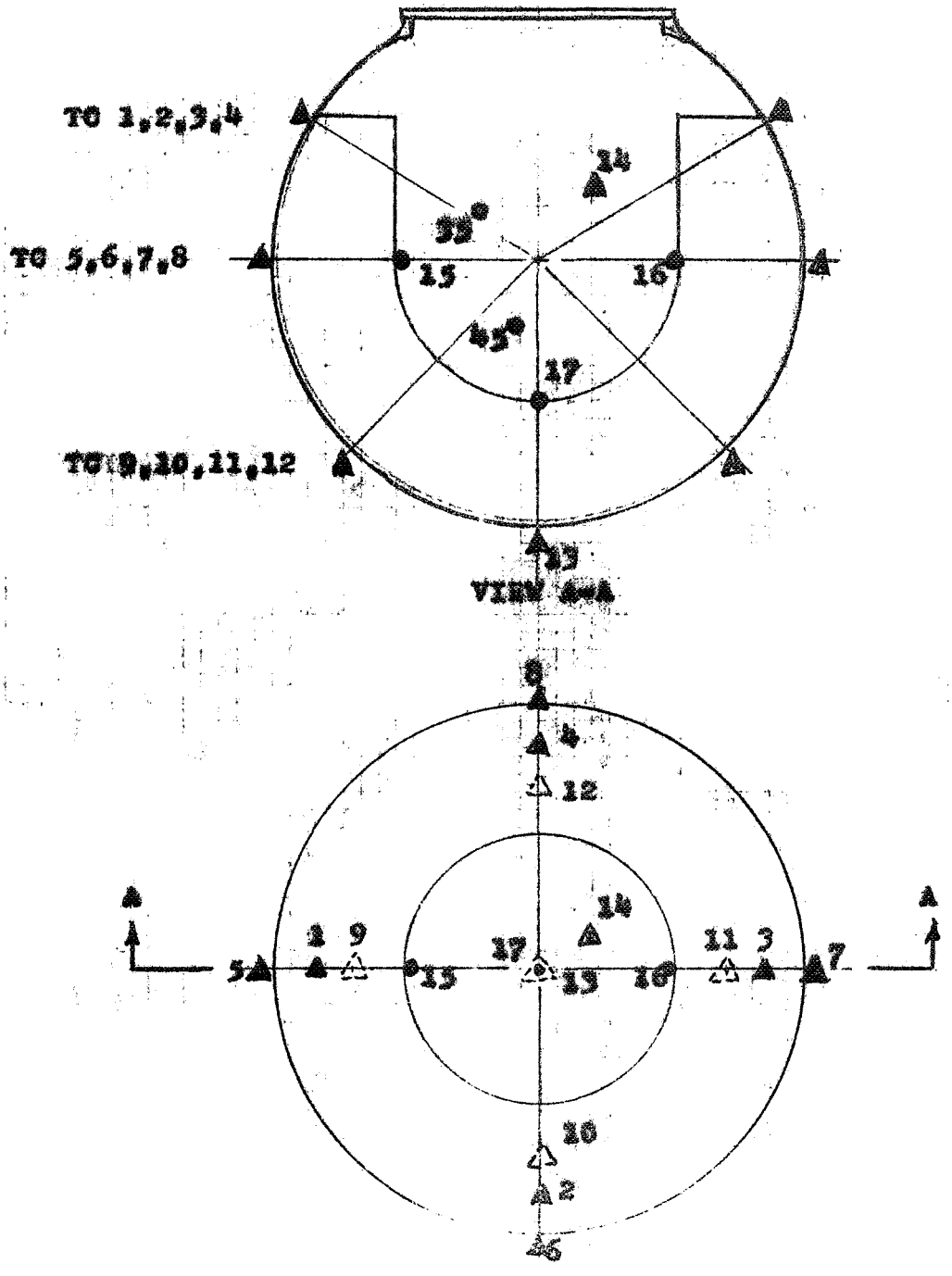

FIGURE 5-10

MOTOR POSITIONS IN OVEN

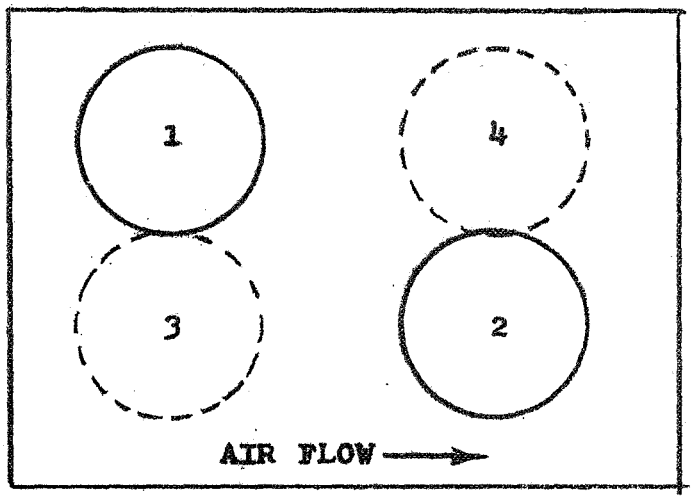


TOP VIEW

NOTE: TC's 1, 5, & 9 FACE AIR FLOW

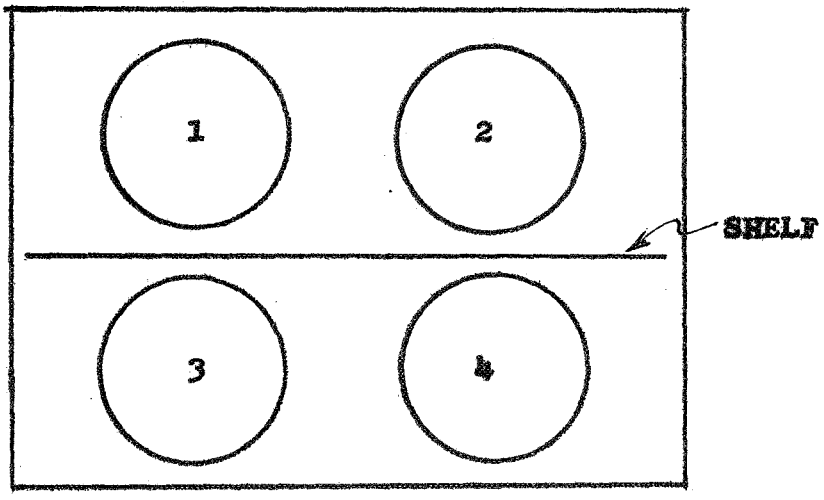


FRONT VIEW

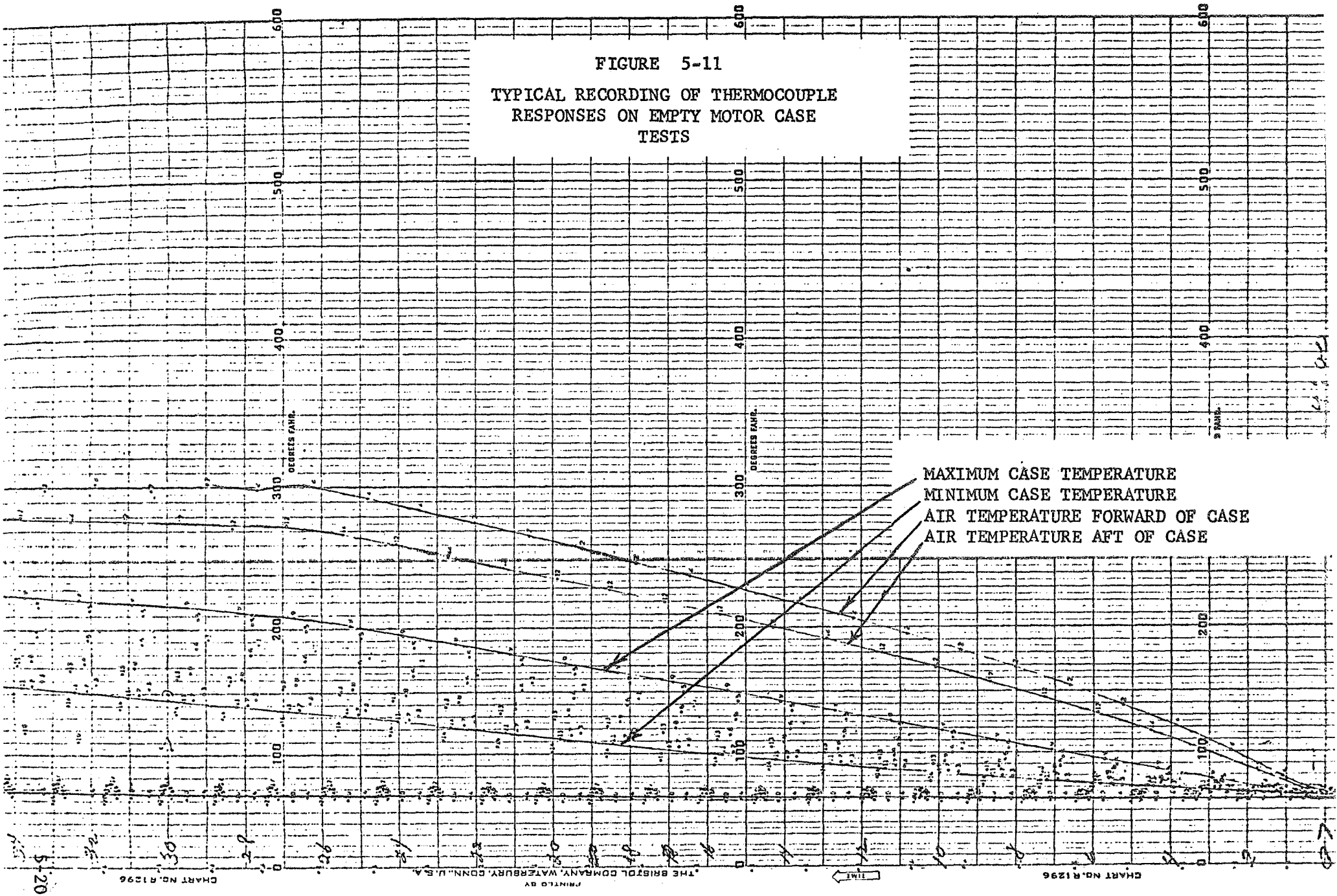


FIGURE 5-11

TYPICAL RECORDING OF THERMOCOUPLE RESPONSES ON EMPTY MOTOR CASE TESTS

heat balance to the empty case wall including internal and external heat transfer. This heat balance assumed that all of the air inside the case was heated by heat transferred through the wall.

The recorded temperature data and the accompanying calculated heat transfer coefficients are shown in figures 5-12 through 5-33. Because the heat transfer coefficient calculations involve division by small differences in measured temperatures, small measured errors can lead to the large random fluctuations shown in these plots. It is possible, nevertheless, to determine approximate values and trends in heat transfer coefficients. The coefficients at the point of maximum response vary roughly between 1.0 and 6.0 Btu/hr-ft$^2$-°F. At the point of slowest response, the values range from 1.0 to 2.0 Btu/hr-ft$^2$°F. The wide variation of heat transfer coefficients and the fluctuations can probably be related to one or more of the following factors:

A. The convection to a surface is dependent upon temperature levels of the gas and wall,

B. Hot air leakage into the empty case through the top,

C. Variation of air flow around the case due to uneven flow distribution,

D. Error between titanium wall thickness assumed and actual values,

E. Error between titanium thermal properties assumed and actual.

Since more tests were to be run with the inert and live motors, no attempt was made to investigate these possible problem areas. These tests were designed to yield a rapid value of oven temperature response in the early stages of the analysis, and they accomplished that task.

# STERILIZABLE MOTOR EMPTY CASE TEST

FIGURE 5-12 - EMPTY CASE POSITION NUMBER 1, TEST 1
LOW VALUE CASE TEMPERATURES

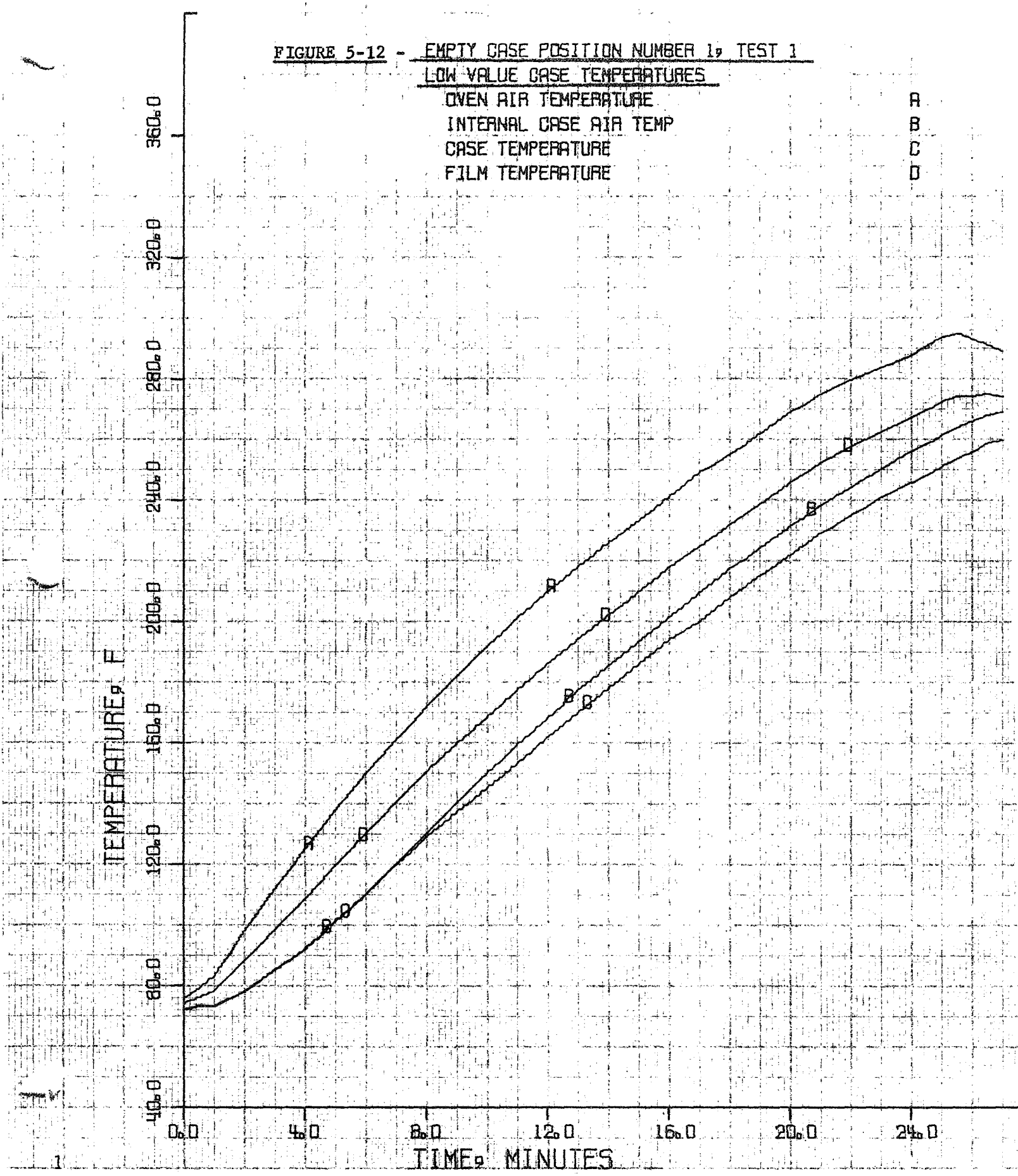

# STERILIZABLE MOTOR EMPTY CASE TEST

**FIGURE 5-13 - EMPTY CASE POSITION NUMBER 1, TEST 1**
**HIGH VALUE CASE TEMPERATURES**

| | |
|---|---|
| OVEN AIR TEMPERATURE | A |
| INTERNAL CASE AIR TEMP | B |
| CASE TEMPERATURE | C |
| FILM TEMPERATURE | D |

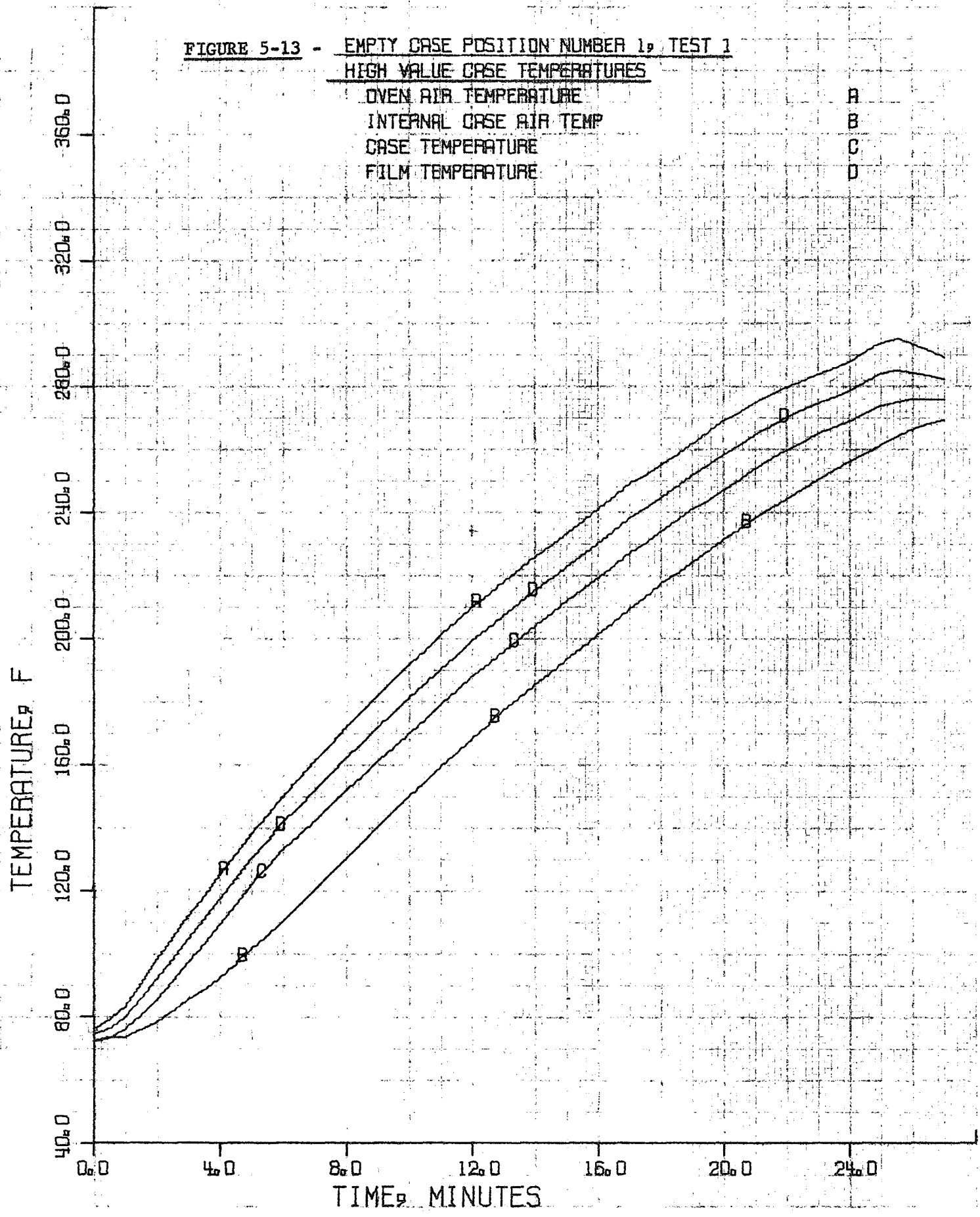

10 APR 1969

# STERILIZABLE MOTOR EMPTY CASE TEST

FIGURE 5-14 - EMPTY CASE POSITION NUMBER 1, TEST 1
LOW VALUE CASE TEMPERATURES, HTC RESULTS

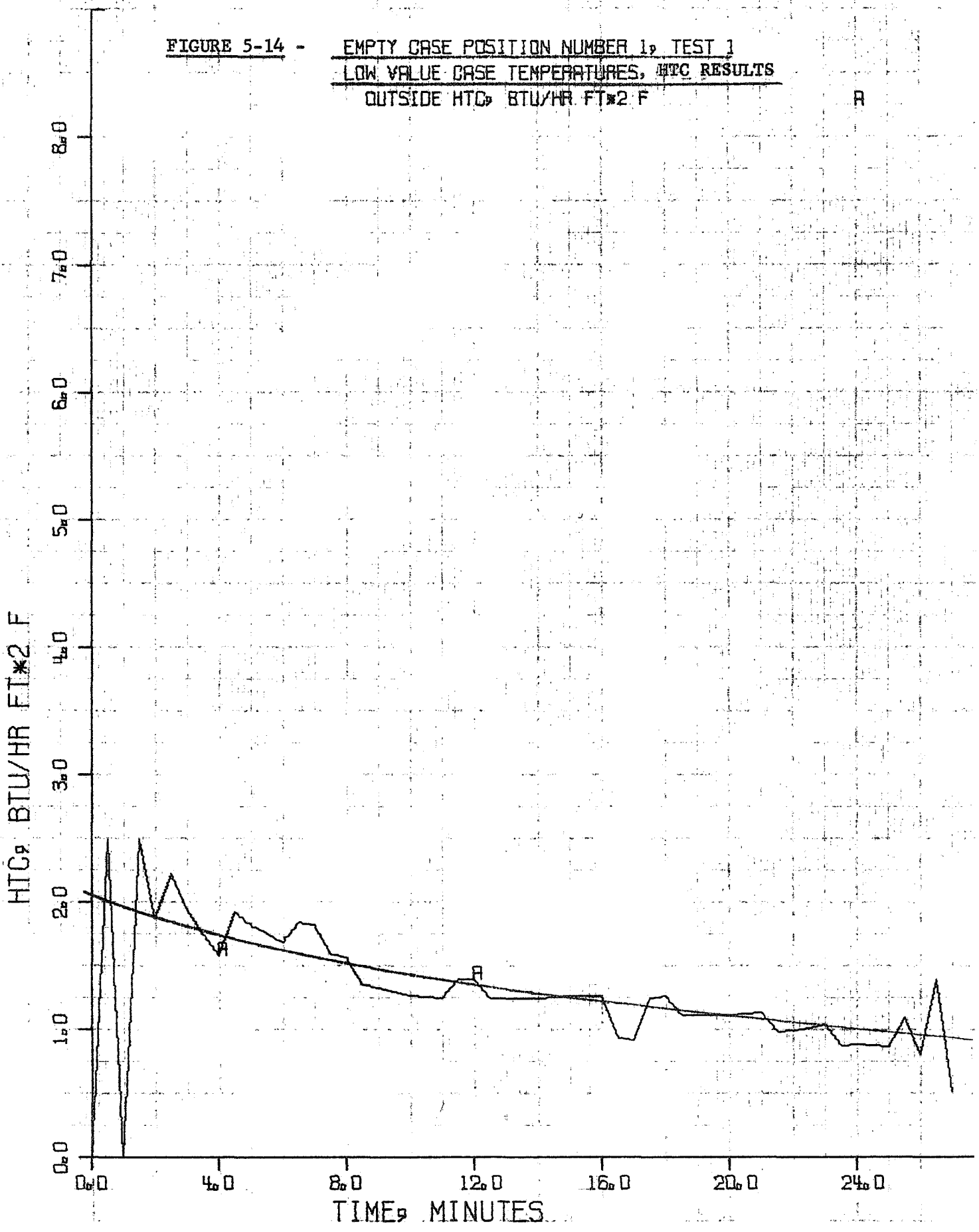

10 APR 1969

# STERILIZABLE MOTOR EMPTY CASE TEST

FIGURE 5-15 - EMPTY CASE POSITION NUMBER 1, TEST 1
HIGH VALUE CASE TEMPERATURES, HTC RESULTS

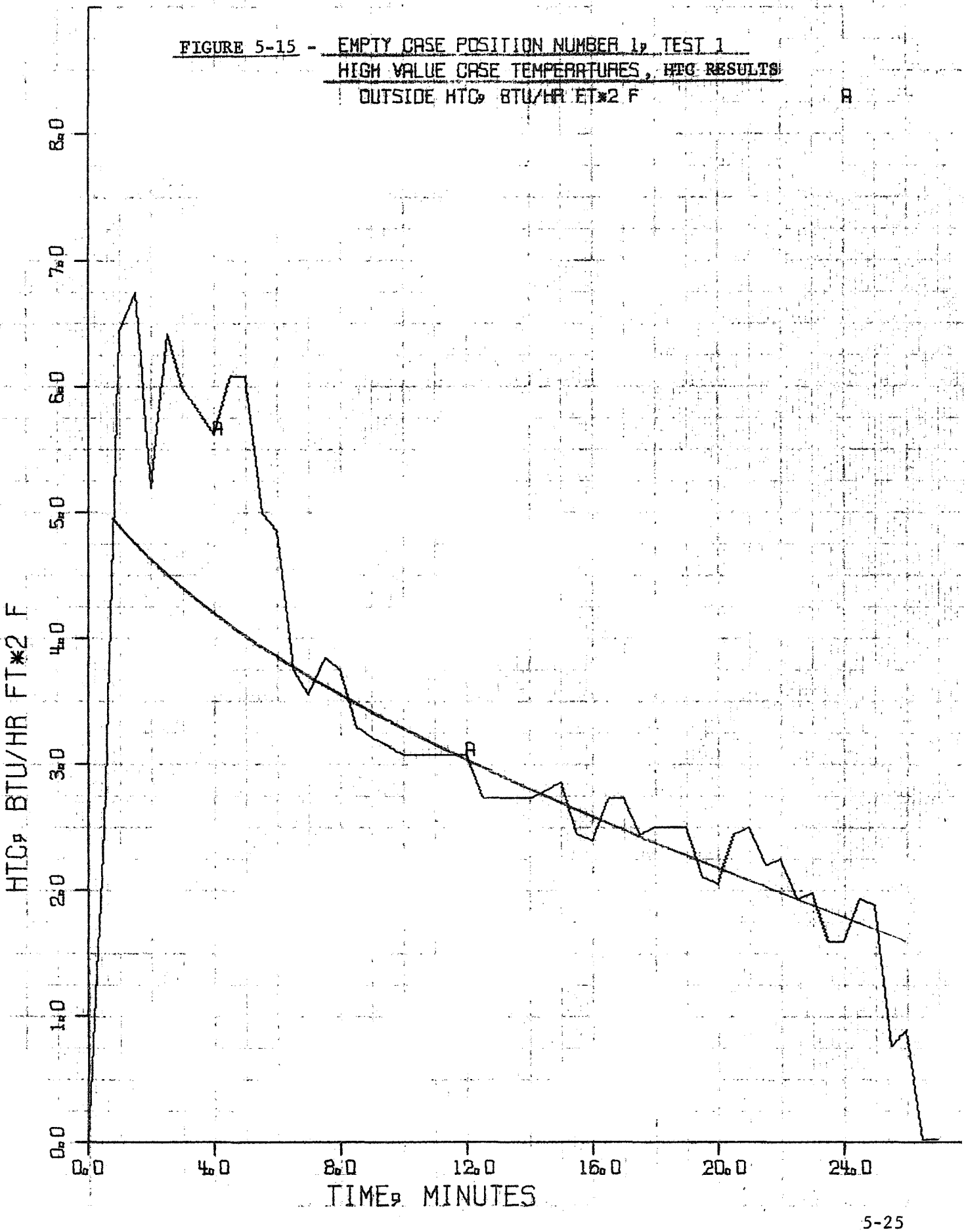

10 APR 1969

# STERILIZABLE MOTOR EMPTY CASE TEST

FIGURE 5-16 - EMPTY CASE POSITION NUMBER 4, TEST 2
LOW VALUE CASE TEMPERATURES

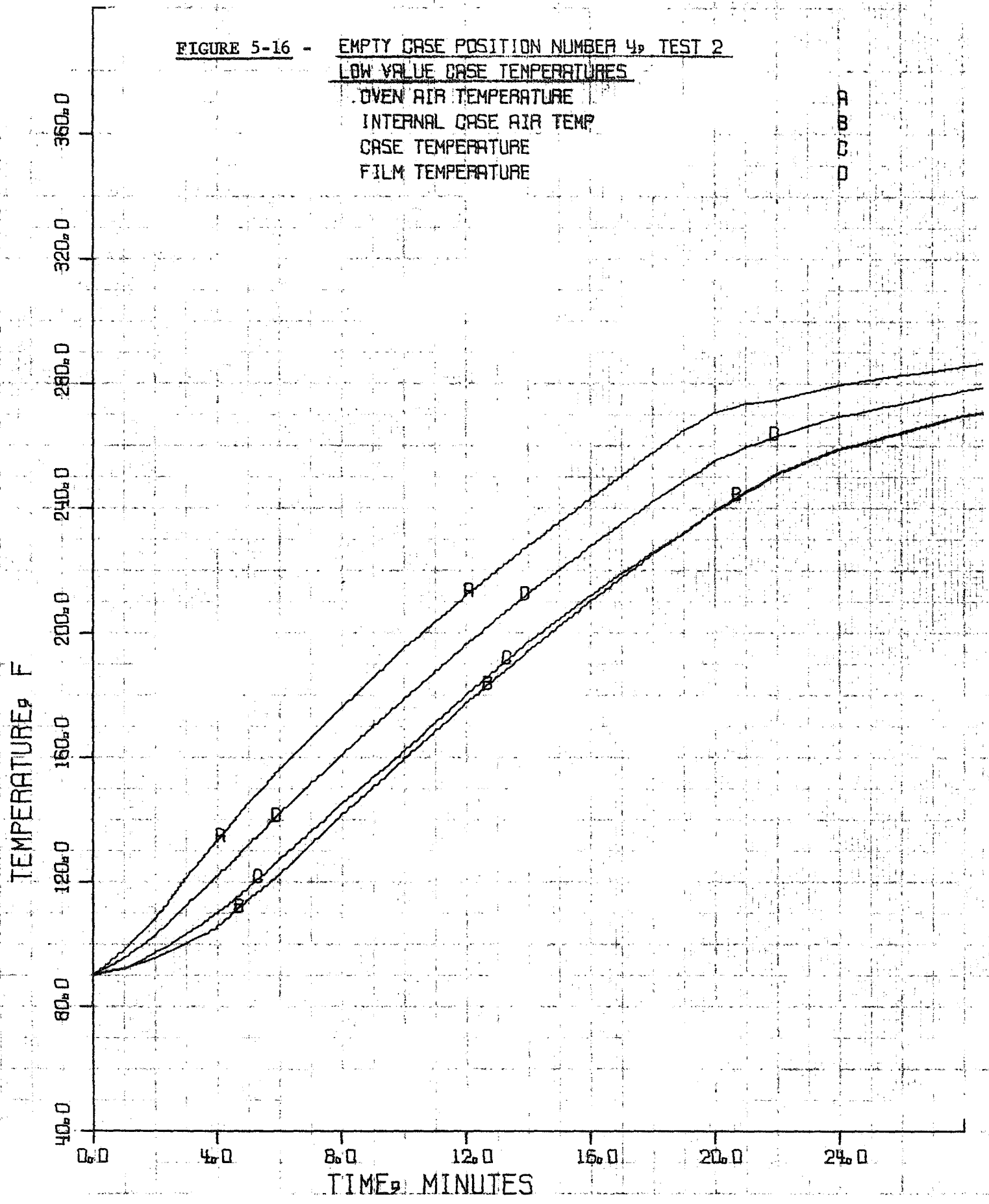

# STERILIZABLE MOTOR EMPTY CASE TEST

FIGURE 5-17 - EMPTY CASE POSITION NUMBER 4, TEST 2
HIGH CASE TEMPERATURE VALUES

| | |
|---|---|
| OVEN AIR TEMPERATURE | A |
| INTERNAL CASE AIR TEMP | B |
| CASE TEMPERATURE | C |
| FILM TEMPERATURE | D |

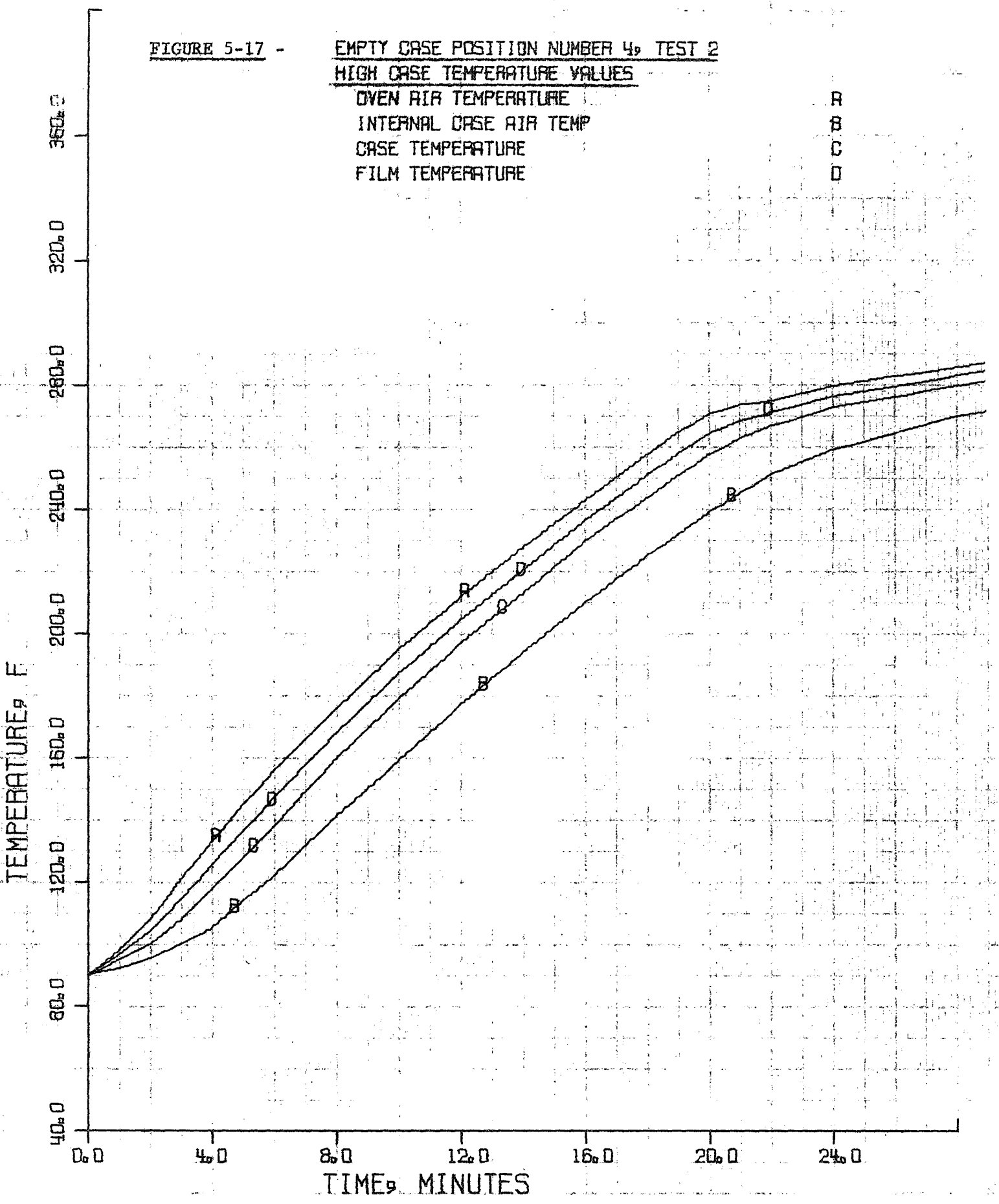

# STERILIZABLE MOTOR EMPTY CASE TEST

FIGURE 5-18 - EMPTY CASE POSITION NUMBER 4, TEST 2
LOW VALUE CASE TEMPERATURES, HTC RESULTS
OUTSIDE HTC, BTU/HR FT**2 F

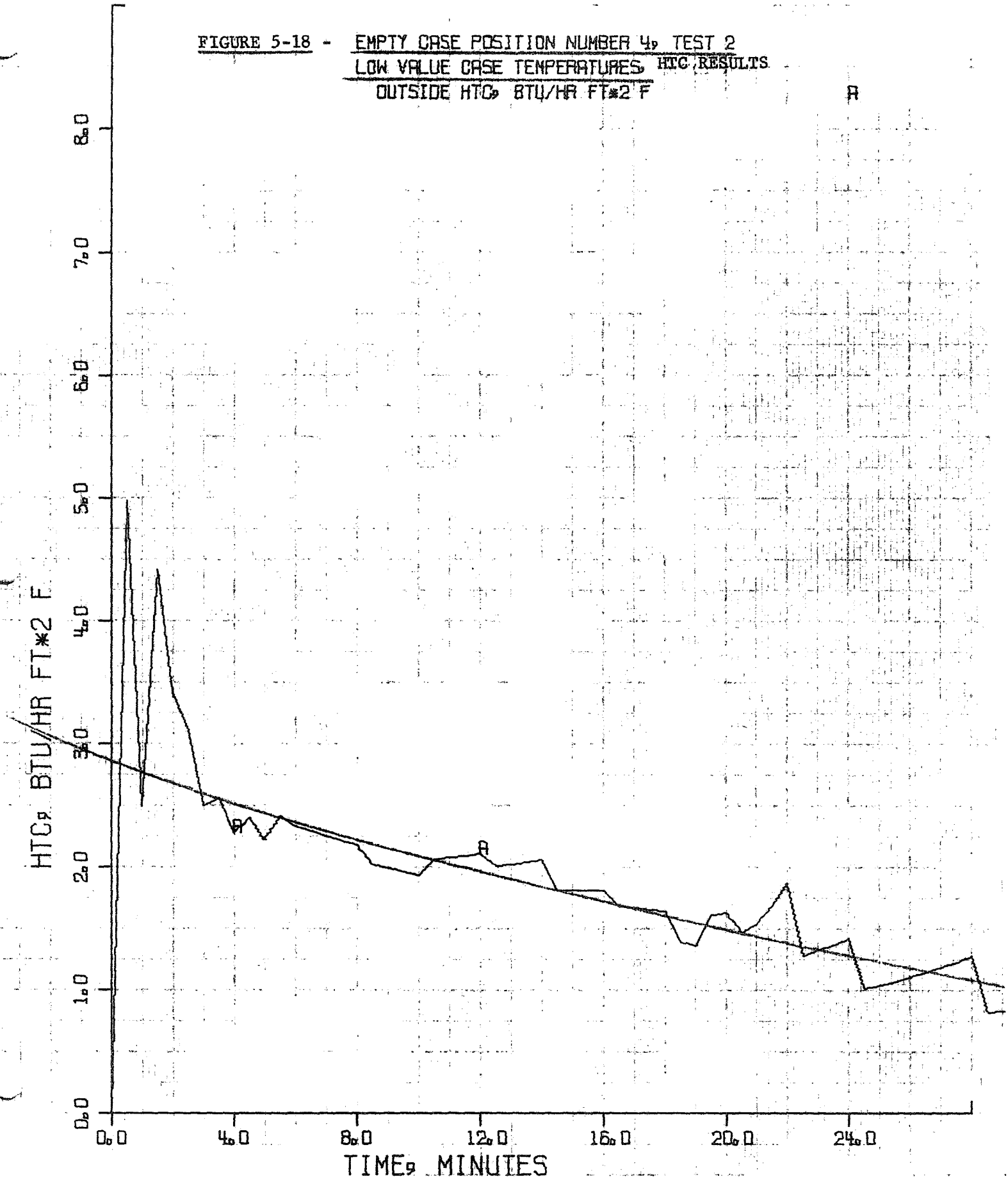

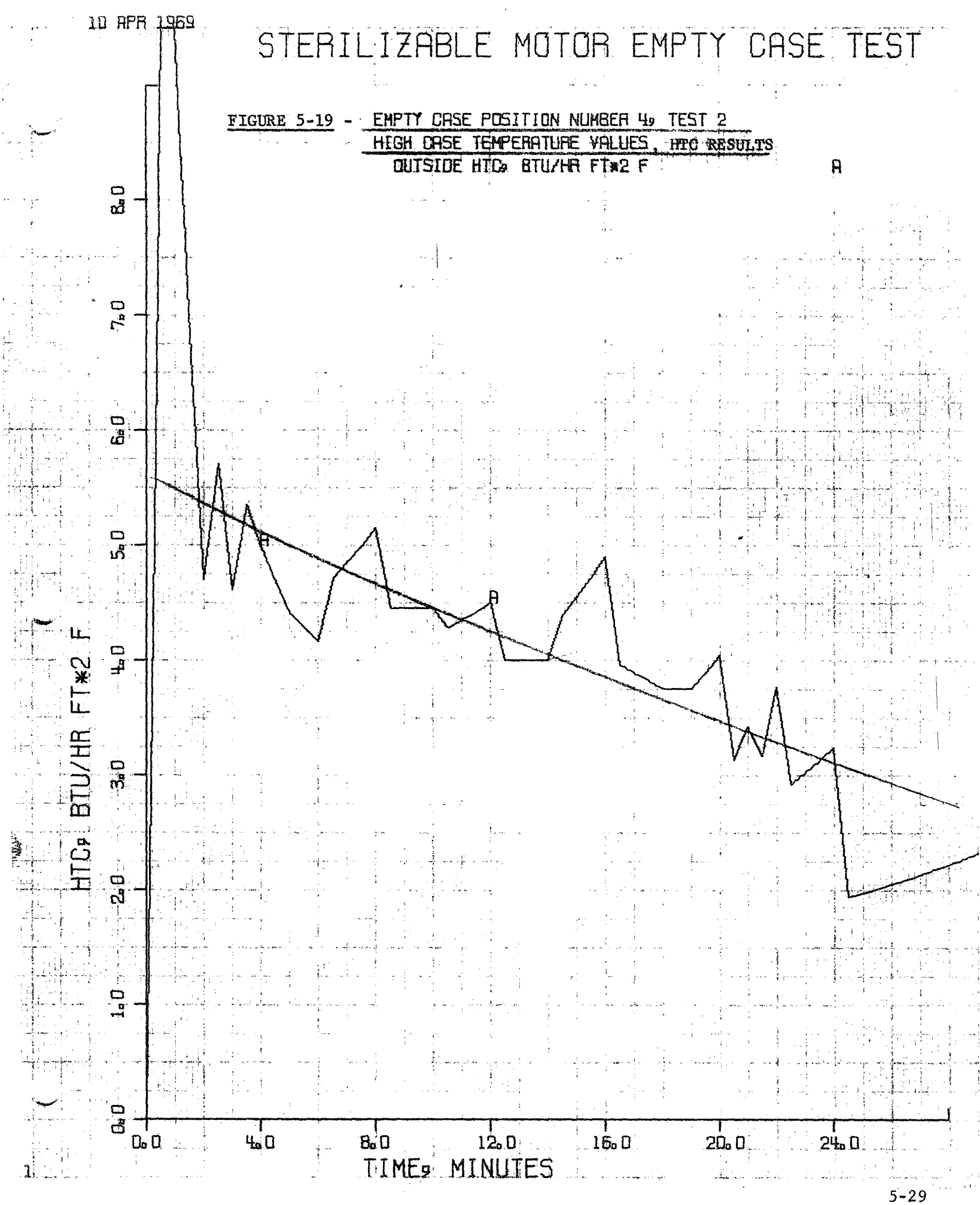
10 APR 1969
STERILIZABLE MOTOR EMPTY CASE TEST
FIGURE 5-19 - EMPTY CASE POSITION NUMBER 4, TEST 2
HIGH CASE TEMPERATURE VALUES, HTC RESULTS
OUTSIDE HTC, BTU/HR FT**2 F
A
HTC, BTU/HR FT**2 F
0.0
1.0
2.0
3.0
4.0
5.0
6.0
7.0
8.0
0.0
4.0
8.0
12.0
16.0
20.0
24.0
TIME, MINUTES

# STERILIZABLE MOTOR EMPTY CASE TEST

FIGURE 5-20 - EMPTY CASE POSITION NUMBER 2, TEST 3
LOW CASE TEMP. VALUES, PRE-HEAT OVEN

| | |
|---|---|
| OVEN AIR TEMPERATURE | A |
| INTERNAL CASE AIR TEMP | B |
| CASE TEMPERATURE | C |
| FILM TEMPERATURE | D |

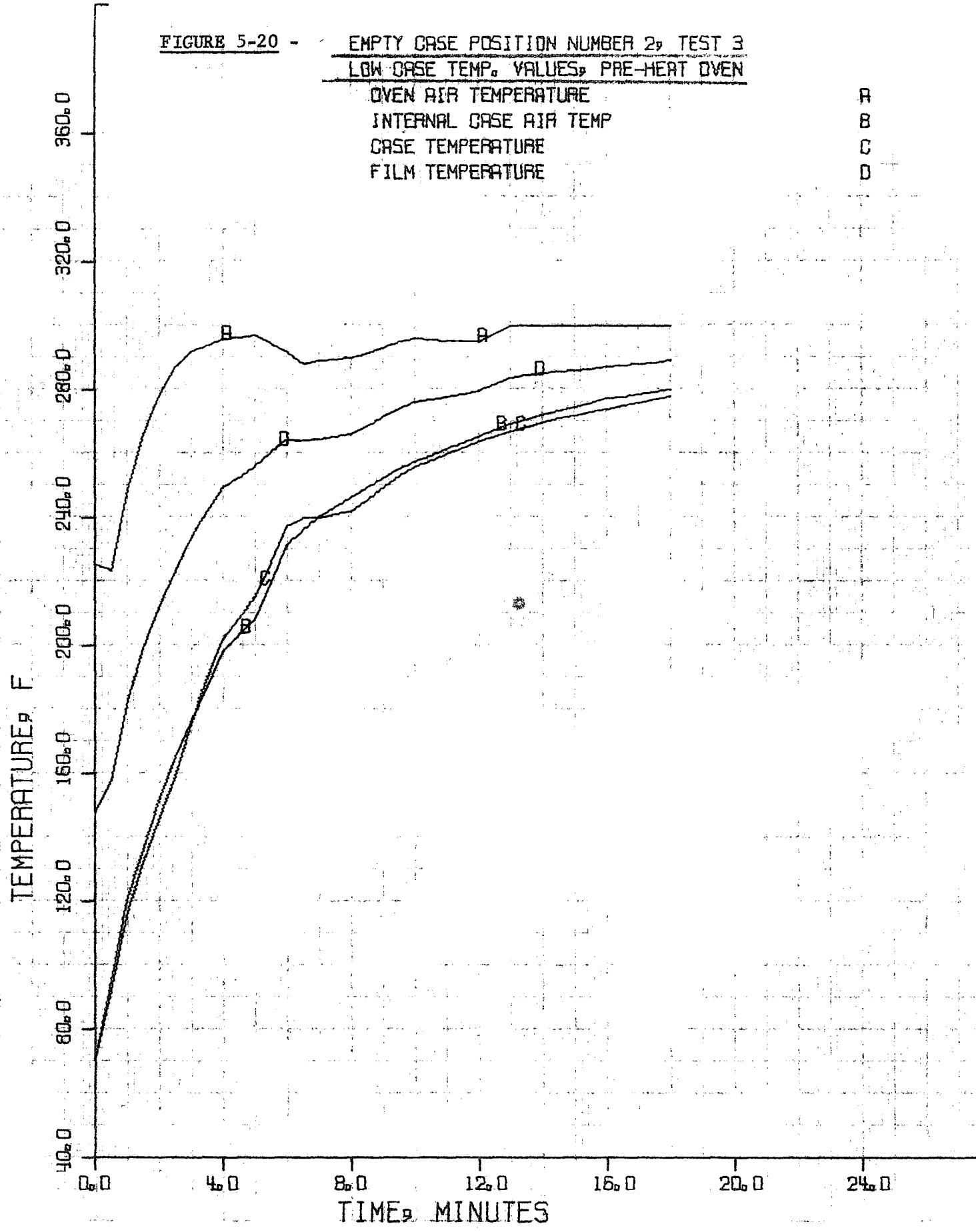

# STERILIZABLE MOTOR EMPTY CASE TEST

FIGURE 5-21 - EMPTY CASE POSITION NUMBER 2, TEST 3
HIGH CASE TEMP VALUES, PRE-HEAT OVEN

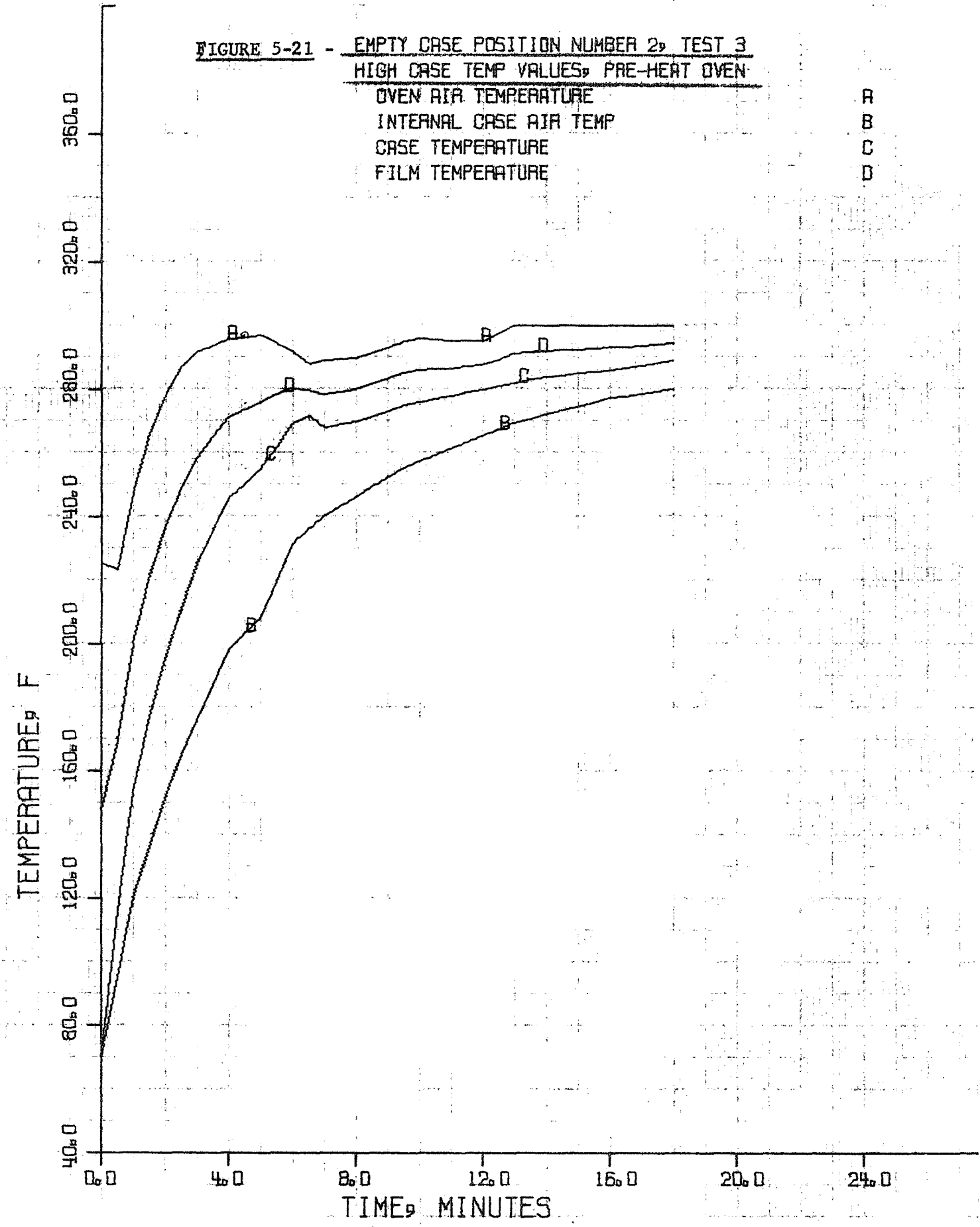

# STERILIZABLE MOTOR EMPTY CASE TEST

FIGURE 5-22 - EMPTY CASE POSITION NUMBER 2, TEST 3
LOW CASE TEMP. VALUES, PRE-HEAT OVEN, HTC RESULTS
OUTSIDE HTC, BTU/HR FT**2 F A

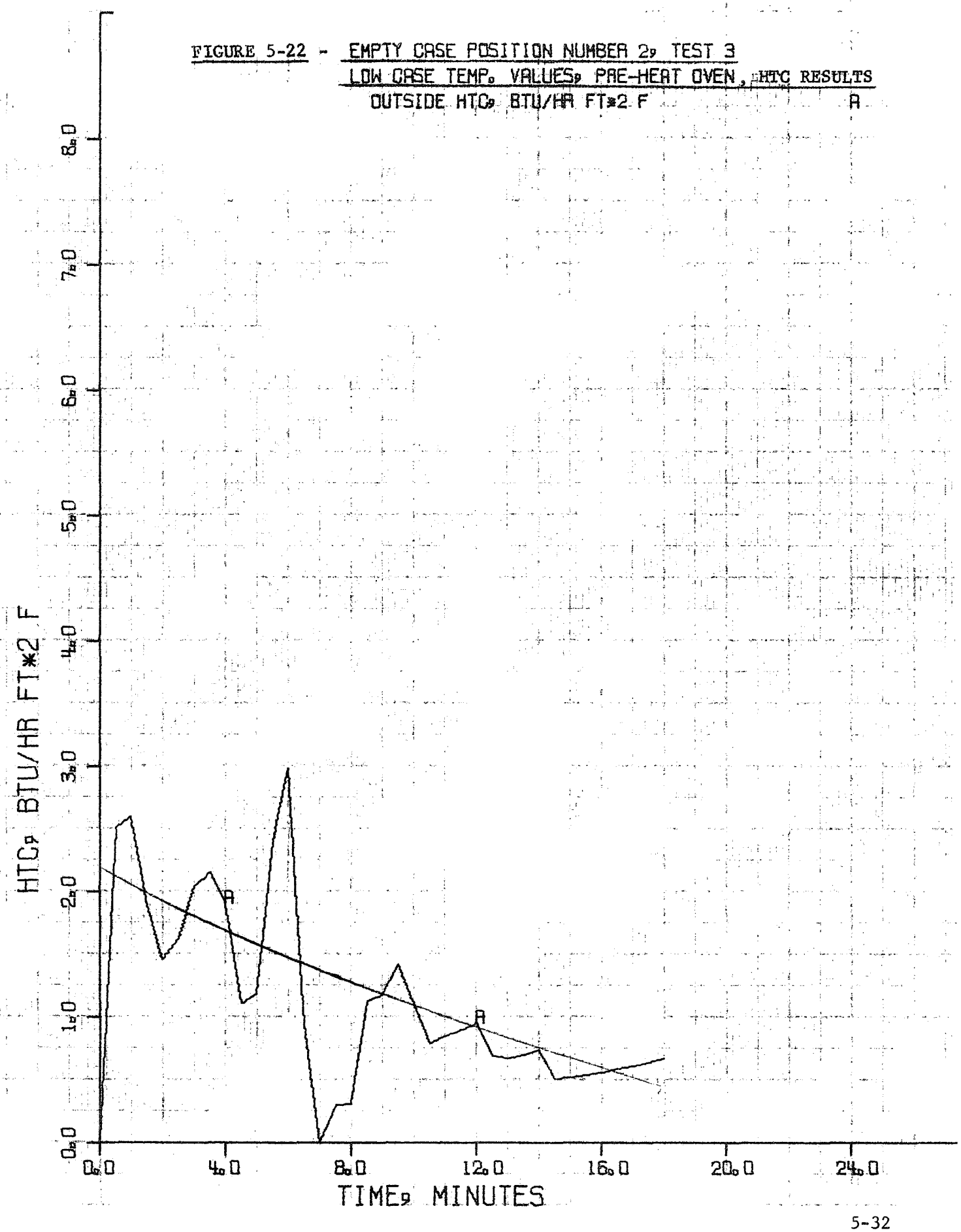

# STERILIZABLE MOTOR EMPTY CASE TEST

FIGURE 5-23 - EMPTY CASE POSITION NUMBER 2, TEST 3
HIGH CASE TEMP VALUES, PRE-HEAT OVEN , HTC RESULTS
OUTSIDE HTC, BTU/HR FT**2 F

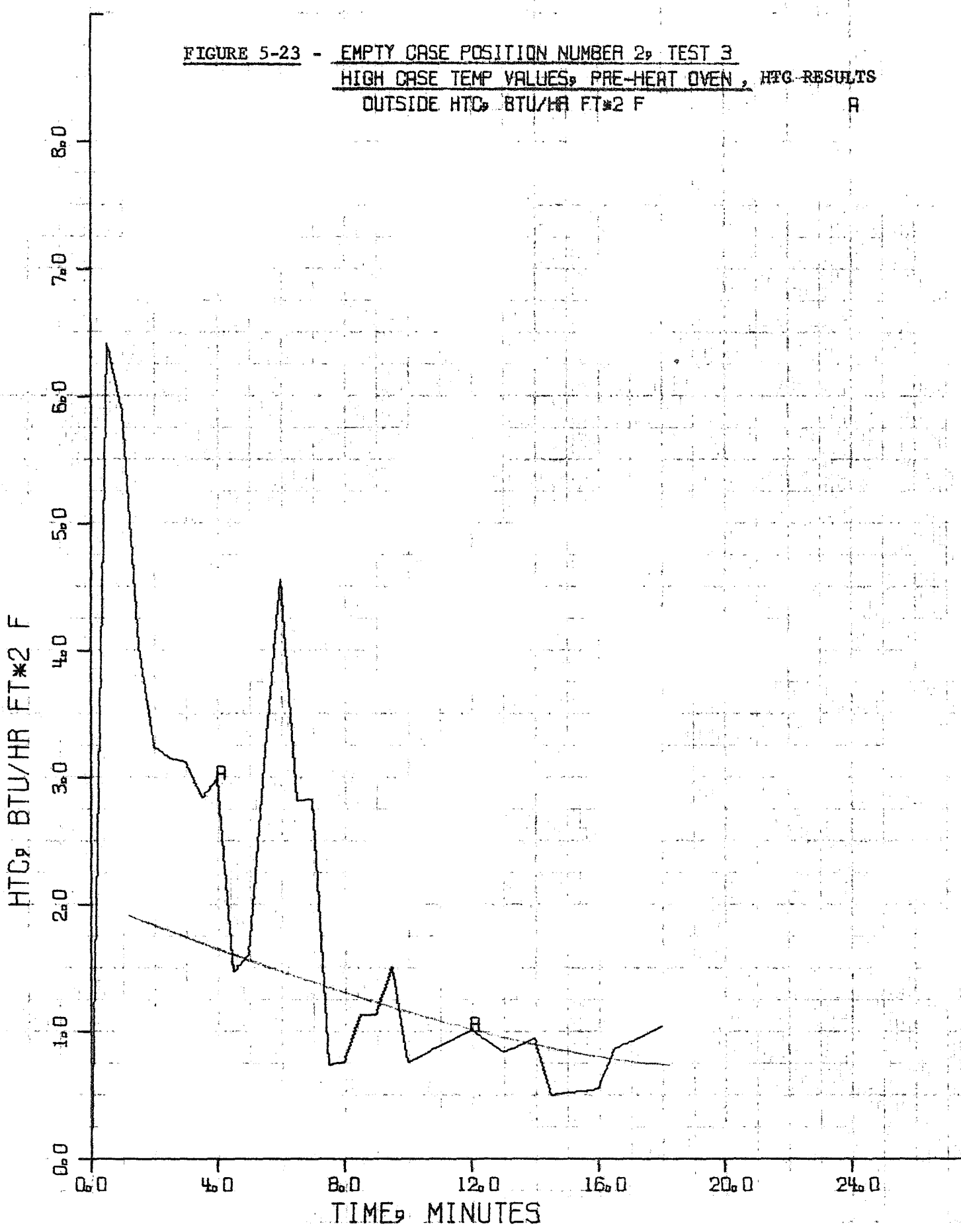

# STERILIZABLE MOTOR EMPTY CASE TEST

FIGURE 5-24 - EMPTY CASE POSITION NUMBER 3, TEST 4

LOW CASE TEMPERATURE VALUES

| | |
|---|---|
| OVEN AIR TEMPERATURE | A |
| INTERNAL CASE AIR TEMP | B |
| CASE TEMPERATURE | C |
| FILM TEMPERATURE | D |

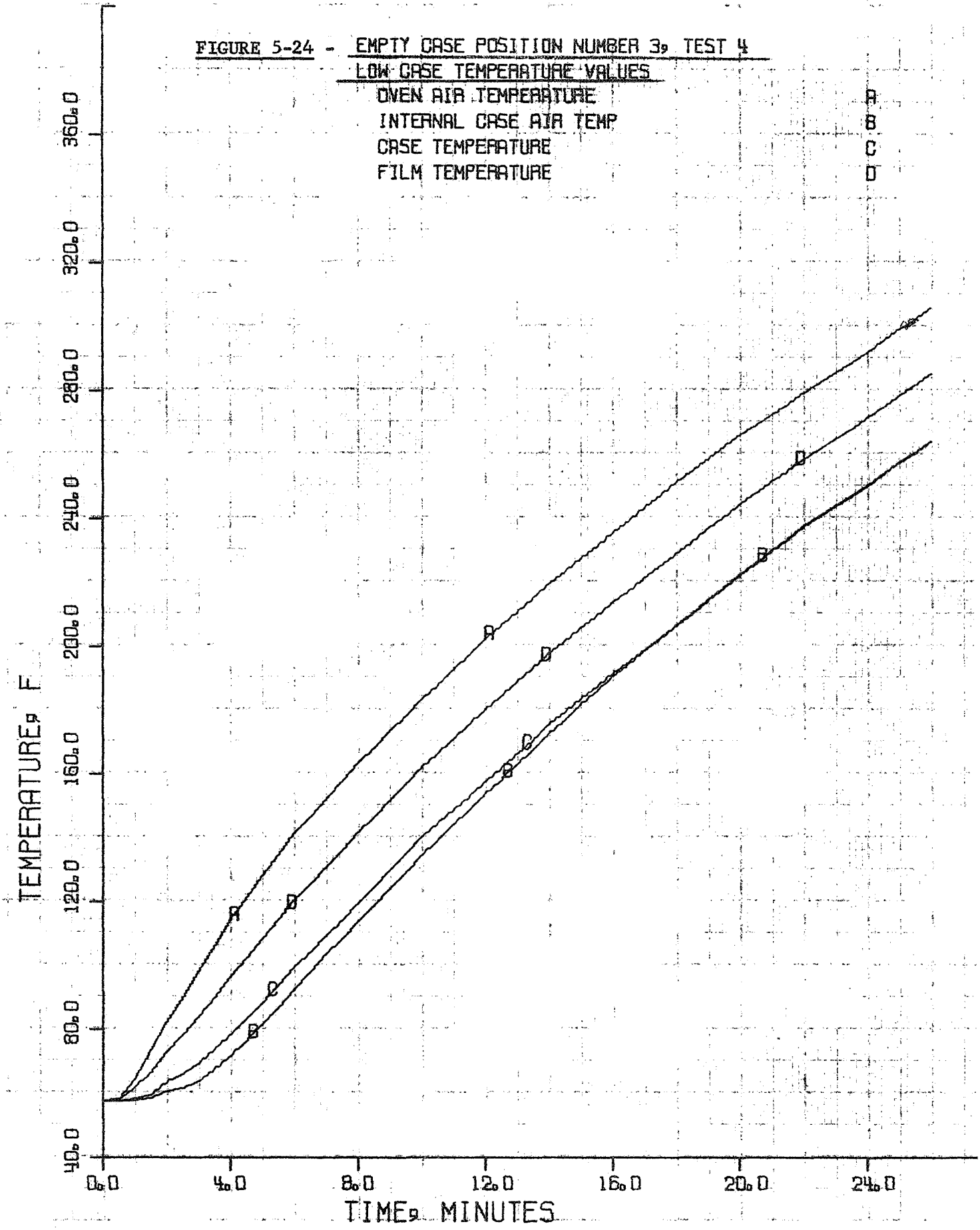

# STERILIZABLE MOTOR EMPTY CASE TEST

FIGURE 5-25 - EMPTY CASE POSITION NUMBER 3, TEST 4
HIGH CASE TEMPERATURE VALUES

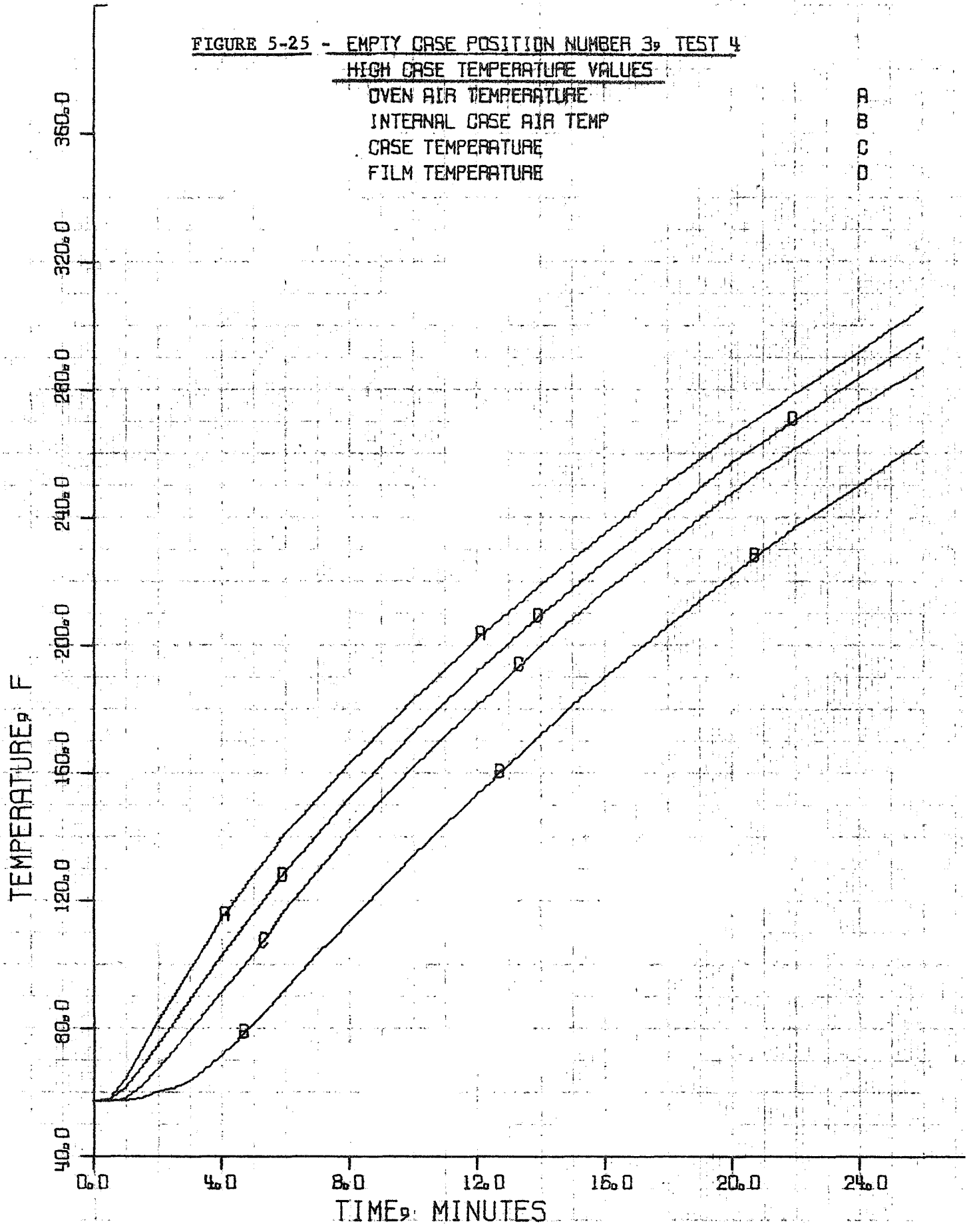

# STERILIZABLE MOTOR EMPTY CASE TEST

FIGURE 5-26 - EMPTY CASE POSITION NUMBER 3, TEST 4
LOW CASE TEMPERATURE VALUES, HTC RESULTS
OUTSIDE HTC, BTU/HR FT**2 F

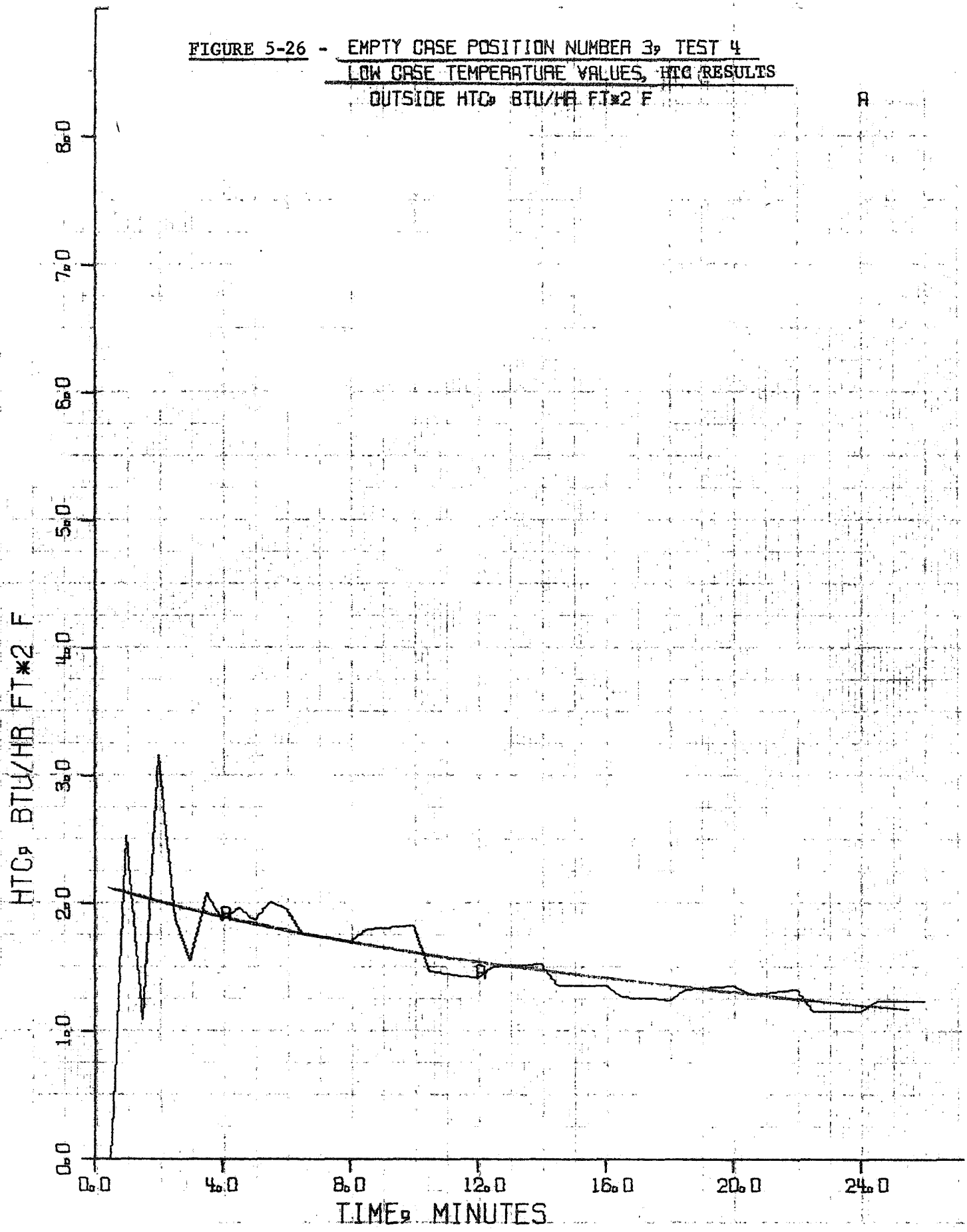


2

# STERILIZABLE MOTOR EMPTY CASE TEST

FIGURE 5-27 - EMPTY CASE POSITION NUMBER 3, TEST 4
HIGH CASE TEMPERATURE VALUES, HTC RESULTS
OUTSIDE HTC, BTU/HR FT**2 F

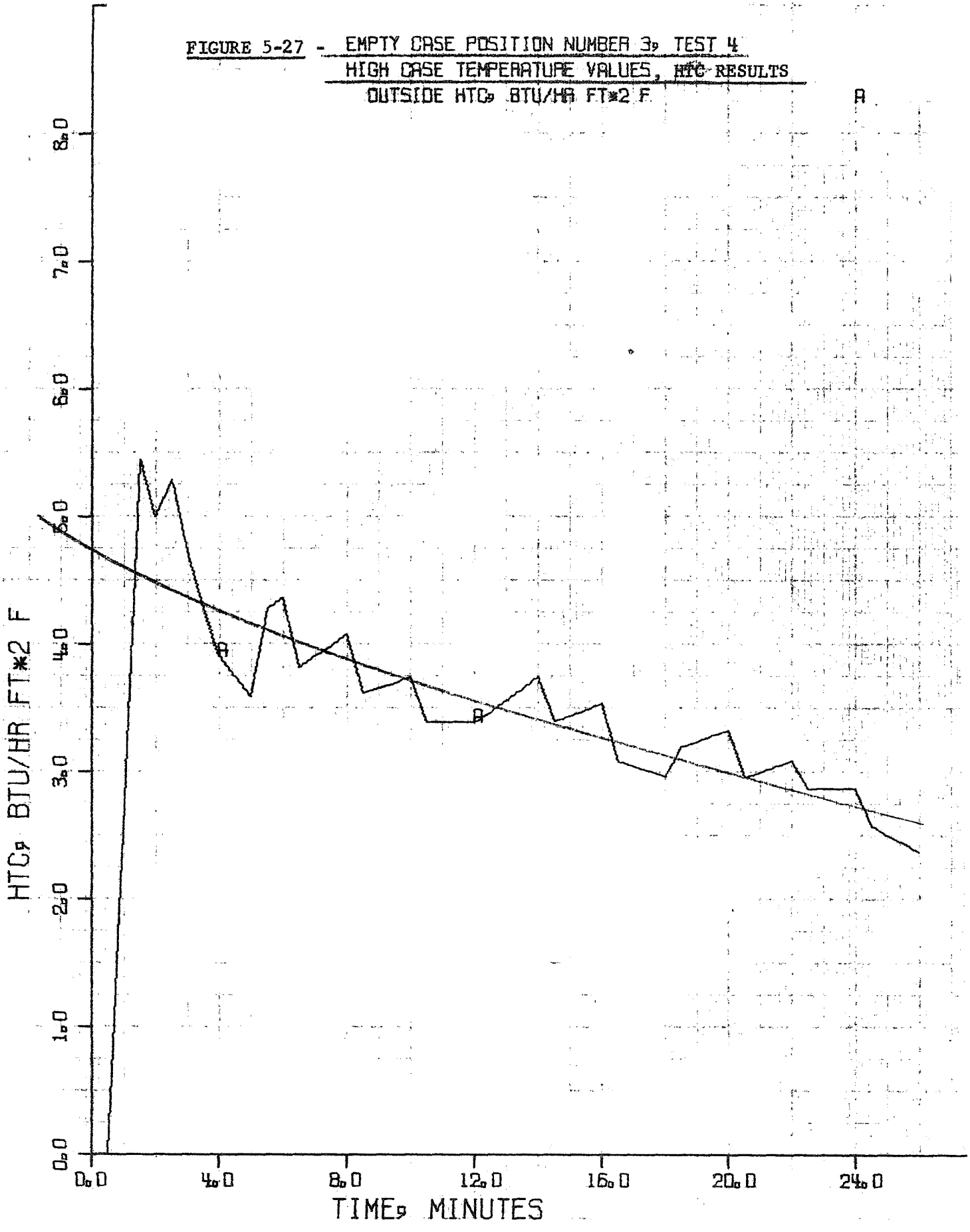

10 APR 1969

# STERILIZABLE MOTOR EMPTY CASE TEST

FIGURE 5-28 - EMPTY CASE POSITION NUMBER 4, TEST 5
LOW CASE TEMPERATURE VALUES

| | |
|---|---|
| OVEN AIR TEMPERATURE | A |
| INTERNAL CASE AIR TEMP | B |
| CASE TEMPERATURE | C |
| FILM TEMPERATURE | D |

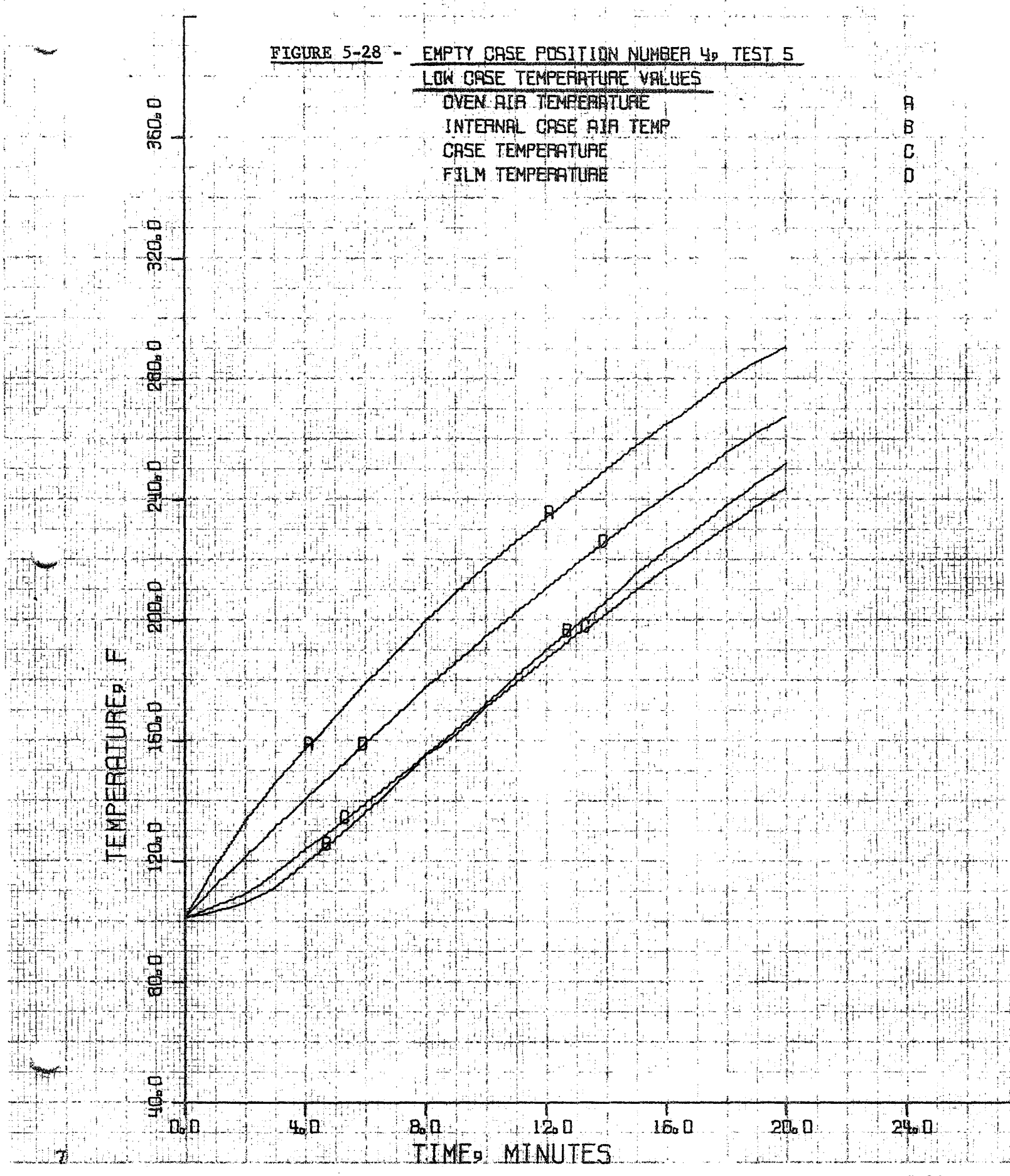

# STERILIZABLE MOTOR EMPTY CASE TEST

FIGURE 5-29 - EMPTY CASE POSITION NUMBER 4, TEST 5

HIGH CASE TEMPERATURE VALUES

| | |
|---|---|
| OVEN AIR TEMPERATURE | A |
| INTERNAL CASE AIR TEMP | B |
| CASE TEMPERATURE | C |
| FILM TEMPERATURE | D |

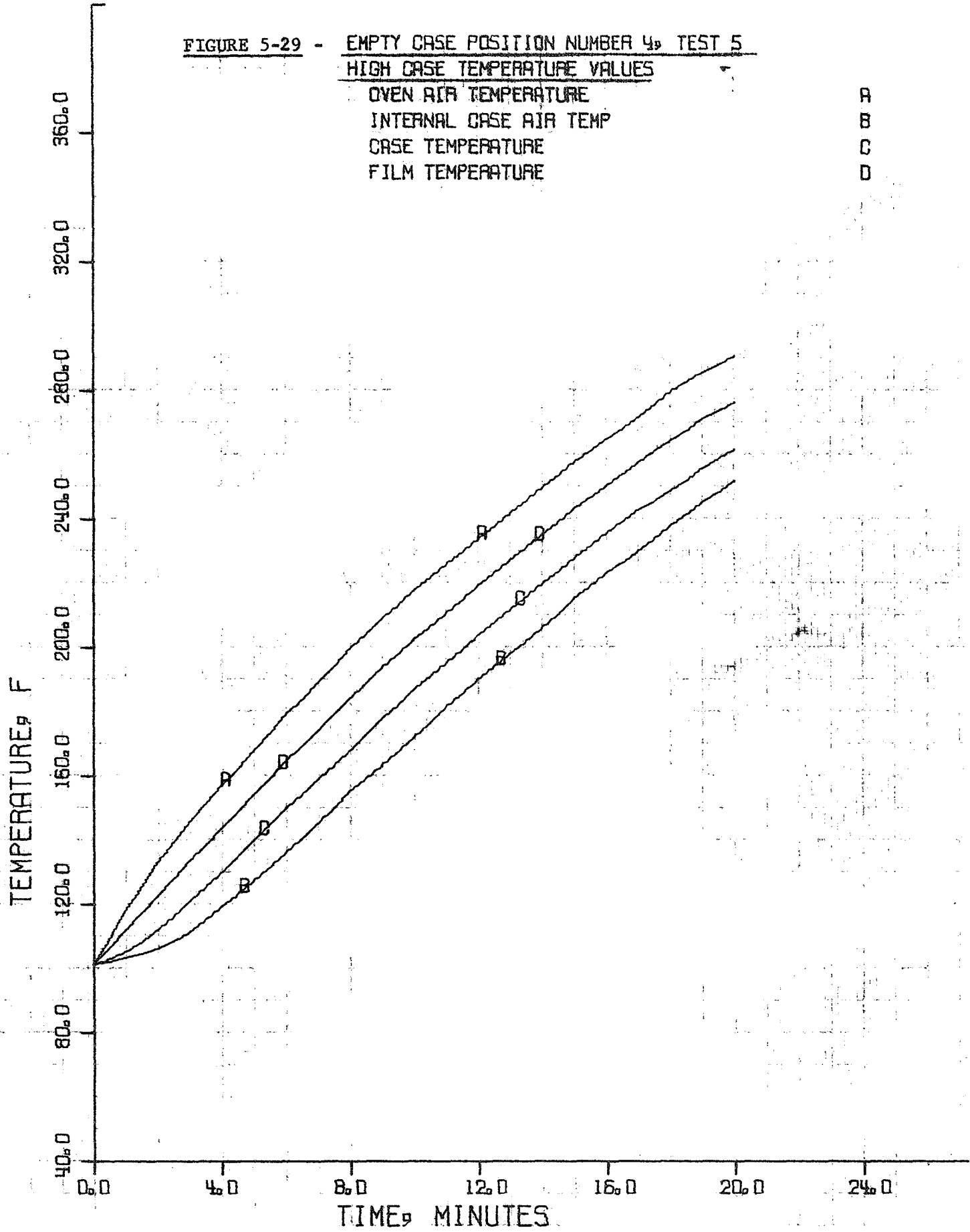

# STERILIZABLE MOTOR EMPTY CASE TEST

FIGURE 5-30 - EMPTY CASE POSITION NUMBER 4, TEST 5
LOW CASE TEMPERATURE VALUES, HTC RESULTS
OUTSIDE HTC, BTU/HR FT**2 F

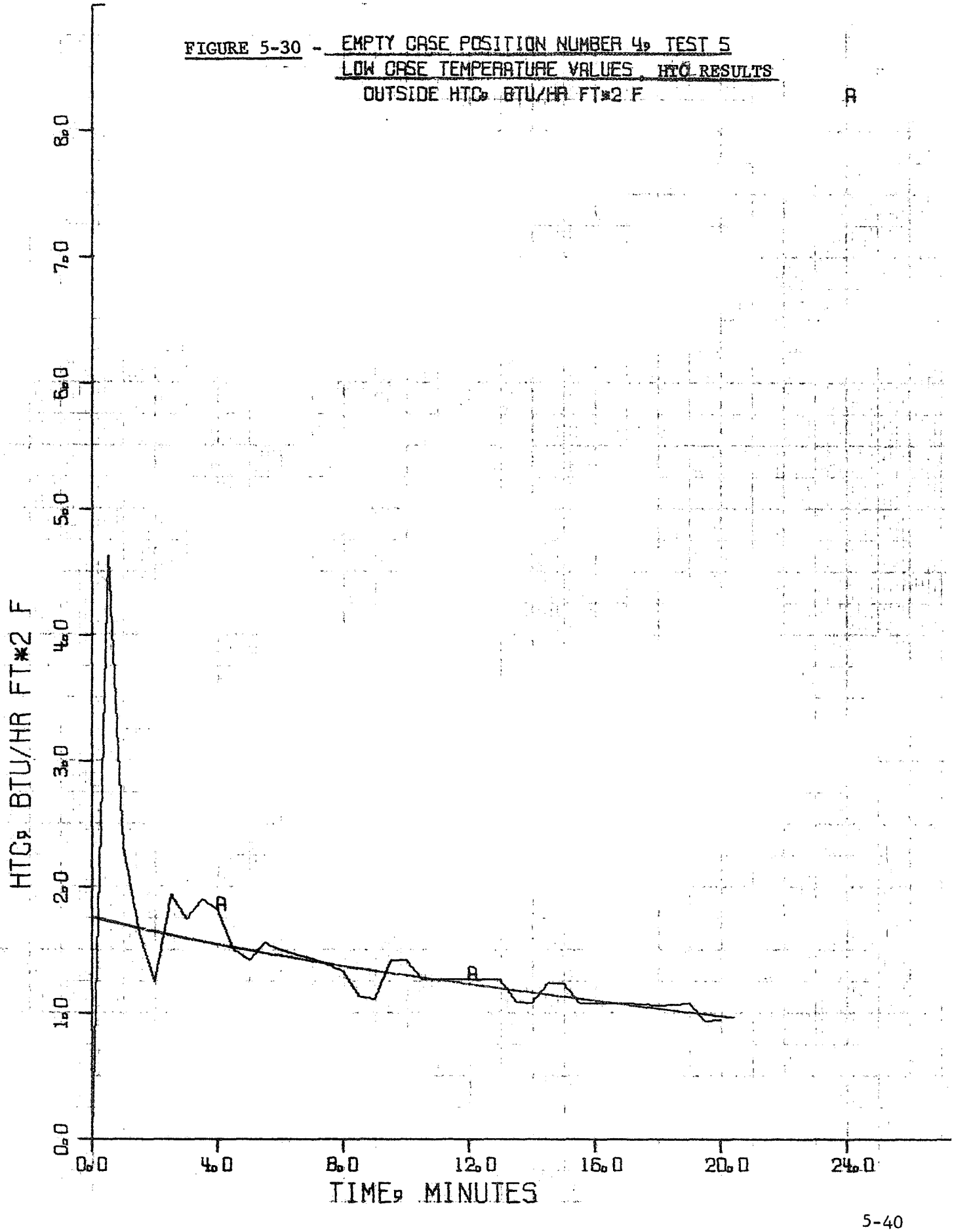

# STERILIZABLE MOTOR EMPTY CASE TEST

FIGURE 5-31 - EMPTY CASE POSITION NUMBER 4, TEST 5
HIGH CASE TEMPERATURE VALUES, HTC RESULTS
OUTSIDE HTC, BTU/HR FT*2 F

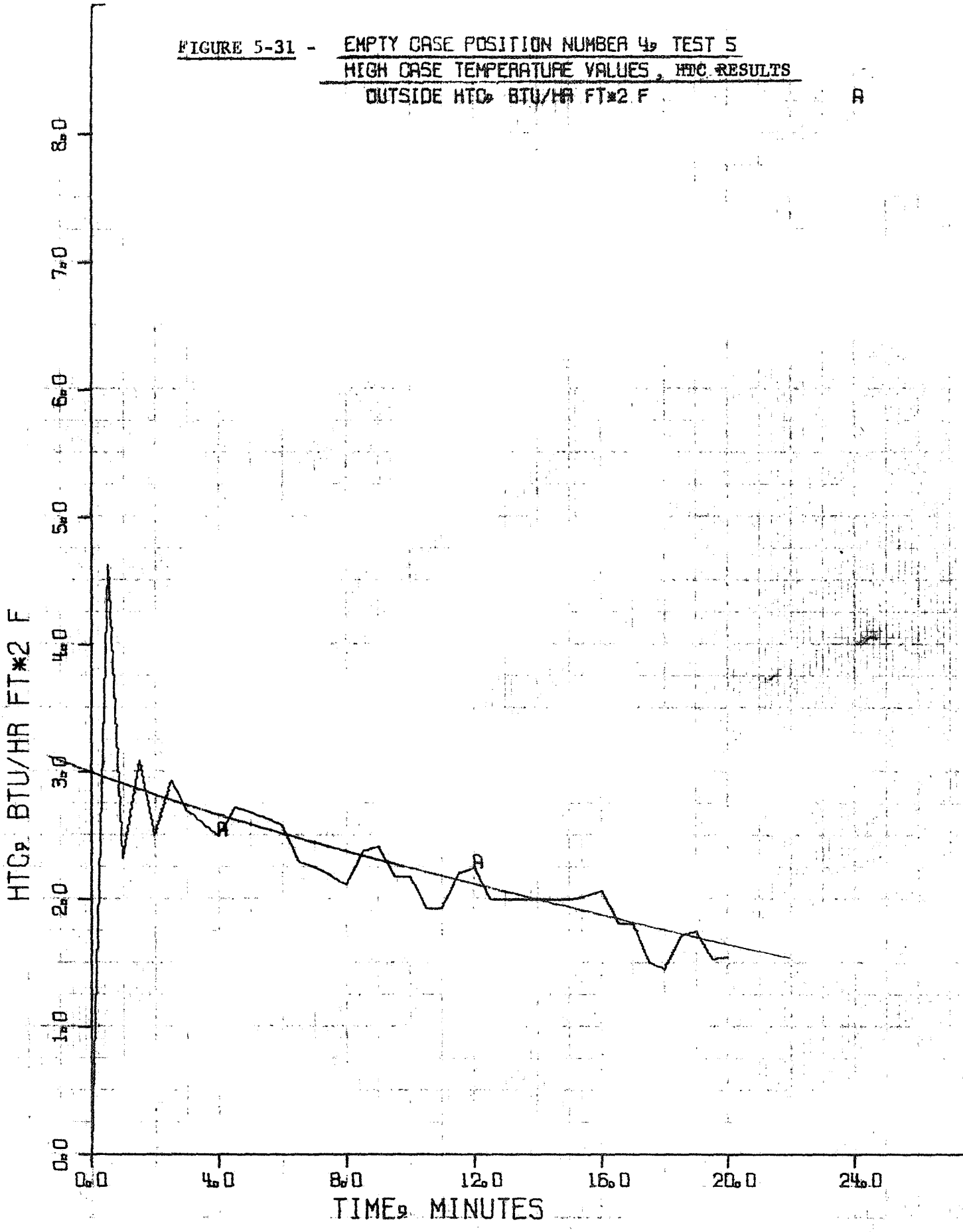

# STERILIZABLE MOTOR EMPTY CASE TEST

FIGURE 5-32 - EMPTY CASE POSITION NUMBER 4, TEST 5
COOL DOWN TEST

| | |
|---|---|
| OVEN AIR TEMPERATURE | A |
| INTERNAL CASE AIR TEMP | B |
| CASE TEMPERATURE | C |
| FILM TEMPERATURE | D |

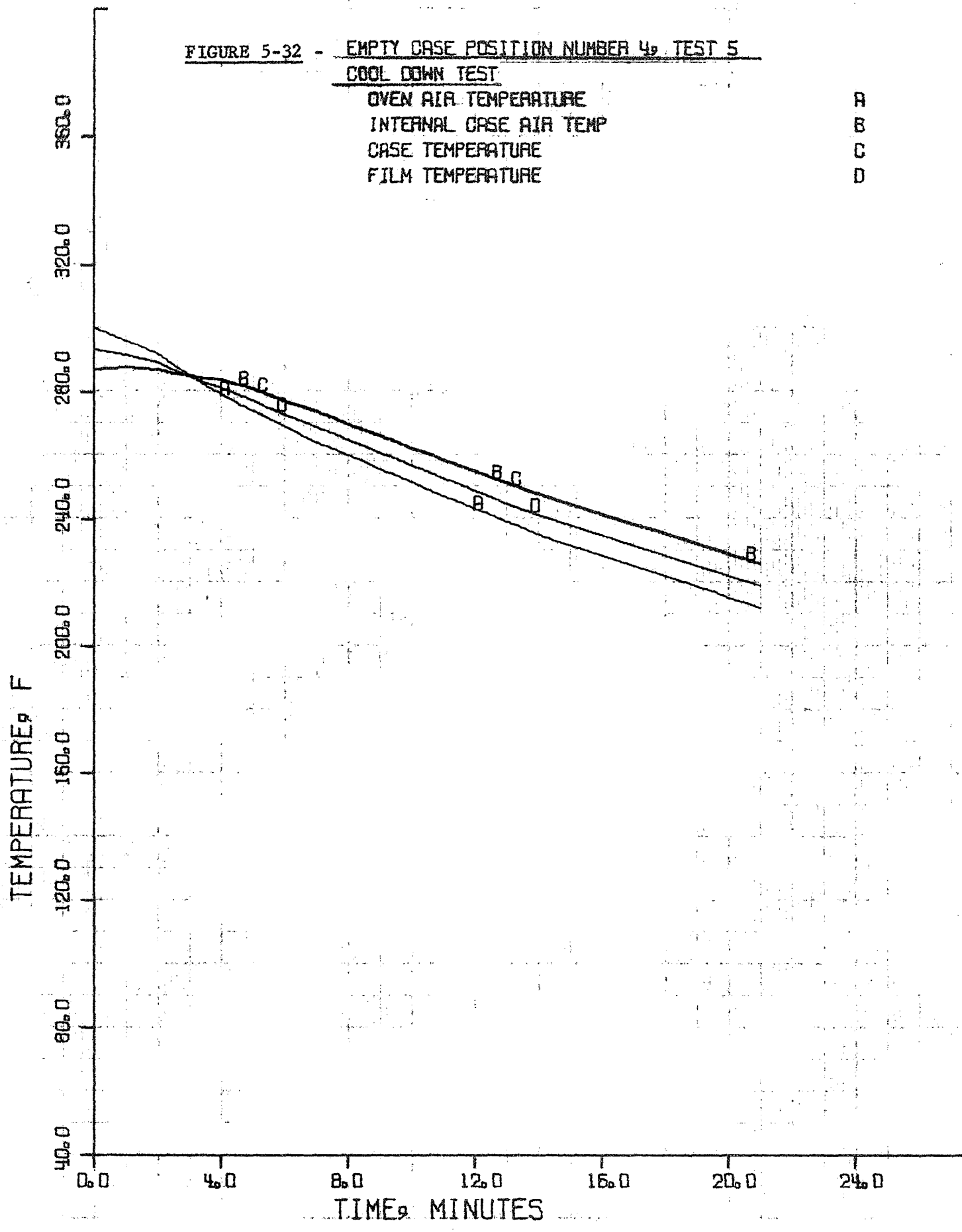

# STERILIZABLE MOTOR EMPTY CASE TEST

FIGURE 5-33 - EMPTY CASE POSITION NUMBER 4, TEST 5
COOL DOWN TEST, HTC RESULTS
OUTSIDE HTC, BTU/HR FT**2 F

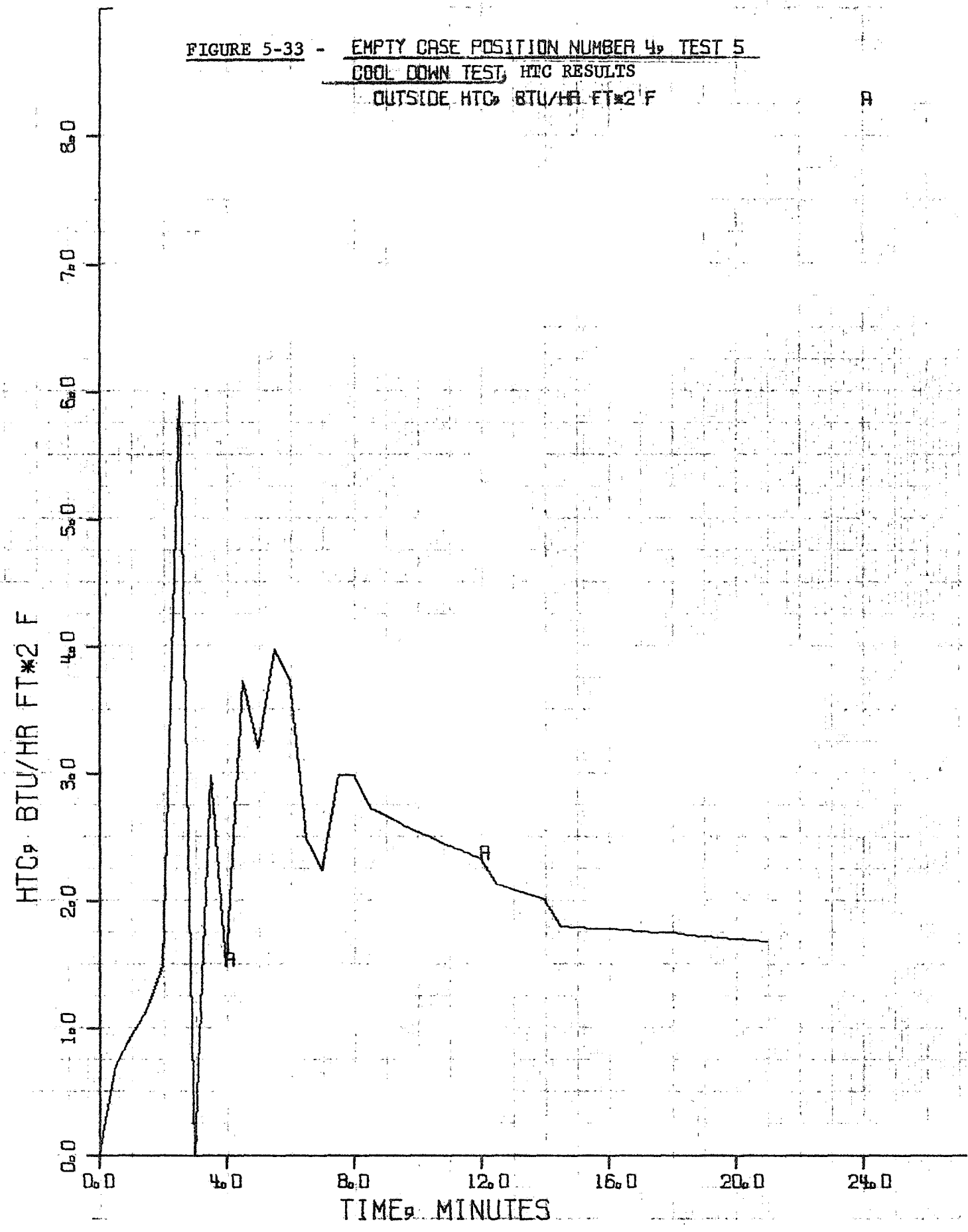

## 5.3 OVEN TESTS USING AN INERT PROPELLANT MOTOR

Following the tests using the empty motor case, oven heating tests were conducted using a motor case loaded with an inert propellant in the configuration shown in figure 5-9. The tests were designed to accomplish:

A. A more refined determination of the external surface heat transfer coefficients; this should be possible due to the slower response of the case wall when backed by propellant.

B. Verification of the in-depth heat conduction model used to predict temperature profiles through the grain.

The external surface of the loaded motor case was instrumented with thermocouples in the same way as the empty case, as shown in figure 5-9. In addition, thermocouples were placed in contact with the inside grain surface and within the grain itself. These locations are also shown in figure 5-9. As with the empty motor case test, two thermocouples were used to record the oven air temperature, one forward and one aft of the case with respect to flow of air in the oven. Using the temperature responses of the case and the appropriate air temperature, heat transfer coefficients were calculated for the fastest and slowest responding points on the case. These calculations were performed by a one-dimensional axisymmetric heat conduction program (LA15ZAZ), described in section 5.1, using its capability to back out the heat transfer coefficient required to produce the surface temperature measured in the test. The heat conduction program was also used to determine the in-depth thermal response of the grain. Figure 5-34 shows temperature profiles across the grain at the fastest responding point at various times in the cycle. Figure 5-35 shows the gas temperature, internal surface, and interface temperature between the grain and liner as a function of time for

# INERT GRAIN STERILIZABLE MOTOR

FIGURE 5-34- TEST 1, POSITION 1, HIGH CASE

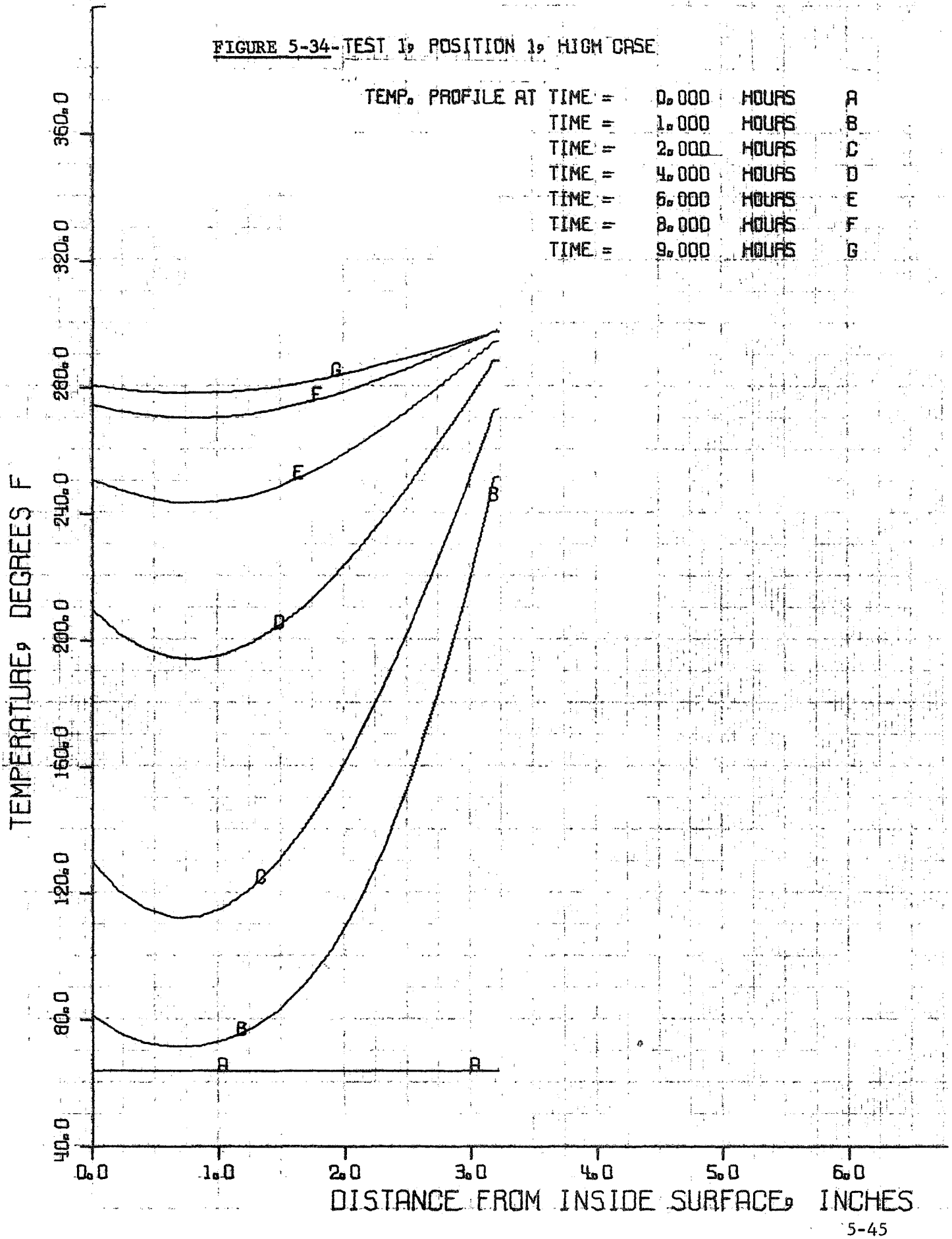

# INERT GRAIN STERILIZABLE MOTOR

FIGURE 5-35 - TEST 1, POSITION 1, HIGH CASE

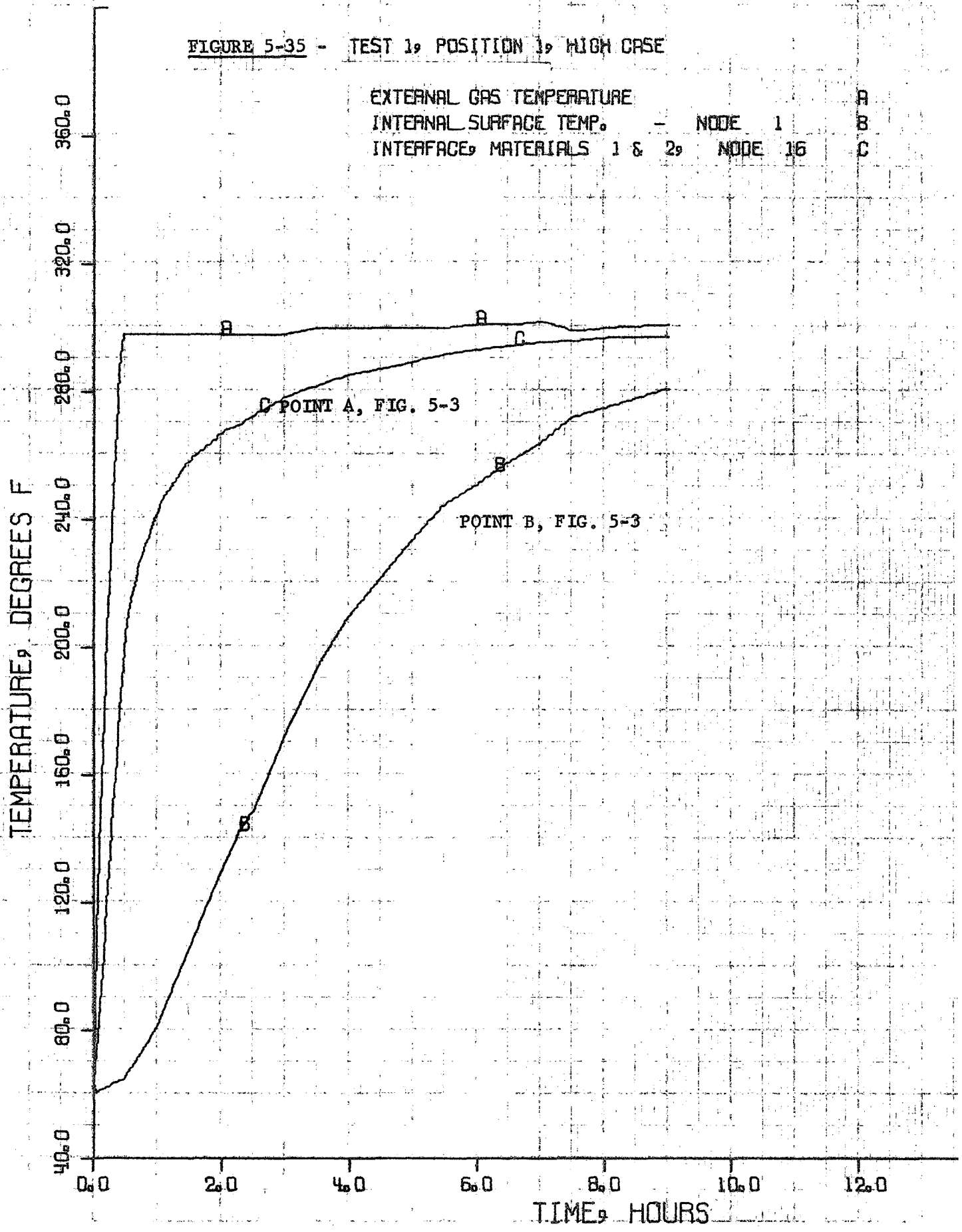

the first oven cycle using the inert propellant. The thermocouples placed within the grain yielded no useful results apparently due to either electrical shorts between the thermocouple wire and the motor case or due to the crack which appeared in the grain during the heating cycle.

Although the propellant grain failed structurally during the first oven heating cycle, the test objective of refining the determination of external heat transfer coefficients was met. During the first oven heating cycle, the test motor was placed in oven position 1, as shown in figure 5-10. A second oven heating cycle was run with the test motor in oven position 2. The crack in the grain was not expected to have a significant effect on the heat transfer between the oven air and the external motor. The heat transfer coefficients calculated from these two oven cycle runs had smaller variations and were more repeatable than those determined using the empty motor. The temperature responses and heat transfer coefficients calculated for the fastest and slowest responding points on the external surface are shown in figures 5-35 through 5-42. The coefficients calculated are considerably higher than those obtained in the empty case tests ranging between roughly 2.0 and 6.0 Btu/ft$^2$-hr-°F at the slowest responding point and between 6.0 and 12.0 Btu/ft$^2$-hr-°F at the fastest responding point. The heat transfer coefficient calculations require a knowledge of the thermal conductivity of the propellant. Before the inert grain was cast, thermal conductivity measurements were made using a modified Cenco-Fitch thermal conductivity apparatus.

It is possible, however, that the thermal conductivity of the propellant undergoes changes during the sterilization heating cycle. Such a change in thermal conductivity could account for the differences between

# INERT GRAIN STERILIZABLE MOTOR

FIGURE 5-36 - TEST 1, POSITION 1, HIGH CASE

EXTERNAL SURF. HEAT TRANSFER COEFFICIENT A

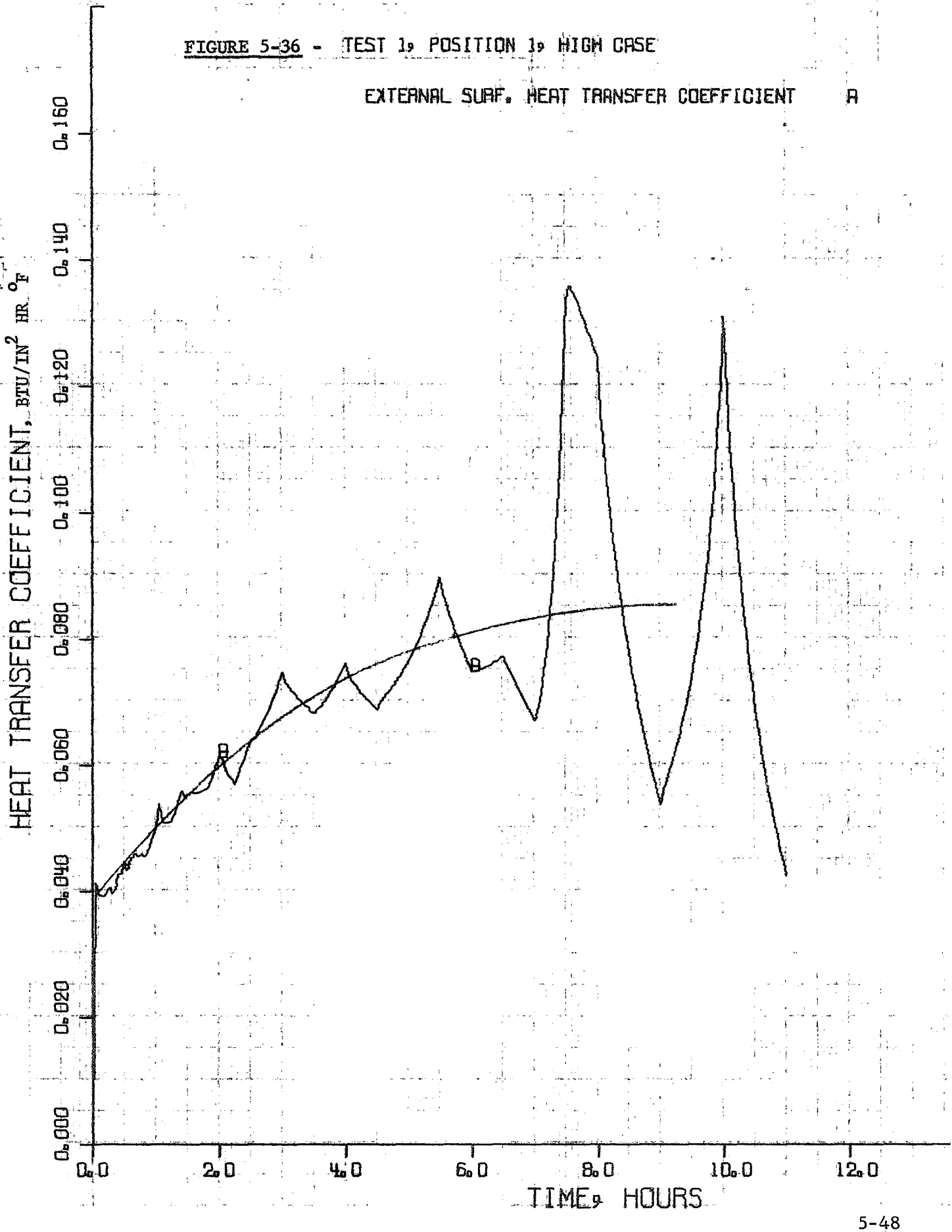

# INERT GRAIN STERILIZABLE MOTOR

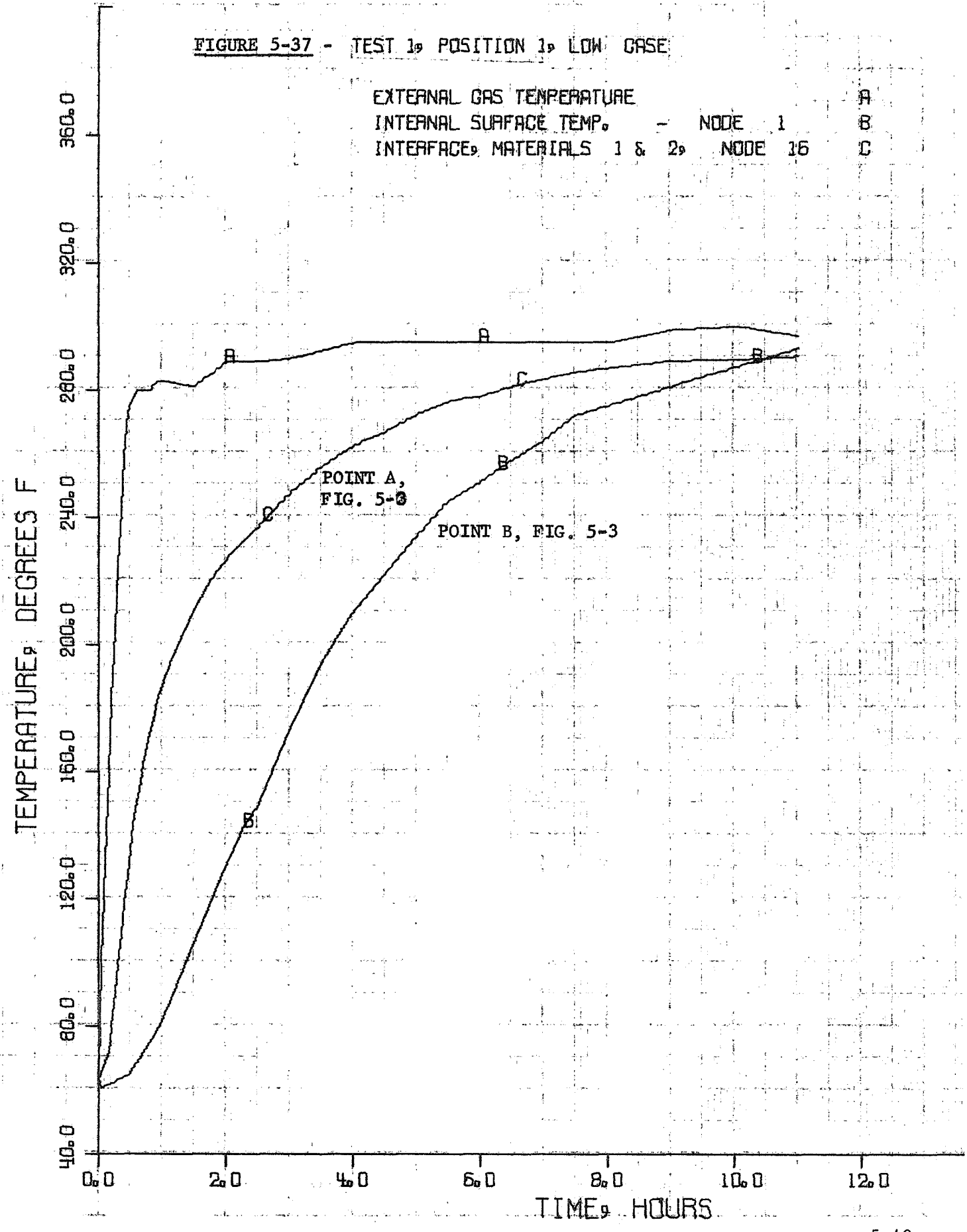

# INERT GRAIN STERILIZABLE MOTOR

FIGURE 5-38 - TEST 1, POSITION 1, LOW CASE

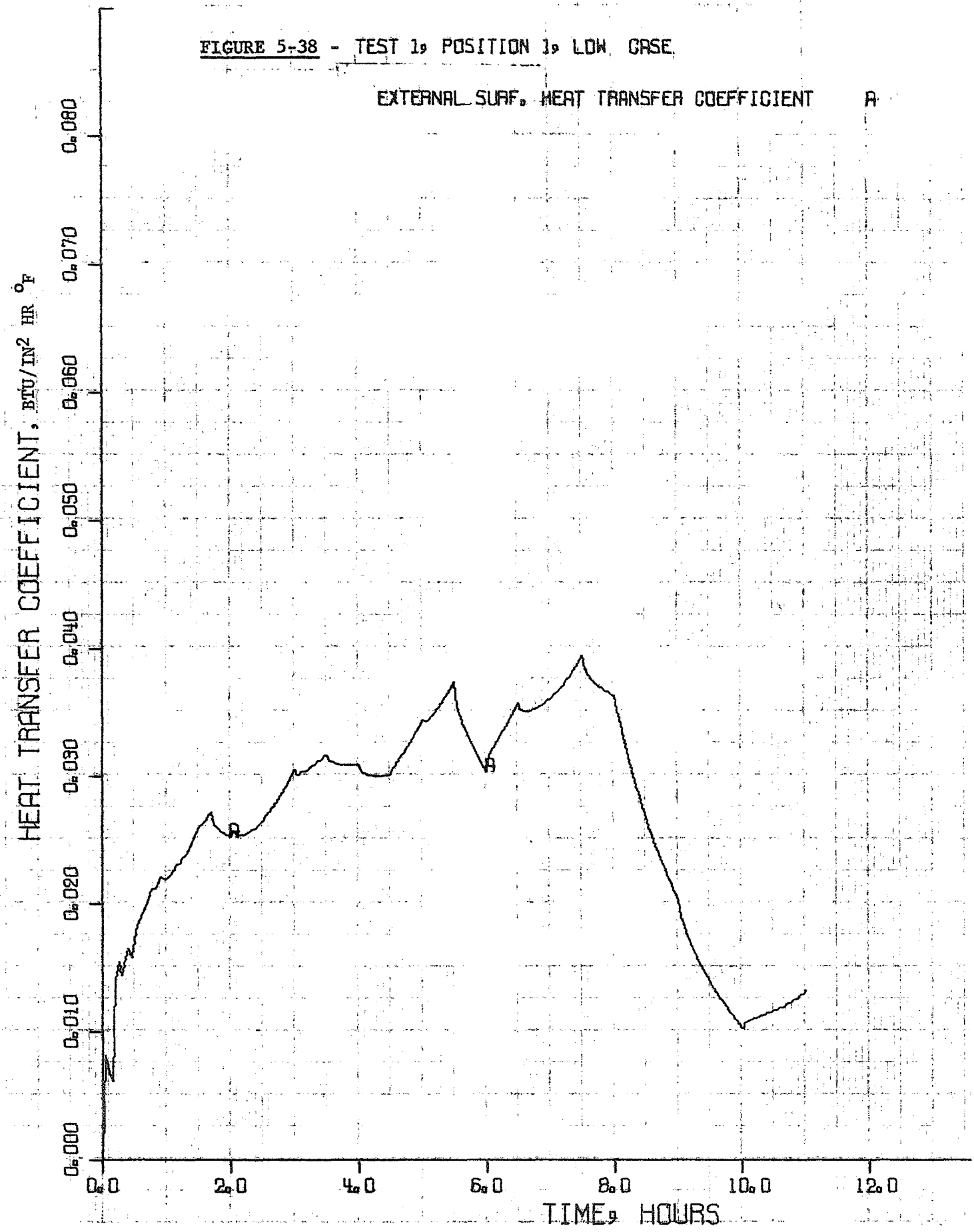

# INERT GRAIN STERILIZABLE MOTOR

FIGURE 5-39 - TEST 2, POSITION 2, LOW CASE

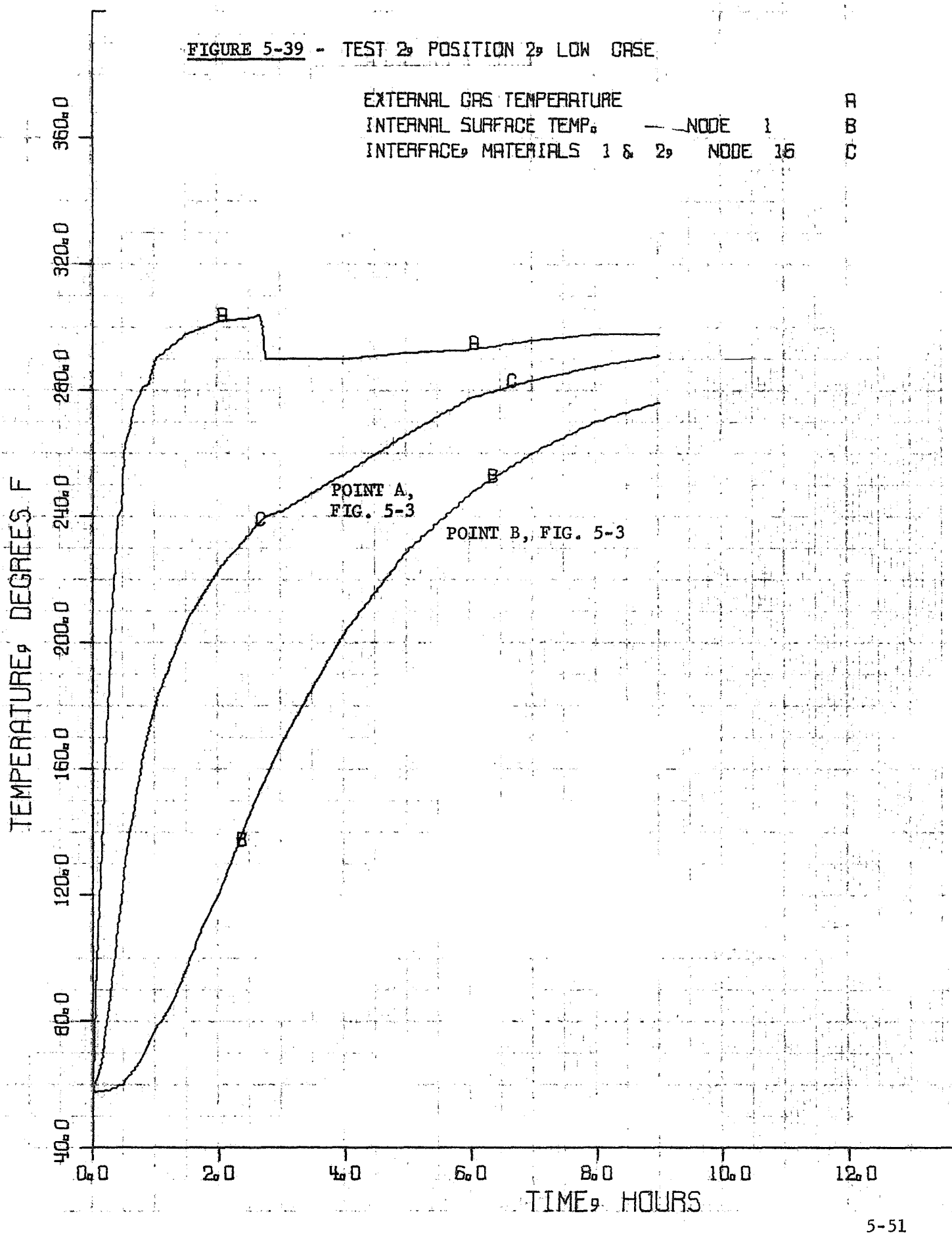

# INERT GRAIN STERILIZABLE MOTOR

FIGURE 5-40 - TEST 2, POSITION 2, LOW CASE

EXTERNAL SURF. HEAT TRANSFER COEFFICIENT A

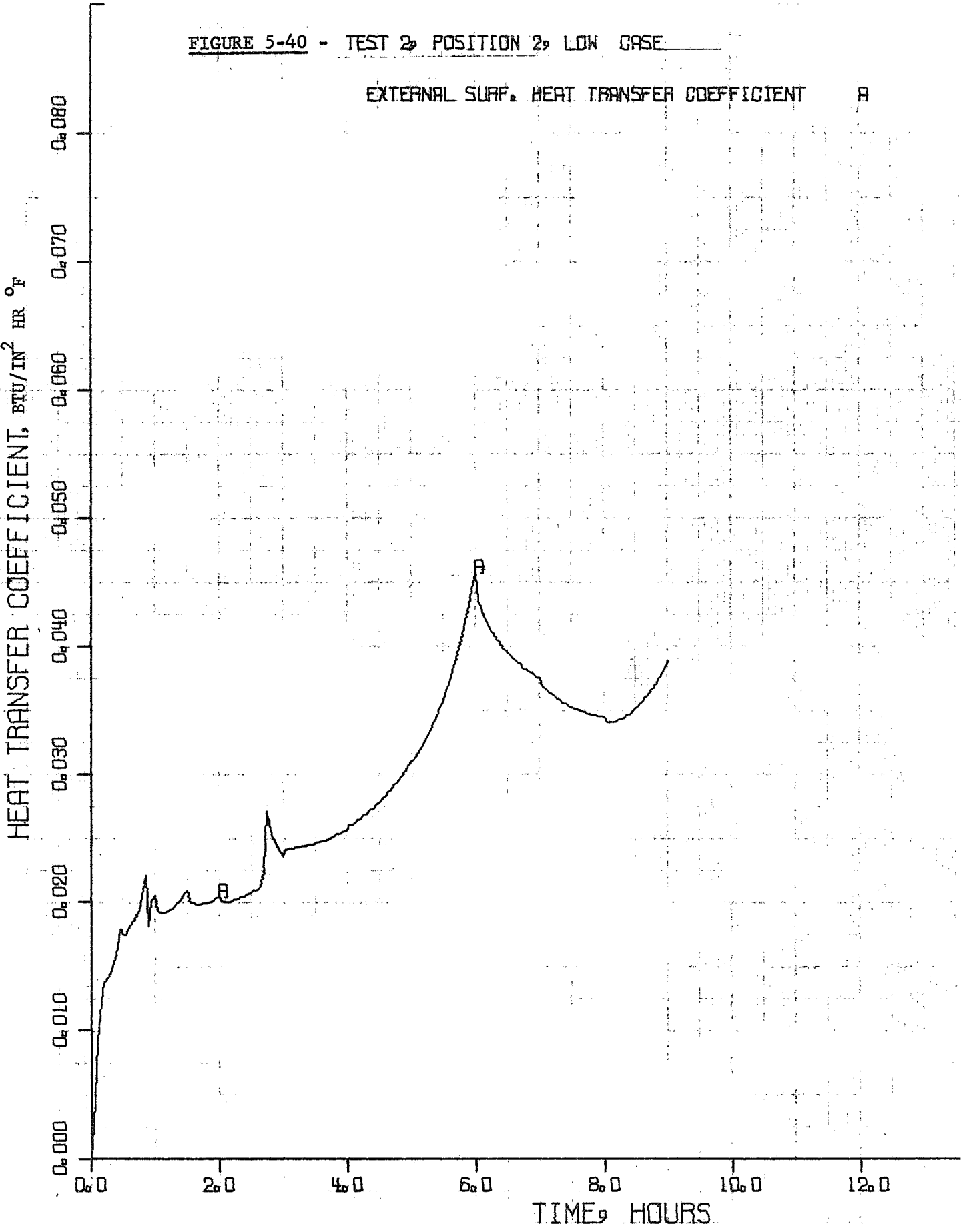

# INERT GRAIN STERILIZABLE MOTOR

FIGURE 5-41 - TEST 2, POSITION 2, HIGH CASE

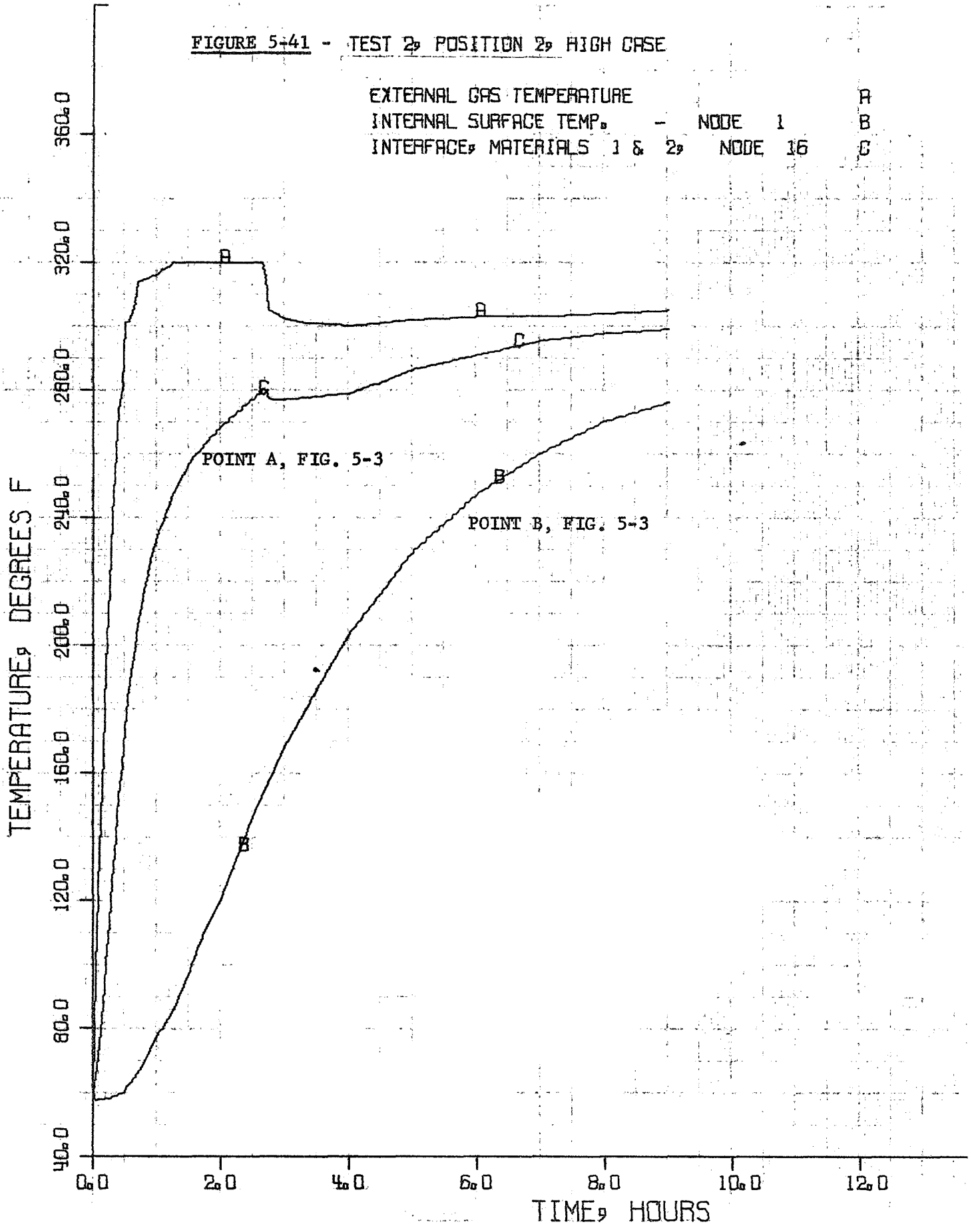

# INERT GRAIN STERILIZABLE MOTOR

FIGURE 5-42 - TEST 2, POSITION 2, HIGH CASE

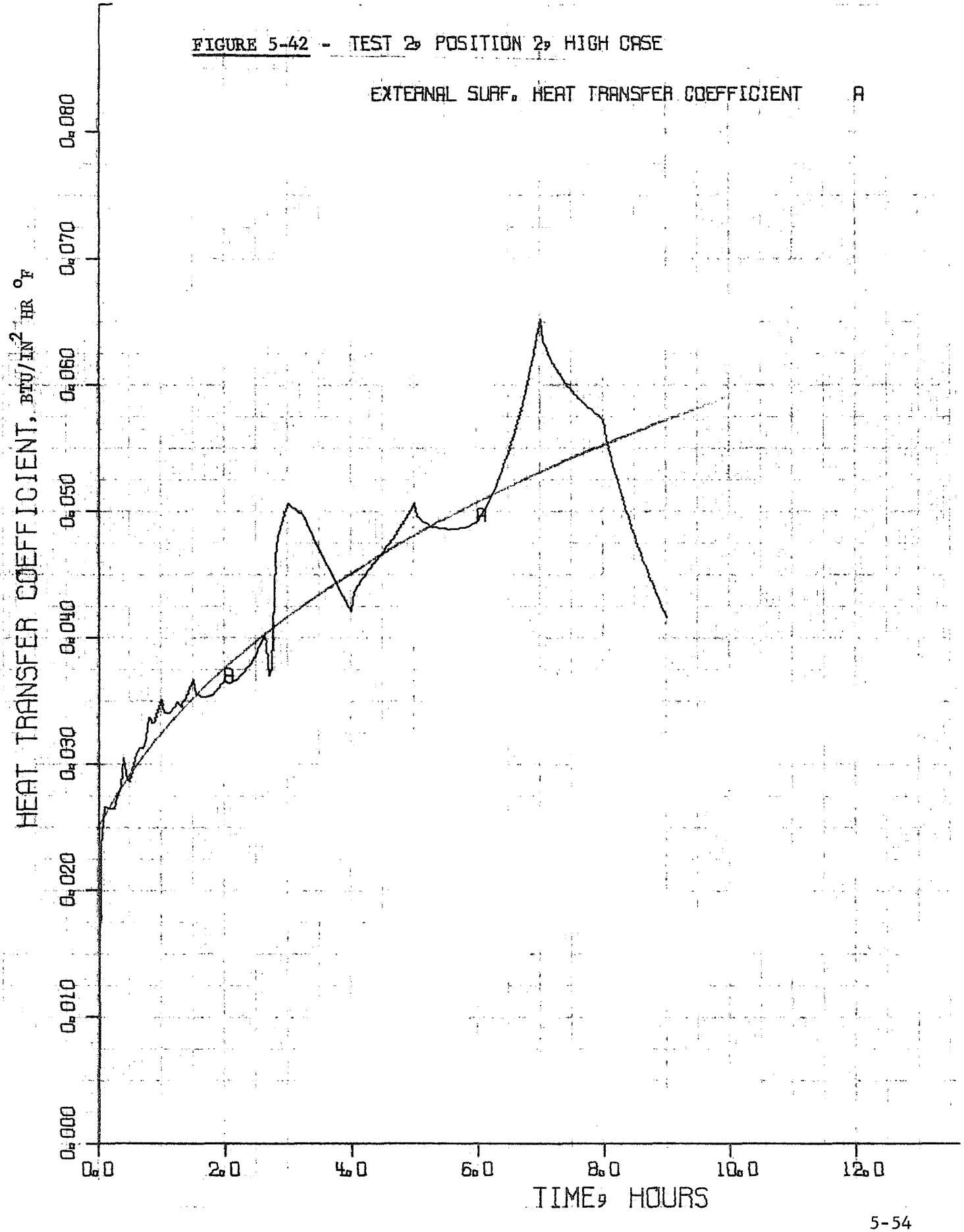

the heat transfer coefficients calculated from the empty motor case tests and those calculated from the tests using inert propellant, since knowledge of the thermal conductivity is an integral part of the process whereby the heat transfer coefficients are determined.

The second objective of the inert propellant oven tests, verification of the in-depth heat conduction, was only partially satisfied because of the failure of the thermocouples within the grain.

## 5.4 STERILIZATION HEATING CYCLE USING LIVE PROPELLANT

After the structural failure of the inert propellant grain, the live grain was reexamined for structural failure modes. Heating cycles were designed to minimize the difference in mean bulk temperature between the motor case and the propellant grain. Three manually controlled step changes in oven air temperature were used. Numerous cycles were evaluated for stress and degradation resulting in a heating cycle selected for the first live propellant sterilization cycle. This cycle included an oven air temperature of 190°F for 6 hr, followed by an increase to 235°F for 6 hr, then to 300°F for 8 hr, and finally lowered to 275°F and remain at that level for the remainder of the cycle. The first live grain motor was placed in oven position 1 and subjected to the heating cycle. The thermocouple data from the test were reduced and are shown in figure 5-43 along with the grain mean bulk temperature obtained from a one-dimensional heat conduction analysis. Figure 5-44 presents the thermal profiles at various times during the cycle. These plots are for the fastest responding point on the motor. Figures 5-45 and 5-46 show the predicted response for the slowest and fastest responding points on the motor based on heat transfer coefficients calculated from the

# LIVE GRAIN STERILIZABLE MOTOR

FIGURE 5-43

FIRST CYCLE, POSITION 1, IMPRESSED
HEAT CONDUCTION RUN USING FIRST LIVE MOTOR DATA

| | |
|---|---|
| EXTERNAL GAS TEMPERATURE | A |
| EXTERNAL SURFACE TEMP. - NODE 21 | B |
| INTERFACE, MATERIALS 1 & 2, NODE 36 | C |
| INTERNAL SURFACE TEMP. - NODE 1 | D |

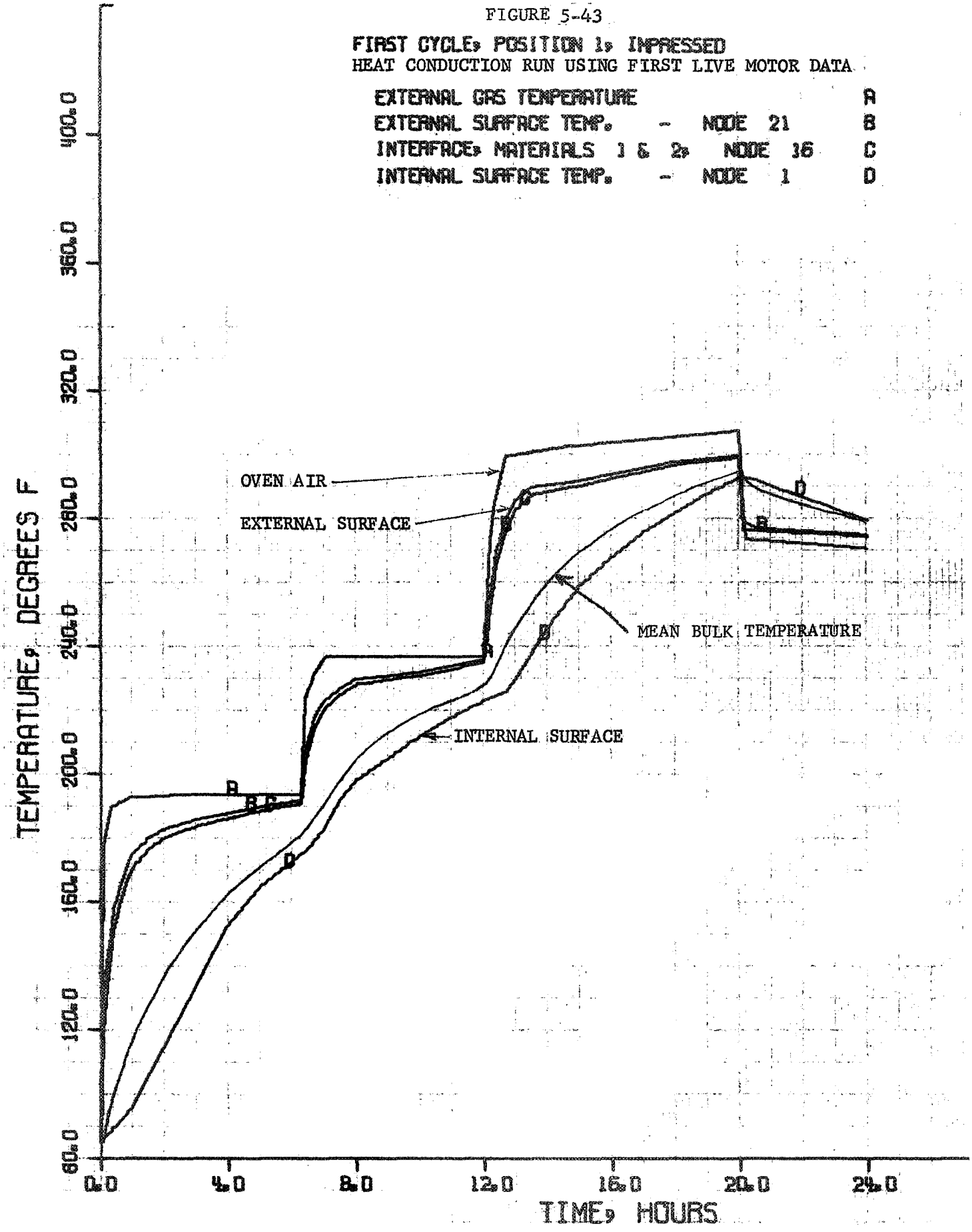

26 JUN 1969

# LIVE GRAIN STERILIZABLE MOTOR

FIGURE 5-44

FIRST CYCLE, POSITION 1, IMPRESSED

PROFILES FROM HEAT CONDUCTION RUN USING FIRST LIVE MOTOR DATA

| | | | |
|---|---|---|---|
| TEMP. PROFILE AT TIME = | 0.000 | HOURS | A |
| TIME = | 1.000 | HOURS | B |
| TIME = | 2.000 | HOURS | C |
| TIME = | 6.000 | HOURS | D |
| TIME = | 12.000 | HOURS | E |
| TIME = | 16.000 | HOURS | F |
| TIME = | 20.000 | HOURS | G |
| TIME = | 24.000 | HOURS | H |

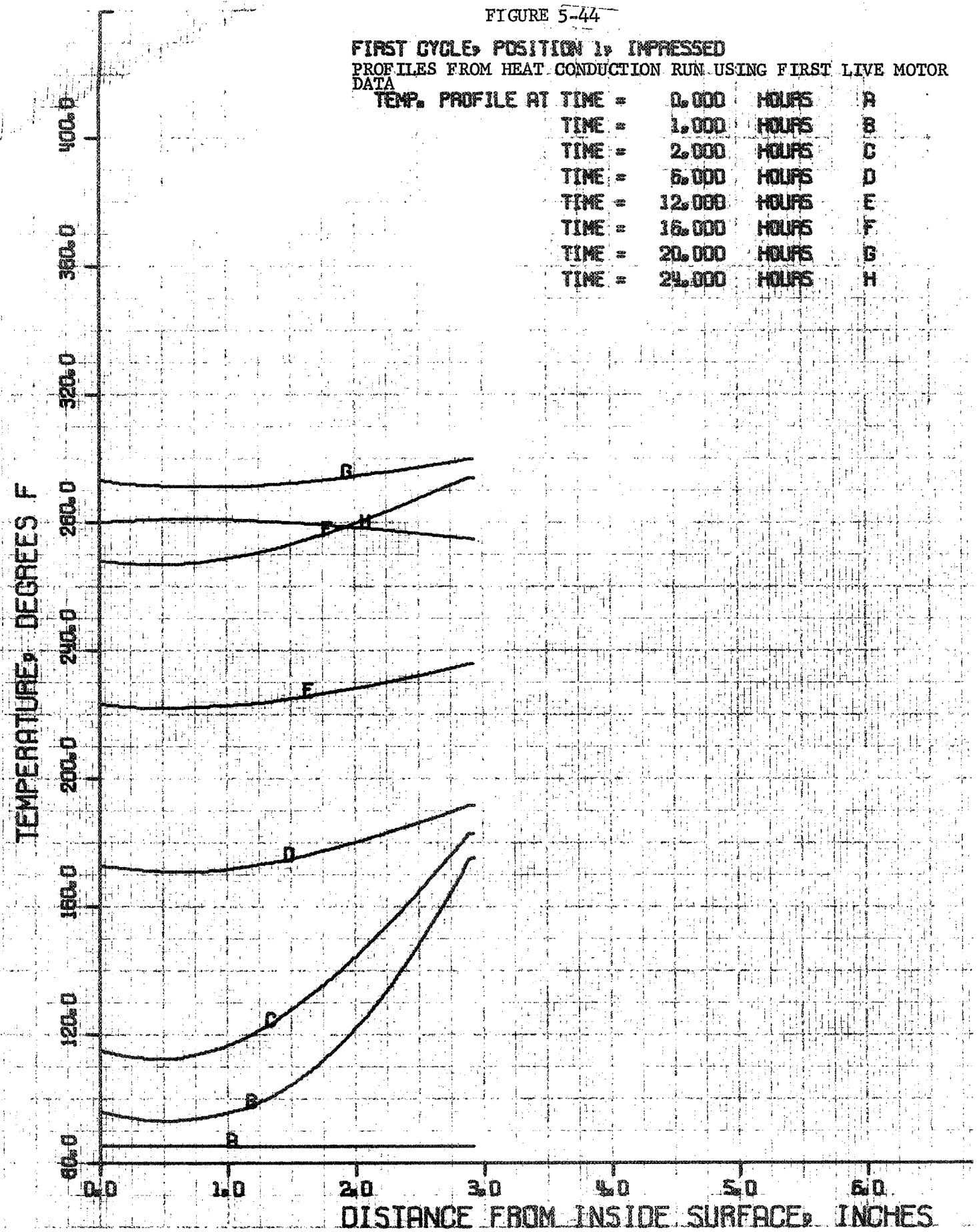

# STERILIZABLE MOTOR

FIGURE 5-45 - PREDICTION FROM INERT MOTOR DATA FOR LOW VALUE HTC

LIVE GRAIN, CYCLE 6, 190 FOR 6,
240 FOR 6, 300:

| | | |
|---|---|---|
| INTERNAL SURFACE TEMP. | NODE 1 | A |
| INTERFACE, MATERIALS 1 & 2, | NODE 16 | B |
| INTERFACE, MATERIALS 1 & 2, | NODE 17 | C |
| INTERFACE, MATERIALS 2 & 3, | NODE 19 | D |
| INTERFACE, MATERIALS 2 & 3, | NODE 20 | E |
| EXTERNAL GAS TEMPERATURE | | F |

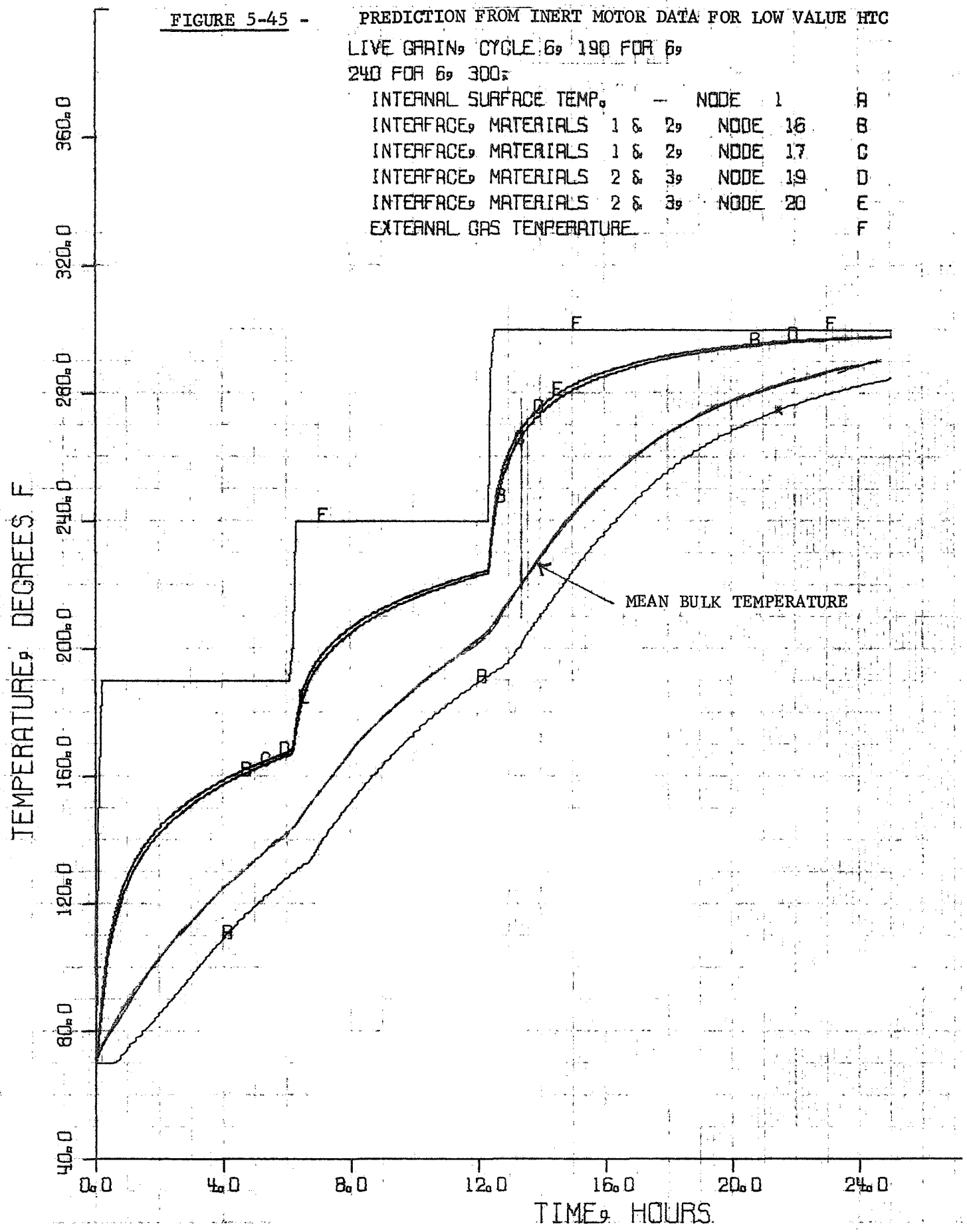

22 MAR 1969

# STERILIZABLE MOTOR

FIGURE 5-46 - PREDICTION FROM INERT MOTOR DATA FOR HIGH VALUE HTC

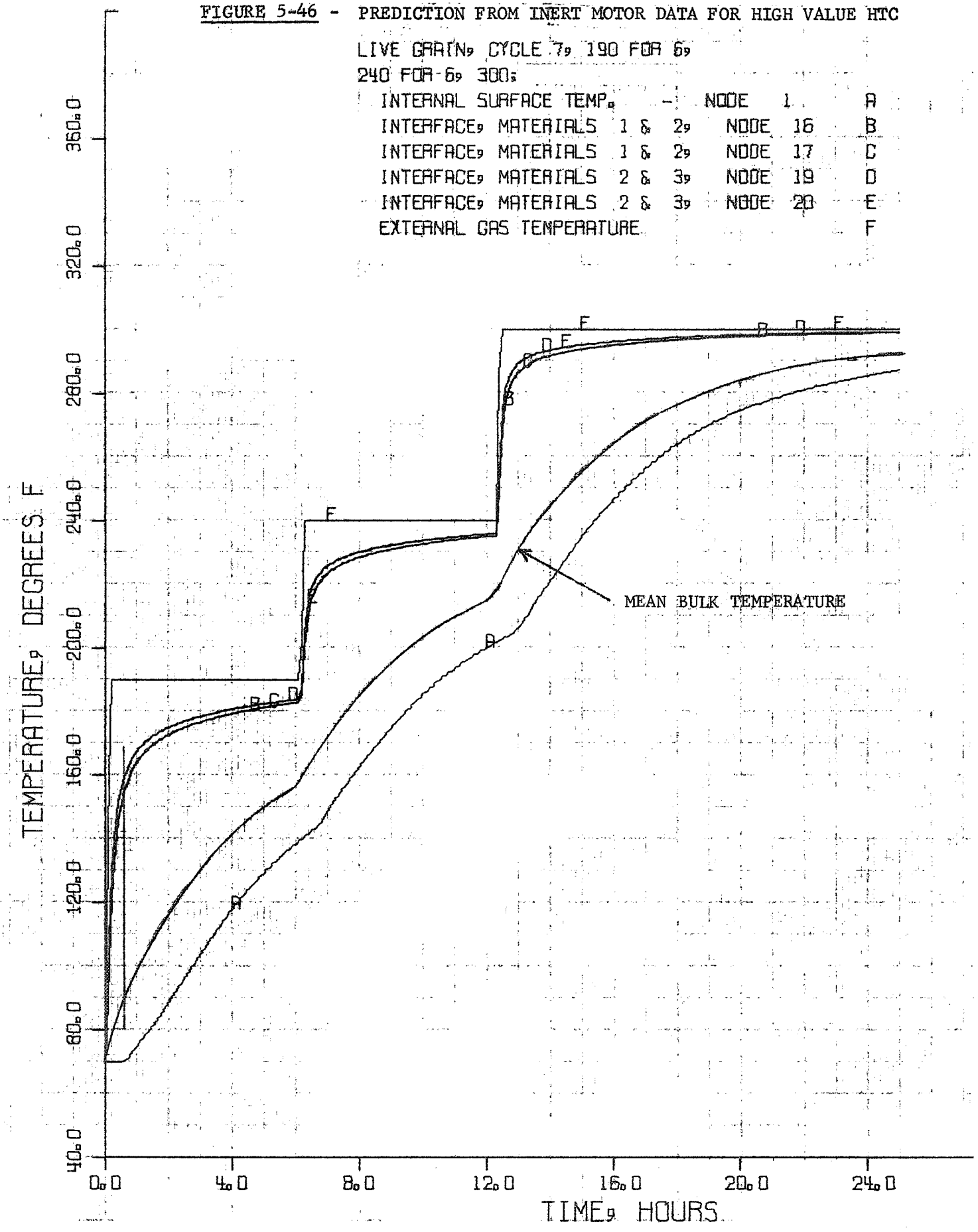

inert propellant test. Although the motor case wall thermal response agrees well with the predicted response for the higher heat transfer coefficients, the response of the inside grain was considerably faster than has been expected. This was probably the result of using a thin foil to seal the open end of the motor rather than the wooden seal used in previous tests. The foil would be expected to transfer heat more readily. A second oven cycle was run with one live motor in oven position 1 and another in position 2. The thermocouple results of this test were compared to the first cycle and found to be in close agreement. There was, in fact, little variation as a function of oven position.

Because more heat reaches the inside surface of the grain than had been predicted, a less severe oven cycle was possible and was analyzed. The new cycles called for the oven air temperature to be at 180°F for 5 hr, 230°F for 5 hr, and 285°F for 9.5 hr. The new cycle is presented in figure 5-47, and the thermal profiles are presented in figure 5-48. Degradation of the grain was calculated for the inside and outside surfaces of the grain for three cycles: (1) as predicted for the low and high heat transfer coefficients from the inert tests, (2) as experienced for the first live propellant heating cycle, and (3) for the new cycle. These results, in 275°F equivalent degradation hours, are as follows:

Grain Degradation

| Grain Surface | Predicted Low HTC | Predicted High HTC | Actual First Cycle HTC | New Cycle HTC |
|---|---|---|---|---|
| Inside | 4.09 | 5.4 | 7.3 | 4.9 |
| Outside | 15.8 | 21.4 | 17.3 | 11.1 |

27 JUN 1969

# LIVE GRAIN STERILIZABLE MOTOR

FIGURE 5-47 - FINAL CYCLE PREDICTION FOR LIVE MOTOR BASED UPON FIRST LIVE MOTOR DATA
CYCLE, 180 FOR S, 230 FOR S, 285 FOR
10

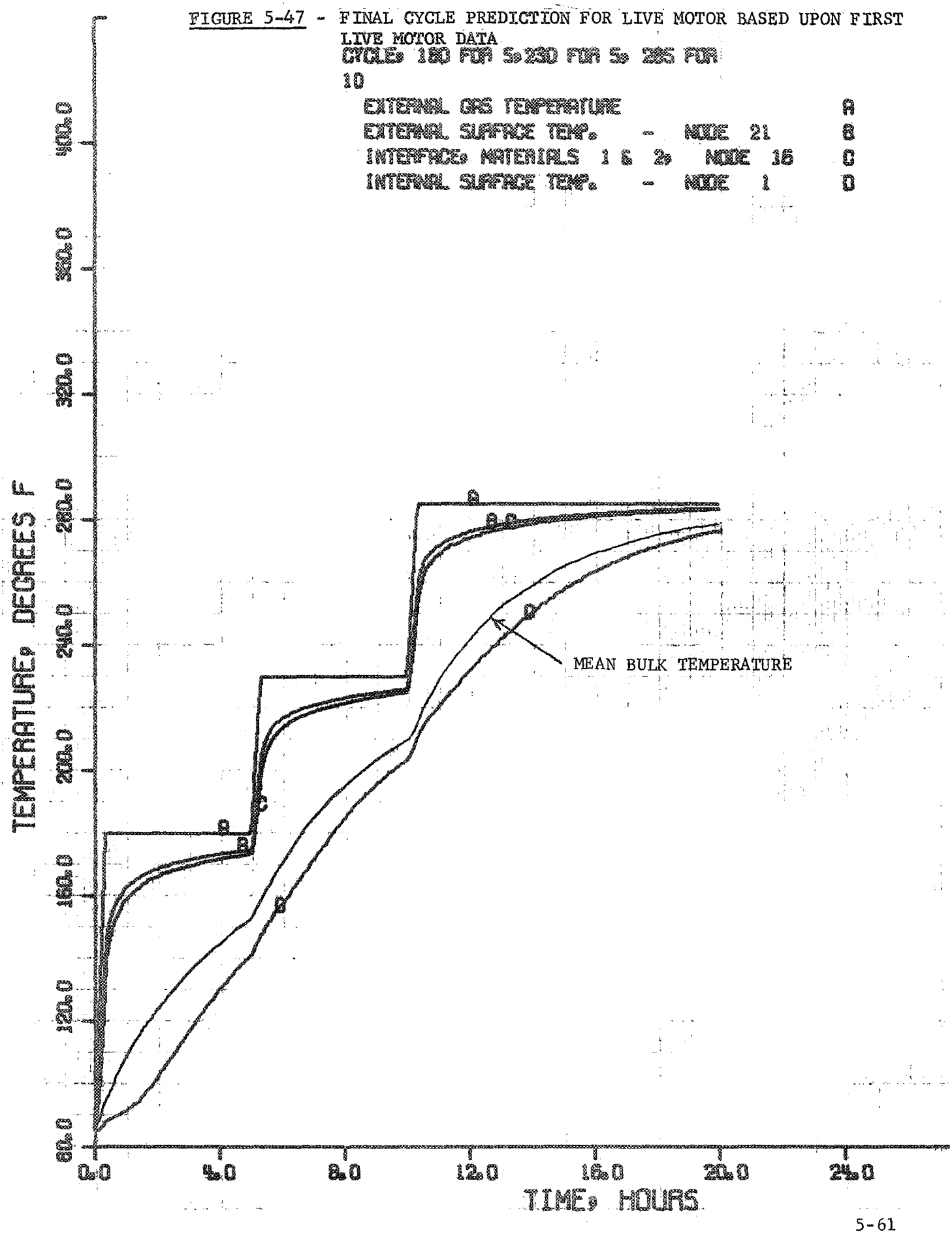

27 JUN 1959

# LIVE GRAIN STERILIZABLE MOTOR

FIGURE 5-48 PROFILES FOR FINAL LIVE MOTOR CYCLE PREDICTION

CYCLES 180 FOR 5,230 FOR 5, 285 FOR 10

TEMP. PROFILE AT TIME = 0.000 HOURS A
TIME = 1.000 HOURS B
TIME = 2.000 HOURS C
TIME = 5.000 HOURS D
TIME = 10.000 HOURS E
TIME = 12.000 HOURS F
TIME = 15.000 HOURS G
TIME = 16.000 HOURS H

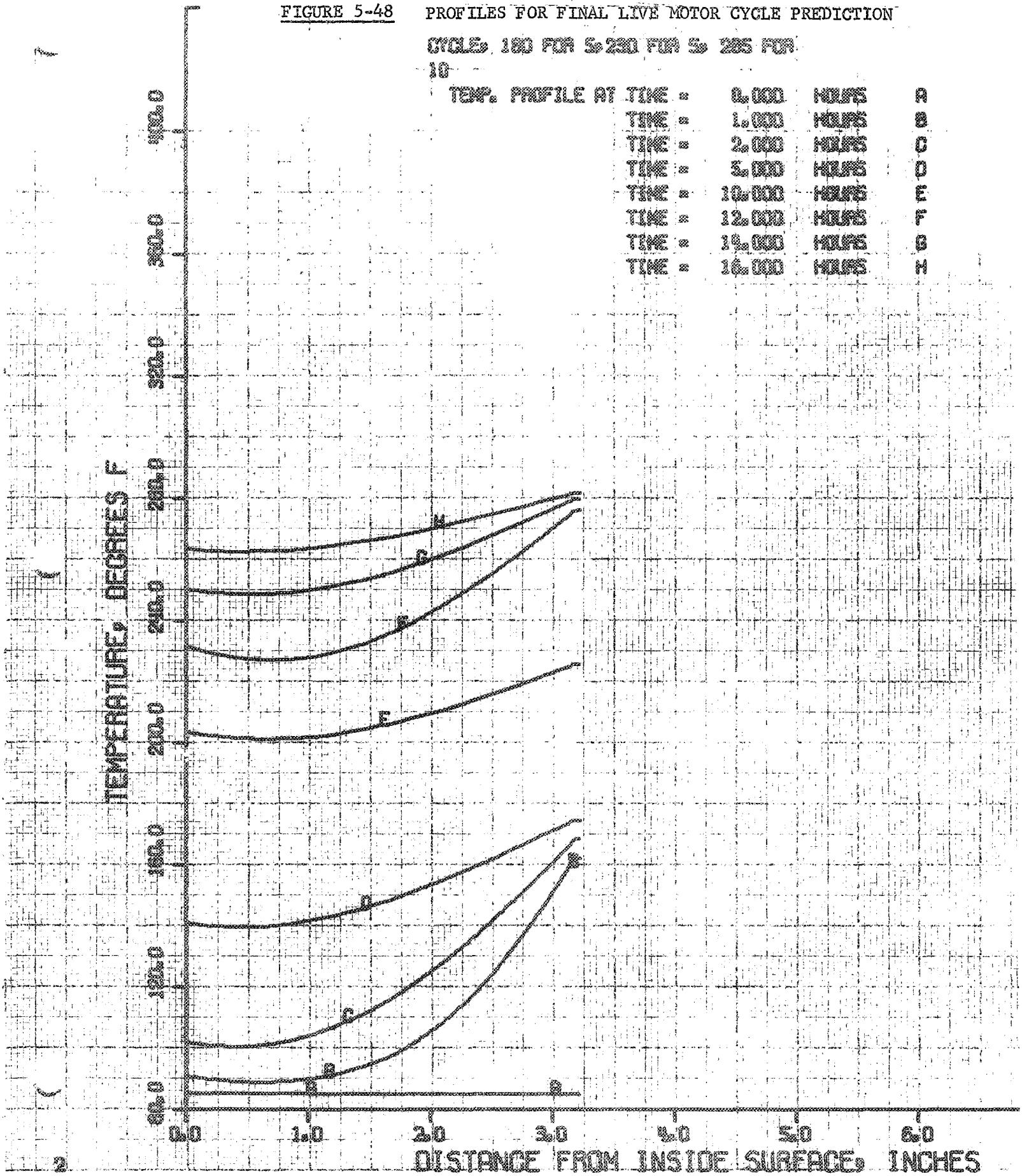

The maximum differences between the case temperature and grain mean bulk temperatures were: for the predicted cycle (high heat transfer coefficient), 69°F; for the first actual oven cycle, 60°F; and for the proposed new cycle, 56°F. The new cycle was not used due to the grain-to-liner bond failure of the live propellant test motors.

## 5.5 CONCLUSIONS AND RECOMMENDATIONS

In conclusion, an optimum heatup transient for the sterilization cycle was found that fell within the three major constraints: aging degradation, thermal stress, and oven hardware. This transient heatup cycle would thermally age the propellant 11.1 hr longer than the standard 53 hr cycle, for a degradation factor (excluding cooldown) of 1.21 for one cycle. This factor is found to be acceptable for six sterilization cycles.

It was found during this phase of the program, that:

A. Propellant surface temperatures should be kept as close to the sterilization temperature as possible to minimize the aging degradation,

B. The heatup transient portion of the cycle is controlled by the thermal stress restraints for the propellant system used,

C. Consideration of the heating of the propellant from both the external and internal surfaces must be made where the nozzle closure is not perfectly insulated or sealed.

The following suggestions and recommendations are made for future work on the sterilizable cycles:

A. Thermal properties should be determined for room and elevated sterilization temperatures, both before and after each sterilization

cycle to determine variations that may exist. The thermal properties directly affect the rate at which the propellant heats and cools,

B. Oven heating distribution on a loaded live or inert motor should be determined as described previously for any new oven configuration to be used for sterilization; accurate mapping of the flow should be made to aid in the placement of the motors in the oven,

C. For ovens in which the heating around the motor case is nonuniform, either baffles should be used to more evenly distribute the air flow, or the cases can be rotated or moved from cycle to cycle to eliminate any one spot from having more "aging" than another due to higher local heating rates,

D. Investigation should be made regarding sterilization within a liquid bath, where the sealed motor would be immersed in a constant temperature bath. This would have several advantages. For example, the liquid could be increased in temperature at any desired rate and accurately controlled, and sufficient mixing could be provided so that there would be no uneven heating as there is in an oven. Plastic bags could enclose the motor to protect the case and to also seal it from the liquid, thus eliminating poststerilization cleaning or drying.

# 6.0 MOTOR DESIGN, DESCRIPTION, AND PERFORMANCE SUMMARY

The rocket motor studied under this contract, as specified by NASA, used an existing spherical titanium motor case of sufficient volume to simulate the impulse needs of a MARS lander deorbiting motor. The motor design was to provide a propulsion system capable of withstanding a preflight sterilization process (six cycles of 275°F for 53 hr) as well as the vehicle flight environment.

Various grain designs were considered for use in the demonstration motor: (1) tubular port, (2) spherical star, (3) tubular perforations with conocyl, and (4) transverse slotted tubes with central port at the forward dome.

A single tubular grain configuration was selected for use in the demonstration test motor because of its ease in processing, low grain stresses, high reliability, and absence of slivers. After casting and cure, the tubular port is machined to its final dimension, thus allowing a high dimensional and weight accuracy with no delay for tooling in off-loading to the desired system performance. When cast and trimmed to the proper dimensions, the motor contained 44.5 lb of propellant giving a total sea level impulse of 10,370 lb-sec.

Insulation and liner materials were investigated during the UTC research and development programs for the proposed UTP-11439 propellant. The propellant/liner/insulation system had to be compatible and could not contain ingredients that would adversely affect bonds or properties during the NASA temperature sterilization cycling requirement. Silica-asbestos loaded butyl rubber insulation was found to be fully compatible with UTP-11439 and to be capable of the heat sterilization cycling. UTC developed a liner material, UTL-0026, which

showed excellent compatibility with UTP-11439 and with the silica-asbestos loaded butyl rubber insulation.

The spherical titanium motor case, steel aft closure, and steel igniter housings were GFE. UTC designed the grain configuration, case insulation, nozzle, and ignition system to make best use of the government-supplied hardware and to achieve the desired motor ballistic performance.

The design summary in table 6-I shows the design features of the demonstration motor. Table 6-II lists the UTC drawings which comprise the design of the demonstration motor.

## 6.1 GRAIN DESIGN AND PERFORMANCE SUMMARY

An internal burning cylindrical port grain was selected because it exhibited over-all superiority in comparison to star, slot, and conocyl designs in ease of processing, flexibility for future modifications, low grain stresses, and absence of slivers. The tubular port design has an exposed aft face terminating in a closed hemisphere at the forward end (see figure 6-1). The spherical dome has a constant 3.125-in. web thickness, thereby eliminating slivers and allowing the burning surface to be regulated by the thickness and location of the end surface. The 3.125-in. web gives the motor a 15.8-sec burn time. The web burnback history is shown in figure 6-2. The 3.125-in. web thickness allows a b/a of 2.1 and a factor of safety at allowable strain of 1.5%.

The specified performance for the test motor was a minimum total sea level impulse of 8,670 lb-sec, an average thrust of 682 lb for a minimum duration of 12.8 sec, and a propellant mass fraction of 0.692. The UTC demonstration motor performance completely satisfies these design goals. Fully

TABLE 6-I

DESIGN SUMMARY

| | |
|---|---|
| Propellant | UTP-11439 (sterilizable CTPIB) |
| Grain design | Spherical, cylindrical tube |
| Port cylindrical diameter, in. | 6.25 |
| Port spherical radius, in. | 3.125 |
| Motor case material | Titanium sphere, 0.040-in. wall (E14247) |
| Motor OD | 12.700 in. |
| Motor case insulation | Silica-asbestos loaded butyl rubber and FM-5504 tape, silica cloth-phenolic |
| Liner | UTL-0026 |
| Nozzle throat diameter, in. | 0.95 |
| Nozzle throat material | G-90 graphite |
| Throat backup insulation | FM-5504 tape, silica cloth-phenolic |
| Exit diameter, in. | 2.25 |
| Nozzle half angle, degrees | 15 |
| Expansion ratio | 6:1 |
| Exit cone material | FM-5504 tape, silica cloth-phenolic |
| Ignition | Two squib-initiated, cartridge-loaded pyrogen igniters |
| Total motor weight (loaded), lb | 66 |
| Propellant weight, lb | 44.5 |
| Propellant mass fraction | 0.674 |

TABLE 6-II

DRAWING LIST

| Title | Drawing No. |
|---|---|
| Spherical Motor Assembly Sterilizable Motor Vibration | C05814 |
| Spherical Motor Assembly Sterilizable Motor | C05806 |
| Case, Insulated - Spherical | C05778 |
| Nozzle Assembly | C05804 |
| Insulated Aft Closure Sterilizable Motor | C05812 |
| Closure, Aft | C05815 |
| Adapter Pressure Tap Sterilizable Motor | C05808 |
| Adapter, Igniter | C05816 |
| Nut, Locking Sterilizable Motor | C05807 |
| Clamp Half | C05819 |
| Support Bracket Sterilizable Motor | C05813 |
| Loaded Case | C05856 |
| Igniter Assembly Sterilization Motor | C05820 ECO 14314 |
| Cap Head Igniter Sterilization Motor | C05821 |
| Gasket | C05873 |
| Booster | C05830 |
| Cartridge, Igniter Sterilization Motor | C05811 |
| Case, Cartridge, Igniter - Sterilizable Motor | C05810 |
| Igniter Assembly Inert, Sterilization Motor | C05822 |
| Shipping Configuration Spherical Motor, Sterilizable Vibration Test | C06001 |
| Container, Shipping - Rocket Motor, Sterilizable | C05987 |
| Cap, Protective Shipping/Lifting | C05988 |
| Insert, Igniter | C06130 |

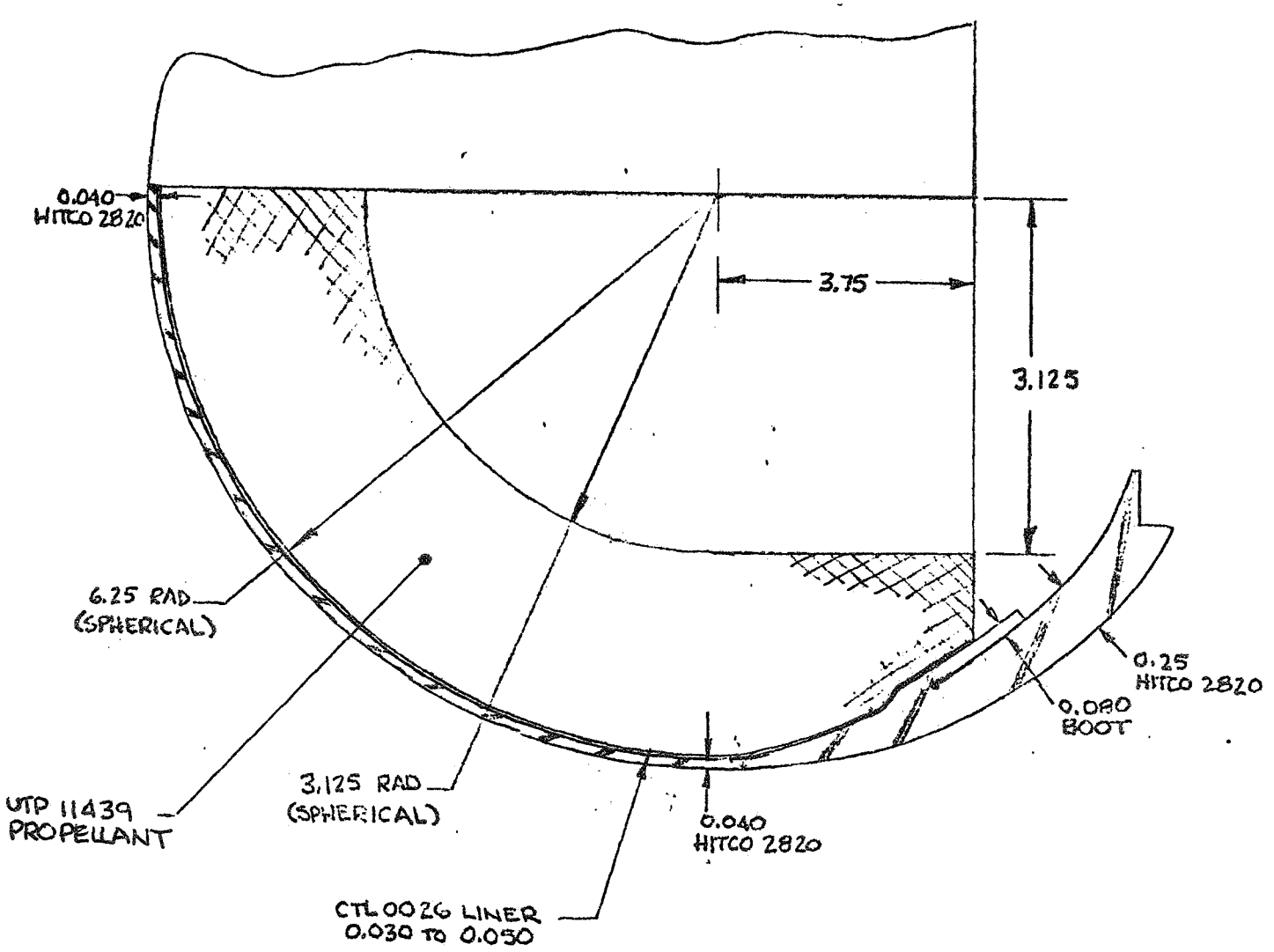


Figure 6-1. Grain Design

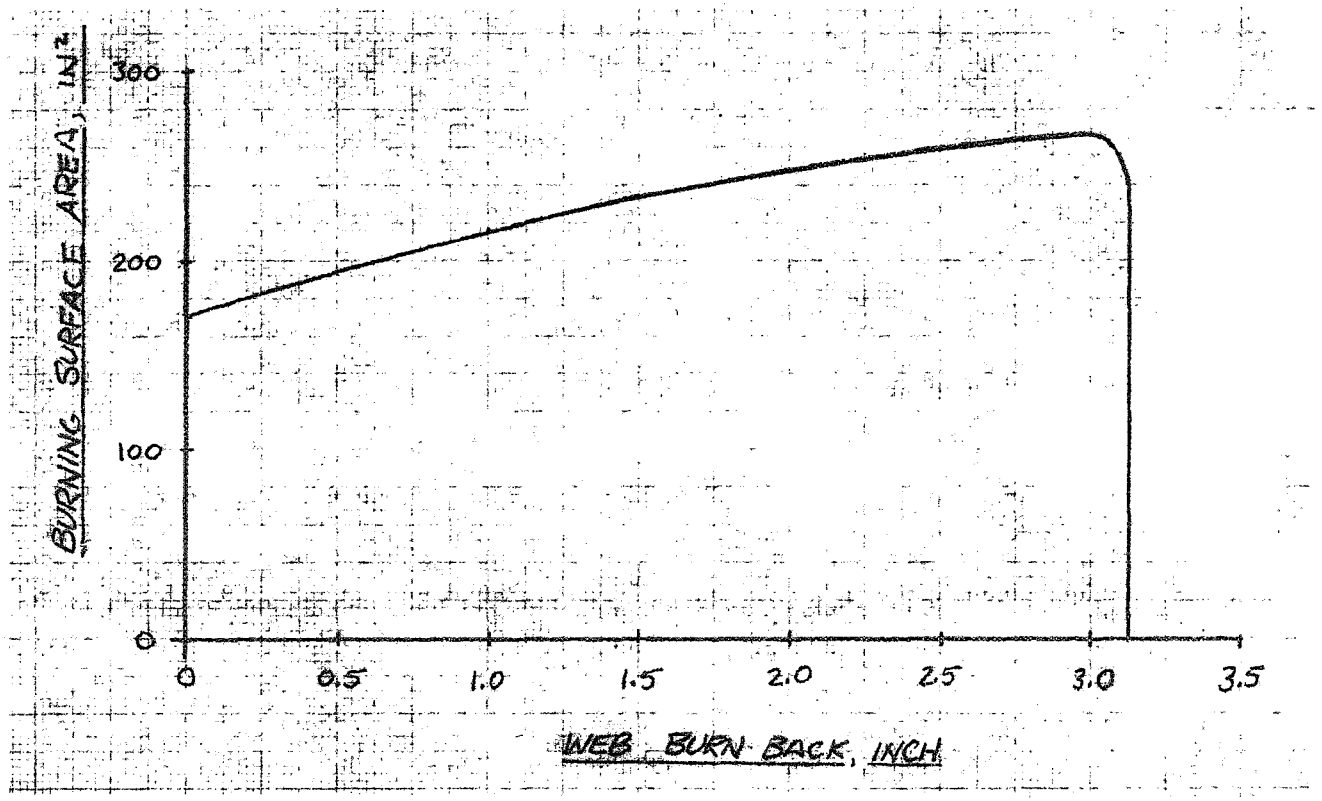


Figure 6-2. Burning Surface Area vs Web Burnback

loaded and prepared for testing, the demonstration motor weighs 66 lb with 44.5 lb of propellant, giving a propellant mass fraction of 0.674. The predicted average thrust is 600 lb for a burn time of 17.3 sec, giving a total impulse of 10,370 lb-sec.

A summary of the predicted ballistic performance is presented in table 6-III. This performance was determined using a standard sea level nozzle with an expansion ratio of 6:1 and a 15° half-angle utilizing a high density nonablating throat insert. The predicted motor thrust and chamber pressure (see figures 6-3 and 6-4, respectively) are progressive with time. With minor changes to the grain design, the shape of the thrust and pressure history could be modified if required.

TABLE 6-III

BALLISTICS SUMMARY
(PREDICTED)
NOMINAL - SEA LEVEL - 70°F

| | |
|---|---|
| Burn time, sec | 17.3 |
| Average pressure, psia | 600 |
| Average thrust, lb | 600 |
| Average delivered specific impulse, sec | 233.0 |
| Total impulse, lb-sec | 10,370 |
| Maximum pressure, psia | 710 |
| Maximum thrust, lb | 740 |

## 6.2 MOTOR CASE DESIGN

The motor case assembly for flightweight demonstration firings utilizes a NASA-supplied case and aft closure modified for use with UTC-designed igniters and pressure monitoring system. The assembly, modeled as for a flightweight motor,

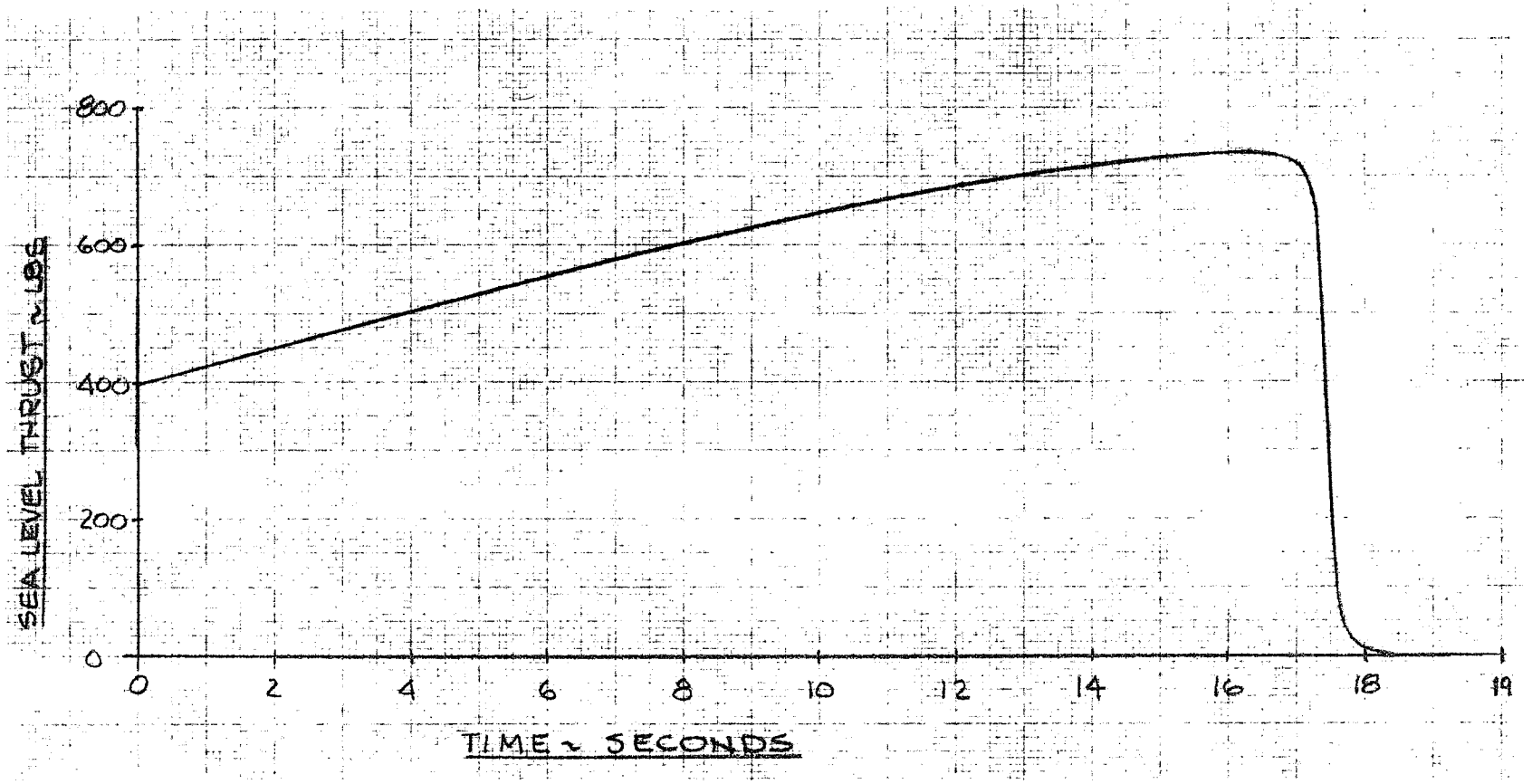


Figure 6-3. Sea Level Thrust vs Time
(Nominal ~ 70°F)

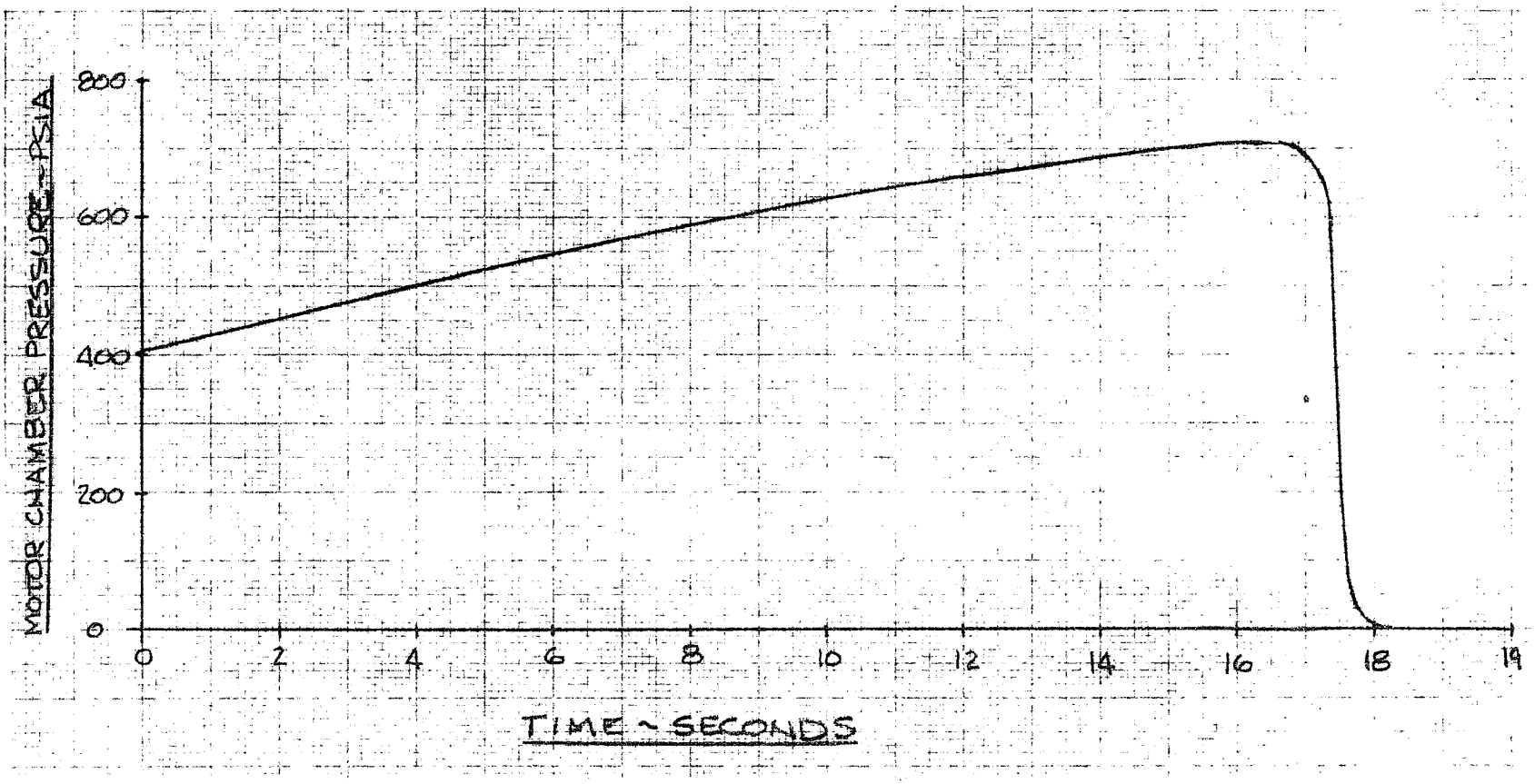


Figure 6-4. Motor Pressure vs Time
(Nominal ~ 70°F)

includes a NASA-furnished case and aft closure, two UTC igniter port adapters, and a UTC pressure tap adapter. The titanium 6AL-4V alloy motor case is a 12.7-in.-diameter sphere with a 0.040- to 0.047-in. wall thickness. Two integral attach lugs are included in the case, and a single opening with a bolted flange joint is provided for the aft closure. The cases supplied were successfully proof tested to 1,000 psi at UTC and were used without modification.

The NASA-furnished aft closure is a flat conical bulkhead with integral cylindrical nozzle housing. Included in the closure are ports for pressure tap and for igniters and joint provisions for attachment to the case and nozzle. Nozzle retention is accomplished using 12 ball bearings to engage a circumferential groove in the nozzle shell. The ball bearings are restrained by clamps against radial motion. Closure material is 17-4 ph stainless steel.

The closures supplied were modified to provide clearance and sealing surfaces for the UTC igniter adapters. As received, the igniter ports are threaded and without provisions for seals. Evidently the original closure-igniter joints were sealed with potting compound, a practice with only marginal reliability. To improve performance reliability, the closures were modified by machining igniter port threads to provide interfaces for O-ring packings. Other closure modifications included locally cutting away nonstructural portions of the closure to provide clearance for the igniter adapters since the nozzle attachment features intended for ease of thrust termination by nozzle ejection leave an inadequate igniter envelope. Adapters have been designed which, with completion of the minor closure modifications mentioned previously, successfully join the closure and UTC components. The pressure tap adapter and two igniter adapters are retained by threaded nuts installed at the inside of the closure before insulation, and are sealed using O-ring packings.

Several problems were experienced in modifying the NASA-supplied aft closures for use with UTC components. Visual inspection of the closures on arrival detected some parts with pitted pressure tap sealing surfaces. Two closures were rejected for use with UTC components and several others required minor rework in the seal area.

During closure igniter port modification, discrepancies were found between actual closure dimensions and supplied component detail drawings. Discrepant features included igniter port locations, major thread diameters, and closure contours adjacent to the igniter ports. The closure defects made redesign of the UTC igniter adapters necessary.

## 6.3 NOZZLE/AFT CLOSURE ASSEMBLY DESIGN

The nozzle/aft closure assembly was designed to meet the motor performance characteristics. Although it was not intended that the nozzle be subjected to the sterilization cycles or to vibration, these requirements were considered in the design. In addition, the nozzle does not incorporate an environmental seal; however, provisions for such a seal on a flight nozzle would require no changes in the basic design concept.

The nozzle assembly consists of a G-90 graphite throat insert supported in a conical silica cloth-phenolic insulator and a tapewrapped silica cloth-phenolic exit cone liner. Structural support is provided by a 4140 steel shell. Approximately 50% of the nozzle is submerged in the motor with OD insulation on the submerged portion comprised of silica-phenolic at the forward end and asbestos-silica reinforced butyl rubber at the high area ratio regions. The nozzle configuration is shown in figure 6-5.

The backed-up G-90 graphite throat design concept is similar to that used in the fourth stage Scout nozzle. The graphitite throat insert is backed over

its entire length with a conical OD insulator tapewrapped silica cloth-phenolic. This insert subassembly is supported on a tapered (5° half-angle) steel support which transmits ejection loads to the nozzle steel housing. In Scout nozzle fail-safe tests (reference UTC report No. UTC 2293-FR) this throat configuration has been shown to adequately contain graphitite throat inserts with built-in longitudinal and circumferential cracks.

The tapewrapped silica-phenolic exit cone liner is bonded to the steel housing at the forward end of the cone with an O-ring seal. The O-ring seal prevents possible exposure of the bond to the exhaust gases and prevents pressurization of the backside of the cone which could cause exit cone ejection.

The throat insert insulation and exit cone liner are fabricated of high silica cloth-phenolic (U. S. Polymeric's FM5504) tapewrapped parallel to the centerline in the case of the exit cone liner and parallel to the OD of the G-90 graphite in the case of the throat insert insulation. The material and fabric orientation provide required hoop tensile strength, maximum dimensional stability when charred, low thermal conductivity, and adequate ablation resistance for the exit cone liner application.

The nozzle housing is subjected to relatively low stresses, therefore annealed 4140 steel was chosen for this application. In the area of the groove for the ball attachment joint, the housing is flame hardened to Rockwell C44 to obtain the necessary bearing strength for this type of joint.

The adhesive used for bonding is Bloomingdale Rubber Company's HT-424. This material is an epoxy-phenolic resin, aluminum filled on a glass cloth carrier; it is known for its good structural properties at elevated temperatures. The material meets the requirements of the type III structural adhesive described in specification MMM-A-132.

The butyl rubber insulation on the submerged portion of the nozzle is the same as that on the motor case.

All of the basic design concepts, materials, and fabrication methods used in the nozzle design could be used in a flightweight nozzle. An expansion ratio of 50:1 could be provided by the incorporation of a stainless steel skin-supported, lightweight silica-phenolic exit cone similar to that used on UTC's fourth stage Scout nozzle.

The insulated aft closure assembly is shown on UTC drawing C05812. The closure itself is modified GFE. It is insulated in the same manner and with the same materials as used for the insulated case. The method of attaching the nozzle to the aft closure (clamp ball joint) could be used in a flight assembly. This method of attachment would provide a means of terminating thrust through the use of explosive nuts or bolts on the clamp which, when initiated, would release the clamping pressure on the balls and allow the entire nozzle assembly to be ejected. On the demonstration assembly, the clearance between the clamps and the pressure tap and igniter adapters is insufficient to allow for total release of the clamping pressure. A simple modification to this design, such as moving the aft closure/nozzle interface inboard, would provide sufficient clearance to ensure total release of clamping pressure.

A thermal analysis of the nozzle design shown in figure 6-5 was made to assure the thermal adequacy of the components and to provide temperature profiles to be used in the stress analysis. The analysis consisted of two parts: (1) a prediction of the ablative response of all surfaces exposed to the hot gas environment and (2) a prediction of the in-depth thermal response of the various nozzle components. Both parts of the analysis were conducted using standard techniques developed at UTC for the analysis of rocket motor

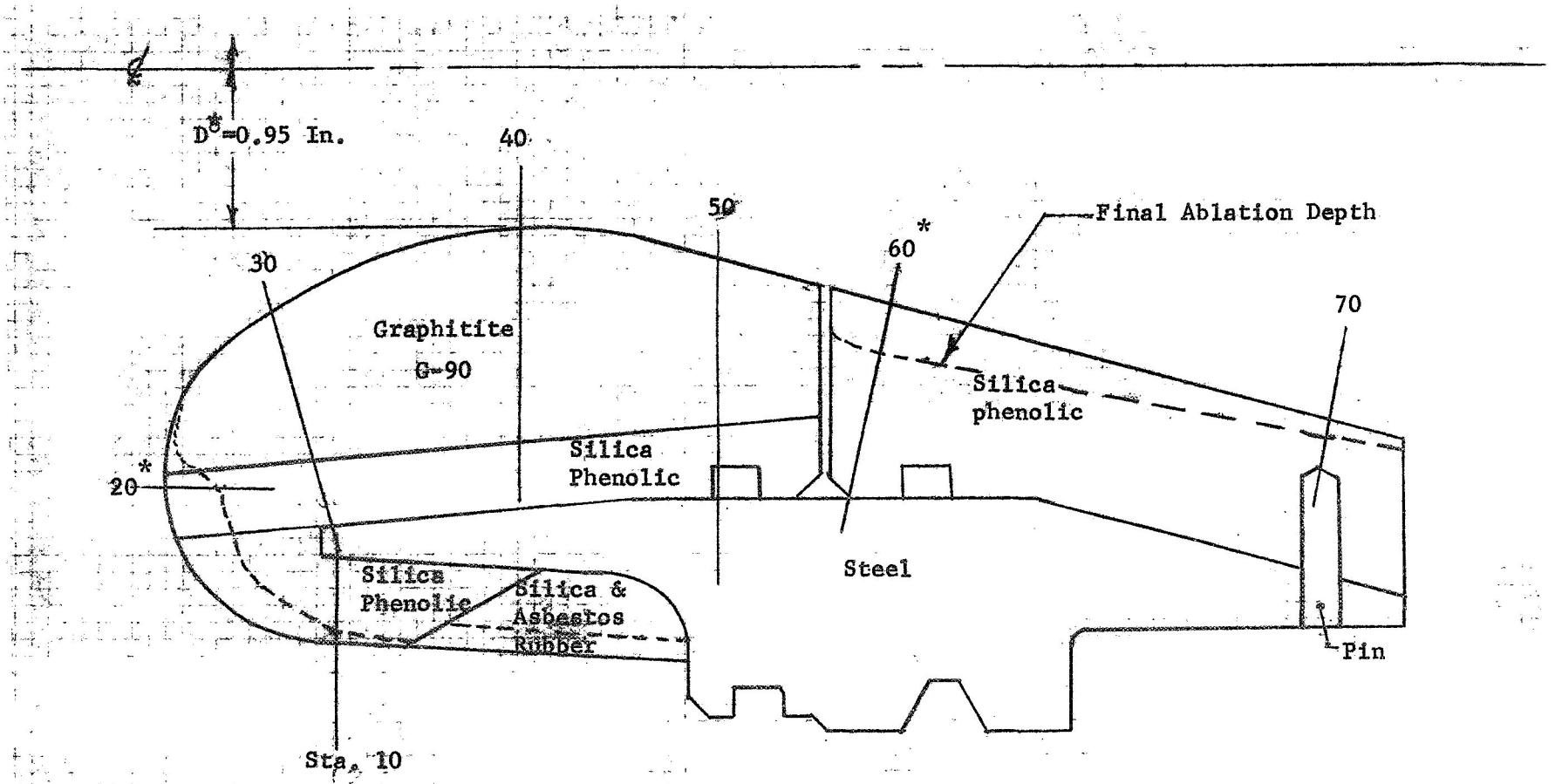


* A thermal analysis was not conducted at this location.

Figure 6-5. Thermal Analysis Stations for Nozzle

components. Descriptions of the computer programs used for this contract begin on page 6-24.

The prediction of ablation rates on the nozzle surfaces is based on empirical correlations of ablation rate as a function of heat flux calculated using a modified Bartz equation. These correlations have been developed from data taken from previous static test firings. The correlations for silica-asbestos loaded rubber and silica-phenolic are shown in figures 6-6 and 6-7. Based on data from numerous other test firings using G-90 graphite, similar propellants, and similar chamber pressures, negligible ablation is expected on the throat insert. Ablation predictions for the silica-asbestos loaded rubber and the silica-phenolic components were made using the computer program ABLATE/MACH which calculates ablation rates based on the previously mentioned correlations, motor chamber pressure obtained from internal ballistics analysis, and the Mach number calculated as a function of the instantaneous diameter. The predicted postfire ablation contour is shown in figure 6-5.

The in-depth thermal response of the nozzle components was calculated using a one-dimensional axisymmetric heat conduction program (LA15ZAZ). The thermal properties of the graphite and silica-phenolic materials in the nozzle are shown in figures 6-8 and 6-9.

The convective boundary conditions were calculated using the Bartz simplified heat transfer coefficient correlation for turbulent flow. The radiative boundary condition was determined on the basis of gas emissivity calculated with the use of Beer's law. These boundary conditions along with the ablative boundary conditions were input to the one-dimensional heat conduction program. The temperature response at the stations indicated in figure 6-5 is shown in figures 6-10 through 6-13. As can be seen from these

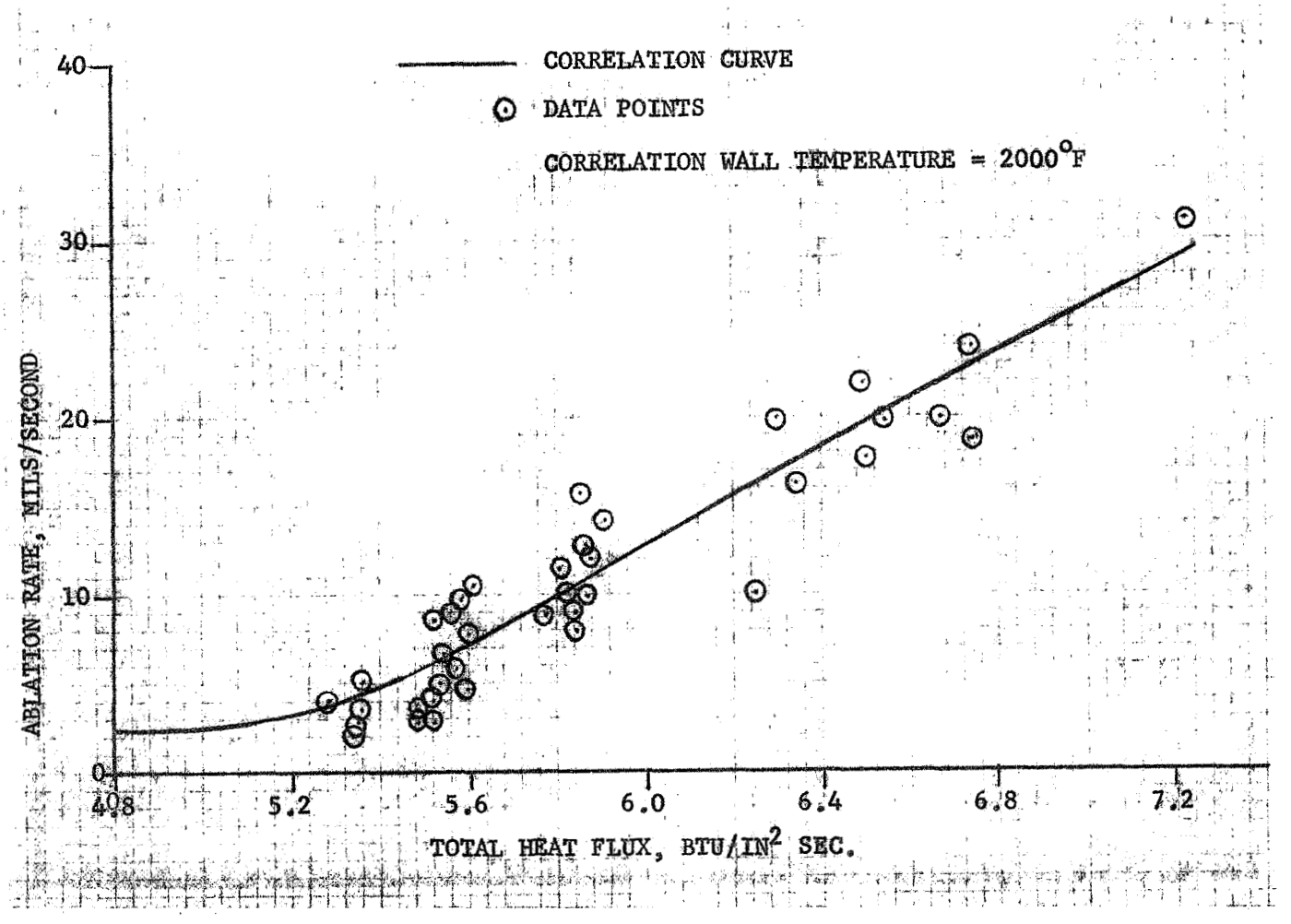


Figure 6-6. Ablation Rate vs Heat Flux
for Silica and Asbestos Rubber Insulation

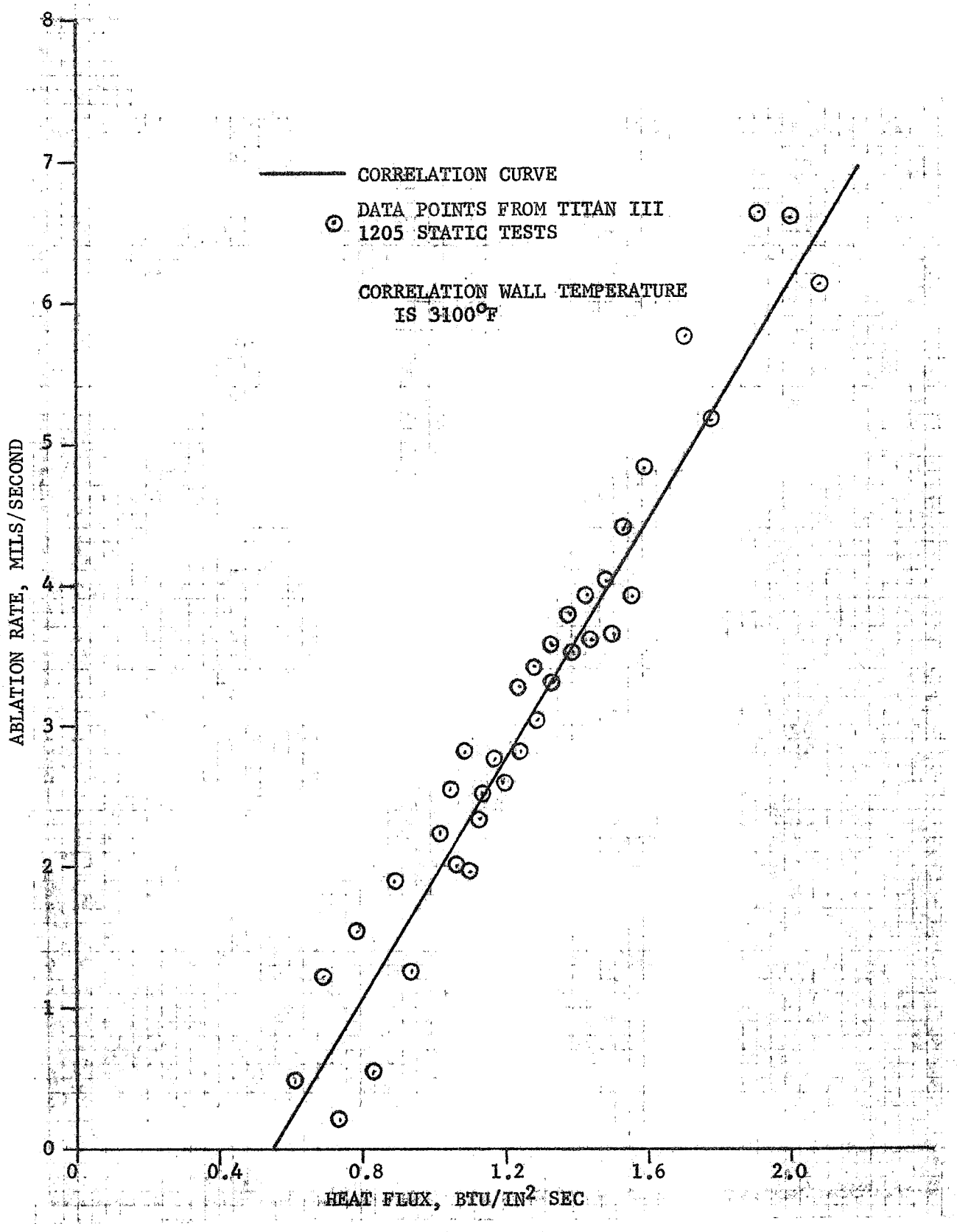


Figure 6-7. Ablation Rate vs Heat Flux for Silica Cloth-Phenolic Insulation

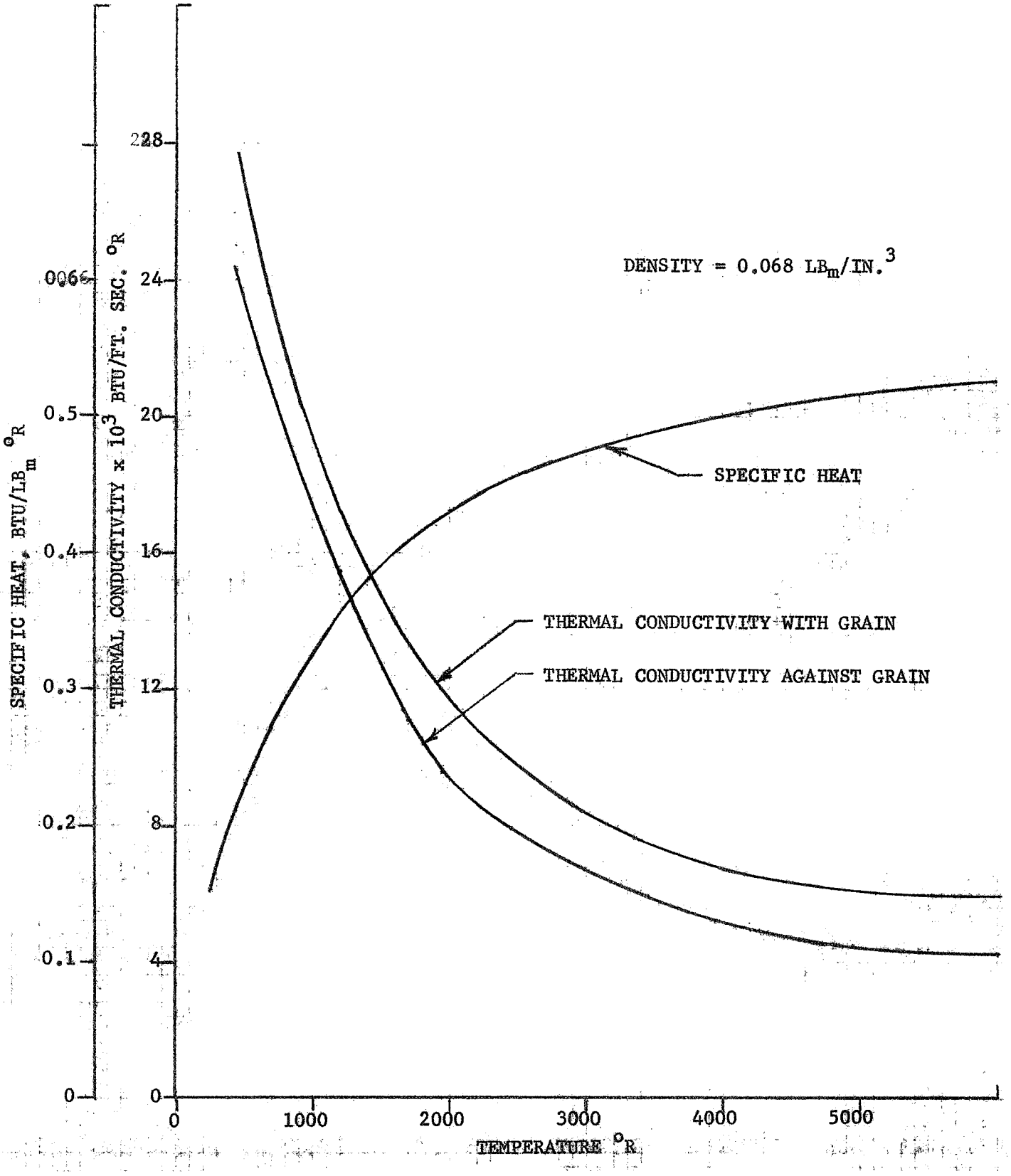


Figure 6-8. Thermal Properties of G-90 Graphite

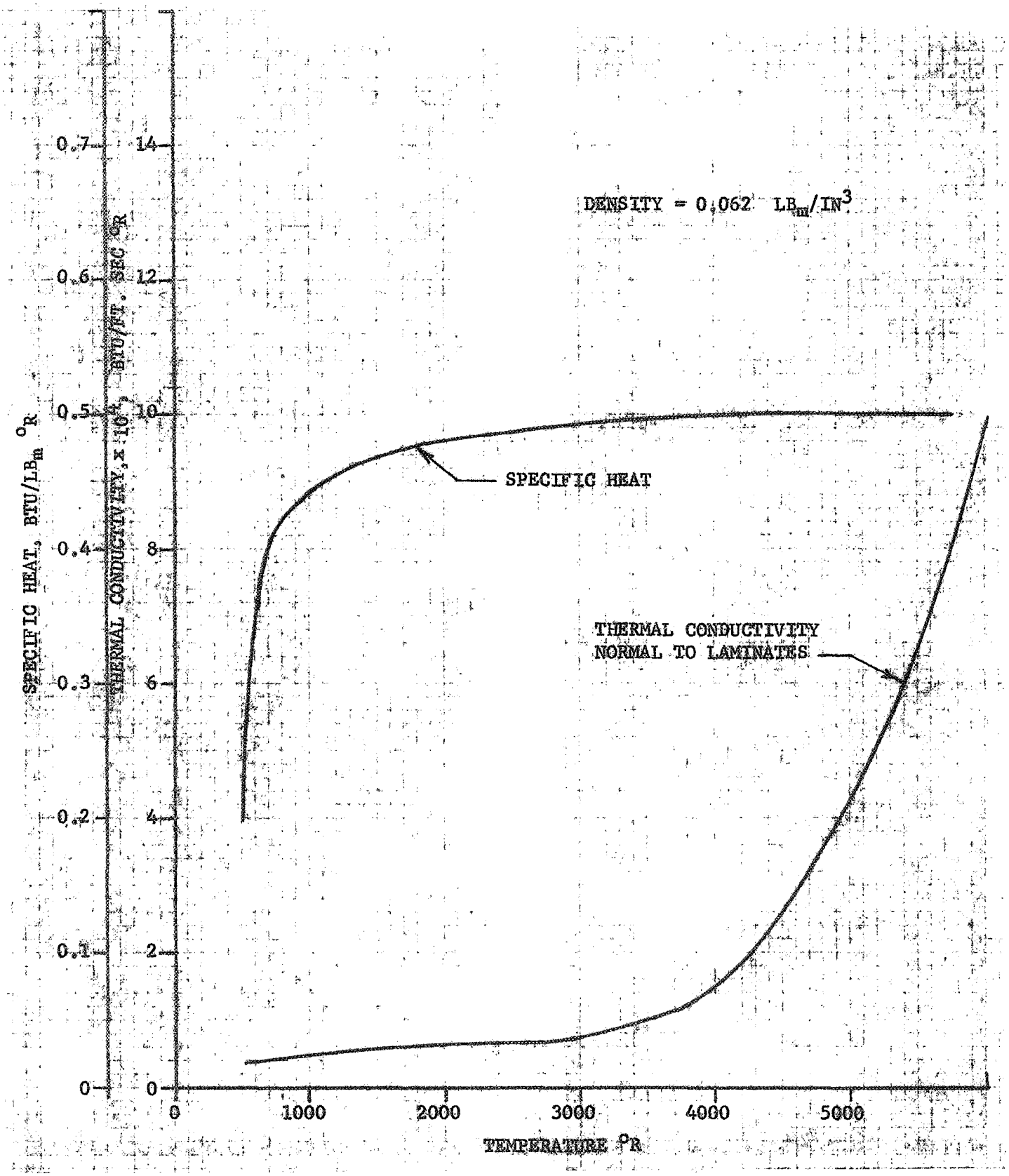


Figure 6-9. Thermal Properties of Silica-Phenolic

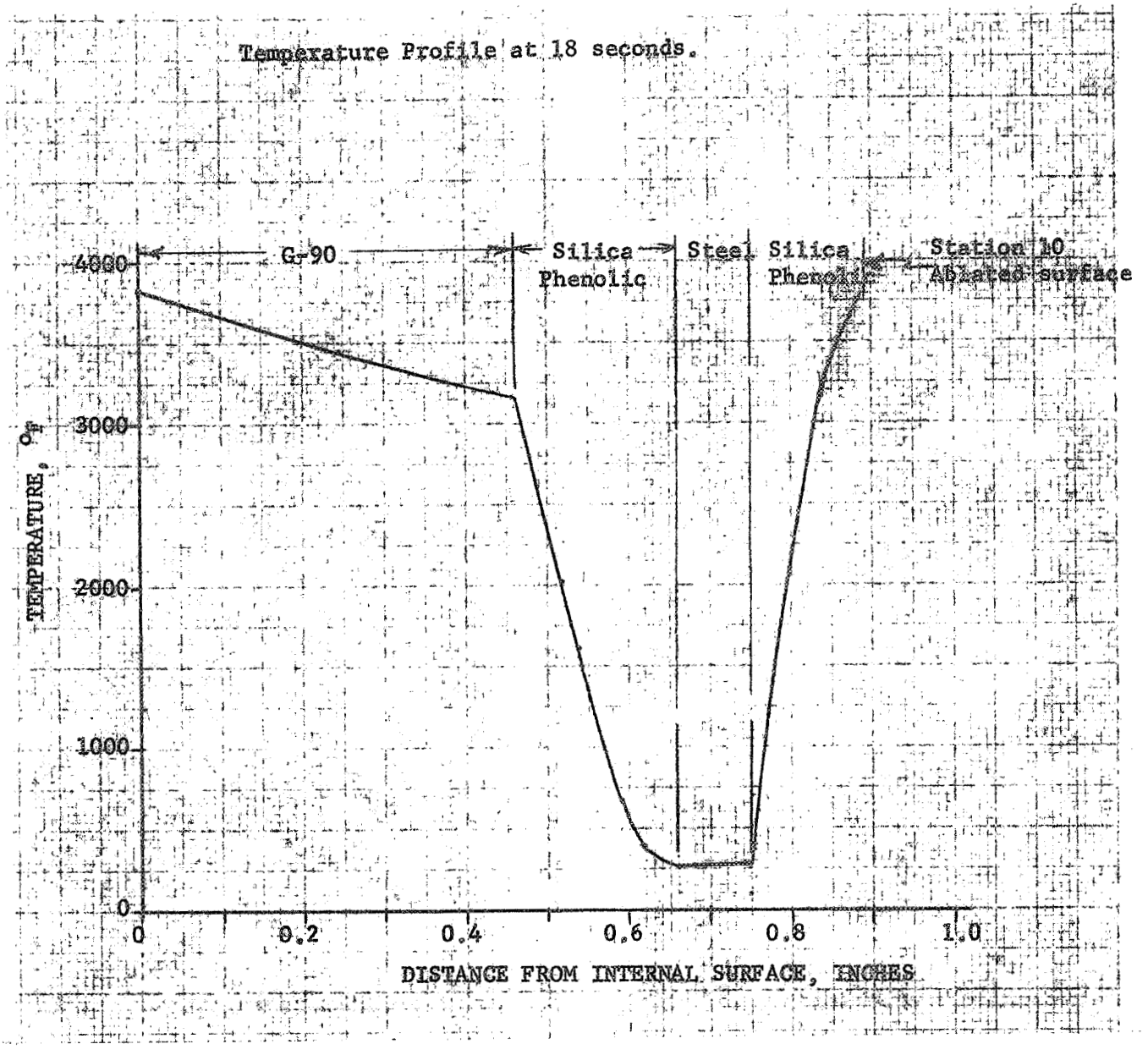


Figure 6-10. Sterilizable Motor Nozzle, Station 10-30

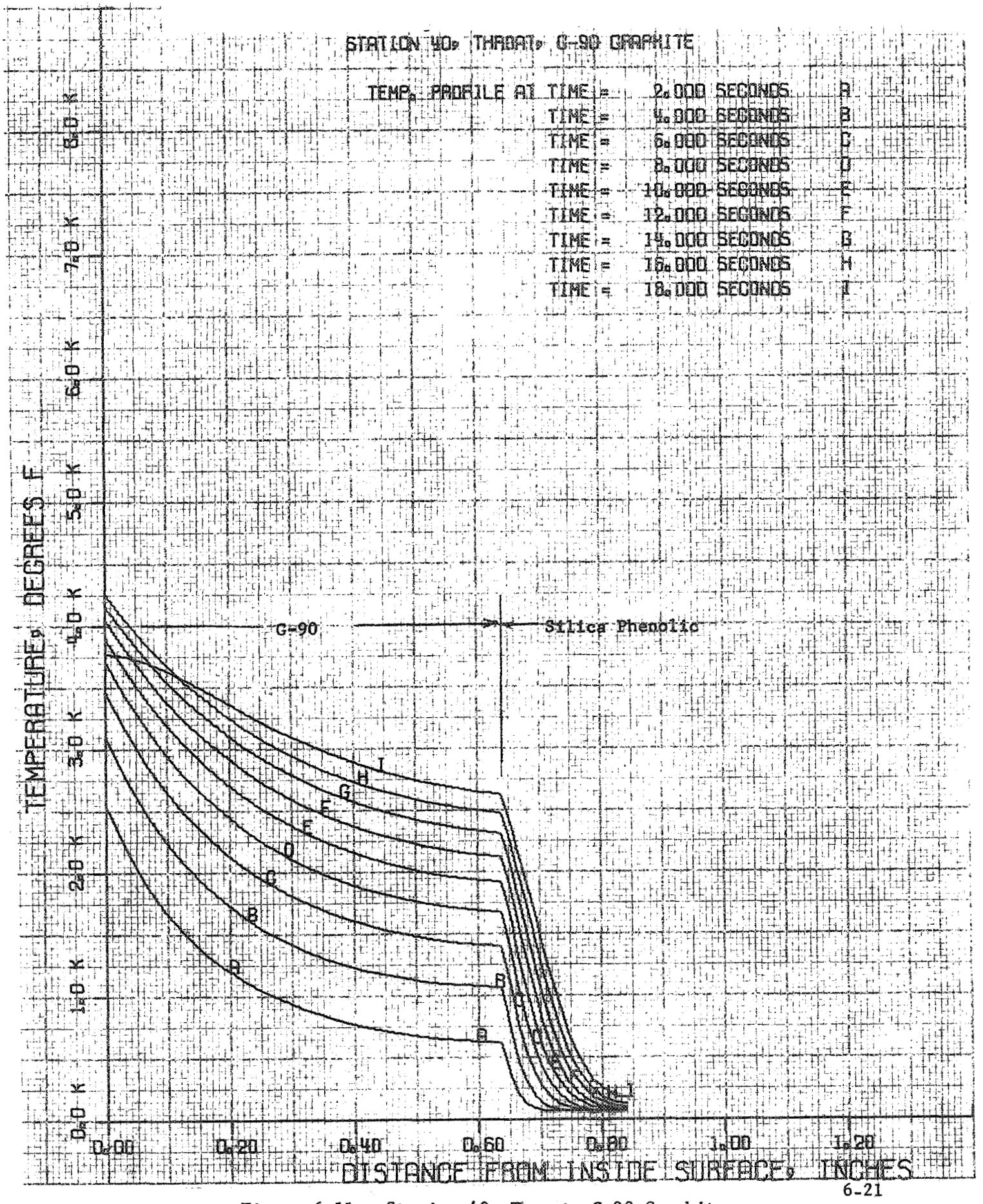




Figure 6-11. Station 40, Throat, G-90 Graphite

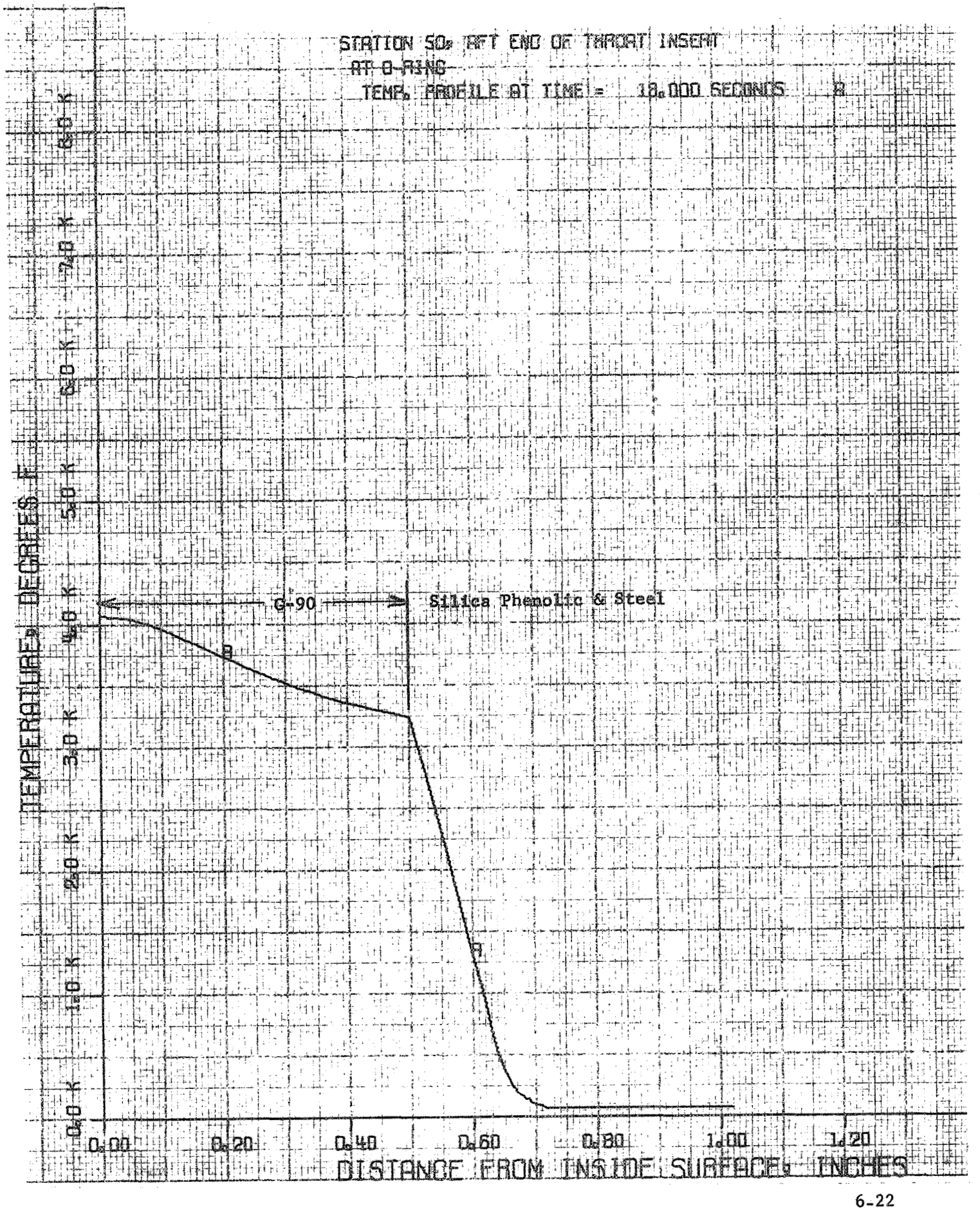




Figure 6-12. Station 50, Aft End of Throat Insert at O-Ring

Temperature Profile at 18 Seconds.

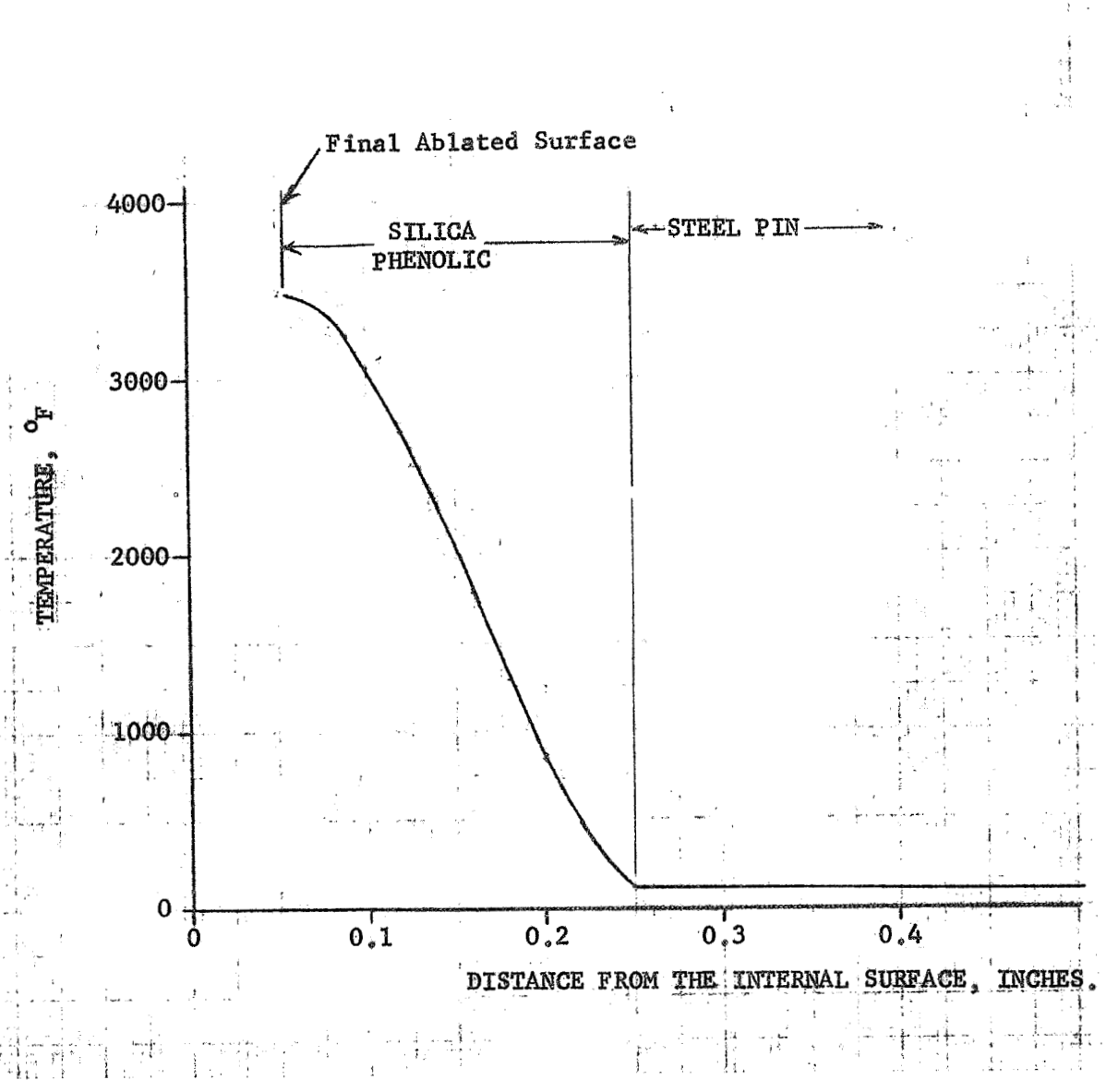


Figure 6-13. Sterilizable Motor Nozzle, Station 70

figures, the backside temperatures at the end of the firing are sufficiently low to maintain structural integrity of the steel shell. The analysis is conservative in that one-dimensional heat conduction model does not consider the endothermic charring reactions of the silica-phenolic, which tends to lower the resulting temperatures.

Following are brief descriptions of the thermal and ablation models which were used for this analysis. The techniques described are standard and would be utilized for a similar propulsion system analysis.

A. One-Dimensional Heat Conduction Program, LA15ZAZ (HC-8)

This analysis tool is a computer program finite difference numerical solution to the heat equation using the implicit or backward difference technique. The following differential equation for an axisymmetric, one-dimensional body is solved by this technique.

$$\frac{\partial^2 T}{\partial_R 2} + \frac{1}{R}\frac{\partial T}{\partial R} = \frac{1}{\alpha}\frac{\partial T}{\partial t}$$

where:

T = temperature

R = radius

t = time

NOTE: Thermal diffusivity ($\alpha$) may vary with temperature.

This program accepts a variety of boundary conditions separately or in combination. The boundary conditions available on either internal or external surfaces include convective coefficient, incident radiation, surface reradiation, and a specified surface temperature history. It also contains a moving surface feature to simulate an ablating wall. The

convection and radiation conditions may be both surface temperature and time dependent, the impressed temperature is time dependent, and the ablation is time dependent and can be turned off and on during a problem run. No in-depth charring or material degradation is handled by this program.

B. Ablation Prediction Program

The ABLATE/MACH ablation prediction computer program makes use of empirical correlations of ablation rate versus heat flux which assumes that the ablation rate of a material is a function of the heat flux that is being absorbed by the material at some arbitrary correlation wall temperature.

The program computes the heat flux using the Bartz simplified heat transfer coefficient correlation equation and radiation from the gas stream to determine the convective and radiative components of the total flux. One-dimensional gas dynamics using instantaneous local and throat diameters is used to determine local Mach numbers at the location being analyzed. It is also possible to utilize a Mach number-time function if one-dimensional gas dynamics do not apply. A chamber pressure-time function can also be used, and the local pressure is computed assuming isentropic flow. The program proceeds in a stepwise-in-time-manner, in which all of the necessary quantities are evaluated and updated for each time-step. The corresponding flux, the resulting ablation rate, and integrated total ablation are found as functions of time. The ABLATE/MACH ablation prediction program outputs the ablation velocity as a function of time in a form directly usable by the one-dimensional heat conduction

computer program. This program is a useful analysis and design tool and is used with all of the ablation correlations.

## 6.4 CASE INSULATION DESIGN

The material chosen for the case insulation was Hitco-2820, an asbestos-silica reinforced butyl rubber compound (figure 6-14). Evaluation tests of several materials showed that this material could withstand the required sterilization cycles; it also exhibited good erosion-resistant characteristics in subscale motor firings.

The case insulation is designed to limit the temperature rise in the case wall to 30°F during the motor firing. The required insulation configuration is shown in figure 6-14. The insulation varies in thickness from 0.25 in. at the nozzle/aft closure boss area to 0.04 in. at the point of propellant burnout. These thicknesses include a 1.5 safety factor on erosion and were determined as follows:

Required thickness - (Erosion rate x time exposed to exhaust gases x 1.5 safety factor) + (thickness required to limit the case wall to a 30°F temperature rise)

The design includes a boot located at the aft end of the propellant grain to relieve the stresses which occur in the grain as a result of shrinkage during the curing process. The insulation is bonded into the case with Chemlock 205 primer and Chemlock 234 adhesive. This bonding system provides a good bond between the titanium case and the butyl rubber compound, and will maintain adequate bond strength at the temperatures required for sterilization. The bond is cured during the insulation fabrication process. In this process the case is cleaned as specified on the drawing, and the primer and adhesive are applied and allowed to dry. Unvulcanized rubber insulation is then layed up in the motor case to the required configuration. The rubber is vacuum bagged

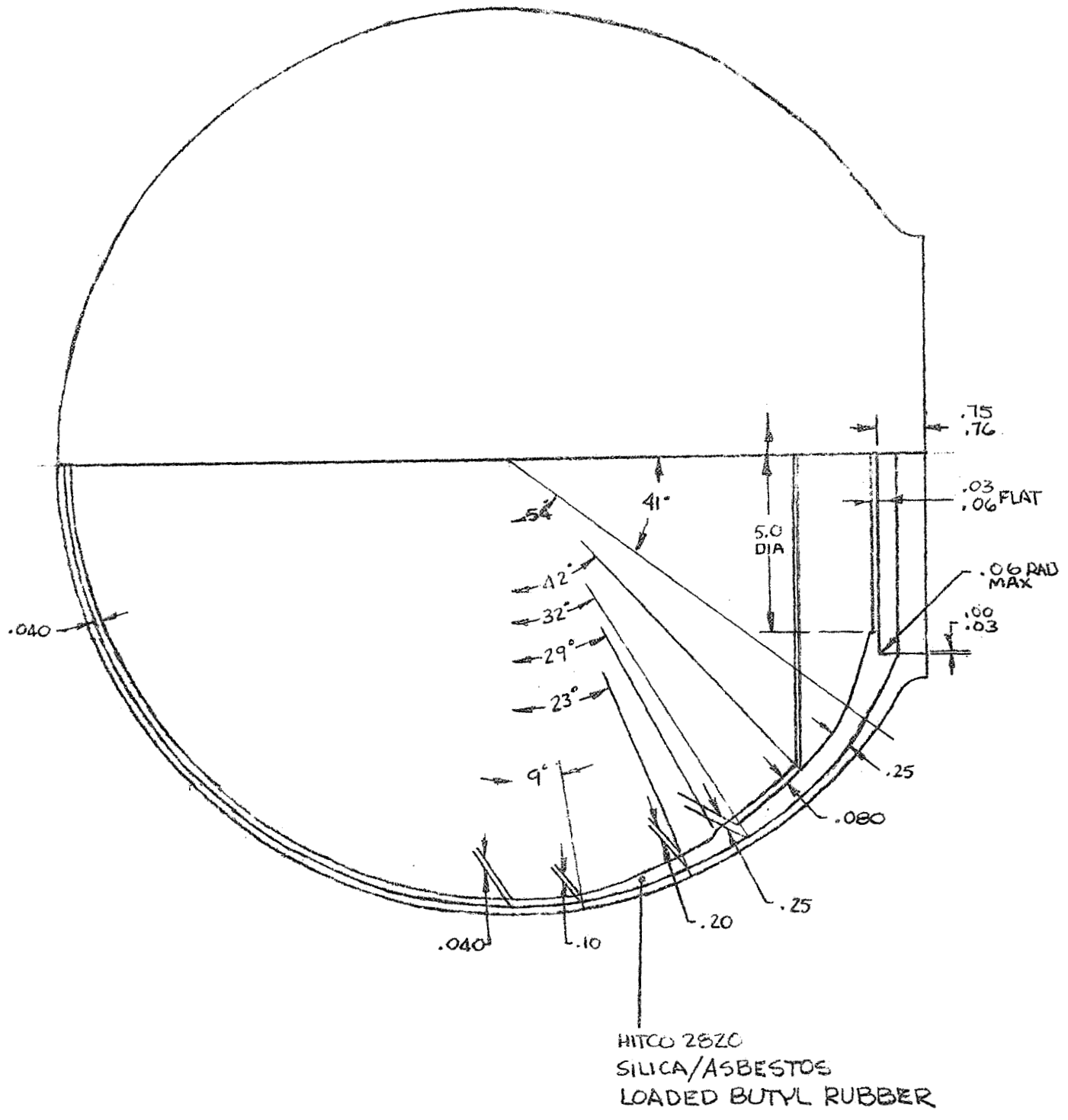


Figure 6-14. Insulated Motor Case

and cured (vulcanized) in an autoclave under 200 psi and 300°F. During this vulcanization process the insulation-to-case bond is also cured.

Thermal and ablation analysis of the motor case insulation was conducted using the Hitco-2820 silica and asbestos rubber insulation. The objective of the analysis was to demonstrate that the motor was sufficiently insulated to provide adequate thermal protection to the motor case and nozzle components. The analysis procedure was to first determine the ablation rates and then determine the thermal response of the titanium case to the heating and ablation. For the location of the insulation (area ratios greater than 13.5), the pressure, chamber temperature, and heat flux values are low, resulting in relatively low ablation rates. UTC data for ablation correlation of rubber insulation materials in solid motors indicates that the ablation rate would be 2.5 mils per second. Based upon this, the ablation depth of the insulation at a location exposed to the full duration would be 0.044 in. The minimum insulation thickness for a fully exposed region is 0.2 in. at the location just behind the nozzle throat. The thickness at other locations varies relative to the exposure time. Worst case heating would take place where the exposure time is the longest. As a result, a thermal analysis was conducted with the one-dimensional heat conduction program, LA15ZAZ, for 2.5 mils per second and an impressed ablation temperature of 2,000°F. This ablation temperature is considered conservative based upon postfire analysis of static test motors with similar insulation designs. These results are shown in figure 6-15 where a plot of the titanium case temperature versus time is shown. The maximum case temperature rises less than 4°F for these conditions.

These results show that the insulation on the motor case is thermally and ablatively adequate. Any other location would have less heating since the exposure times are shorter, thus producing a lower thermal gradient.

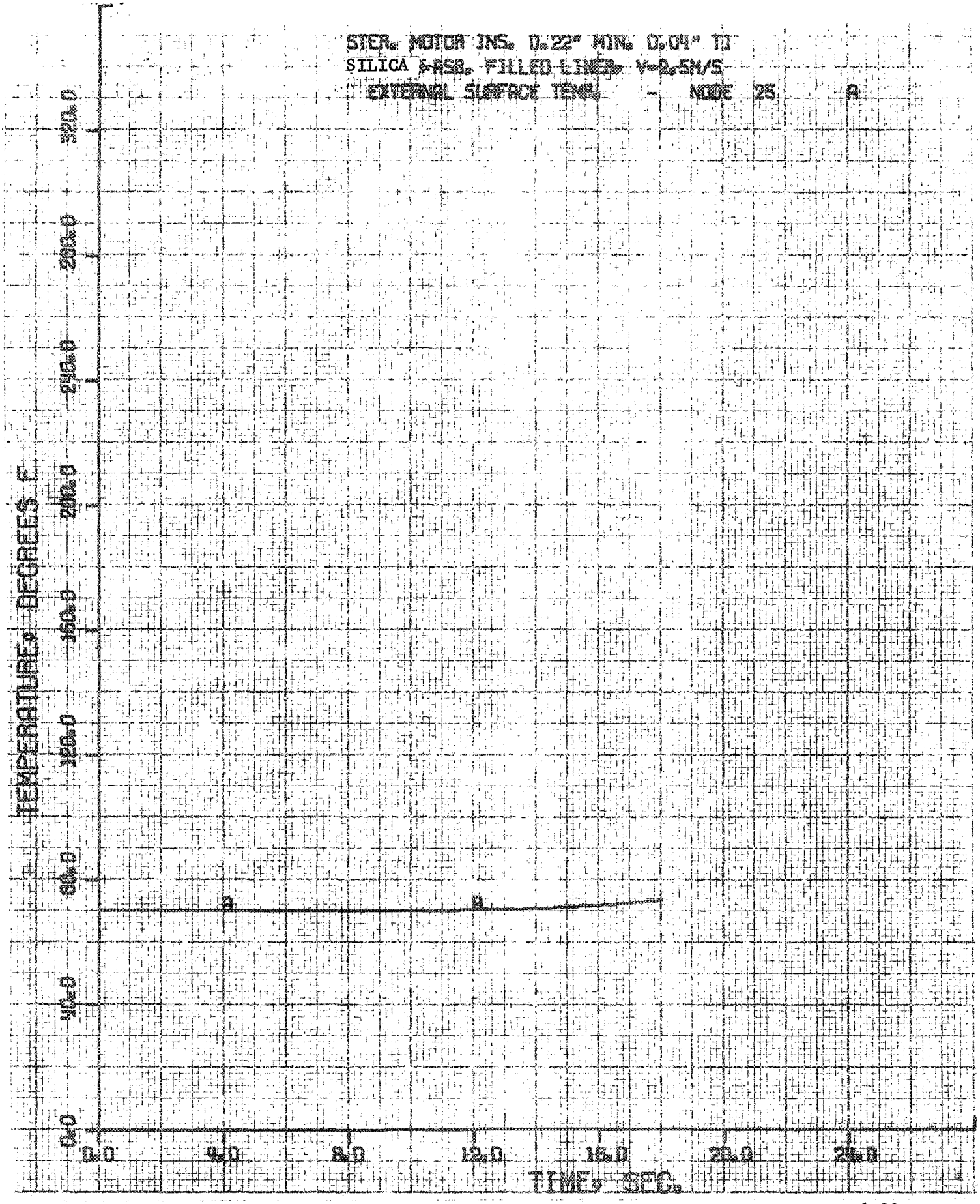




Figure 6-15. Sterilizable Motor Case Insulation

## 6.5 IGNITER DESIGN AND SIZING

### 6.5.1 Design

The igniter is an aft-mounted pyrogen igniter. The design was based upon the use of the NASA-furnished igniter body. A pyrotechnic booster is added to implement ignition. Initiation of the ignition sequence is by means of an off-the-shelf EED. The main igniter charge is a cartridge-loaded solid propellant grain.

The assembled igniter is shown in figure 6-16, less the ignition booster, and consists of the following components.

| Component | Drawing No. |
|---|---|
| Igniter body | E15502 (Thiokol) |
| Grain cartridge | C05811 |
| Head cap | C05821 |
| Gasket | C05873 |
| Insulation insert | C06130 |
| Initiator (EED) | Holex model 2074 |
| O-Ring | MS28775-024 |
| O-Ring | Parker No. 3-6 |
| Booster | C05830 |

A. Igniter Body

Ten igniter bodies were furnished by NASA and were delivered fully machined. An insert was designed to provide thermal protection at the aft end during motor operation and to act as the igniter nozzle. Body insulation was provided by the grain cartridge, which was adhesively held in the body during firing. The body material was 303-stainless steel. The igniter was threaded into bosses located at the aft end of the demonstration motor.

B. Insert

The insert consists of a molding from Fiberite MX2625, which is adhesively bonded to the igniter body with HT-424 adhesive.

C. Head Cap

The cap is machined from 303-stainless steel and is threaded to the forward section of the igniter body. A MS boss is provided at the forward end to interface with the Holex 2074 EED.

D. Grain Cartridge

The grain, a tubular design, consists of UTP-1095, a high burning rate PBAN formulation, cast into a paper phenolic cartridge. The loaded cartridge is adhesively bonded to the igniter body with Epon-934 adhesive. The weight of each propellant grain is 0.068 $lb_m$ or 0.136 $lb_m$ for the ignition system.

E. Gasket

The gasket, used as a grain support, obduration seal, and head cap insulation, is fabricated from 40 Shore neoprene rubber and is adhesively bonded to the head cap with Epon-934 adhesive.

F. Ignition Booster

The booster is comprised of 5 g of $BKNO_3$ No. 2A pellets with 1 g of $BKNO_3$ factory fines interspersed among the pellets and heat sealed in a static-free velostat plastic bag. The sealed bag is placed in a paper phenolic tube and is mounted in line with the nozzle of the igniter.

G. EED

The EED is an off-the-shelf design from Holex, Inc. The main charge of the EED contains approximately 1 g of a pressed $BKNO_3$ pellet, which is sufficient to ignite the igniter grain.

6.5.2 Sizing

A NASA-furnished igniter body was used, and it was desirable that its performance characteristics be similar to those of the parent igniter. The grain cartridge was, therefore, designed to deliver a mass flow rate of 0.25 lb/sec over a period of 0.35 sec. This results in a total mass flow of 0.5 lb/sec for each motor. With this flow rate, the calculated flux delivered to the grain surface is 30 cal/cm$^2$-sec. Although ignition should occur at this relatively low flux, it was felt advisable to augment the heat flux. Based on the following empirical relationship*

$$W = \frac{38}{\Delta H}\left[A_B q_c \left(\frac{L}{A_B}\sqrt{4\pi A_p}\right)^{0.59}\right]^{1.06}$$

where:

$W$ = charge weight = g

$\Delta H$ = heat of combustion = 1,500 cal/g

$A_B$ = surface area = 1,110 cm$^2$

$q_c$ = ignition energy = 0.3 cal/cm$^2$ (arbitrarily reduced from 0.5 cal/cm$^2$ since pyrogen is a primary ignition mode)

$L$ = grain length = 17.8 cm

$A_p$ = port area = 198 cm$^2$.

a total charge weight of 10 g or 5 g per igniter was calculated. One gram of fines was added to aid in ignition of the pellets.

* "A Method for Predicting Ignition Energy Requirements of Practical Propellant Systems", NAVORD Report No. 6134, 2 February 1959.

The use of the augmentation charge added only 80 psi to the initial peak, or a maximum of 180 psi when coupled with the pyrogen igniters.

### 6.5.3 Igniter Thermal Analysis

A thermal analysis was conducted on the igniter throat to determine the ablation of the silica-phenolic insert during the igniter burn and the soakout response of the throat region after igniter burn. This analysis was required to ensure thermal and structural integrity of the igniter installation during the firing. The approach used was to analyze the most severe location for ablation and thermal penetration, assuming that all other locations within the igniter were thermally less severe. The throat region experiences the most severe environment since the heat transfer and ablation is the greatest there, while being less at all locations upstream.

The determination of the throat heat flux and ablation requires a knowledge of the igniter pressure and propellant characteristics. Since the ablation of the igniter throat and the calculation of the pressure trace was interrelated, a ballistics analysis must be made which simultaneously computes the ablation of the throat and pressure trace. Igniter ballistics computer program IGNITER/CODE was used for this purpose and incorporates the standard ballistics and gas dynamic equations plus the capability to predict throat ablation using the empirical ablation correlation for silica-phenolic. This correlation relates heat flux to the ablation rate of the silica-phenolic as shown in figure 6-6. The heat flux is computed using the Bartz convective heat transfer coefficient for turbulent flow with which the ablation rate may be found for each time step of the ballistics analysis, thus updating the throat diameter with time.

With the UTC one-dimensional heat conduction computer program, LA15ZAZ, the thermal penetration into the throat structure was computed at the thin steel section as marked in figure 6-16. At the end of the igniter firing duration, the steel temperature increase was predicted to be less than 30°F. For the remainder of motor firing, it is assumed that the gas within the igniter remains stagnate, and the energy within the igniter chamber is convected to the walls during the motor firing. It is assumed that the igniter chamber temperature decreases during this process and that only enough chamber gas is introduced to maintain equilibrium pressure. This maximum energy can be found from the product of the maximum mass of gas that can be in the chamber, the gas specific heat, and the chamber temperature. The maximum mass of gas is a product of the chamber volume and the gas density evaluated for maximum motor chamber pressure and ambient temperature. This energy was then combined with that remaining within the igniter throat wall at the end of the igniter firing to obtain a final steel and insulation temperature at the end of motor burn. This temperature is computed to be 733°F. These results are conservative for the following reasons:

A. The heat transfer analysis was conducted using a noncharring heat conduction solution for both the igniter burn and soakout phases. The absorption of energy by the silica-phenolic charring would significantly reduce the final steel temperature.

B. The analysis location chosen contains the least amount of steel on a one-dimensional basis. Since the structure is quite three-dimensional in nature, the computed temperature would be reduced due to three-dimensional conduction effects.

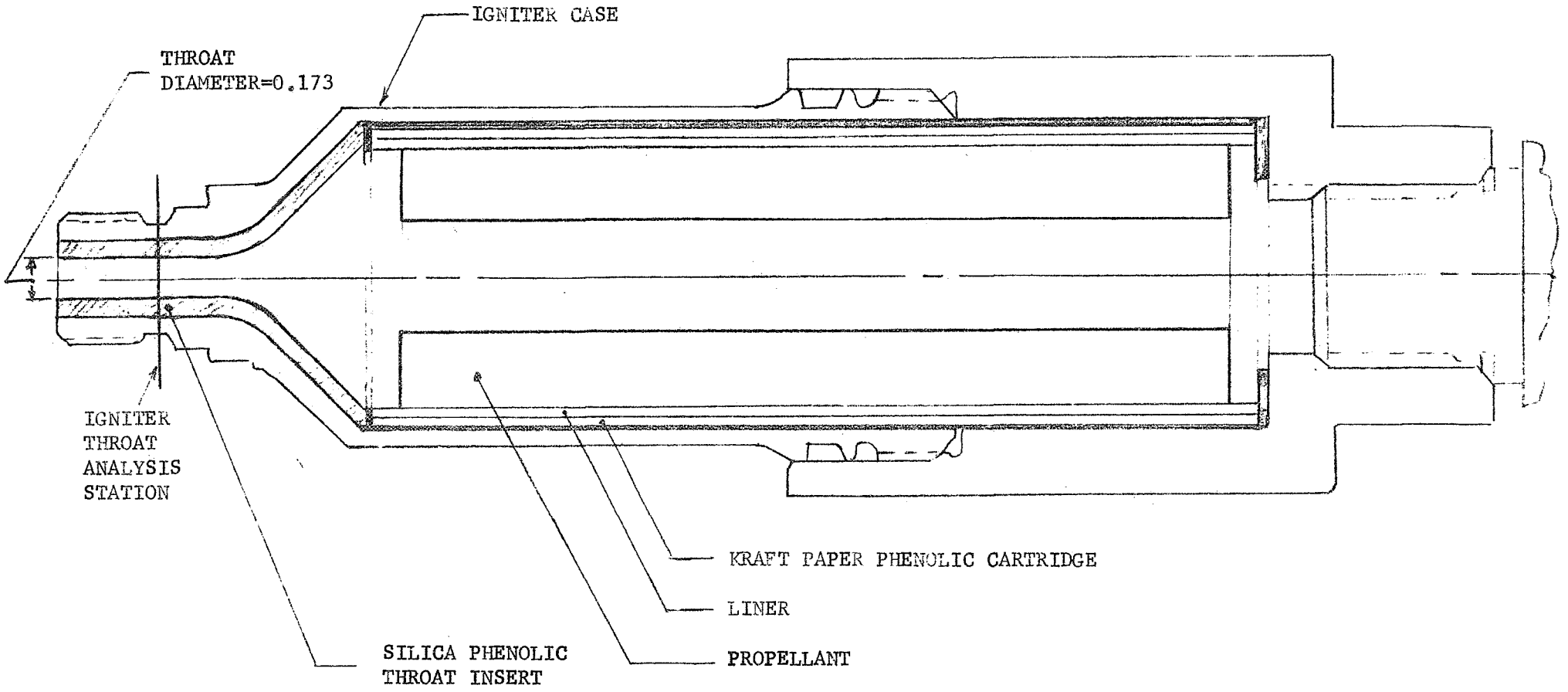


Figure 6-16. Igniter Schematic Showing Location of Thermal Analysis

Since the throat region had the greatest residual energy from the igniter firing, it is the most severe location for thermal analysis. All other regions have more mass and a significantly lower heating rate than the throat. On this basis the igniter is thermally adequate from both the igniter burn and motor burn environments.

Inspection of the assembly drawing for the static test motor revealed that the igniter assembly protruded significantly beyond the exit plane of the nozzle, where radiation heating could be quite severe on the igniter case. To ensure adequate protection during the static test, an evaluation was made of insulation that might be required. A prediction of maximum radiant heat flux was made by determining the view factor to the igniter case from the jet plume and combining it with radiant heat flux emitted from the jet (based upon exit plane static temperature). It was determined that 0.25 in. of cork, such as Insulcork 2755, would be adequate to protect the igniter case during the firing.

## 6.6 MOTOR LOADING AND CURING

### 6.6.1 Processing Procedures

The preparation, loading, and curing of spherical demonstration motors has been conducted in accordance with standard operating procedures as modified by specific quality control requirements to assure that the necessary quality is obtained for each casting. Motors were cast from separate propellant mixes in accordance with program objectives.

One motor was employed to experimentally verify the optimized thermal sterilization cycle, and two were processed for demonstration tests. Motor processing includes case inspection; hydrostatic proof testing; cleaning; insulation fabrication; liner preparation; application to the insulation; propellant mixing, casting, and curing; and grain machining to the final configuration.

The motor processing flow chart, figure 6-17 shows the fabrication and processing procedures pertinent to this task. Each phase was monitored by quality control to assure conformance with UTC specifications and procedures.

A. Case Inspection, Hydrotest, and Cleaning

Each case (GFE) was visually and dimensionally inspected upon receipt to verify conformance to drawing E-1424F, then hydrostatically tested in the following manner:

1. The motor case was secured in a handling dolly assembly (GFE), capped with an aft closure (GFE), and sealed with a UTC-fabricated hydrotest plug. The hydrotest assembly, including pressurization equipment, is shown in figure 6-18.

2. The case was filled with ethylene glycol pressurized to 75± psig then vented to release entrapped air.

3. Hydrostatic proof pressure of 900±20 psig (1.5 MEOP) was held for 1 min. Pressurization and depressurization rates were 500 to 1,000 psi/min.

4. At the conclusion of the hydrotest, the motor case assembly was cleaned with undiluted toluene, followed by a caustic-free detergent bath and a thorough rinsing with tap water.

5. The motor case was visually inspected for hydrotest damage, then dye-penetrant inspected. This was followed by cleaning the case prior to further processing.

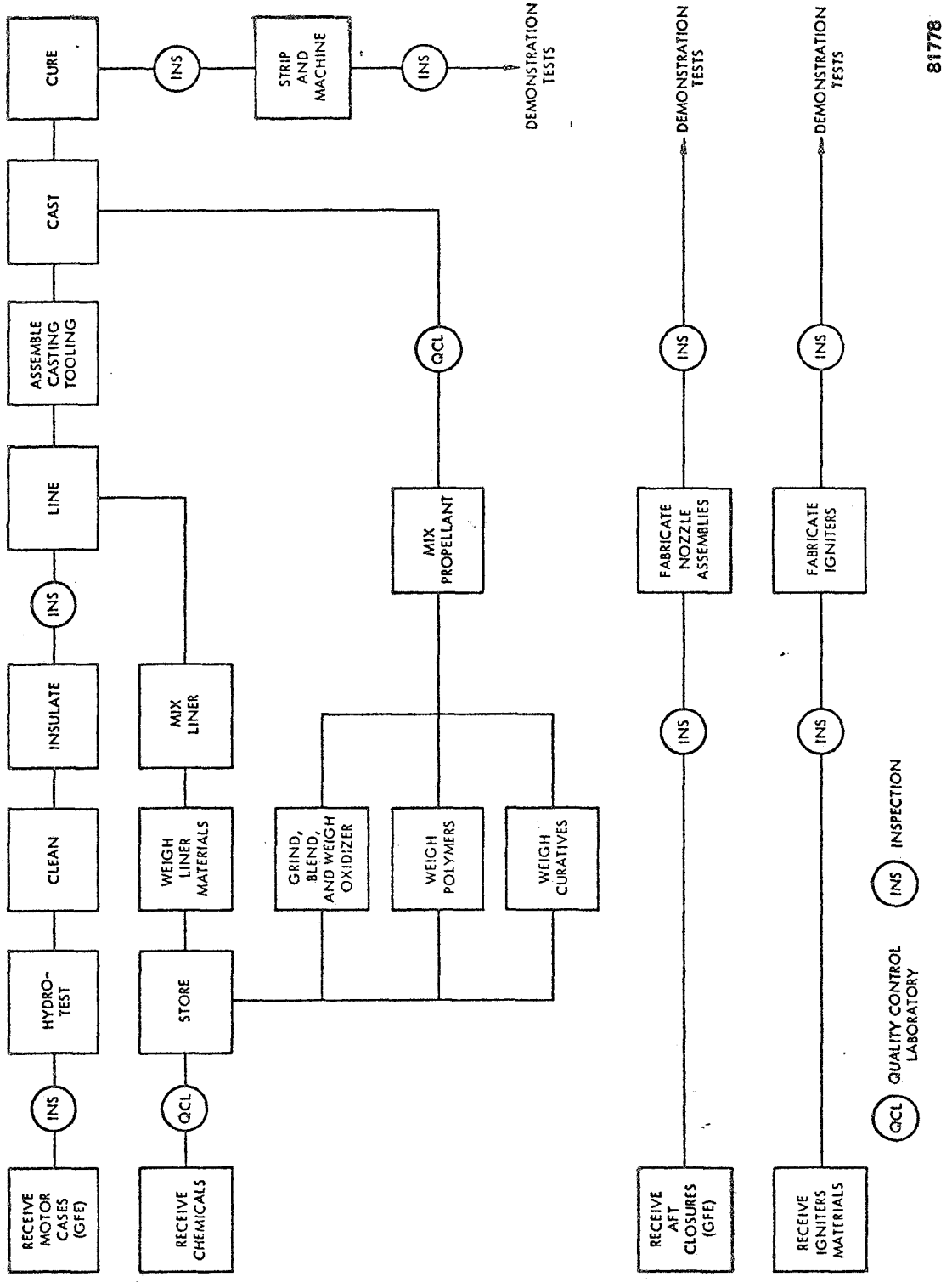


Figure 6-17. Motor Processing Chart

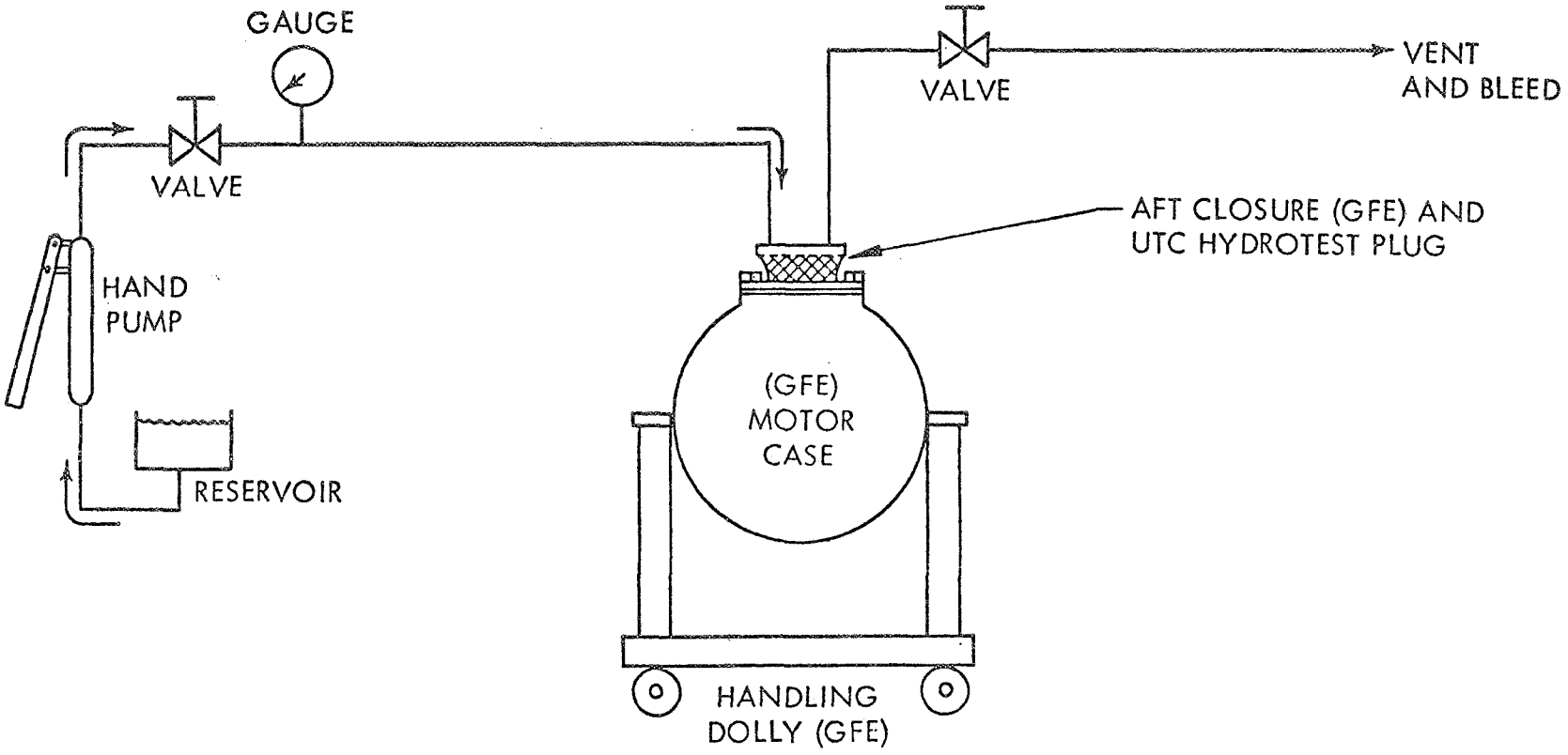


Figure 6-18. Hydrotest Assembly

B. Case Insulation Fabrication

Following successful completion of the proof pressure test, insulation was fabricated within the motor case. The process involved laying up uncured plies of butyl rubber insulation to the required thickness on the prepared case surface using a release cloth where applicable for the stress relief boot. The layed up material was vacuum bagged, and both the insulation and insulation-to-case bond were cured in an autoclave at a pressure of 200 psi at 300°F. Volatiles were removed by exposing the unit to one simulated thermal sterilization cycle.

C. Liner and Propellant Processing

Insulated motors were wash-coat lined with UTL-0026 prior to casting. The lined motor was weighed, then masked to prevent undesired bonding of the propellant to the insulation adjacent to the aft closure.

A 5-gal. Day Regal mixer was employed, providing a capacity of 80 lb per batch.

Propellant processed in each 75-lb demonstration motor batch was apportioned in the following manner:

1. 2 lb for liquid strand burning rate and quality control analysis prior to casting,
2. 10 lb for three NASA/LRC sample blocks, each 3 in. by 3 in. by 5 in.,
3. 10 lb for 35 JANNAF specimens for UTC propellant evaluations,
4. 45 lb for motor casting,
5. 8 lb for mix bowl and valve residual.

Propellant was processed under vacuum in facilities arranged to permit remote operation of all ingredient mixing activities. Mix procedures were in accordance with specifications established during sterilizable propellant

development and include detailed records of mixer coolant temperature, mix temperature, and mixer power.

The mixing operation was conducted in the following sequence:

1. All ingredients except curatives and oxidizer were mixed under vacuum at 180°F for 30 min,

2. Curatives were added and mixed under vacuum at 165°F for 5 min,

3. Oxidizer was added remotely; vacuum mixing was continued at 165°F for 30 min after all oxidizer was added.

The propellant was then vacuum cast to a specified volume, a mandrel was inserted, and the motor was moved to the cure oven. The casting installation is outlined in figure 6-19. The motor was pressure cured at 100 psi.

Upon completion of curing, the motor and samples were removed to ambient temperature, the mandrel was removed from the motor, and a preliminary visual examination was conducted. The propellant was then remotely machined to the final contour.

### 6.6.2 Processing Propellant for Evaluation

As indicated in previous sections of this report, the candidate propellant developed for sterilizable motor systems is based on CTPIB, a polymer developed at UTC and scaled up by Enjay Chemical Company. Inasmuch as the polymer does not have an extensive background of manufacture and use, it was decided to characterize more than one 5-gal. mix prior to processing the spherical demonstration motors. This was considered particularly critical since previous 1-gal. mixes had indicated variations based on polymer sublots. In addition, polymer equivalent weights varied with each batch of polymer subjected to

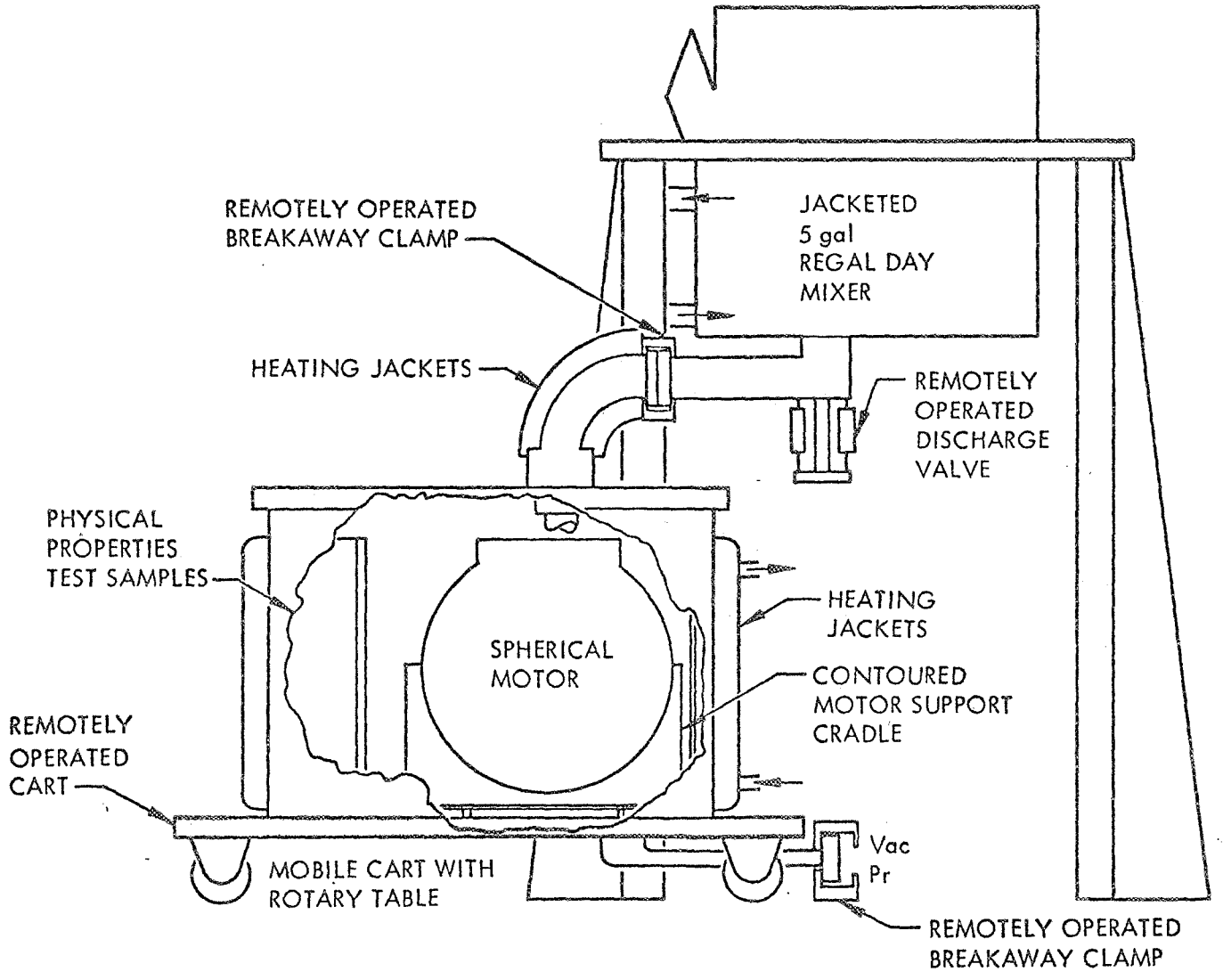


Figure 6-19. Remote Casting Installation

acetone fractionation. As discussed earlier, the effect of acetone fractionation was to remove the very low molecular weight polymer fractions resulting in a higher equivalent weight for the polymer. The result of the fractionation on final propellant properties was to decrease stress capability with a slight increase in strain capability.

Altogether four 5-gal. propellant batches were processed before the first demonstration motor was cast. All of these batches utilized a curative-to-carboxyl functional ratio of 1.2:1. The initial stress-strain data for these batches is shown in table 6-IV.

TABLE 6-IV

FIVE-GALLON CHARACTERIZATION BATCHES
(UTP-11439)

| Batch No. | Polymer Lot No. | Equivalent Weight, g | Stress/Strain, psi/% | |
|---|---|---|---|---|
| | | | After Cure | After One Cycle |
| 5/1 | 474A | 1,405 | 111/22.5 | 213/17 |
| 5/2 | 476 | 1,010 | 114/22 | 207/12.5 |
| 5/3 | 476A | 1,318 | 95/22 | 173/14.5 |
| 5/4 | 276A2 | 1,566 | 85/22.4 | -- |

Concurrent with the processing and evaluation of propellant mixes for characterization of propellant, one inert batch was cast into a spherical motor to experimentally verify the optimized thermal sterilization cycles. The inert propellant cracked during the test, but the data required to calculate the necessary heat transfer parameters were not compromised. As a result of the cracking of the inert grain, the propellant properties were again analyzed with respect to the motor grain design. The stress-strain properties of the inert grain are presented in table 6-V.

TABLE 6-V

UTX-12335 STRESS-STRAIN PROPERTIES

| | Stress, psi | Strain, % |
|---|---|---|
| After cure at 75°F | 149 | 41.2 |
| After one cycle at 75°F | 196 | 10.3 |
| After one cycle at 275°F | 89 | 6.3 |

In addition to the very substantial postcure experienced by the inert propellant during the sterilization cycle, the inert grain was bonded directly to the case with no insulation or relief boots to relieve excessive strain on the bore cavity.

An engineering analysis of propellant physical properties and the grain configuration showed that failure of the inert propellant would have been predicted based upon its physical properties. Nevertheless, this event focused emphasis on the zero strain temperature shift and the strain capability of the propellant.

### 6.6.3 Processing Propellant for Demonstration Motors

As a result of the stress-strain properties exhibited by the four propellant batches at the 5-gal. scale and the cracking of the inert grain, it was concluded by NASA that a reduced curative ratio should be used in the first motor batch to increase strain capacity. On the basis of earlier propellant work conducted at UTC with other lots of polymer in which adequate physical properties had been obtained using reduced curative ratios, a decision was made that the first motor (No. 2348-002) should be loaded with propellant having a curative ratio of 1.1:1.

Cartons of propellant cured with the motor exhibited a decided lack of cure after the normal cure cycle; therefore, the motor was subjected to an extended cure cycle. After 19 days at 160°F and 5 days at 180°F, the motor was inspected. Some evidence of propellant unbond at the propellant/liner interface was observed. Radiographic inspection after one sterilization cycle revealed major separations near the propellant/insulation bond area. A very thin layer of propellant generally appeared to cover the liner at the separated areas. Although some evidence of propellant separation was observed after propellant cure, the areas of separation were more apparent after sterilization.

Based on the initial very soft propellant cure resulting from the first motor mix, the second live spherical motor (No. 2348-003) was cast using a functional equivalence ratio of curative to polymer of 1.15 (reference UTP-11439-5/6). The motor was cured at 100 psig for 2 days at 180°F and for 7 days at 160°F. The extended cure schedule was used to minimize the upward strain-free temperature shift during subsequent sterilization cycles.

The second live spherical motor also experienced unbonding at the propellant/insulation interface after one sterilization cycle. The unbonded area was extensive around the aft portion of the case. Table 6-VI indicates the propellant physical properties as a function of the number of sterilization cycles to which it was exposed.

## 6.7 INSPECTION AND QUALITY CONTROL

The primary objectives of the UTC quality assurance program for NASA Contract No. NAS-1-8937 were: (1) to assure motor-to-motor uniformity and (2) to provide specific inspections between sterilization cycles with acceptance of the motors based on specific contract acceptance criteria. To accomplish these objectives, the UTC quality assurance program focused its attention on

TABLE 6-VI

PROPELLANT PHYSICAL PROPERTIES

| | UTP-11439-5/5 Motor No. 2348-002 | | UTP-11439-5/6 Motor No. 2348-003 | |
|---|---|---|---|---|
| | True Stress, psi | True Strain, % | True Stress, psi | True Strain, % |
| After cure at 75°F | 57.0 | 22.5 | 168 | 15.2 |
| After cure at 250°F | 23.5 | 27.0 | 79.7 | 11.7 |
| One cycle at 75°F | 52.7 | 37.2 | 157 | 19.4 |
| One cycle at 250°F | 13.8 | 40.5 | 65.6 | 17.8 |
| Two cycles at 75°F | 28.0 | 32.6 | 110 | 23.8 |
| Two cycles at 250°F | 10.8 | 41.4 | 40.2 | 27.2 |
| Three cycles at 75°F | 24.7 | 31.5 | 122 | 22.0 |
| Three cycles at 250°F | 3.3 | 43.8 | 41.2 | 26.6 |
| Four cycles at 75°F | 34.0 | 31.4 | 125 | 21.1 |
| Four cycles at 250°F | 5.8 | 46.7 | -- | -- |
| Five cycles at 75°F | 31.3 | 31.8 | -- | -- |
| Five cycles at 250°F | -- | -- | -- | -- |
| Six cycles at 75°F | -- | -- | 117 | 25.0 |
| Six cycles at 250°F | -- | -- | 30 | 25.0 |

two major areas of inspection: (1) propellant and liner processing and (2) sterilization effects on loaded motor integrity. Generally, the inspections supporting ingredient acceptance and mixing and casting were routine inspections to assure proper composition and weighout of ingredients and chemical, ballistic, and physical properties analysis of the processed propellant to verify the mixing cycle and propellant performance. From an analysis standpoint, UTP-11439 propellant was analyzed as routinely and reliably as other families of propellants processed at UTC. Existing quality control laboratory analysis procedures were employed for all analyses.

To evaluate sterilization effects on system integrity, the demonstration motors were inspected before and after each sterilization cycle. These inspections consisted of dimensional inspection, radiographic inspection, and tap test inspection. These inspection techniques were able to detect propellant grain defects such as cracking, voids, unbonds, separations, and slump, and were able to detect changes in these conditions from one sterilization cycle to the next. These inspections provided the necessary confidence to evaluate the integrity of the sterilized motors and were conducted quite routinely and economically.

Figure 6-20 illustrates the master inspection plan utilized during the program. The following paragraphs will discuss the major inspections conducted and the results of these inspections.

### 6.7.1 Propellant Inspections

#### 6.7.1.1 Propellant Constituents

The quality control laboratory obtained complete analysis of all propellant constituents prior to mixing of the propellant. This was accomplished through use of supplier certified test analysis or by quality control laboratory analysis, as required.

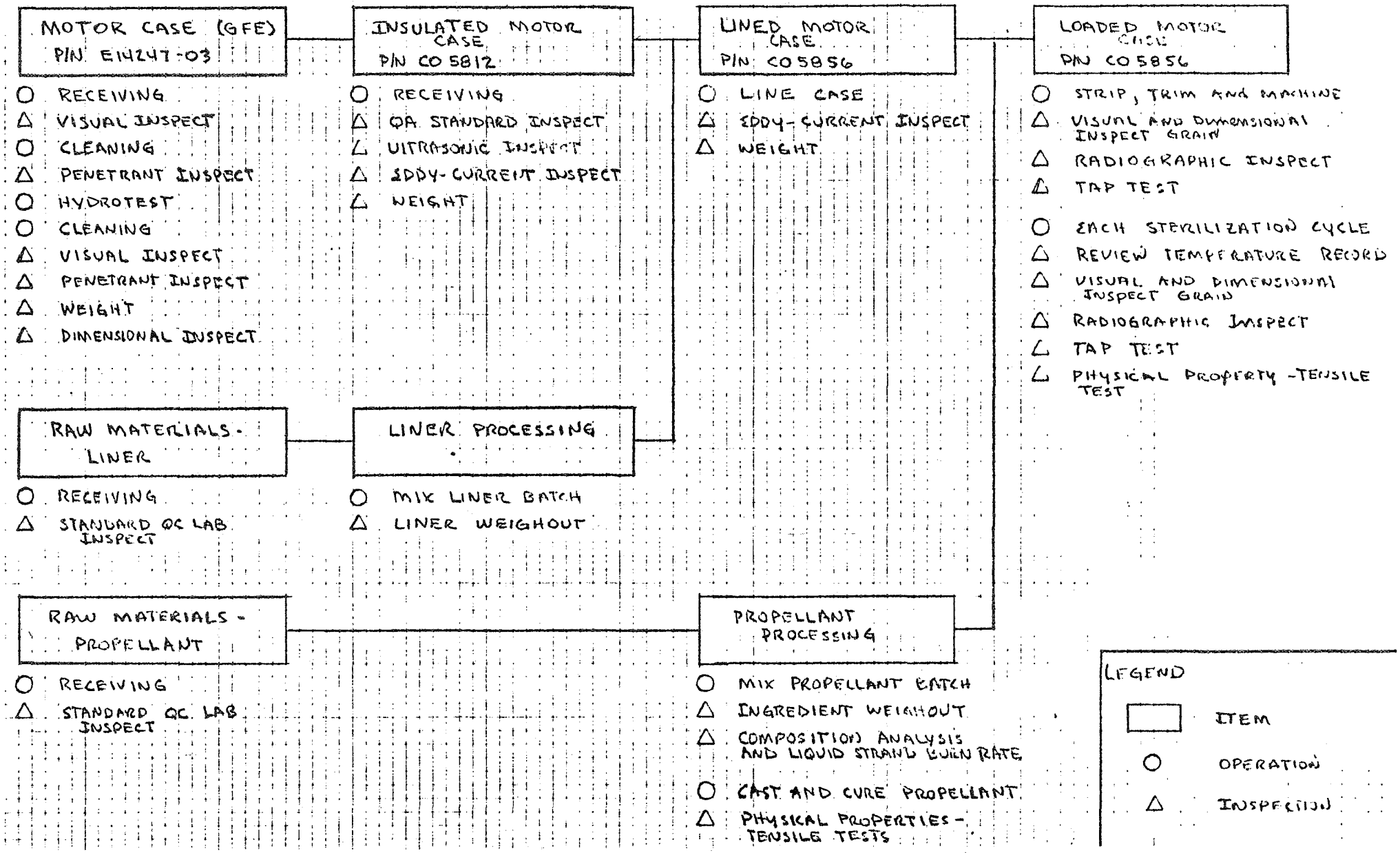


Figure 6-20. Master Inspection Plan

6.7.1.2 Uncured Propellant Analysis Prior to Loading

The quality control laboratory performed the following tests on each batch of propellant prior to loading into the motor: (1) percent ammonium perchlorate, (2) percent aluminum, (3) unreacted acid equivalents, (4) unreacted crosslinker equivalents, and (5) liquid strand burning rate at 500 and 1,000 psig (75°F).

6.7.1.3 Cured Propellant Physical Properties

Five propellant specimens from each propellant mix were set aside for physical property testing. The results of the pre-motor batches are presented in table 3-VII. The results of tests of samples from the motor batches are presented in table 6-VII.

6.7.2 Motor Case and Loaded Motor Inspections

6.7.2.1 Motor Case Inspections

Upon receipt at UTC the GFE motor cases were visually and penetrant inspected for cracks, scratches, dents, and stress risers. Penetrant inspection was in accordance with MIL-I-6866, type 1.

Penetrant inspection was repeated after hydrotest of the motor cases to 1,000±20 psi. All GFE motors successfully passed the penetrant inspections. Proper cleaning techniques compatible with titanium were employed to remove the residue from penetrant inspection.

6.7.2.2 Insulated Case Inspection

Each insulated case was ultransonically inspected for insulation-to-case bond. Ultrasonic inspection was conducted in accordance with UTC specification 4MGS-90410, type 1, class 1. All cases were 100% inspected; no unbonds were detected. The contact method was used utilizing the Sperry UN-700 Model with a 3/8-in.-diameter 2.25-mHz transducer.

TABLE 6-VII

PROPELLANT DATA - MOTORS NO. 1 AND 2

| | Batch UTP-11439-5/5 Motor No. 1 | | Batch UTP-11439-5/6 Motor No. 2 | |
|---|---|---|---|---|
| Stress (psi) at | 70°F | 250°F | 70°F | 250°F |
| 0 cycle | 57.0 | 23.5 | 168 | 79.7 |
| 1 cycle | 52.7 | 13.8 | 157 | 65.8 |
| 2 cycles | 28.0 | 10.8 | -- | -- |
| Strain (%) at | | | | |
| 0 cycle | 22.5 | 27.0 | 15.2 | 11.7 |
| 1 cycle | 37.2 | 40.5 | 19.4 | 17.8 |
| 2 cycles | 32.6 | 41.4 | -- | -- |

The insulated cases were then inspected to verify insulation thickness. This inspection was conducted using eddy currents (ED-510 unit). These measurements were taken at specific stations located from the nozzle boss and were recorded every 90° to verify insulation thickness and to serve as a baseline for subsequent liner measurements. Insulation thicknesses were within B/P tolerance. The specific technique employed was accurate to 0.001 in.

Peel strength values, insulation to case, were obtained for UTC's supplier. Specification requirements were 35 lb/in.-min. Preproduction, production, and case samples obtained values in excess of 87 lb/in.

6.7.2.3 Lined Motor Case

Liner thickness measurements were made at the same stations that the insulation thickness measurements were made. Liner thickness required by B/P was 0.030 in. to 0.050 in. and all cases were found to be acceptable. Accuracy of the test measurement was 0.001 in.

6.7.2.4 Loaded Motor Inspection

Each loaded motor was visually, dimensionally, radiographically, and tap test inspected. These tests were conducted prior to and after each sterilization cycle and were planned and designed to provide reproducible results from inspection to inspection. Dimensional inspection was conducted of the bore of the motor at specific stations to measure changes in the bore due to grain movement, shrinkage, or slump. Radiographic inspection was conducted as illustrated in figure 6-21. The results of radiographic inspection were recorded on specially prepared NDT records for this program.

The radiographic technique conformed to the requirements of MIL-STD-746, and the sensitivity requirement of 1% was satisfied.

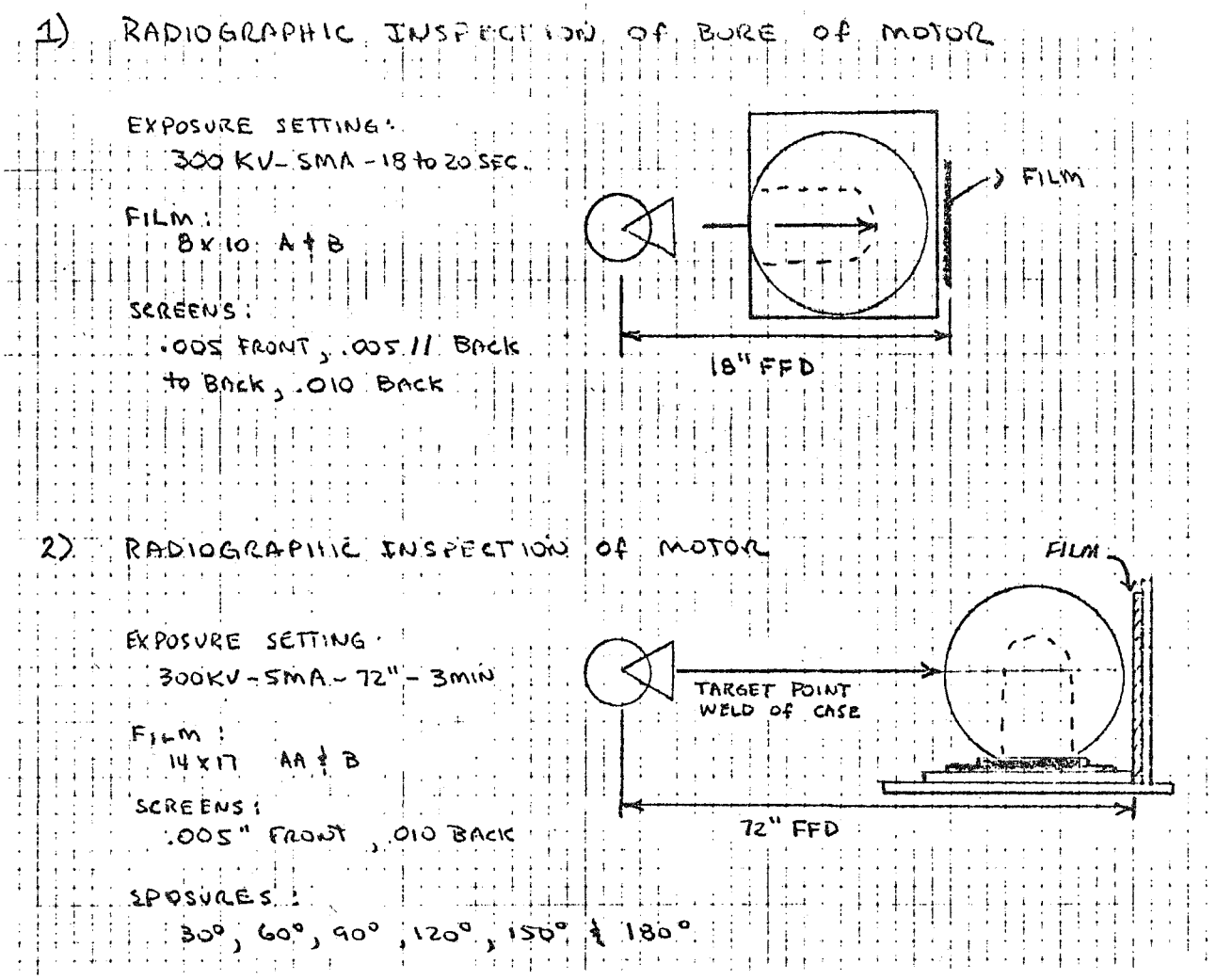


Figure 6-21. Radiographic Inspection Technique

Accept/reject criteria as defined by the contract included: (1) motors will be unacceptable if there is any evidence of grain cracking or separation between propellant and liner or liner and insulation, (2) maximum allowable void size of 0.125 in. in diameter with no more than five voids of this size in any 14 in. by 17 in. film area, (3) the presence of porosity shall be cause for rejection, (4) no foreign objects in the propellant grain, and (5) unbonds between the case and insulation shall be reported.

UTC's radiographic inspection was capable of identifying the above anomalies. Results of the inspections on demonstration motors No. 1 and 2 are contained in tables 6-VIII and 6-IX and in figures 6-22 and 6-23.

In addition, a tap test was conducted to locate unbond areas. The tap test was conducted starting in the area of the boot and working toward the igniter end. The tap test was conducted to detect fundamental change initially, then harmonic change depending upon the degree of fundamental change. The boot area was used as a standard for unbond. The tap test was conducted in accordance with the UTC established technique for tap testing the fourth stage Scout motor.

A summary of project nonconformances is contained in table 6-X.

## 6.8 MOTOR ENVIRONMENTAL TESTS

One thermal control motor and two demonstration motors, with related propellant samples, have been subjected to dry heat thermal sterilization cycles. The selected cycle, optimized by the analyses of section 5.0, meets the requirements of the statement of work while minimizing propellant thermal exposure and operating time.

Sterilization was conducted in a 3 ft by 3 ft by 2 ft electrically heated, forced-draft oven (Despatch Company, model V-29) capable of simultaneously cycling three motor assemblies.

TABLE 6-VIII

LOADED CASE, STERILIZABLE MOTOR (PROJECT 2348)
P/N CO5856-01-01, S/N 0176 - MOTOR NO. 1

| Event | Temperature °F | Bore Measurements, in. (A) 2.5 | (B) 4.0 | (C) 6.0 | Average | Depth | X-ray Results (See Attached NDT Reports) |
|---|---|---|---|---|---|---|---|
| Mandrel | 75 | -- | 4.696 | 4.640 | -- | -- | |
| Before machining | 75 | -- | 4.795 | 4.800 | 4.789 | -- | Quick series of X-rays were taken to provide general evaluation of the grain and to locate any major anomalies - no major anomalies were noted. |
| After machining | 75 | 6.955 | 6.955 | 6.945 | 6.952 | 9.545 | X-rays revealed excessive porosity 360° around in the first 1 in. of propellant in the aft end. Average size 0.100 in., striation in two parts 0.25 in. from aft end, one part 0.200 in. long, the other 0.850 in. long and appeared for 360° and one void 1.5 in. long by 300 in. wide located dead center in the forward end. |
| After first cycle | 100 | | 6.955 | 6.945 | 6.950 | 9.570 | Porosity expanded and extended to 1-1/2 in. (fine to medium porosity) and for another additional 1-1/2 in. (minute to fine porosity); opening of striation in the boot area; scattered unbonds determined in the dome section identified by tap test. |
| After second cycle | 100 | 6.75 | 6.60 | 6.70 | 6.68 | 9.30 | Porosity further expanded and extended; unbonds detected by X-ray indicating separation of liner to propellant (scattered unbond); definite unbond revealed by tap test. |

TABLE 6-IX

LOADED CASE, STERILIZABLE MOTOR (PROJECT 2348)
P/N CO5856-01-01, S/N 0177 - MOTOR NO. 2

| Event | Temperature °F | Bore Measurements, in. (A) 2.5 | (B) 4.0 | (C) 6.0 | Average | Depth | X-ray Results (See Attached NDT Reports) |
|---|---|---|---|---|---|---|---|
| Mandrel | 75 | -- | 4.896 | 4.640 | -- | -- | --- |
| Before machining | 75 | -- | 4.750 | 4.855 | 4.802 | 9.102 | None taken. |
| After machining | 75 | 6.75 | 6.90 | 6.85 | 6.83 | 9.20 | X-rays revealed porosity 360° around in the first 2 in. of propellant in the aft end. Average size 0.150 in., concentration volume medium, also separation of liner to boot at aft end and possible start of separation liner to insulation and liner to propellant in dome section. Definite but minute audio change in tap test. |
| After first cycle | 100 | 6.15 | 6.005 | 6.03 | 6.06 | 9.20 | Porosity extended and expanded; propellant separation at boot peeled from insulation, liner to propellant separation over 50% of the motor (verified by tap test), inside the propellant separations perpendicular to thrust axis 2 to 3 in. in from the aft end (propellant to propellant separation). |

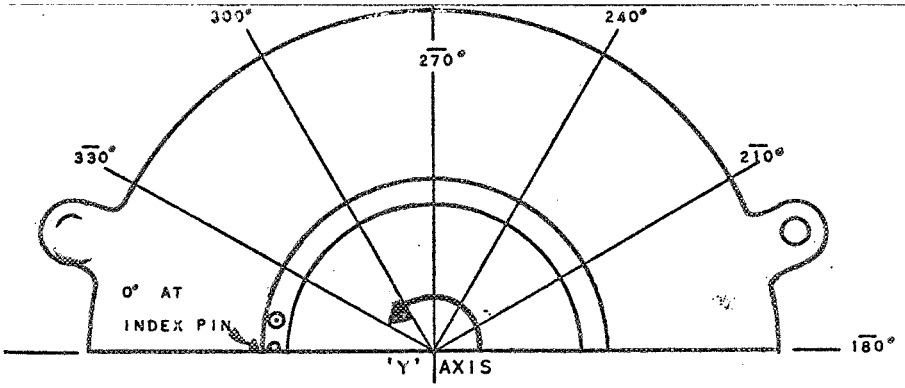


DEGREES OF REVOLUTION ARE MEASURED FWD. LOOKING AFT.
CLOCKWISE ABOUT 'Y' AXIS

# X-RAY REPORT GRAPH

PART NO. C05856 S/N 0176

DATE 6-11-69 INSP. [illegible]

SPEC. _____ CYCLE _____

REMARKS Initial X-Ray

1) Porosity 360° Around

LEFT TANGENT AT REVOLUTION OF

RIGHT TANGENT AT REVOLUTION OF

X-RAY TARGET AT REVOLUTION OF

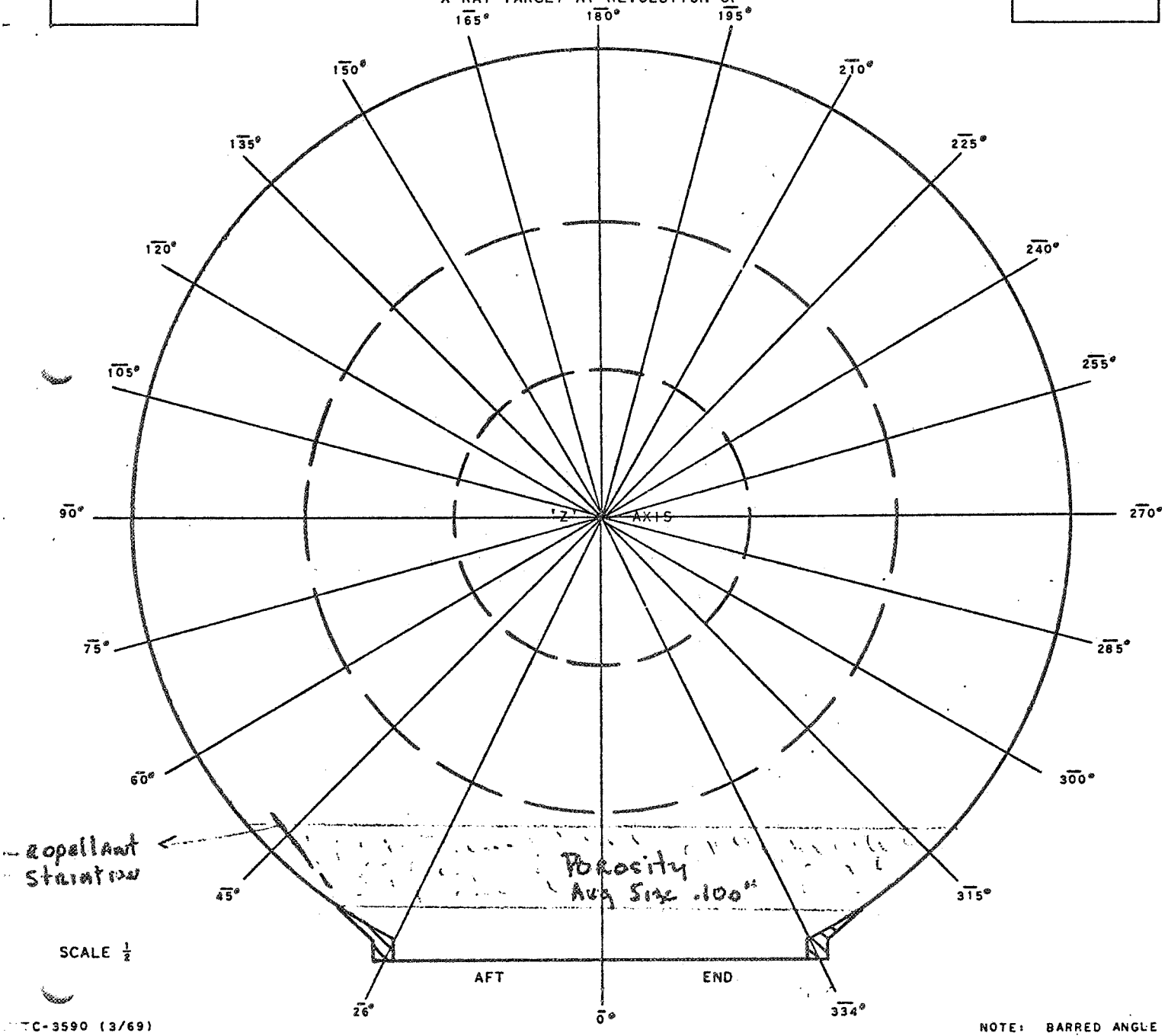


SCALE ½

TC-3590 (3/69)

NOTE: BARRED ANGLE IS MEASURED FROM 'Y' AXIS CLOCKWISE ABOUT 'Z' AXIS

$\overline{\text{O}}^{\circ}$ BARRED ANGLE IS POSITION IN X-Y PLANE ABOUT THE CENTER OR 'Z' AXIS

R DISTANCE FROM CENTER OR 'Z' AXIS TO DEFECT

Figure 6-22

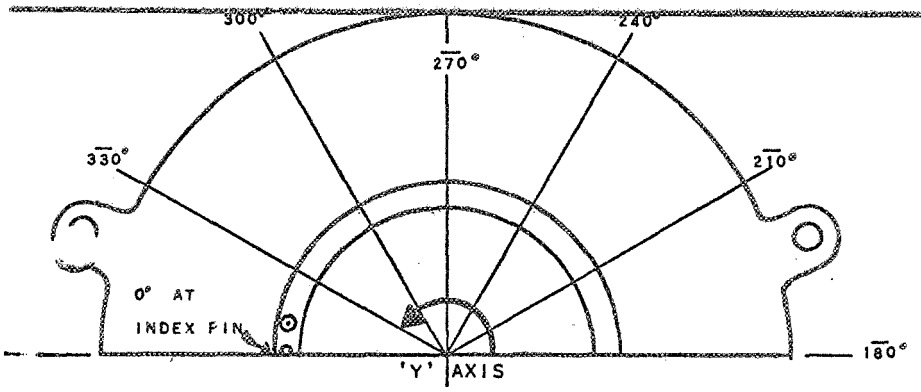


DEGREES OF REVOLUTION ARE MEASURED FWD. LOOKING AFT.
CLOCKWISE ABOUT 'Y' AXIS

# X-RAY REPORT GRAPH

PART NO. C05856 S/N 0177

DATE 6-19-69 INSP. COUSINS

SPEC. _____ CYCLE _____

REMARKS INITIAL X-RAY

1) Porosity is 360° around

2) AFT END Separation is 360° around

LEFT TANGENT AT REVOLUTION OF

RIGHT TANGENT AT REVOLUTION OF

X-RAY TARGET AT REVOLUTION OF

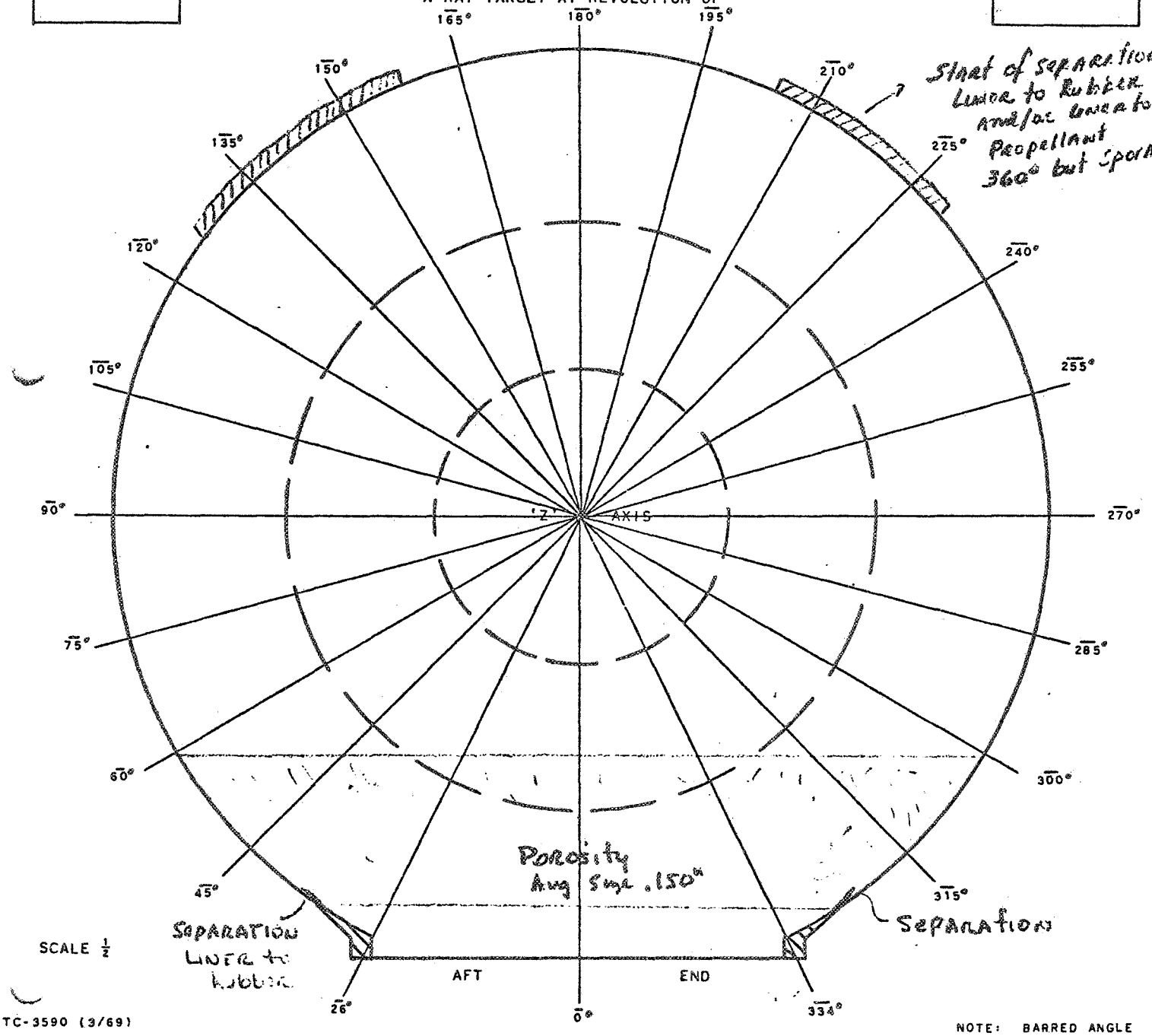


Start of separation Liner to Rubber and/or Liner to Propellant 360° but spora

Porosity Avg 5mil .150"

Separation

Separation Liner to Rubber

SCALE ½

TC-3590 (3/69)

$\overline{0}^{0}$ BARRED ANGLE IS POSITION IN X-Y PLANE ABOUT THE CENTER OR 'Z' AXIS

R DISTANCE FROM CENTER OR 'Z' AXIS TO DEFECT

NOTE: BARRED ANGLE IS MEASURED FROM 'Y' AXIS CLOCKWISE ABOUT 'Z' AXIS

TABLE 6-X

DISCREPANCY SUMMARY

| UTC Discrepancy Document No. | Part No. | Discrepancy |
|---|---|---|
| IDR 24800 | P/N C05778 Insulated Case, S/N 176 | 0.75 dimension undersize |
| IDR 24794 | P/N C05778 Insulated Case, S/N 179 | 0.03 dimension undersize<br>0.75 dimension undersize |
| IDR 24269 | P/N C05778 Insulated Case, S/N 168 | 0.75 dimension undersize |
| IDR 24753 | P/N C05856 Loaded Motor, S/N 176 | Excessive porosity<br>Separation<br>Propellant voids |
| IDR 01834 | P/N C05856 Loaded Motor, S/N 177 | Excessive porosity |
| IDR 24674 | P/N E 14247-03 Motor Case | Masking tape residue<br>Heat affected zone |
| IDR 00687 | AP Lot MS-57 | $P_H$ water solution is 4.9; should be 5.5/6.5 |

Uniform heating was obtained by baffling air flow while monitoring a control motor thermocoupled to provide a comprehensive thermal profile. A thermal profile confirmed in this manner insured that the most thermally remote portion of demonstration motors were, in fact, at 275°F for 53 hr.

Prior to sterilization cycling, each demonstration test motor was instrumented with four thermocouples, two on the case exterior and two on the propellant surface. During sterilization cycling the specified thermal profile will be verified and documented by a continuous temperature with time record of oven air, case exterior, and grain surface. Each motor was inspected visually and radiographically prior to the first and following each successive thermal sterilization cycle.

# 7.0 SUPPLEMENTAL TESTS

In addition to the uniaxial constant strain rate tests required for monitoring the effect of heat sterilization on propellant properties, some additional testing has been conducted in response to other problems which developed on this program. As a result of experience with the thermal control motor in which the inert grain cracked during heat sterilization, increased concern regarding propellant strain properties dictated a reevaluation of the propellant strain capability. The thermal control motor contained a CTPB system loaded with aluminum and ammonium sulfate which was case-bonded with liner directly to the case wall. This system experienced considerable postcure during the sterilization cycle.

To more realistically evaluate propellant strain capability in the demonstration motors, analog motors (2.8 in. in ID by 13.5 in. in length) were cast with propellant UTP-11439 (batch 5/4) at a curative ratio of 1.2. Polymer lot No. DL-476A2 (equivalent weight 1,566 g) was used. A set of six motors in lined steel cylinders having bore dimensions designed to yield nominal bore strains of 18%, 12% and 8% was processed. The motors were cured for 5 days at 160°F and were measured. Three of the motors were then given an additional 5-day cure. Changes in the propellant bore diameter were measured and related to changes in the strain level at the bore surface and to the strain-free temperature of the propellant. The results are presented in table 7-I. The strain levels increased slightly in the analog motors that were cured for an additional 5 days. After subjecting the complete set of motors to one heat sterilization cycle, those grains which had strain levels of approximately 13%

and 18.5% exhibited cracks on the bore surface. The grains having the least strain (approximately 10%) survived the first sterilization cycle but cracked on the second cycle.

TABLE 7-I

MEASURED STRAIN IN ANALOG MOTORS

Propellant UTP-11439-5/4
Curative ratio 1.2

| Motor No. | Measured Strain, % 5-Day Cure | 10-Day Cure | One Sterilization Cycle | Two Sterilization Cycles |
|---|---|---|---|---|
| 3 | 18.6 | -- | Cracked | -- |
| 2 | 12.9 | -- | Cracked | -- |
| 1 | 8.7 | -- | 10.0 | Cracked |
| 4 | 8.5 | 9.8 | 10.0 | Cracked |
| 5 | 12.7 | 13.6 | Cracked | -- |
| 6 | 18.4 | 19.5 | Cracked | -- |
| JANNAF* Specimens | 22.4 | 17 | -- | 14.5 |

* Constant strain rate of 2 in./min

Based on the degree of shrinkage determined from the grain bore measurements, a strain-free temperature of 180°F for this propellant was established. The strain-free temperature is the temperature to which the motor would need to be conditioned to expand the propellant grain sufficiently to reduce the bore dimension to the original mandrel dimension. After one sterilization cycle, the strain-free temperature increased to 198°F, indicating some additional crosslinking resulting in increased strain in the motors. For comparative

purposes, the propellant strain capability measured for uniaxial constant strain rate tests is also presented in table 7-I.

As a result of these tests, the safety margin, with respect to the strain requirements of the demonstration motor, was considered marginal. A decision was made to reduce the propellant curative level from 1.2 to 1.1 curative/carboxyl equivalent ratio. The first spherical demonstration motor containing UTP-11439 (batch 5/5) cured to a relatively soft propellant. As a result of the obvious low degree of cure of batch control specimens, the spherical motor was given an extended cure cycle (21 days at 160°F followed by 3 days at 180°F). The uniaxial stress-strain test results for control specimens, presented previously in section 6.0, indicate a low stress capability for this batch. After one heat sterilization cycle, some scattered propellant/insulation separation was discovered in the motor by the tap test. After the second cycle, some additional unbonded areas were identified and confirmed by radiographic inspection.

As a result of the abnormally soft cure experienced with the low curative level, the second live motor (No. 2348-003) was processed using a curative level of 1.15. X-rays and tap tests revealed separation of liner-to-boot at the aft end and the possibility of propellant/insulation separation in the dome section. After one sterilization cycle, the areas of separation were more extensive.

Visual inspection of both motors confirmed separations at the propellant/liner interface. A very thin layer of propellant generally appeared to cover the liner at the separated areas. As discussed in section 4.0, several factors were considered to be probable causes for the motor unbonding: (1) migration of materials from the insulation through the liner and into the propellant causing loss of bond strength near the propellant/liner interface and (2) loss

of bond strength of propellant-to-liner during sterilization. A third factor which must be considered is the high temperature endurance stress capability of the propellant. In the spherical demonstration motor, the propellant grain experiences positive shear stresses during heat sterilization at the propellant/insulation interface. These stresses reach a maximum near the aft end of the motor. This shear occurs in addition to the compression stress at the same interface and is exerted throughout the high temperature portion of the sterilization cycle.

An investigation of possible deleterious materials in the Hitco-2820 insulation system, discussed in section 4.0, resulted in the formulation of a modified Hitco insulation which was subsequently installed for testing in cylindrical analog motors. Propellant grains cast into these motors became unbonded after heat sterilization conditioning, but the results were not conclusive because the insulation had not received a sterilization pretreatment prior to casting the propellant. Subsequent attempts by the supplier to bond the modified Hitco insulation into the steel analog motors were unsuccessful. However, additional cylindrical analog motors were processed utilizing UTL-0026 as insulation which was bonded into the cases in the form of 0.125-in. sheets. These cases were then lined according to standard procedures and were loaded with propellant from batch UTP-11439-5/8 (curative ratio 1.15). The cured motors were subjected to one heat sterilization cycle. Radiographic inspection revealed substantial unbonding. Also, in a test in which a thin web of propellant was cast directly to a steel shell, no unbonding occurred. These tests eliminated the insulation as a factor in unbonding, and the bond failures could only be attributed to a failure of the liner/propellant bond or to a lack of endurance stress capability in the propellant.

# 8.0 CONCLUSIONS AND RECOMMENDATIONS

UTP-11439 propellant was demonstrated to be thermally stable up to 275°F for extended time periods. It was successfully processed at the 5-gal. mix scale. Propellant specimens were subjected to extended heat sterilization cycles with essentially no effect on mechanical properties, as determined by constant strain rate uniaxial tensile tests. The liner and the insulation systems survived the required sterilization procedures with no substantial loss of properties. In addition, system tests involving the insulation, liner, and propellant in the bond-in-tension configuration indicated acceptable properties in excess of six sterilization cycles. However, complete motor castings in 13-in. spherical demonstration motors resulted in debonded areas between propellant and insulation after heat sterilization. In addition, the casting of some cylindrical analog motors also resulted in apparent propellant/insulation debonding.

A review of the test results leads to several critical observations pertinent to the debonding problem:

A. Inital analog motors cast into lined steel cases and having bore strains considerably in excess of that in the demonstration motors (up to 18%) all eventually cracked in the bore area after two sterilization cycles. These grains did not debond from the liner. At the same time, uniaxial tensile properties of the propellant showed a lower strain capability than had previously been obtained with propellant with a lower curative ratio. At this point a decision was made to use the spherical motors as a test bed for

propellant screening because of uncertainties with laboratory results, and the first spherical motor was cast with propellant at an arbitrarily selected curative ratio of 1.1. The degree of cure was obviously substrandard for this mix, and the propellant debonded from the insulation during the first sterilization cycle. A second spherical motor was then processed at a curative level of 1.15. The propellant exhibited a reasonable cure but debonded from the insulation after one sterilization cycle. The insulation system in both spherical motors was Hitco-2820.

B. After this, a series of bond-in-tension tests and cylindrical analog motor tests were conducted to investigate whether or not the migration of ingredients from the insulation was causing the debonding. Analog motors with and without Hitco-2820 insulation were prepared using propellant with an equivalence ratio of 1.15. The propellant debonded from the liner whether or not Hitco-2820 was used.

Based upon these observations several conclusions can be reached:

A. The mode of failure in motor systems differs depending upon the propellant functional curative ratio. Motors loaded with a propellant having a curative ratio of 1.2 exhibited bore cracks after sterilization and motors with a propellant having a curative ratio of 1.15 or less showed propellant/liner separation. In the first tests the test strains ranged from two to four times that imposed on the demonstration motors, and therefore were not indicative of demonstration motor failure.

B. Noxious materials in motor insulations, which may inhibit bonds or destroy them by migration, can be removed either during rubber compounding or motor processing. While this is a potential danger it does not appear to be a major factor causing propellant debonding.

C. Based on the effect of sterilization on tensile properties and an examination of ingredients of UTL-0026 liner it is difficult to visualize how this material could be a problem, although it is possible that propellant/liner bond strength could be reduced by sterilization procedures even though the tensile properties of the liner itself remain more than adequate.

There was no provision under this contract for further investigation of the failures. It can only be hypothesized that propellant/liner separation was caused by one or both of the following factors:

A. During the heatup phase of sterilization, the motor case and propellant/liner interface are much hotter than the mean bulk temperature of the grain. This produces a transient tensile stress of reasonable magnitude across the bondline when the bondline is at a temperature of 300°F. The bond strength at this temperature could be less than allowable without special bonding materials.

B. Changes in propellant and/or liner surface condition as the result of extended exposure to high temperature could weaken the bond. Functional curative ratio could play a part in this phenomena.

Propellant made from CTPIB has been shown to have exceptional thermal stability. Difficulties in utilizing this propellant in a practical motor

system seem to stem from improper usage rather than from a fundamental problem with the propellant or its associated components. Should additional work be done, it is recommended that the work start with curative ratio optimization and that screening be based upon constant load endurance tests and strain analog motor results.